ANALYSIS OF NERVE TERMINAL DYSFUNCTION IN AUTOIMMUNE NEUROPATHY

Ian Morrison, B.Sc. (Med. Sci.) (Hons), MB ChB

A thesis submitted in fulfilment of the requirements of the University of Glasgow for the degree of Doctor of Philosophy

Division of Clinical Neurosciences

University of Glasgow

March, 2008

Dedication

To my wife, Susan and my parents,

for their love and support.

Acknowledgements

The experiments described in this thesis are the result of my own research, except where credit is noted otherwise.

Dr Susan Halstead, Mr Peter Humphreys, Mr Eric Wagner, Mrs Jean Veitch, Ms Dawn Nicholl, and Ms Kate Shaw (Division of Clinical Neurosciences, University of Glasgow) have been a source of friendship, technical support, and academic guidance throughout my time in the laboratory in Glasgow, for which I am very grateful.

The staff of the Central Research Facility in Glasgow, including Dr Joyce Ferguson, Mrs Jean Wilson, Mr Colin Hughes, Mr Ryan Ritchie and Miss Lindsay Campbell, were extremely helpful when I was establishing the *in vivo* imaging facility. They also helped with general breeding, husbandry, and post-operative recovery of the animals, and I very much benefited from their advice and experience.

In Texas, Drs Christopher Hayworth (University of Texas, Austin) and Yi Zuo (UC, Santa Cruz) made me especially welcome in the laboratory, and provided many stimulating discussions concerning glia, the neuromuscular junction and bird watching. Mrs Michelle Mikesh (University of Texas, Austin) was a tremendous source of technical assistance. Outside the laboratory, Michelle and her husband's friendship made my wife and I feel a real part of the community, and showed us how to be Texans.

I'd also like to especially acknowledge Miss Yue Li (University of Texas, Austin), who spent a great deal of time helping me with my *in vivo* experiments in Austin. Her knowledge, technical skill, and patience were crucial whilst undertaking the *in vivo* studies. I very much value and appreciate her input into these studies, and the friendship shown by Yue and her husband outside work.

During my studies, I have been very fortunate to spend time in two highly respected laboratories, under the guidance of Professor Hugh Willison (Division of Clinical Neurosciences, University of Glasgow) and Professor Wes Thompson (Division of Neurobiology, University of Texas in Austin).

Professor Thompson welcomed me to his lab group, and throughout my year in Austin, his patience, knowledge and attention to detail taught me the importance of these areas in laboratory science. I very much appreciate the continued guidance and support offered by Professor Thompson, and the friendship extended by him and his family. Not only was my time in his laboratory very productive, but I also left with many fond memories.

Professor Willison has been a great help during my studies, providing advice and guidance on my research. He has taught me the importance of a rigorous, and thorough approach to science, whilst also maintaining awareness of the human impact of disease. He has also been tremendously supportive of my clinical career, and his example as a respected clinician-scientist is one of the main reasons why I chose to specialise in Neurology.

I would also like to offer my thanks to the Patrick-Berthoud Trust for funding my research studies. Their generous support allowed me to study in both Glasgow, and the United States, and develop fascinating new techniques and strategies that I hope will advance research into neuromuscular disease.

Finally, I would like to thank my wife, Susan for all her support (and serum) over the past three years. Despite being so far away from her friends and family, she agreed to move to Texas without hesitation. I cannot thank her enough.

Declaration of Authorship

All experiments are the work of the author unless specifically stated otherwise.

Ian Morrison, B.Sc. (Med. Sci.) (Hons), MB ChB

University of Glasgow, March 2008

Contents

List of Figures

List of tables

List of Publications

Papers

Halstead,S.K., Morrison,I., O'Hanlon,G.M., Humphreys,P.D., Goodfellow,J.A., Plomp,J.J., and Willison,H.J. 2005. Anti-disialosyl antibodies mediate selective neuronal or Schwann cell injury at mouse neuromuscular junctions. *Glia* 52:177-189.

Morrison, I., Li Y., Halstead, S.K., Humphreys, P.D., Thompson W.J., Willison H.J. Mammalian motor nerve terminals survive in the short-term absence of terminal Schwann cells (in preparation)

Abstracts

Morrison,I., Halstead,S.K., O'Hanlon,G.M., Humphreys,P.D., Goodfellow,J.A., Plomp,J.J., and Willison,H.J An anti-disialosyl antibody causing perisynaptic Schwann cell death at mouse neuromuscular junctions. J. Per. Nerv. Syst 2005 10:64

Morrison, I., Li Y., Halstead, S.K., Thompson W.J., Willison H.J. The consequences of terminal Schwann cell ablation at the murine neuromuscular junction observed through *in vivo* imaging J. Per. Nerv. Syst 2007 12:59

List of Abbreviations

3D	Three-dimensional
ACh	Acetylcholine
AIDP	Acute inflammatory demyelinating polyneuropathy
AMAN	Acute motor axonal neuropathy
AMSAN	Acute motor and sensory axonal neuropathy
Anti-GalC	Anti-Galactocerebroside
APAN	Acute panautonomic neuropathy
BTx	α-Bungarotoxin
CANOMAD	Chronic ataxic neuropathy with ophthalmoplegia, IgM paraprotein, cold agglutinins and disialosyl antibodies
CER	Ceramide
CFA	Complete Freunds Adjuvant
CFP	Cyan fluorescent protein
CIDP	Chronic inflammatory demyelinating polyneuropathy
C. jejuni	*Campylobacter jejuni*
CK	Thy1-CFP, S100-GFP transgenic mouse
CMAP	Compound muscle action potential
CMV	Cytomegalovirus
CNPase	2',3'-cyclic nucleotide 3'-phosphodiesterace
CNS	Central nervous system
CSF	Cerebro-spinal fluid
CTb	Cholera toxin b-subunit
DAF	Decay accelerating factor
DRG	Dorsal root ganglia

EAN	Experimental autoimmune neuritis
EBV	Epstein-Barr virus
ELISA	Enzyme-linked immunosorbent assay
EM	Electron microscopy
EthD-1	Ethidium homodimer
FcR	Fc receptor
GalC	Galactocerebroside
GalNAc-T	GalNAc transferase
Gal T2	Galactose transferase II
GAP-43	Growth-associated phosphoprotein
GBS	Guillain-Barré syndrome
GD3s	GD3 synthase
GFAP	Glial fibrillary acidic protein
GFP	Green fluorescent protein
GGF2	Glial growth factor 2
GlcCer	Glucosylceramide
IFA	Incomplete Freunds Adjuvant
IgE	Immunoglobulin E
IgG	Immunoglobulin G
IgM	Immunoglobulin M
i.p.	Intraperitoneal
i.v.	Intravenous
KO	Knockout
LacCer	Lactosylceramide
LOS	Lipooligosaccharides

LPS	Lipopolysaccharide
LTx	α-Latrotoxin
MAC	Membrane attack complex
MAG	Myelin-associated glycoprotein
MBL	Mannan-binding lectin
MEPP	Miniature end plate potential
MFS	Miller Fisher syndrome
MS	Multiple sclerosis
NF	Neurofilament
NHS	Normal human serum
NMJ	Neuromuscular junction
NO	Nitric oxide
Nrg-1	Neuregulin-1
NT-3	Neurotrophin 3
PBS	Phosphate buffered saline
PCR	Polymerase chain reaction
PNA	Peanut agglutinin
PNS	Peripheral nervous system
RFP	Red fluorescent protein
SEM	Standard error of mean
SGPG	Sulfated glucuronyl paragloboside
SNAP	Sensory nerve action potentials
ST1	Sialyl transferase 1
ST2	Sialyl transferase 2
ST3	Sialyl transferase 3

ST4	Sialyl transferase 4
ST5	Sialyl transferase 5
TIA	Transient ischaemic attack
TS	Triangularis sterni
TSC	Terminal Schwann cell
TLC	Thin-layer chromatography
WT	Wild type
YFP	Yellow fluorescent protein

Abstract

In studies on the pathophysiology of the autoimmune neuropathy, Miller Fisher syndrome (MFS), monoclonal antibodies to the disialosyl epitopes on GQ1b, GT1a and GD3 gangliosides have been produced. Antibodies to these complex gangliosides are thought to be crucial in the pathogenesis of MFS.

These antibodies have recently been shown to produce complement dependent, glial and/or neuronal injury at mouse neuromuscular junctions (NMJs). Three antibodies (EG1, LB1 and R24) were identified as producing selective terminal Schwann cell (TSC) injury whilst sparing neuronal membranes at NMJs in BALB/c and C57BL/6 mouse strains in a dose dependent manner. These changes occur in the absence of observable acute physiological or morphological changes to the nerve terminal, suggesting that TSC injury or loss has no major short-term influence on synapse function. Having compared the suitability of two common *ex vivo* muscle preparations for use in characterisation studies, TSC selective antibodies were compared, and EG1 was identified as most suitable for further investigations on the role of the TSC in mammalian NMJ function and as a possible disease target in MFS. The effect of this antibody when combined with normal human serum as a source of complement in *ex vivo* hemidiaphragm preparations was independent of complement regulators DAF and CD59a.

Cell specific promoter sequences have been used to produce a mouse line that expresses green-fluorescent protein (GFP) in TSCs, and cyan-fluorescent protein (CFP) in axons (CK mouse). Live imaging techniques were used to study the acute

and chronic effects of EG1 mAb mediated, complement dependent glial injury in this system. It is shown that TSC injury is characterised by loss of GFP staining, occurring within 20 minutes of complement exposure. Repopulation of the NMJs with GFP-positive cell bodies is first evident at day 2. The origin of these returning Schwann cells is discussed, and three possible sources are considered – the last myelinating Schwann cell, non-myelinating Schwann cells lying more proximally in the peripheral nervous system, and muscle stem cells. At day 7, the number of GFP-positive cell bodies seen at the NMJ is higher (7-12 per NMJ) than prior to antibody exposure (3-5 per NMJ). This process of enhanced repopulation is not dependent on an intact axon as it is retained following axotomy. At 3 months, minor remodelling of the NMJ is seen, and is more pronounced at one year. Repeat antibody exposure within 48 hours does not injure returning processes, or delay repopulation. Instead, extra-junctional TSC processes are formed, with associated axon sprouts in the absence of gross terminal axon injury.

Anti-GQ1b containing serum from a MFS patient is shown to induce murine TSC death in a similar manner to murine monoclonal antibodies described previously. This suggests that TSCs are a potential new disease target in human disease if the ganglioside profile of mouse and human TSCs is equivalent. Ganglioside distribution and antibody binding are examined on a series of human muscles. These studies demonstrate for the first time that components of the human NMJ are potentially susceptible to anti-ganglioside antibody mediated injury, by virtue of their ganglioside profile.

This study suggests that TSCs may be a previously unrecognised site of immune-mediated nerve injury. It also describes a new technique for observing chronic TSC injury and recovery in an *in vivo* mouse model system, which could be used for human disease modelling.

Chapter 1: Introduction

The aims of my thesis are outlined in section 1.6. Briefly stated, these aims are to: 1) Identify and characterise an antibody suitable for producing selective terminal Schwann cell injury; 2) Examine ways of increasing the effect of this antibody by removing complement regulators; 3) Adapt a new fluorescent mouse system to study the effects of immune mediated injury in the peripheral nervous system; 4) Characterise the chronic effects of selective terminal Schwann cell injury in the mammalian neuromuscular junction; and 5) Identify the ganglioside profile, and potential binding targets in human tissue to establish whether the human neuromuscular junction, and in particular the terminal Schwann cell could be a disease target in Miller Fisher syndrome. The following introduction is intended to provide the clinical and experimental context in which these aims can be evaluated.

1.1 Autoimmune neuropathies

1.1.1 Background

Autoimmune neuropathy is a generic term to describe syndromes resulting from both axonal and glial injury caused by inflammation in the peripheral nerve (Willison and Yuki, 2002)**.** The acute diseases, Guillain-Barré syndromes (GBS) are the foremost cause of neuromuscular paralysis with a global incidence of ~$1.5/10^5$ (~750 UK cases per year). These syndromes include the acute motor axonal neuropathy (AMAN), acute inflammatory demyelinating polyneuropathy (AIDP); and the focal variant,

Miller Fisher syndrome (MFS) which is characterised by a distinct clinical triad of ataxia, areflexia and ophthalmoplegia (Fisher, 1956).

GBS and variants are post-infectious illnesses, occurring approximately 2 weeks after diverse and ubiquitous infections in individuals with unpredictable sensitivity. These are characterised by inflammation and loss of function in peripheral nerves; and can cause severe axial, limb and respiratory paralysis. A study from the south of England highlighted the considerable morbidity and mortality associated with the illness. In this study, 79 patients were recruited over a 12 month period, and followed up for a year. This study demonstrated that in approximately 25% of patients, the paralysis is so severe that prolonged mechanical ventilation is required, and 4% of patients remained bedbound or ventilator dependent one year from illness onset. The authors also described a mortality rate of 8% in the first year, (all of these patients were over 60 years of age), with 9% of survivors being left unable to walk after 12 months (Rees *et al*, 1998). Studies have also demonstrated the substantial economic burden of this illness, with the financial impact on the US economy of *Campylobacter* related GBS being estimated at between US$0.2-1.8 billion annually (Buzby *et al*, 1997).

1.1.2 Guillain-Barré and its clinical forms

The first description of GBS was made by a French Physician in 1859, called Jean Baptiste Landry. In this early work, he described a group of 10 patients who had a form of ascending paralysis associated with various forms of sensory disturbance, and respiratory paralysis as a terminal event (Landry, 1859). The condition was subsequently known as “Landry’s Ascending Paralysis”.

It took over 50 years until the next influential paper was published in the field. In 1916, three French Physicians, George Guillian, Jean Alexandre Barré and Albert Strohl published the paper: ”Sur un syndrome de radiculo-neurite avec hyperalbuminose du liquide cephalo-rachidien sans reaction cellulaire: remarques sur les caracteres cliniques et graphiques des reflexes tendineux” (Guillain *et al*, 1916). In this study, they described two soldiers in the First World War who developed clinical weakness associated with loss of tendon reflexes. In addition, CSF analysis from these patients demonstrated an acellular CSF with a high protein[1].

Some debate existed around the clinical definition of the disease, with Guillain arguing for a number of years that his description was distinct from “Landry’s Ascending Paralysis”, as it followed a relatively benign course, and respiratory paralysis was not a feature of the illness. Guillain’s opinion was widely accepted for almost 3 decades, until Webb Haymaker and James Watson Kernohan published a study in 1949, describing post mortem data from over 50 patients with severe, rapid onset fatal peripheral neuropathy consistent with a diagnosis of GBS. This post mortem study was also supported with a very comprehensive literature review of similar cases (Haymaker and Kernohan, 1949). The literature review in particular, concluded that many peripheral neuropathies (including GBS and Landry’s Ascending Paralysis) represented a spectrum of the same condition, rather than distinct clinical entities. They concluded that it was more appropriate from a clinical and research perspective to classify them together as a single, distinct syndrome.

[1] More contemporary studies have shown that CSF protein levels may be normal, particularly during the first week of illness (Ropper, 1992)

In addition to the new classification based on the literature review, the post mortem data also suggested that an as yet unidentified agent was responsible for the tissue damage, rather than the widely held belief that injury resulted from direct inflammatory injury. Although methodological difficulties exist with this study, including issues of tissue preparation and pathology that was not consistent with the geographical area of the patient sample; the study was the first to suggest that a foreign agent may be the initiating factor of GBS.

Aside from the original descriptions by Landry and Guillain, Barré and Strohl, the Haymaker and Kernohan paper is possibly one of the most important publications in the field of GBS research, as it identifies a heterogenous group of disorders as a single clinical condition while also offering an important insight into disease pathogenesis. This conclusion provided an important basis for further research into the condition.

1.1.3 AIDP

1.1.3.1 Background

The demyelinating form of GBS is known as acute inflammatory demyelinating polyneuropathy (AIDP), and is particularly common in Europe and North America. In this condition, patients present with the typical flaccid paralysis in conjunction with absent tendon reflexes. Nerve conduction studies on these patients are often inconclusive, due to the patchy nature of the demyelination and this can lead to equivocal or negative results. When present however, certain features are thought to be highly specific for AIDP.

1.1.3.2 Electrophysiological features

Two common tests of motor function in neurophysiology are testing the H-reflex and F-wave, and both are sensitive for AIDP. The H-reflex is the muscle response to stimulation of 1a sensory afferent nerves arising from the muscle spindles in their innervating nerves, in a way analogous to tendon reflexes producing a knee or ankle jerk via the spinal reflex arc. Its absence is one of the most common neurophysiological changes in AIDP patients (Gordon and Wilbourn, 2001) but it can also occur in other conditions, therefore its absence is not exclusively diagnostic.

The F-wave measurement represents the antidromic activation of motorneurones. The distal portion of a nerve is stimulated transcutaneously, and the impulse travels antero- and retrogradely along the nerve. The anterograde conduction produces muscle contraction, known as the M-response while the retrograde response travels back up the nerve to the cell body, where it is "reflected back" to produce a second muscle contraction. It is this second, antidromic response that produces the F-wave. However, this technique has the potential for considerable variation in measurement and as a result, its analysis is subject to a number of strict protocols that account for nerve length, stimulation frequency, and age of the subject (Fisher, 1998). Despite this, absent or prolonged F-wave latencies are seen in up to 80% of patients with AIDP.

Often distal compound muscle action potential (CMAP) amplitudes are preserved in patients with AIDP. These CMAP amplitudes represent a group of simultaneous muscle action potentials that are combined as a summated action potential following stimulation of the innervating motor nerve and, when preserved, suggest that the muscle bulk and

axon are intact, and are responding appropriately to nerve action potentials. A preserved CMAP in conjunction with absent or delayed F-waves latencies is highly suggestive of GBS (Al Shekhlee *et al*, 2005; Gordon and Wilbourn, 2001).

Another electrophysiological marker of AIDP is the presence of multifocal demyelination in the absence of any entrapment neuropathies. Studies have shown that proximal conduction block and temporal dispersions are highly specific for AIDP, in addition to slowing of the nerve conduction velocity in the first 3 weeks of illness (Ropper *et al*, 1990). However, these findings are only present in approximately 20% of patients and are not sensitive for AIDP.

Although AIDP is considered primarily a motor weakness, sensory abnormalities are also often present, particularly in the first 3 weeks of illness. At this time, patients will display sensory abnormalities on nerve conduction in the upper limbs with relative sparing in the lower limbs, particularly the sural nerve. This finding is thought to be highly specific for acquired demyelination, particularly under 60 years of age (Al Shekhlee *et al*, 2005; Gordon and Wilbourn, 2001).

1.1.3.3 Clinical features

Although there are no clinical features which are exclusively diagnostic of AIDP in isolation, a combination of several features in conjunction with a suitable history are very suggestive of AIDP, and are used in diagnosis as defined by Asbury and Cornblath (Asbury and Cornblath, 1990). Clinical features that are consistent with a diagnosis of GBS, and AIDP include:

- Progressive, relatively symmetrical motor weakness lasting until 4th week of illness, not restricted to limb musculature
- Limited sensory involvement
- Autonomic dysfunction
- Recovery within 4 weeks after motor progression stops
- Absence of fever at disease onset.

However, variation in the disease symptomatology means that many patients have a unique clinical presentation, which limits the practical application of strict diagnostic criteria with GBS. It is also important to recognise that certain presentations can suggest other diseases, including marked asymmetry of symptoms, persistent bladder or bowel weakness, and a high levels of mono- or poly-nuclear lymphocytes in the CNS. In which examples, conditions such as botulism, poliomyelitis and other peripheral nerve disorders should be excluded in the first instance.

1.1.3.4 Pathological features

While both the clinical presentation and electrophysiological features are well documented, the exact mechanism of injury in AIDP has yet to be clearly elucidated. The original paper by Asbury in 1969 described pathological samples from patients showing lymphocytic infiltration, suggesting that the process was mediated by T-cells and therefore similar to allergic neuritis (figure 1.1) (Asbury *et al*, 1969).

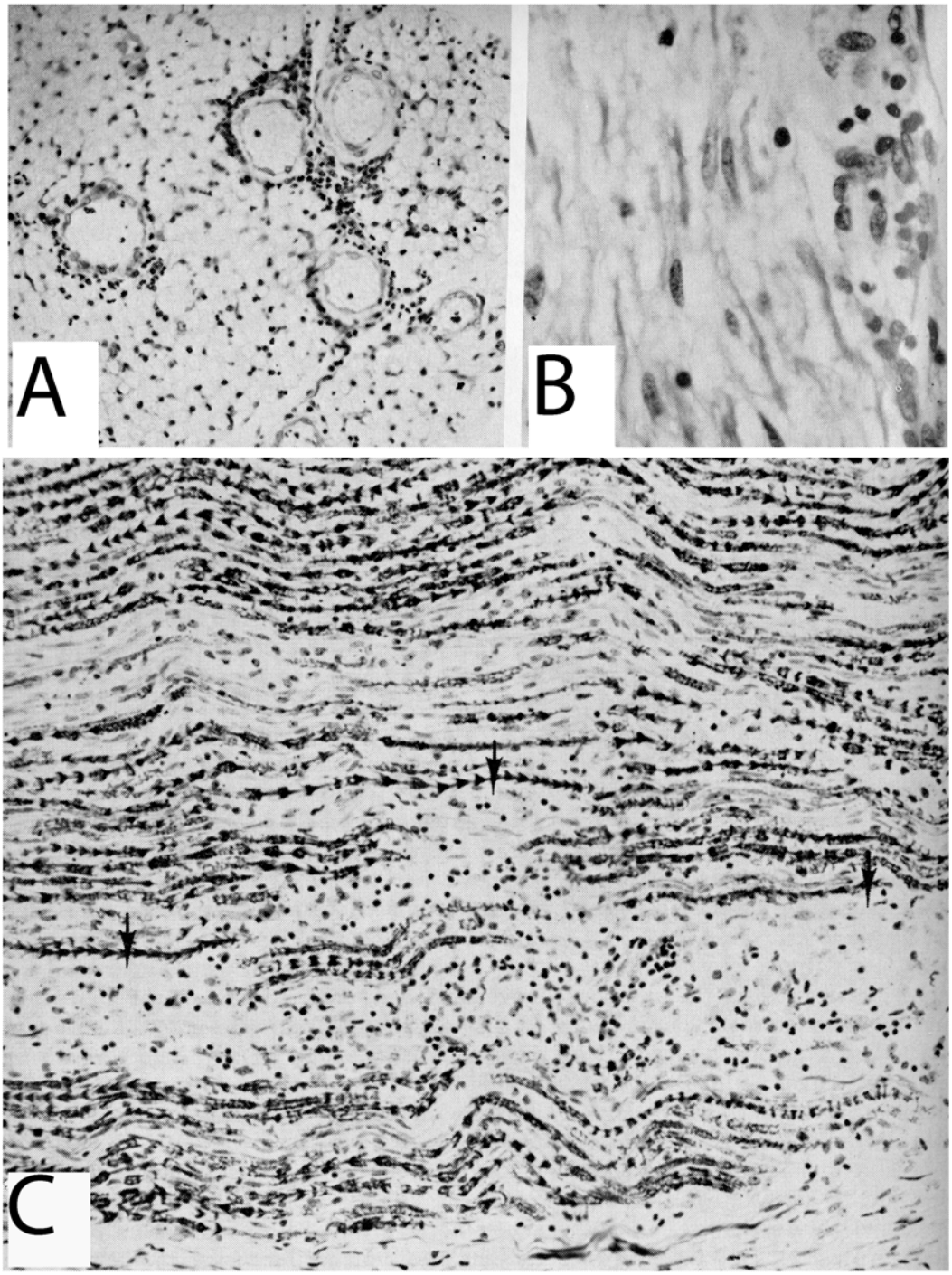

Figure 1.1: Illustration of injury in AIDP.

A: Perivascular infiltrate contains many polymorphonuclear lymphocytes, as well as leucocytes in areas of tissue damage. (Cross section through several roots at the level of the cauda equina, 200x)

B: Small subperineurial exudates composed of a mixture of lymphocytes and polymorphonuclear leukocytes. Transforming cells derived from

invading lymphocytes are also seen (large, pale nuclei with prominent nucleoli and marginated chromatin) (Cross section through several roots at the level of the cauda equina, 490x)

C: Extensive myelin destruction and inflammatory infiltrate. Arrows indicate areas of myelin breakdown. Small dark cells are predominantly lymphocytes. (Radial nerve, 170x). Taken from Asbury (1969)

However, a more recent study examined post mortem tissue from 3 patients who had symptoms of AIDP at the time of death. These immunohistochemical studies examined the distribution of complement activation products on the surface of myelin, using a combination of resin imbedded tissue and EM studies. This work showed complement activation products on the surface of myelin, and vacuolar changes occurring prior to the ingress of macrophages to the area. This suggests, at least in these cases of AIDP, that the injury is an antibody-mediated, complement dependent injury to myelin, with subsequent macrophage recruitment to remove the damaged myelin (figure 1.2) (Hafer-Macko *et al*, 1996b). There may also be subsequent axonal degeneration associated with the demyelinating process (Albers *et al*, 1985), and while the exact mechanism of this damage is unclear, it is most likely due to loss of trophic support from the Schwann cells (so called “bystander effect”).

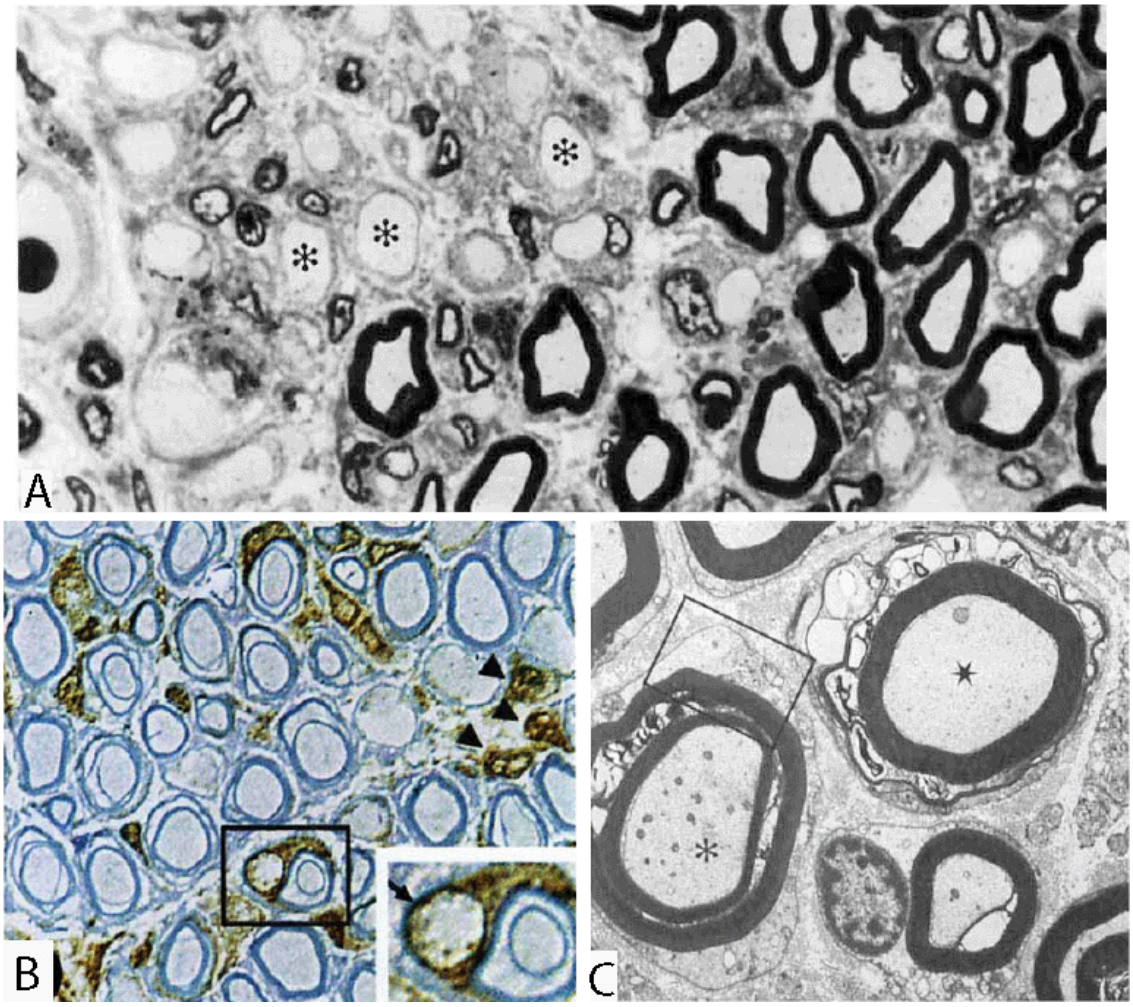

Figure 1.2: Contemporary study of injury in AIDP.

A: Post mortem study of ventral roots. At day 9, there were large plaque-like areas (outlined with asterisks) with demyelinated nerve fibres. (Ventral roots, day 9 post mortem, 910x).

B: C5b-9 deposition. In addition to extensive C5b-9 deposition on the Schwann cell surface, macrophages were also identified in close association, and also expressed C5b-9 antigen (black arrowheads). Macrophages on the outer surface of myelin sheaths also stained for C5b-9 (black arrow in boxed region) (Etched immunostained plastic sections counterstained with toludine blue, day 8 post-mortem)

C: EM study of nerve injury at day 8. C3d is seen on the outer surface of two fibres. Myelin disruption in fibres with C3d immunostaining is associated with vesicular changes in the sheath, and was seen in the outermost myelin lamellae (seen in fibre with asterisk). However, it is not possible to fully exclude post-mortem artefact as a cause for these structural changes. (Thick and thin sections, day 8 post mortem, 4830x) Taken from Hafer-Macko *et al* 1996b)

1.1.4 AMAN

1.1.4.1 Background

Although axonal degeneration can result from the "bystander effect", it was proposed in the 1980s that axonal degeneration could result from an entirely separate pathological process, where the injury was directed towards the axon itself, rather than the surrounding myelinating Schwann cells (Feasby *et al*, 1986). These forms of GBS are called acute motor axonal neuropathy (AMAN) (McKhann *et al*, 1993) and acute motor sensory axonal neuropathy (AMSAN) (Griffin *et al*, 1996).

The injury in AMAN and AMSAN is believed to be antibody-mediated, usually directed towards the GM1 and GD1a gangliosides. Unlike AIDP, post mortem studies from these cases have shown axonal degeneration associated with immunoglobulin and complement deposition at the nodes of Ranvier in the absence of significant demyelination (Hafer-Macko *et al*, 1996a). It is thought that the initial immune response can then recruit macrophages to this site by complement co-factors,

including C5a. The macrophages can then travel in the periaxonal space between internodes to produce degeneration of the axon, often extending as far as the ventral root to produce extensive Wallerian degeneration (figure 1.3) (Griffin *et al*, 1996).

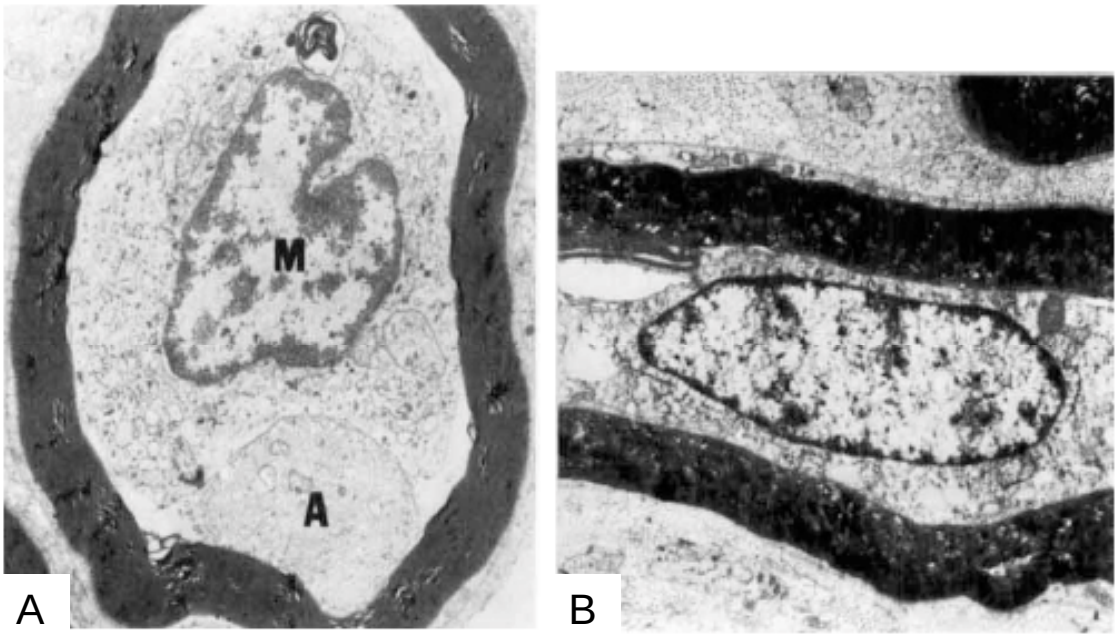

Figure 1.3: Illustration of damage in AMAN.

A: Electron micrograph of a sectioned nerve fibre shows a macrophage (M) in the periaxonal space, with a normal myelin sheath and a condensed, but otherwise normal intact axon (A) (1mm plastic embedded sections of the ventral nerve, 6826x)

B: Electron micrograph of a sectioned nerve fibre. The axon has denegerated, and a macrophage is present in the space normally occupied by the axon. The myelin sheath is intact. (1mm plastic embedded sections of spinal roots, 7600x before 5% reduction) (Taken from Griffin, 1996)

Interestingly, these predominantly axonal forms of GBS are more prevalent in the developing world, particularly rural China, in contrast to AIDP, which is common in Europe and North America. The exact reason for this geographical difference is unknown.

1.1.4.2 Electrophysiological features

Unlike AIDP, patients with AMAN will demonstrate normal motor distal limb latencies and conduction velocities, with apparently normal sensory electrophysiology and F-waves. Significantly however, they may have reduced CMAP amplitudes because the axon is damaged, and therefore present as a pure motor axonal neuropathy in contrast to AIDP (McKhann *et al*, 1993). Patients who have AMSAN may have the same motor features as AMAN, in addition to reduced or absent sensory nerve action potentials (SNAP).

1.1.4.3 Recovery

Understandably, if the injury is proximal, recovery from such extensive axonal degeneration will be prolonged, as the axons will have to grow a considerable distance during reinnervation. However, certain subgroups of patients exhibit relatively rapid recovery from AMAN. In this group, it is thought that the antibodies bind transiently to the nodes of Ranvier, and produce a short-lived electrophysiological disruption. This antibody complex does not cause significant axonal degradation, therefore recovery is rapid as regeneration does not need to occur (Ho *et al*, 1997).

1.1.5 Acute Panautonomic Neuropathy

A very severe GBS-like condition is Acute Panautonomic Neuropathy (APAN), which is also known as autoimmune autonomic gangliopathy. Although the condition in its purest form affects only the autonomic nervous system, many presentations also have a somatic component, and it is considered to be very similar to GBS as a result. Patients may experience an ascending sensory disturbance initially, which is also associated with widespread autonomic dysfunction (Low *et al*, 1983). The autonomic dysfunction can be purely cholinergic, or can also involve the adrenergic and other organ systems, particularly the GI tract (Low, 1994). This may result in significant cardiovascular instability characterised by labile blood pressure; and GI paresis. Recent work suggests that antibodies bind to acetylcholine (ACh) receptors in the autonomic ganglia to produce a conduction block analogous to myasthenia gravis (Wang *et al*, 2007). Unlike other forms of GBS, the prognosis for this variant is particularly poor due to the autonomic features, and therapeutic options are limited. However, a study suggests that high dose intra-venous immunoglobulin may be appropriate in certain cases (Smit *et al*, 1997).

1.1.6 Miller Fisher syndrome

1.1.6.1 Clinical features

1.1.6.1.1 Background

MFS is another variant of GBS, and was first described by Charles Miller Fisher in 1956 (Fisher, 1956), a Canadian neurologist who is also renowned for his work on stroke disease, and transient ischaemic attacks (TIAs). Although the disease only accounts for less than 5% of all cases of GBS, it provides an interesting experimental model for the disease. Patients were originally described as presenting with a clinical triad of: ophthalmoplegia, areflexia and ataxia; often occurring after antecedent infection that may include a diarrhoeal illness caused by *Campylobacter jejuni* (Endtz *et al*, 2000). However, recent reviews have suggested that other clinical features, including papillary abnormalities, ptosis, and bulbar and facial weakness should be considered as variants of the clinical presentation, in addition to the original clinical triad described by Fisher (Mori *et al,* 2001). It is also possible that components of the syndrome may present in isolation, including isolated ophthalmoplegia or bulbar and facial palsies, and these are believed to represent a more limited variant of MFS (Overell *et al*, 2007).

Although variations do exist in the presentation of MFS, the original description and subsequent studies have emphasised that limb weakness is not considered a feature of pure MFS (Fisher, 1956; Sauron *et al,* 1984). Recent reviews suggest however that a

"GBS overlap" syndrome may exist where limb weakness is a feature, but its long-term morbidity may be different from isolated MFS (Overell *et al*, 2007).

1.1.6.1.2 Electrophysiological features

Interestingly, despite the lack of limb symptoms, electrophysiological studies have shown some degree of peripheral nerve dysfunction in MFS. In particular, a reduction in sensory nerve potential amplitude in the limbs is often seen (Fross and Daube, 1987, Durand *et al,* 2001), suggesting involvement of the afferent spinal nerves and possibly the dorsal root ganglia. However, the exact pathophysiological mechanism behind these findings has yet to be elucidated. Motor nerve dysfunction in the limbs has also been described in the absence of weakness, but these data are more variable than studies of sensory abnormality. Some studies describe an axonal neuropathy (Fross and Daube, 1987), while others conclude that a form of proximal demyelination is present (Jamal and Ballantyne, 1988). The exact nature of the motor limb lesion is therefore unclear.

There are few studies examining the nature of motor cranial nerve dysfunction in MFS, as these nerves are often very difficult to examine. However, a recent paper demonstrated a neuromuscular junction conduction defect in the extraocular muscles using single fibre EMG techniques (Sartucci *et al,* 2005), while transcranial magnetic stimulation studies suggest that facial nerve weakness results from demyelination of the proximal nerve segments (Arányi *et al,* 2006). However, it is widely accepted that further work is required to characterise the nature of the defects in more detail, to assist in diagnosis and understanding the disease pathogenesis.

1.1.6.1.3 Prognosis

In contrast to other forms of GBS, MFS is generally considered to have a relatively benign, self-limiting course. One retrospective review of MFS cases demonstrated that all of their untreated patients with MFS (28 patients) had returned to normal approximately 6 months after disease onset, with a median period of recovery of 32 days (range from 8 to 271 days) for symptoms of ataxia, and 88 days (range from 29 to 165 days) for ophthalmoplegia (Mori *et al,* 2001). Although both immunoglobulin and plasma exchange therapy are commonly used in the treatment of MFS, there is little evidence to establish their value in the treatment of the condition at present (Overell *et al*, 2007).

1.1.6.2 Anti-ganglioside antibodies

During the acute phase of the illness, over 90% of patients with MFS will have demonstrable titres of antibodies to the GQ1b ganglioside (figure 1.4) (Chiba *et al*, 1993; Willison *et al*, 1993a). Serum titres of these antibodies often become undetectable during the recovery phase (Mizoguchi, 1998), and these observations have led investigators to believe that anti-ganglioside antibodies are strongly implicated in the disease pathogenesis.

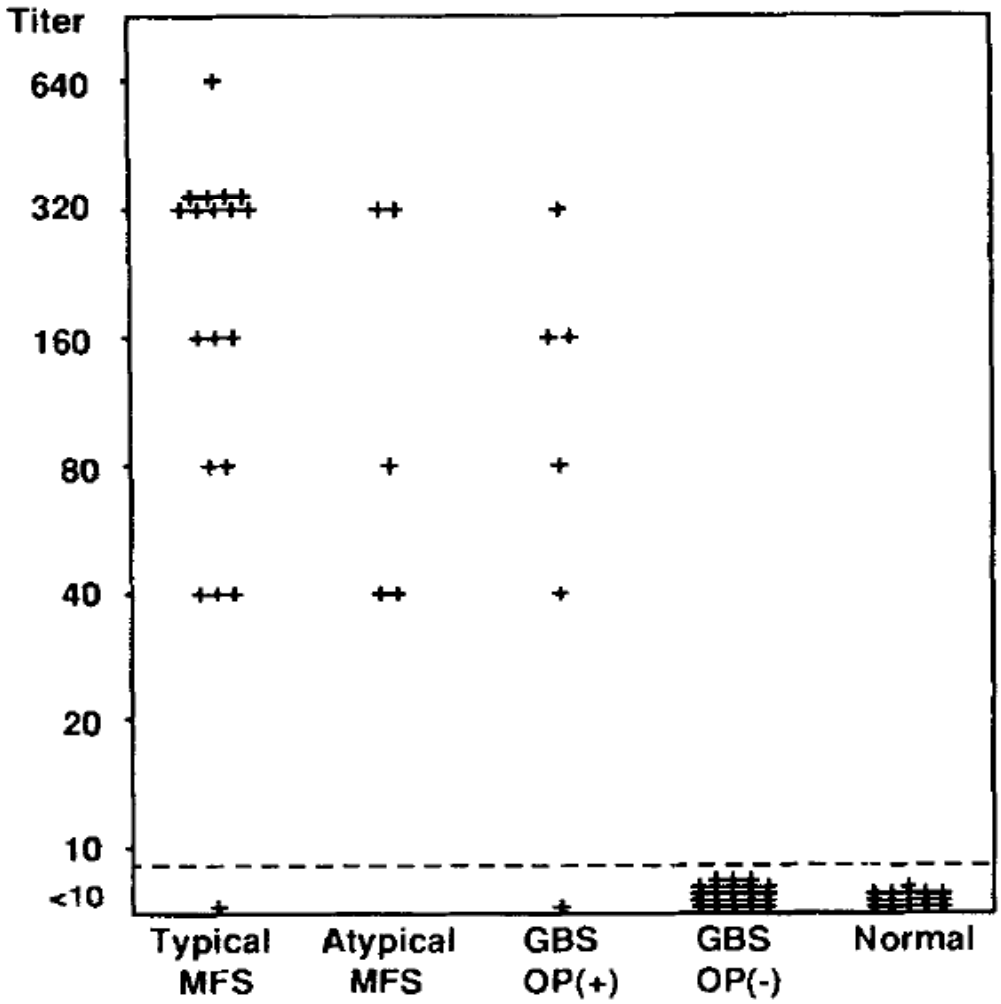

Figure 1.4: GQ1b IgG antibody titres from patients during acute neurological weakness.

18 of the 19 patients with typical MFS, and all 5 patients with atypical MFS (no ataxia, variable limb reflexes) had demonstrable titres of GQ1b. In addition, 5 of the 6 patients with GBS with ophthalmoplegia (GBS OP(+)) also had GQ1b antibodies. This suggests that antibodies to complex gangliosides, in particular GQ1b are present in MFS, and may be involved in the mechanism of ophthalmoplegia (Taken from Chiba *et al*, 1993).

Although anti-ganglioside antibodies are highly specific for MFS, they are also found in Bickerstaff's brainstem encephalitis (Yuki *et al*, 1993a). There is considerable debate over the similarities between these diseases, particularly their clinical signs and pathogenesis. For example, the original description of Bickerstaff's encephalitis identified patients with ophthalmoplegia, and ataxia, with 50% displaying either hypo- or areflexia (Winer, 2001). These features are consistent with MFS leading some authors to suggest that they may represent a spectrum of the same condition, supporting the similar anti-ganglioside antibody profiles in both (Odaka *et al*, 2001). Similarities also exist between MFS and diseases like acute ophthalmoparesis and ataxic GBS, including clinical presentation and ganglioside profile (Willison and Yuki, 2002), and "GBS overlap" syndromes have also been described with features of MFS or Bickerstaff's encephalitis in association with limb weakness (Overell *et al,* 2007). This has led some authors to propose the concept of an "anti-GQ1b antibody syndrome", classifying patients with anti-GQ1b antibodies and ophthalmoplegia as a distinct clinical entity, regardless of the primary diagnosis. However, this new classification has yet to be accepted, as the clinical outcome of the "anti-GQ1b antibody syndrome" often varies according to the primary presentation, making it difficult to classify as a single disease entity (Winer, 2001)

1.1.6.3 Disease targets

One of the more interesting hypotheses recently proposed identifies the neuromuscular junction (NMJ) as a possible target of antibody-mediated injury in GBS variants, particularly MFS (Sartucci *et al*, 2005). The antibody-mediated injury is thought to result from the formation of pores in the nerve membrane, by activation

of complement and resulting production of membrane attack complex. These pores allow entry of calcium, and induce vesicle release with subsequent nerve terminal destruction caused by activation of calpain (a calcium dependent proteolytic enzyme) (figure 1.5) (O'Hanlon *et al*, 2003). Certain cranial nerves, particularly the oculomotor nerve, are relatively rich in complex gangliosides (Chiba *et al*, 1997), and as antibodies to these structures are strongly associated with the MFS (Willison and Veitch, 1994), it is likely that these sites are the target for antibody binding and give the symptom of ophthalmoplegia.

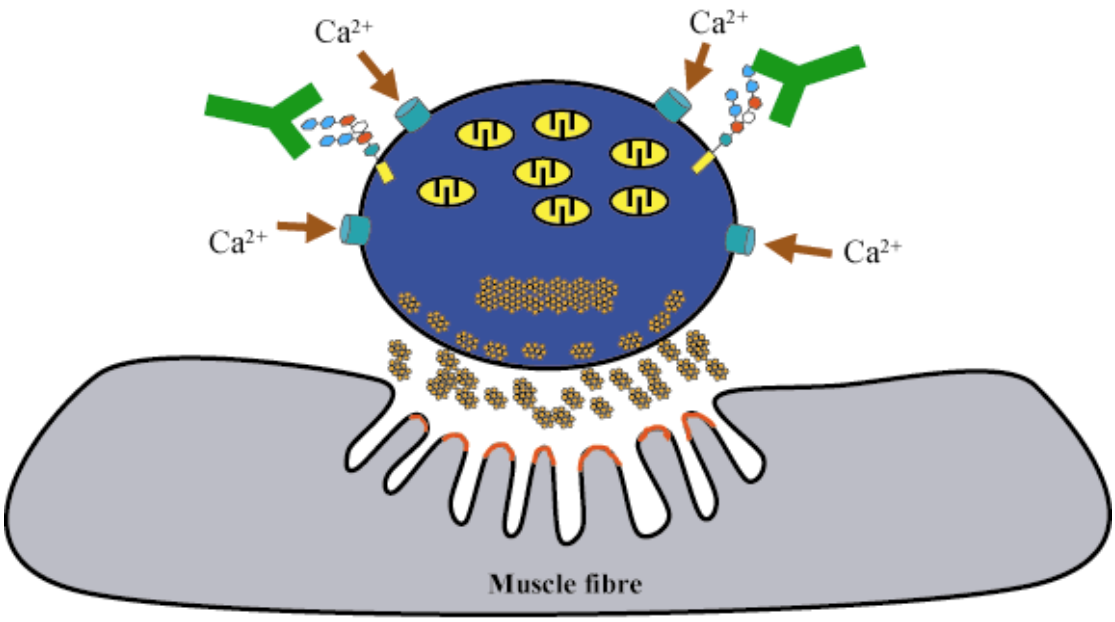

Figure 1.5: Cartoon illustration of nerve terminal injury.

Antibodies bind to ganglioside on the surface of the nerve, and activate complement to form MAC. The resulting MAC pores cause the influx of calcium into the nerve terminal, causing massive exocytosis of ACh vesicles. Calcium also activates calpain to induce nerve terminal destruction.

A number of other factors exist that suggest the NMJ is the likely source of injury in MFS. For example, the NMJ is more vulnerable to circulating antibodies than other structures in the nervous system, as it is not bound by the blood-nerve barrier and can be easily accessed by antibodies in the circulation. Also, many other autoimmune diseases of the nervous system, including myasthenia gravis, and Lambert-Eaton myaesthenic syndrome, produce induce injury at this structure. Aside from autoimmune disease, a number of toxins have been shown to target the NMJ. One of these toxins, from the bacterium *Clostridium botulinum*, shares many of the clinical and electrophysiological features of MFS, and exerts its initial effect at the NMJ by binding to gangliosides (O'Hanlon *et al*, 2002). This interesting similarity provides strong support for ganglioside involvement in the pathogenesis of MFS. Finally, a recent case study suggests that the conduction defect in MFS occurs at the NMJ (Sartucci *et al*, 2005), although the patient in this example did not have demonstrable titres of anti-ganglioside antibody in their serum.

Neuromuscular conduction defects are also seen in animal models exposed to complex ganglioside antibodies, and support the electrophysiological studies from the human. In these *ex vivo* animal studies, the antibody caused spontaneous release of ACh vesicles (measured by miniature end plate potentials), followed by failure of end plate potentials evoked by nerve stimulation (O'Hanlon *et al*, 2001). This effect is similar to the injury caused to the nerve terminal by the black widow spider venom, α-latrotoxin.

Although injury to the NMJ is one possible mechanism for paralysis in MFS, it should be noted that antibodies to GQ1b have been noted to bind at other sites, including the nodes of Ranvier in oculomotor nerves (Chiba *et al*, 1993). It is therefore possible that the variants of disease represent antibodies binding to different neural sites, including the TSC.

However, the clarity of data surrounding the possible pathogenesis of MFS make it a desirable model, not just for MFS, but for other antibody-mediated nerve injuries. In particular, work towards an animal model will allow new therapeutic strategies to be tested that may significantly reduce the morbidity and mortality of the disease.

Syndrome	Identified ganglioside targets	Electrophysiology	Probable Site of injury
AIDP	GalC, LM1, GM1 SGPG, GM2	Absent F- and H-reflex Normal CMAP	Myelinating Schwann Cells
AMAN	GD1a, GM1a, GM1b	Normal distal limb latencies Reduced CMAP	Axon (possibly via node of Ranvier)
AMSAN	GD1a, GM1a, GM1b	Normal distal limb latencies Reduced CMAP Reduced or absent SNAPs	Axon (possibly via node of Ranvier)
APAN	Unknown	Autonomic instability	Autonomic ganglia
MFS	GQ1b, GD3 GT1a, GT1b	Reduced SNAP amplitudes Abnormal blink reflexes Reduced facial CMAP Variable motor studies	NMJ

Table 1.1: Clinical summary of GBS variants.

1.1.7 Therapeutic options

Although it is clear that the immune system is strongly implicated in the pathogenesis of GBS, only a limited number of current therapies are successful in modulating the immune response in this condition. Current literature suggests that plasma exchange and high dose intravenous immunoglobulin therapy (at 2g/kg over 2 days) are equally effective at improving functional outcome (for example shortening the time to walking independently) (Shahar, 2006) .

During plasma exchange, the patient's blood is filtered and the plasma is substituted by an albumin solution. As plasma contains the pathological antibodies, its removal reduces the concentration of circulating antibody, and moderates the disease effect. The technical requirements of this process and equipment costs however, restrict this method to specialist tertiary referral centres. There are also certain complications specific to plasma exchange, rendering it slightly less safe than immunoglobulin therapy. These complications include those arising from insertion of dialysis catheters, and also bleeding diatheses (Raphael *et al*, 2002).

The current alternative to plasma exchange is high dose intravenous immunoglobulin therapy. During this treatment, the patient receives a high concentration of purified plasma taken from at least 1000 donors. One of the earliest uses of immunoglobulin therapy was described in 1981 for the treatment of autoimmune thrombocytopenia in children, and then later for GBS (Imbach *et al*, 1981; Kleyweg *et al*, 1998). While the exact mechanism of action is unknown, it is thought that the high concentration of immunoglobulin can suppress the immune response. This may occur by blocking Fc receptors on macrophages to prevent them being directed to Schwann cells by antibodies; inhibiting the action of cytokines or autoantibodies; or by inhibiting the components of the complement cascade (Dalakas, 2004). Another, more complex hypothesis suggests that the immunoglobulin accelerates the breakdown of IgG by overwhelming the immunoglobulin recycling process in endothelial cells (a mechanism dependent on FcRn receptors on the cell surface) and diverting excess IgG towards lysosomes, increasing its rate of breakdown (Yu and Lennon, 1999). Another mechanism, which uses a model of MFS, suggests that immunoglobulin may inhibit antibody binding to the NMJ (Jacobs *et al*, 2003).

Regardless of the mechanism, recent reviews have clearly shown that concentrated immunoglobulin therapy is efficacious for the treatment of GBS to reduce overall morbidity (Hughes *et al*, 2007). Although immunoglobulin therapy is widely considered to be safer than plasma exchange, there are risks with transfusion reactions, although these are normally self-limiting and are generally associated with hyperviscosity. The risk of infection is also limited by the careful screening of donors, and there have been no documented cases of transmission of HIV through immunoglobulin blood product, and only a small number of cases of hepatitis C. However, the large number of donors required for the therapy, and the difficulty with identifying and eliminating prion proteins, suggests that exposure to variant Creutzfeldt-Jakob disease is possible. While the transfusion services have made attempts to minimise this risk, the long-term effects of the potential exposure are still unknown (Hughes *et al*, 2006a).

Another well established immunosuppressive treatment is the corticosteroid therapy. This technique has been used extensively in medicine as a treatment for autoimmune illness, and it would be expected to play a similar role in modulating the immune response in GBS. However, a recent Cochrane review did not show any evidence that steroids alone produce an improvement in symptoms, and indeed their use was associated with a slight (statistically insignificant) increase in steroid related complications including diabetes but not surprisingly, hypertension (Hughes *et al*, 2006b). Steroids are widely recognised as being effective modulators of inflammation, and this surprising result may due to the effect of steroid myopathy masking any improvement in nerve function.

Clearly current therapy is effective but has a number of limitations, in particular failure to reduce the overall mortality of the condition (Hughes *et al,* 2007). It is therefore highly desirable to explore other treatment options. These new therapies could even be used in other autoimmune diseases beyond the nervous system that share a common pathogenesis.

1.1.8 Possible future treatments

Current therapies in GBS are directed towards modifying the immunological response, by either removing the causative antibodies, or directly influencing the immune response with high dose immunoglobulin. However, recent work suggests that it may be possible to inhibit the damage caused by the activation of complement, allowing prompt recovery from the initial insult.

As discussed previously, damage in MFS is thought to arise from the entry of calcium into the nerve, through pores created by the complement product C5b-9 (membrane attack complex). The injury results from calcium binding to the cysteine proteases: calpains, producing damage to cytoskeletal proteins, including neurofilament (Chan and Mattson, 1999). Although they potentially contribute to injury in disease, calpains are also thought to be important in maintaining normal synaptic structure, as application of calpain inhibitors in a healthy preparation causes abnormal accumulations of neurofilament (Roots, 1983). Experiments have also shown a therapeutic role for calpain inhibitors, as their administration *in vivo* can have

beneficial effects following brain injury by preventing axonal breakdown (Bartus *et al*, 1995).

As a result of these observations, calpain was studied in the context of antibody-mediated nerve injury, as a method of inhibiting damage to neurofilament resulting from calcium ingress secondary to MAC activation (O'Hanlon *et al*, 2003). These experiments demonstrated that while application of calpain inhibitors (calpeptin and calpain inhibitor V) did not stop the electrophysiological changes associated with antibody-mediated injury, their application did inhibit subsequent breakdown of axonal neurofilaments. This suggests that while calpain inhibitors may not prevent the initial insult that produces paralysis, they may expedite recovery by limiting the damage resulting from antibody-mediated neuropathy.

Other therapeutic strategies that attempt to modify or prevent the initial injury are also being investigated, including the use of complement inhibitors to limit the formation of MAC, and prevent significant terminal destruction. This could be achieved by inhibitors of C3 and C5 convertase enzymes in the complement cascade, using APT070, which is a substance based on the active component of CD35 (a naturally occurring complement regulator) (Halstead *et al*, 2005a).

The formation of MAC can also be inhibited by the use of antibodies to C5, a key component in the MAC complex. These antibodies bind to C5 to prevent its cleavage into C5a and C5b, and thus prevent its use in the MAC complex. This has been shown to prevent nerve terminal injury caused by antibodies to complex gangliosides (Halstead, submitted).

Another treatment possibility involves refining the technique of plasma exchange to produce therapeutic columns through which blood is passed. Anti-ganglioside antibodies are then removed by immuno adsorption onto glycan-conjugated filtration devices (Willison *et al*, 2004). This would selectively remove pathogenic antibodies, without causing significant disruption or fluid shifts from the patient's plasma.

Once fully developed, these exciting strategies will hopefully offer new, safer treatments that will expedite recovery, and limit long-term injury in patients with GBS. If successful, these new therapies will hopefully reduce the considerable financial, and emotional impact of the disease.

1.2 Disease Pathogenesis

1.2.1 Role of gangliosides

1.2.1.1 Background

As discussed previously, a number of theories exist about the origin of injury in GBS, and anti-ganglioside antibodies are thought to be the most likely cause based on both laboratory and clinical data (Quarles and Weiss, 1999).

Gangliosides are glycosphingolipid structures found extensively through the body, (Yuki *et al*, 1993c; Sheikh *et al*, 1998) and are particularly concentrated in the nervous system (Leeden, 1995), and in the outer leaflet of synaptic membranes (Simons and Ikonen, 1997). They consist of a hydrophobic ceramide "tail" lodged in

the lipid cell membrane, and an extracellular hydrophilic carbohydrate backbone to which sialic acids are attached. The constitution of the carbohydrate varies, as does the number and position of the sialic acid residues, allowing gangliosides to be identified using the widely recognised Svennerholm nomenclature. Firstly, the number and position of the sialic acids on each ganglioside are named as M, D, T or Q corresponding to: mono, di, tetra or quadra-sialosyl groups. A number from 1 to 4 then follows, and this describes the biosynthesis of the carbohydrate backbone. Thus, gangliosides lacking the terminal galactose, galactosyl-N-acetylgalactosamine or internal galactose are assigned the number 2, 3 or 4, respectively. Finally, the position of the sialic acid groups on the backbone are described using a, b, or c and this correlates with the biosynthetic pathway. Most b group gangliosides have disialosyl gangliosides on the internal galactose (with the exception of GM1b) and c group have three internal sialic acids on the internal galactose. This nomenclature is preceded by the letter G, corresponding to “ganglio-series” ganglioside (figure 1.6).

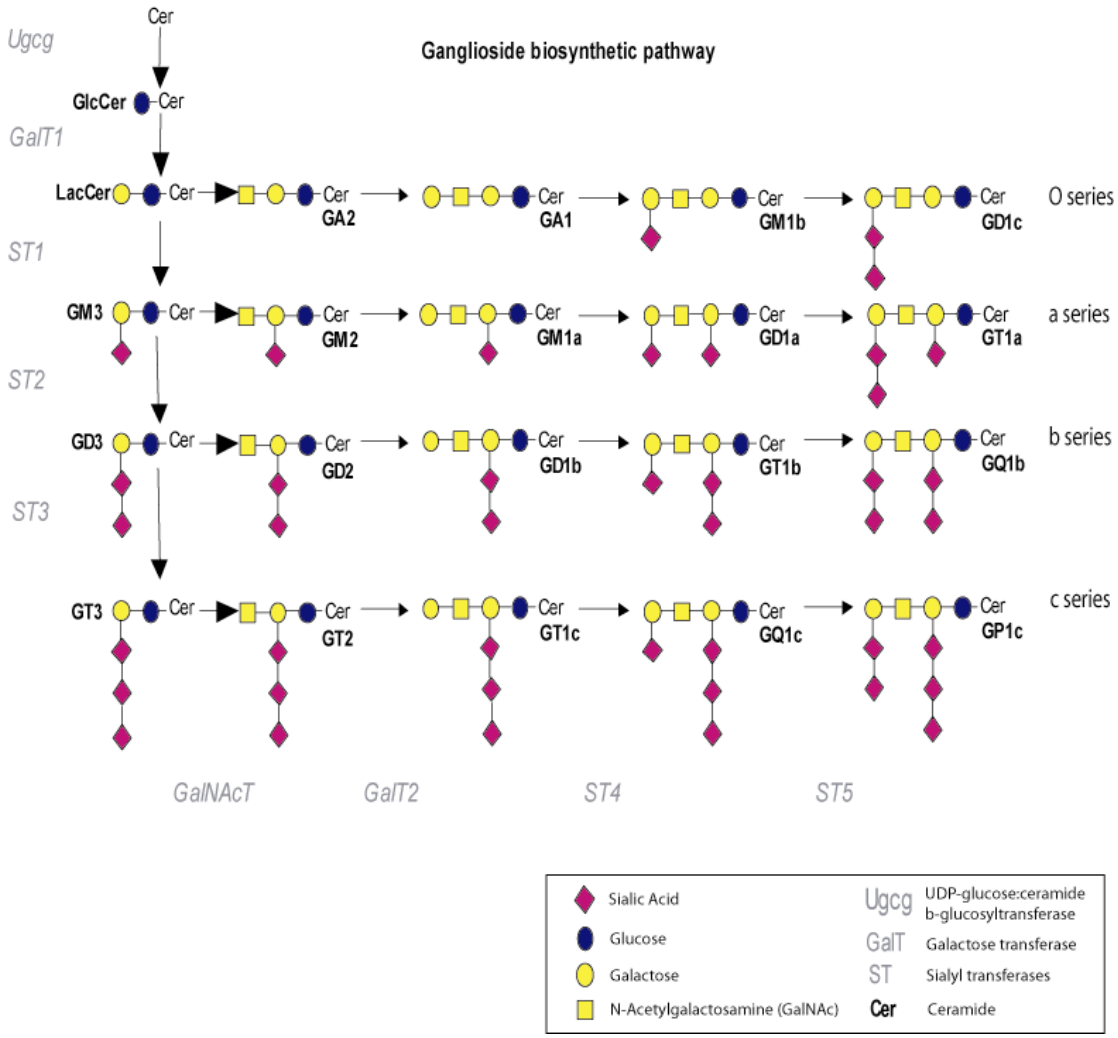

Figure 1.6: Summary of ganglioside biosynthetic pathway.

Thus, a ganglioside with a full carbohydrate "backbone" of galactose, galactosyl-N-acetylgalactosamine, and the internal galactose, with a disialosyl group on the internal glucose would be named: GD1b

1.2.1.2 Ganglioside biosynthesis

Using the Svennerholm nomenclature, the pattern of ganglioside biosynthesis is easily understandable. All gangliosides share a common ceramide, hydrophobic tail that is lodged in the cell membrane. A glucose molecule is added to this by UDP-glucose:ceramide b-glucosyltransferase to form glucosylceramide (GlcCer). A galactose molecule is then added to the structure by galactose transferase to form lactosylceramide (LacCer). This forms the structural backbone of all other gangliosides.

From here, the sialic acids are added to the first, internal galactose molecule by sialyl transferases (ST1-3) to form GM3, GD3 and GT3, respectively. These new gangliosides comprise the first molecules in the a-c series. The molecule then receives a GalNAc residue (using GalNAc transferase) to expand the carbohydrate backbone. A further galactose is added if necessary by galactose transferase, and remaining sialic acid residues are added to the terminal galactose by sialyl transferases where appropriate.

The exact location of these synthetic enzymes is not clear, with variability seen between cell types, and actual gangliosides. However, it has been shown experimentally, using pharmological manipulation, that manufacture of simple gangliosides such as GM3 and GD3 occurs in the proximal Golgi apparatus (Young *et al*, 1990). GalNAcT has also been shown in the trans-Golgi apparatus (Giraudo *et al*, 1999), and it is therefore likely that GM2 and GD2 are synthesised here. Often, enzymes are closely associated along gradients in the Golgi, to ensure efficient

transfer of molecules, and synthesis. This is seen in particular with GalNAc T and Gal T2 (Giraudo *et al*, 1999). However, it should be noted that this arrangement is not static, and can vary between cell types making biosynthesis a very complex arrangement.

There are approximately 50 distinct gangliosides found throughout the body that are synthesised from monosaccharides in the Golgi apparatus using glycosyltransferases. They are usually located in "lipid rafts" with soluble N-ethylmaleimide-sensitive factor attachment protein receptor (SNARE) proteins in the plasma membrane, and are particularly concentrated at NMJs, amongst other sites (Chamberlain *et al*, 2001).

The distribution of gangliosides throughout the nervous system is not uniform as less complex ganglioside structures, such as GM1, are found in the spinal cord, particularly the cauda equina (Ogawa-Goto and Abe, 1998) while complex gangliosides are more commonly found in the motor cranial nerves (Chiba *et al*, 1993, Chiba *et al*, 1997). This results in a cranio-caudal reduction in ganglioside complexity through the spinal cord.

Although the exact role of gangliosides at the synapse is not clear, studies suggest that they can modulate long-term potentiation of the synapse (Furuse *et al*, 1998), influence ion-channel function (Kappel *et al*, 2000), and their addition to incubation baths can cause an increase in synaptosomal neurotransmitter release (Ando *et al*, 1998). Also, in the disease botulism, a paralytic illness caused by a neurotoxin from *Clostridium botulinum,* gangliosides are believed to act as presynaptic ectoacceptors for the toxin, whose incorporation into the presynaptic terminal results in blockade of

ACh release, and paralysis (Schiavo *et al*, 1992). In addition to their role in nerve terminal function, gangliosides also therefore act as targets for paralytic disease in the peripheral nervous system (PNS).

1.2.1.3 Anti-ganglioside antibodies

1.2.1.3.1 Background

Early work highlighted an association between benign monoclonal gammopathies and certain late onset neuropathies, when patients displaying strong IgM antibody titres to myelin associated glycoprotein (MAG) often had characteristic patterns of peripheral neuropathy (Kyle, 1992). Patients with classical MAG related neuropathy usually present with a chronic, progressive, primarily sensory demyelinating neuropathy, characterised by an early onset upper limb tremor (Nobile-Orazio *et al*, 1994). *Ex vivo* studies, and also nerve biopises have shown both immunoglobulin deposition and complement activation products (van den Berg *et al*, 1996) associated with chronic demyelination and secondary axonal degeneration, supporting an antibody-mediated effect.

Later studies also support the hypothesis that anti-ganglioside antibodies are capable of producing neuropathy, by demonstrating a correlation between neuropathy and antibodies to other structures within the PNS including sulfated glucuronyl paragloboside (SGPG), which shares many similar antigenic structures to MAG and gangliosides such as GM1 (Quarles and Weiss, 1999). Also, other anti-ganglioside antibodies have been associated with types of neuropathy, including those to Gal(ß1-

3) GalNAc-bearing glycolipids; or NeuAc (α2-8) NeuAc (α2-3) Gal-configured disialylated gangliosides (Léger *et al*, 2001; Willison *et al*, 2001). Additionally, there is a strong association between GQ1b antibody and MFS (Chiba *et al*, 1993; Willison *et al*, 1993a).

These illnesses give insights into ganglioside distribution in the body, by association with clinical symptomatology. For example, anti-GD1b antibodies can produce a sensory neuropathy, and have been shown to bind to the ventral roots in preference to the dorsal roots (Willison and Yuki, 2002) especially in the head and neck. In addition, the node of Ranvier has been identified as a possible source of injury in the variants of GBS possibly causing both demyelination and axonal degeneration. Gangliosides have been identified on both the axolemma (Ganser *et al*, 1983) and paranodal structures while anti-ganglioside antibody binding has been demonstrated to structures at this site (Molander *et al*, 1997; Willison *et al*, 1996).

However, it should be noted that ganglioside distribution doesn't necessarily correlate with clinical phenotype as both anti-GM1 and anti-GD1b antibodies bind to neurones in the dorsal root ganglia, but only anti-GD1b antibodies are associated with sensory neuropathies, (Maehara *et al*, 1997; O'Hanlon *et al*, 1998). Ganglioside location is clearly important, but other factors may be responsible for clinical presentation in certain cases.

1.2.1.3.2 Antibody production

Although the antibodies may be implicated in the disease, the process that results in the production of antibodies has yet to be elucidated. A recent study examined the incidence of 16 common infections occurring shortly before the onset of GBS, with *Campylobacter jejuni*, cytomegalovirus and Epstein Barr virus being the most common (Jacobs *et al*, 1998). However, other studies have shown that GBS is preceded by a variety of infections. On this basis, it is now clear that many cases of GBS are preceded by an insult to the immune system. Often, these antibodies arise through a process of molecular mimicry.

The process of molecular mimicry is clearly seen with the evolution of MFS following *Campylobacter* infection (Endtz *et al*, 2000). In response to this enteric infection, the body generates an immune response to lipooligosaccharides (LOS) and the outer core oligosaccharides of lipopolysaccharide (LPS) on the bacterial coat of *Campylobacter jejuni* (Boffey *et al*, 2004). These LOS glycan structures are structurally similar to gangliosides (Yuki *et al*, 1993b; Sheikh *et al*, 1998), and it is thought that the resulting antibodies bind these gangliosides in addition to the bacterial epitopes (Ang *et al*, 2004; Goodyear *et al*, 1999). However, less than 1% of all *Campylobacter* infections result in GBS, therefore these LOS structures alone are not sufficient to produce a response (Nachamkin, 2001).

Detailed immunological characterisation of the antibody response is confusing, and does not appear to identify a clear method of antibody generation. There are two main cell types in the immune system: B-cells and T-cells. It has been widely accepted that

T-cells control much of the activity of B-cells, as B-cell activation usually requires antigenic protein binding to immunoglobulin on the surface of a subclass of B-cell (follicular dendritic B-cell), in association with antigen specific T-cell co-stimulation using ligand complexes and cytokine release. These newly activated B-cells either become quiescent memory cells, or plasma cells in the circulation.

However, an earlier mechanism of B-cell activation exists that is independent of T-cell function. In this pathway, subsets of B-cells (B1 cells, and marginal zone B-cells) found particularly in the pleural and peritoneal cavities, can activate independently to produce both IgA and IgM antibodies to respond early to infection (Fagarasan and Honjo, 2000), particularly with lipopolysaccharide expressing bacteria (Kearney *et al*, 1997).

Early mouse anti-ganglioside antibodies were generated from a T-cell independent mechanism. In these studies, mice immunised with ganglioside, or LPS devoid of disialosyl structures, produce IgM and IgG3 antibodies at low levels, in a manner that is consistent with activation of the innate B-cell pool. This suggests that B-cells exist in these pools, and can be polyclonally activated and amplified in response to antigen. Although these responses are weak, it is still possible to clone these antibodies for further study (Goodyear *et al*, 1999).

Further characterisation of these antibodies confirms their T-cell independent origin. Work shows that the antibodies are of relatively low affinity, and are also polyreactive antibodies arising from unmutated V genes, without undergoing affinity maturation (Boffey *et al*, 2004). Despite their polyreactive nature, these antibodies do show

selective binding to polysaccharide structures, and could possibly cause injury in the nervous system (Boffey *et al*, 2005). Indeed, it has been proposed that activation of naturally occurring anti-ganglioside antibody from the innate B-cell pool may cause proliferation and pathologically elevated levels of antibody, causing neuropathy. Similar mechanisms of activation occur as an immediate response to other infections' (Snapper *et al*, 1994; Fagarasan and Honjo, 2000).

However, human work suggests that anti-ganglioside antibodies causing MFS, AMAN and other forms of GBS belong to the IgG1 and IgG3 subtypes (Vedeler *et al*, 1988; Willison and Veitch, 1994; Ogino *et al*, 1995). This suggests that the cells arise from B2 cells, which is consistent with a T-cell dependent response to an antigenic protein, most likely the LOS glycans on the coat of *Campylobacter*. This produces high affinity, specific antibodies that are particularly efficient at activating complement.

Further evidence to support a T-cell dependent pathway in the human was seen from studies using a cloned antibody to the GM1 ganglioside. In this example, the genes were encoded by both diverse, and closely related V genes, some of which exhibited somatic mutation (Paterson *et al*, 1995). The authors suggest this is consistent with an antigen driven immune response, as expected with a T-cell dependent pathway. Other work from using IgM antibodies cloned from a patient with CANOMAD (chronic ataxic neuropathy with ophthalmoplegia, IgM paraprotein, cold agglutinins and disialosyl antibodies) also described somatic mutation and similar gene families, consistent with a T-cell dependent origin (Willison *et al*, 1996) that would produce high affinity, specific antibodies.

The mechanism of antibody generation in the human, and mouse is clearly very different. Although the reason for this difference is not entirely clear, it may reflect the nature of antigen exposure in both groups. In the mouse model, the animal is exposed to a high concentration of antigen very acutely, and this may result in a T-cell independent response. In the human however, exposure to antigen (from the infection) is more chronic, and prolonged, which may result in the T-cell dependent response.

1.2.1.4 Immunological tolerance

The mechanism behind the generation of anti-ganglioside antibodies in the human is further complicated by the concept of "immunological tolerance". Gangliosides are found throughout the body, and most people have low levels of antibodies to gangliosides circulating as natural innate defence against microbial infections (Casali and Schettino, 1996). These antibodies exist in low levels, possibly the result of immunological "tolerance", and do not produce any apparent neuropathy. A failure of this process may account for the high levels of antibody seen pathologically.

The exact mechanism behind this immunological tolerance is unknown, but it is believed that B-cells from the spleen and bone marrow are capable of detecting, and developing tolerance for, gangliosides within the tissues and circulation, but not necessarily when sequestered in the nervous system.

This is supported by experiments where knock-out mice that are deficient in complex gangliosides, are inoculated with the oligosaccharide coating from *Campylobacter jejuni* (which is structurally similar to gangliosides). These mice generate an anti-

ganglioside antibody response far greater than expected from their wild-type controls. These antibodies are also generated in a T-cell dependent manner (Bowes *et al*, 2002). It suggests that, under normal conditions, the presence of complex gangliosides limits the immune response, as the host animal does not recognise inoculated oligosaccharides as foreign. For some reason, there is a breakdown of this tolerance following infection, resulting in a vigorous immune response throughout the body, but especially in the nervous system where the high levels of antibody produces neuropathy.

Detailed studies continue in this area, to develop a greater understanding of the exact mechanisms behind anti-ganglioside antibody production, and eventually develop techniques to interrupt this process that will possibly offer another therapeutic option in the disease.

1.2.1.5 Detection methods

One of the limitations of studying anti-ganglioside antibodies is the relative difficulty in their assay. Indeed, a number of factors exist that vary between laboratories, including source of antigen, handling of sera, and diagnostic criteria which make inter-laboratory comparisons difficult. Although attempts have been made to standardise current assay techniques (Willison *et al*, 1999), the sampling method (ELISA) may itself have inherent difficulties. For example, previously seronegative samples can show mildly positive titres if other molecules (for example, phosphatidic acid) are present on the ganglioside ELISA plate (Kusunoki *et al*, 2003). This suggests that anti-ganglioside antibodies have the capability to bind to complexes of

structures, rather than single ganglioside structures in isolation. This was supported by a recent study using sera from patients, where the anti-ganglioside antibodies bound at the interface between two ganglioside species (Kaida *et al*, 2004). As a result, it may be difficult to correlate clinical disease with antibody sub-species if they are tested in isolation on ELISA.

1.2.1.6 Experimental evidence

However, before anti-ganglioside antibodies can be confirmed as the cause of injury in GBS, the Witebsky's postulates must be satisfied (Rose and Bona, 1993). These state that a disease can be classified as autoimmune if:

1) There is evidence of an autoreactive process (ie molecular mimicry)
2) There is a specific autoantigen
3) The disease can be reproduced using an animal model
4) The disease can be passively transferred to an animal model.

The autoreactive process (molecular mimicry) has been described previously (Endtz *et al*, 2000) in GBS, and confirms the first postulate. Aside from this, it has been very difficult to confirm or refute the other postulates, particularly in the human. However, other investigators have provided indirect evidence, and have also performed animal studies that offer compelling evidence to support the autoimmune nature of injury.

An example of this includes research into the role of gangliosides as a method of directing chemotherapeutic agents towards malignant tissue. Mouse anti-GD2

antibodies were used to target neuroectodermal tumours that are rich in ganglioside GD2. Two of the patients in this clinical trial then developed a sensorimotor polyneuropathy (Saleh *et al*, 1993), and resulting *ex vivo* binding studies using this antibody then showed strong binding to peripheral nerve myelin (Yuki *et al*, 1997), possibly explaining the pathogenesis of the neuropathy. In this study, anti-ganglioside antibodies were, in effect, passively transferred to the patient, and induced a clinical disease (sensorimotor polyneuropathy).

Evidence to support the existence of an autoantigen is seen with AMAN patients who express high titres of antibodies in GM1. Firstly, ganglioside GM1 was shown to be present at the node of Ranvier by cholera toxin binding studies (Sheikh *et al*, 1999). Autopsy studies from patients with AMAN expressing high levels of GM1 showed immunoglobulin and complement binding to the nodes of Ranvier, and paranodal structures (Hafer-Macko *et al*, 1996a). The strong correlation suggests that anti-ganglioside antibodies are binding to GM1 at this site. Although there have been limited studies demonstrating conduction block at the node of Ranvier, it is widely believed that it is the site of injury in anti-GM1 related disease (Willison and Yuki, 2002), thus implicating the ganglioside in the disease pathogenesis, and making it a likely candidate as an autoantigen. This study is supported by work in the rabbit. In this example, rabbits were immunised with bovine brain ganglioside. These animals then produced high titres of anti-GM1 antibodies, and subsequently developed a flaccid paralysis. Post-mortem analysis also demonstrated pathological changes similar to AMAN, and this is strong evidence for an animal model of the disease (Yuki *et al*, 2001), while also supporting the possibility of gangliosides as autoantigens.

Interestingly, while anti-ganglioside antibodies can induce a polyneuropathy in humans, it has been extremely difficult to induce clinical disease in animal models using serum from patients. Aside from the obvious species difference, it is also difficult to break down the blood-nerve barrier in these experimental animals to allow antibody access to the potential sites of injury. While the other postulates have been proved, it remains difficult to absolutely confirm the autoimmune basis of GBS pathogenesis as a result (Sheikh and Griffin, 2001).

1.2.1.7 Other hypotheses

Other theories also exist as to the mechanism of injury in GBS. One such theory suggests that *Campylobacter* infection produces a non-specific activation of B-cells to produce IgM rather than high affinity, class-switched IgG. This is unlikely in GBS, but may be present in chronic neuropathies (Willison and Yuki, 2002).

Another hypothesis identifies T-cells as the cause of injury and inflammation in the PNS, based in part on studies that have shown T-cell infiltration in cases of AIDP (Hughes *et al*, 1992a,b). One of the first animal models of AIDP, called experimental autoimmune neuritis (EAN), was developed in 1955 in rabbits. In this disease model, rabbits were inoculated with either ground sciatic nerve or spinal ganglia, and after 2 weeks developed a progressive, acute flaccid paralysis associated with degeneration of peripheral nerve myelin. However, the pattern of this degeneration was variable, ranging from simple myelin degeneration to complete destruction of the Schwann cell, and its associated axon (Waksman and Adams, 1955). Although the authors couldn't identify the exact pathological mechanism behind this injury, they felt this

model shared a number of similarities with human forms of peripheral neuropathy, and may be a suitable experimental model for the human disease.

Later work using rabbit, and also rats inoculated with myelin or its components e.g. P0, P2 and PMP22, suggested these structures may be antigenic targets, and resulting demyelination was the result of a T-cell mediated injury (Kadlubowski and Hughes, 1979; Linington *et al*, 1992; Gabriel *et al*, 1998) in AIDP. This was further supported by studies examining the effects of transferring CD4+ T-cell lines, which caused demyelination in a timescale that is not compatible with an antibody response (Linington *et al*, 1984). It is thought that this T-cell response to myelin antigens then directs macrophages to the site of injury, to cause demyelination. Interestingly, while the predominant cell type in the T-cell response bears αβ receptors on the surface, a small proportion of cells have γδ receptors, whose antigen presenting molecules are CD1. These molecules are upregulated in GBS, and may recognise non-protein antigens including glycolipids. This may explain the antibody response in cases of AIDP (Hughes *et al*, 1999).

However, it was shown elsewhere in both rat and rabbit that EAN serum could cause demyelination when passively transferred between animals by intraneural injection, and that this injury was primarily based on an antibody-mediated, complement dependent injury (Saida *et al*, 1978). Later work in rat sciatic nerve using passive intraneural transfers of antibody to galactocerebroside (GalC) also supported this observation (Saida *et al*, 1979a), as did work using cell cultures (Saida *et al,* 1979b). The role of anti-GalC antibodies is however controversial, and it has been argued that they represent a secondary phenomenon, unrelated to the pathogenesis of EAN

(Susuki *et al*, 2004), in particular because antibodies to GalC are rarely seen in human GBS, with the exception of those associated with *Mycoplasma pneumoniae* infection (Hughes and Cornblath, 2005). It is possible in this model that both T and B-cell responses co-exist, with the T-cells initially recognising an antigen in the endoneurial compartment, before opening the blood-nerve barrier to allow antibody to access the nerve itself, and produce injury (Hughes *et al*, 1999).

Also, some workers suggest that the initial infection may itself attack and injure the nerve, or nerve injury results from a post infection autoimmune response. While this is unlikely for bacterial infections such as *Campylobacter*, viral infections with CMV may acquire gangliosides from cells during infections, and thus invoke an immune response.

1.2.2 Role of complement

1.2.2.1 Complement Activation

Early work has shown complement in close association with nerves and demyelinated areas in patients with GBS (Luijten *et al*, 1972), and samples of serum and CSF taken during the acute phase of the illness have demonstrated higher than expected concentrations of complement proteins including membrane attack complex (Tonnessen *et al*, 1982; Sanders *et al*, 1986). These clinical findings therefore suggest that antibodies may produce injury in GBS through a complement dependent process. Although anti-ganglioside antibodies have been shown to have influence NMJ quantal release independently in the mouse (Buchwald *et al*, 2002), certain anti-ganglioside

antibodies can produce significant NMJ injury in the presence of a source of serum, due to activation of the complement cascade (Halstead *et al*, 2006b).

Complement was first described in 1898 by Jules Bordet (Bordet, 1898) and later characterised in 1899 by Ehrlich and Morgenroth as a heat-sensitive component of serum that could kill bacteria in conjunction with antibody (Silverstein, 2001; Ehrlich and Morgenroth, 1899). In addition to its bactericidal properties, complement has other functions in the body, including acting as a stimulus to inflammation by causing degranulation of mast cells and basophils via C3a and C5a. These can also produce smooth muscle contraction, and increase vascular permeability, which are all important in the inflammatory process. Complement can also activate neutrophils, and cause their chemotaxis (C5a); solubilise circulating immune complexes to prevent injury to capillary beds (C3b, CR1); and permit the opsonization of bacteria and fungi to allow their subsequent phagocytosis (C3b, C4b) (Walport, 2001b)

Complement can also produce injury at the cellular level by the "complement cascade". This cascade consists of three different pathways that recognise different activating antigenic "targets"; amplification enzymes to increase the effect of the initial target substance, and the final common pathway resulting in the formation of membrane attack complex (MAC).

The "classical" pathway was the first to be described, and results from antibody binding to antigenic targets on the cell surface, activating complement components C1-C9. Antibody binding to the antigenic surface results in the activation of enzyme C1, which then undergoes a conformational change and cleavage of its 4 intrinsic

polypeptide chains. One of these chains (C1s) then cleaves C2b from the membrane bound C4b-C2 complex. The resulting C3-convertase complex then produces C3b.

The “alternative” pathway is more complex, and involves binding of circulating C3b to the cell membrane, which then binds Factor B. This process can be initiated by either circulating immunoglobulins (IgA or IgE), or non-immunological means e.g. particulate polysaccharides (bacterial LPS, yeast, fungi etc). Circulating Factor D then cleaves Factor B into Ba and Bb. The resulting C3Bb complex acts as a C3 convertase to produce C3b.

The other pathway in the complement cascade is known as the Mannose-Binding Lectin pathway. This process is similar to the “classical” pathway, and uses mannose-binding lectin-associated proteases 1 and 2 (MASP1 and MASP2) from the liver to bind to arrays of mannose groups on the bacterial cell surface, and activate C3 or its convertase enzyme. MASP2 activation is thought to lead to the formation of the C3 convertase enzyme, while MASP1 is thought to cleave C3 directly. This leads to further activation of the cascade in a manner similar to the classical pathway. The end result of these pathways is the formation of C5 convertase enzyme, which cleaves C5 to form C5b and is used to form MAC (Walport, 2001a). These pathways are summarised in figure 1.7.

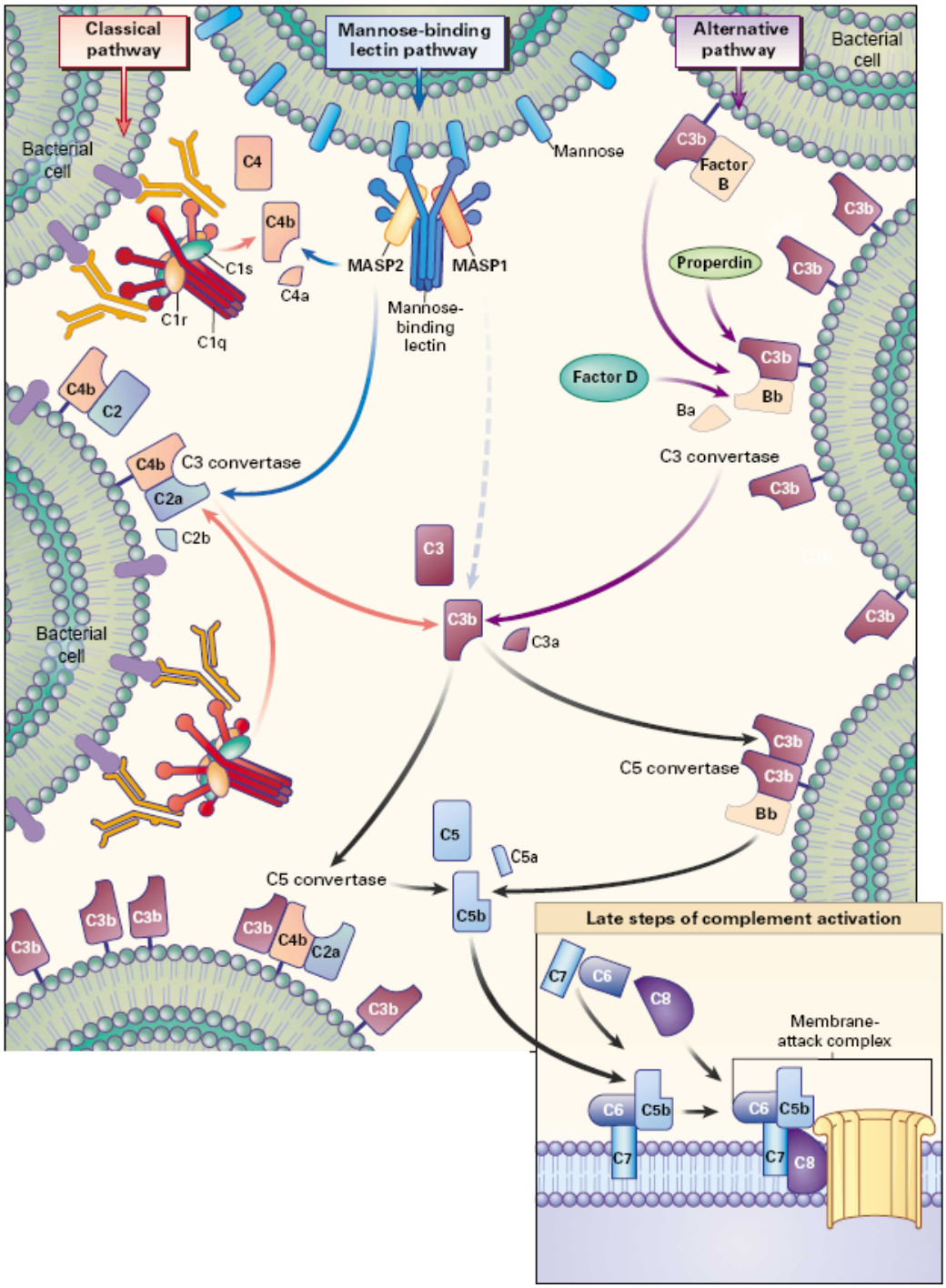

Figure 1.7: Summary of complement cascade.

The Classical, Mannose-Binding-Lectin, and Alternative pathways are shown. In the classical pathway, antibody is seen to bind to the surface of a bacterial cell, with activation of complement products C1-C9 to form MAC. The alternative pathway is also shown, with C3b binding to the

bacterial cell before assembling MAC through a complex series of enzymatic reactions (taken from Walport, 2001).

1.2.2.2 Membrane Attack Complex

MAC is a complex molecule, comprising complement molecules C5b-C9. Although C5b-8 is crucial to the formation of MAC, it is thought that the initiating step of MAC formation is insertion of the C9 molecule into the cell membrane. C9 is an amphipathic molecule that binds to the C5b-8 complex, and inserts through the cell membrane before polymerising to form a transmembranous "pore". The classic "tube-like" structure of MAC usually contains between 16-18 C9 molecules but it is believed that C9 can produce membrane disruption in smaller numbers (one or two C9 molecules) by forming functional, rather than structural pores (Podack and Tschopp, 1984; Bhakdi *et al*, 1991). Functional disruption in the absence of structural "tubes" seen with small numbers of C9 molecules led to the "leaky patch" hypothesis of MAC action. In this hypothesis, C9 insertion into the membrane was thought to disrupt membrane integrity but true, discrete channels were not formed (Esser, 1991). However, the former hypothesis of structural tube formation is currently more widely accepted (Cole and Morgan, 2003).

Interestingly, MAC is not exclusively cytotoxic, and in certain conditions, can act to preserve cells by inhibiting apoptosis, or protecting against lysis. Although MAC has been implicated in Schwann cell injury in GBS (Putzu *et al*, 2000), studies have shown that sub-lethal levels of MAC can actually induce proliferation of Schwann cells in culture (Dashiell *et al*, 2000; Hila *et al*, 2001) and thus may be involved in

Schwann cell recovery following injury. The role of complement on Schwann cells is clearly an interesting area for further study.

1.2.2.3 Complement regulators

In order to limit damage to host tissues from the indiscriminate activation of the complement cascade, regulators exist on cell membranes to minimise injury: membrane cofactor protein (MCP or CD46), decay-accelerating factor (DAF or CD55) and CD59 (Miwa and Song, 2001). MCP acts as a cofactor for serum protease factor I to cleave the C4b and C5 convertase (Brodbeck *et al*, 2000), while DAF limits both C3 and C5 convertase assembly on cell surfaces by limiting their assembly, and accelerating their decay (Hourcade *et al*, 1999). CD59 acts by inhibiting the formation of MAC pores by preventing insertion of C9 into the C5b-8 complex, inhibiting cell lysis (Davies *et al,* 1989). Mouse models deficient in these regulators have been developed to understand their contribution to complement-mediated disease, including nephritis (Lin *et al,* 2004) and paroxysmal nocturnal haemoglobinuria (Holt *et al*, 2001).

Unlike humans who have only single genes, mice have two DAF (DAF1 and DAF2) and two CD59 (CD59a and CD59b) genes. DAF2 is a transmembrane anchored protein mainly expressed in testis and splenic dendritic cells, while DAF1 is a GPI anchored protein expressed in a number of cell membranes (Spicer *et al,* 1995). The distribution of the CD59 regulator genes (CD59a and CD59b) is broadly similar (Harris *et al,* 2003). Both DAF1 and CD59a are considered homologous for the human regulators, and they have been shown to regulate heterologous sources of

complement to an extent (Sun *et al*, 1999; Miwa and Song, 2001). As a result, strains deficient in these complement regulators are a useful tool for understanding the contribution of complement in anti-ganglioside antibody-mediated injury at the NMJ.

1.3 Neuromuscular Junction

1.3.1 Historical context

The NMJ has been under close scrutiny for over 150 years, having first been described by Wagner, Kuhne, Rouget and Krause in the latter half of the 19th Century (cited by Couteaux 1973). In the central nervous system, synapses often receive multiple inputs, and act as processors of data. However, the sole purpose of the NMJ appears to be the transmission of axonal action potentials into muscle fibre contractions, essentially acting as a conduit between two cell types.

1.3.2 NMJ transmission

Although the patterns of transmission at the NMJ are complex, the mechanisms have been described in great detail. Transmission occurs across a synaptic cleft, via ACh. This transmitter substance is stored in the axon in small packets, known as vesicles, which are released in response to action potentials in the axon. Each vesicle can contain between 5000-10000 molecules of ACh (Kuffler and Yoshikami, 1975). However, these vesicles also fuse with the axon membrane spontaneously, releasing their ACh into the synaptic cleft. Some of this ACh reaches the post-synaptic nicotinic-ACh receptors to produce sodium influx into the muscle, and a small

depolarisation (approximately 1mV) of the post-synaptic specialisation that is usually insufficient under normal circumstances to produce muscle contraction. This spontaneous release, known as miniature end plate potentials (MEPPs) was first described famously by Bernard Katz, in his studies of frog muscle fibres, and offered the first description of quantal release at the NMJ.

A proportion of these vesicles lie in clusters at the presynaptic nerve terminal cell membrane, in groups known as "active zones". During active contraction, an action potential from the axon depolarizes the NMJ, and opens voltage dependent calcium channels in the axonal membrane, causing a massive influx of calcium. A number of these calcium channels are believed to lie in close proximity to the "active zones" (Robitaille *et al*, 1993). Calcium-sensitive proteins anchor synaptic vesicles to the membrane, and cause vesicular release in response to calcium influx from the active zones (Sheng *et al*, 1998). A second group of ACh vesicles lies behind the "active zones", and are not involved in neuromuscular transmission under normal circumstances. It is thought that this second group acts as a reserve supply of ACh, to prevent transmission failure in response to high frequency activation of the nerve.

Active zones lie in direct opposition to the open areas of post-synaptic sarcolemmal folding, known as "junctional folds". Junctional folds are deep foldings within the post-synaptic area that are particularly evident in the mammal, and have a high concentration of ACh receptors at their apex. In mammals, the area of contact between the nerve and the post-synaptic specialisation is relatively small (particularly in comparison to the frog). To maximise the effect of neurotransmitter release, junctional folds increase the surface area post-synaptically, and thus increase the

number of available ACh receptors (Wood and Slater, 2001). Their location directly across from active zones also ensures maximum use of any released ACh, and establishes a high fidelity synapse. If a sufficient quantity of ACh therefore binds to post-synaptic receptors, and the resulting depolarization is sufficiently great, voltage sensitive sodium channels deeper within the post-synaptic specialisation will open, and produce a muscle action potential and contraction (figure 1.8).

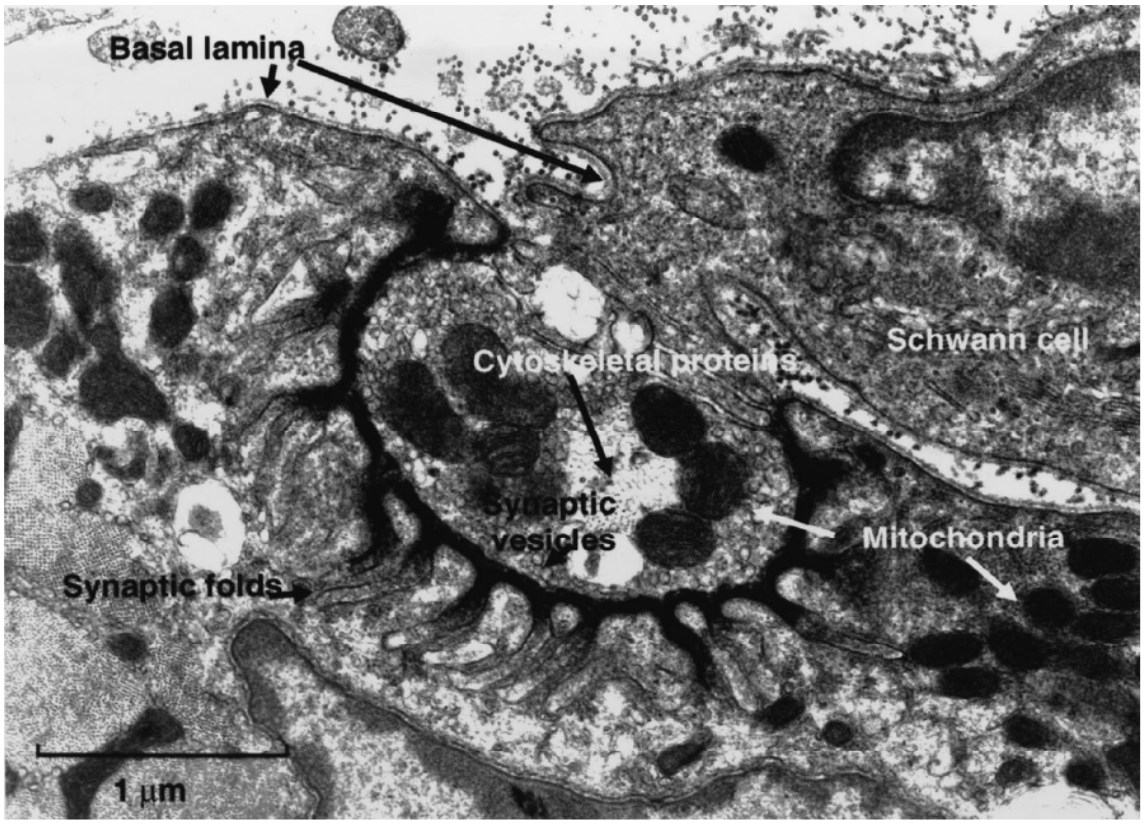

Figure 1.8: Electron micrograph illustrating the structure of a mouse NMJ. Synaptic vesicle and mitochondria are seen in the axon terminal, which lies in a depression on the surface of the muscle. The synaptic vesicles lie in an area adjacent to the synaptic folds. ACh receptors are stained with HRP-bungarotoxin, and are seen at the crests of the junctional folds. A TSC is

seen to cap the terminal (from Wood and Slater, 2001, and Lyons and Slater, 1991)

1.3.3 Age related changes

Once formed, the junction is not static and a number of changes occur with age. The synaptic structure gradually becomes more complex, with increasing branching patterns seen pre- and post-synaptically in most studies in the mouse. The amount of ACh released in response to an action potential also increases, to reach a peak at around 200 days in the mouse before starting to decline. Changes in junction structural complexity may be associated with these changes in ACh release, and while the amount of ACh released does decline with age, it is not sufficient to impair neuromuscular function to any noticeable extent (Wood and Slater, 2001).

1.4 Terminal Schwann cells

1.4.1 Background

Although previously considered a bipartite synapse comprising presynaptic nerve terminal and postsynaptic specialization, recent work has suggested that adjacent glial cells are functionally important at the NMJ (Araque *et al*, 1999). These glial cells, known as peri-synaptic or terminal Schwann cells (TSCs), were first described by Ranvier in 1878 as “arborisation nuclei”, and were thought to be responsible for branching during nerve development. It was only some years later that these nuclei

were identified as derivatives of Schwann cells, which “capped” the nerve terminal junction (figure 1.9) (Birks *et al*, 1960).

Figure 1.9: The morphology of the NMJ, as shown by scanning electron micrography.

The terminal axon is almost detached from the muscle surface, demonstrating grooving on the muscle surface (m) almost identical to the terminal axon. A TSC (s) is seen to overlie the terminal axon, with a capillary (c), pericyte (p) and adjacent nerve (n) lying nearby. (Taken from Matsuda, 1988)

During development, all Schwann cells arise from the same neural crest progenitor cells. These early Schwann cells migrate along nascent axons projecting to peripheral targets, to eventually wrap and segregate the axons or lie adjacent to NMJs. These cells differentiate during maturity depending on their location, morphology, or biological phenotype (Corfas *et al*, 2004).

Previously, distinction was made between Schwann cells based on their myelin expression. Many small calibre axons are encased in Schwann cells that do not express myelin, while thicker axons are often wrapped in several layers of a Schwann cell sheath containing large amounts of myelin. This allowed distinction between myelinating and non-myelinating Schwann cells. However, this distinction is not static, and it has been shown that Schwann cells are pleomorphic. In experiments, a non-myelinated radiolabelled section of nerve was grafted onto a regenerating myelinating nerve in an unlabelled animal, and with time, the radiolabelled Schwann cells adopted a myelinating phenotype (Aguayo *et al*, 1976a). A similar series of experiments demonstrated that Schwann cells can also lose their myelinating phenotype, and this process appears to be under the control of the regenerating axon (Aguayo *et al*, 1976b), possibly via neuregulin-1 signalling (Taveggia *et al*, 2005).

Interestingly, TSCs express many of the proteins found on other Schwann cells, including the low molecular weight, calcium binding protein S100 and P_0 Surprisingly, TSCs also express many myelinating cell markers, including MAG, 2',3'-cyclic nucleotide 3'-phosphodiesterase (CNPase), myelin galactolipid and galactocerebroside (GalC), and suggests that TSCs and myelinating Schwann cells are closely related (Georgio and Charlton, 1990). Despite these similarities, it is now

accepted that the TSC represent a third type of Schwann cell. This distinction was initially made on the location of these cells: overlying the NMJ, and capping the axonal branches at this site. However, they also express more neurotransmitter receptors, and have a greater variety of ion channels than other types of Schwann cell (Descarries *et al*, 1998; Robitaille *et al*, 1996). In their "quiescent" state, TSCs appear to detect, and possibly influence synaptic transmission through changes in intracellular calcium concentrations, while also influencing synaptic morphology. Under certain conditions (for example nerve injury), the cell can change its phenotype, under the influence of neuregulin, to become "reactive" and provide trophic support for the regenerating axon by producing processes that can guide axonal sprouts to adjacent junctions.

1.4.2 Role of terminal Schwann cells following nerve injury

1.4.2.1 Morphological and functional changes

Early work examined the NMJ following nerve sectioning and demonstrated that the TSCs, after axonal damage, became phagocytic and removed subsequent detritus in preparation for nerve regrowth (Miledi and Slater, 1970). During this process, the cells were also noted to move between the muscle fibre and nerve terminal to occupy the spaces vacated by the nerve, and synthesise the enzyme acetyltransferase (Miledi and Slater, 1970). The ACh subsequently produced by this process was then released to the muscle fibre, producing miniature endplate potentials in both the frog, and to a lesser extent, mammals (figure 1.10) (Reiser and Miledi, 1988; Miledi and Slater, 1970). It is unclear if release of this transmitter from TSCs has any role in maintaining

post-synaptic terminal function immediately following denervation. In the amphibian model, TSCs cells produce other neuronal transmitter substances, including nitric oxide and glutamate but again, their role remains unclear (Descarries *et al*, 1998; Pinard *et al*, 2003).

Figure 1.10: An end plate denervated at 12¾ hours.

This plate shows accumulations of high-density material, consisting of mitochondria, dense granular material of unknown origin, and degenerating axonal material. Muscle is shown (m) and processes from the TSC (Sch) are seen to extend into the synaptic cleft. (Taken from Miledi and Slater, 1970). Scale bar 1µm

Other functional changes occur in the cell following nerve injury, including increased muscarinic ACh receptor expression in the amphibious NMJ. (Robitaille *et al*, 1997). It has been demonstrated that other proteins, such as myelin basic protein, may alter the pharmacology of this receptor, suggesting the change in receptor expression may have functional significance (Tucek and Proska, 1995).

1.4.2.2 Molecular changes

Changes have also been shown to occur in the TSC's cytoskeleton with alterations in the levels of growth-associated phosphoprotein (GAP-43) and glial fibrillary acidic protein (GFAP). Alterations in these cytoskeletal components are believed to control the cell's response to neuronal injury.

Other molecules in the cell undergo changes depending on the cell state. Before the development of fluorescent proteins, markers were developed to better understand the changes that occur at the NMJ following denervation. One of these antibody markers, 4E2 bound strongly to the edges of the post-synaptic ACh receptor gutters, and elements of the contractile proteins of the muscle lying near the junctions (Astrow *et al*, 1994). However, following axonal injury, the TSCs also began to express the 4E2 phenotype and this was used as a marker for reactive Schwann cells in studies of axonal injury. Provisional data suggest the antibody may be binding to a component of the intermediate neurofilament, nestin, whose expression is upregulated following denervation (Son and Thompson, 1995a, Vaittinen *et al*, 1999).

1.4.2.3 Post-synaptic maintenance

TSCs have an important role in reinnervation of vacated end plates following axotomy. Axons have the capacity to regrow following incomplete axotomy. To facilitate this process, following partial denervation, the nerve is phagocytosed and the Schwann cells which previously wrapped the axon, regress to leave an endoneurial tube. The new axon then regrows along this tube, remyelination occurs, and the vacant end plate is reinnervated (Kang *et al*, 2003; Rich and Lichtman, 1989).

Rather than regress like their axonal counterparts, TSCs extend following denervation to enter the synaptic site previously occupied by the nerve. Eventually, a newly growing axon will enter the area occupied by the TSC and reinnervate the end plate in a process regulated by the TSC. Immunofluorescence studies have shown that if this process is delayed, there is a loss of post-synaptic ACh receptors, suggesting degradation in synaptic function (Trachtenberg and Thompson, 1996; Kang *et al*, 2003).

The exact reason for this post-synaptic degradation is unclear, but may be due to the changes in TSC morphology following denervation. Although it initially occupies a large proportion of the area vacated by the axon, the TSC begins to withdraw from this site to extend a fine network of cellular processes beyond the synapse to guide reinnervation (Reynolds and Woolf, 1992), leaving some postsynaptic areas "uncovered" and thus unstimulated by ACh (either from the TSC or reinnervating axon). This causes a loss of function in the "uncovered" areas.

It is thought that this loss of function arises through competition between active and inactive post-synaptic areas. This was first described during localised applications of bungarotoxin (an ACh receptor antagonist) to nerve terminals. When this toxin is applied to discrete areas post-synaptically, the "silent area" quickly begins to degenerate. This is thought to result from direct competition between active post-synaptic areas and sites that are electrophysiologically quiescent as a result of bungaratoxin application, although the mechanism of this interaction is not known. This hypothesis is supported by observations where bungarotoxin is applied across the whole end plate, and post-synaptic function is maintained as there is no direct competition within the end plate (Balice-Gordon and Lichtman, 1994). Thus, when TSC processes extend beyond the synapse, leaving areas of the post-synaptic apparatus uncovered and unstimulated, this will result in loss of Ach receptor area through competition with active areas.

1.4.3 Terminal Schwann cells and NMJ reinnervation

1.4.3.1 Complete axotomy

Processes extended beyond the junction by TSCs are often closely associated with regrowing axons, which extend beyond their newly innervated endplate along the TSC extensions (Reynolds and Woolf, 1992). This phenomenon was noted as early as 1944, when these axonal growths were described as "escaped fibres". Extensions from the TSC are thought to provide trophic support for these regenerating axons (Son and Thompson, 1995a,b). This is supported by *in vivo* studies where neurones have been shown to grow along newly formed Schwann cell processes. Live imaging

studies have also shown that the TSC extensions act as a "guide" for the regrowing axon, possibly via this trophic interaction (Bixby *et al*, 1988; Kang *et al*, 2003).

Schwann cell processes can meet similar processes from adjacent synaptic sites, or contact other end plates to form direct connections, and form "Schwann cell bridges". Often, an axon will grow across a bridge to reinnervate an adjacent, vacant end plate and then travel proximally through the end plate's endoneurial tube to grow down an adjacent fibre, and thus innervate further end plates (figure 1.11). If however, both the Schwann cell process and its axon fail to meet an appropriate synaptic site, and reinnervation is delayed, they both regress, stressing the importance of synaptic transmission on Schwann cell process formation (O'Malley *et al*, 1999).

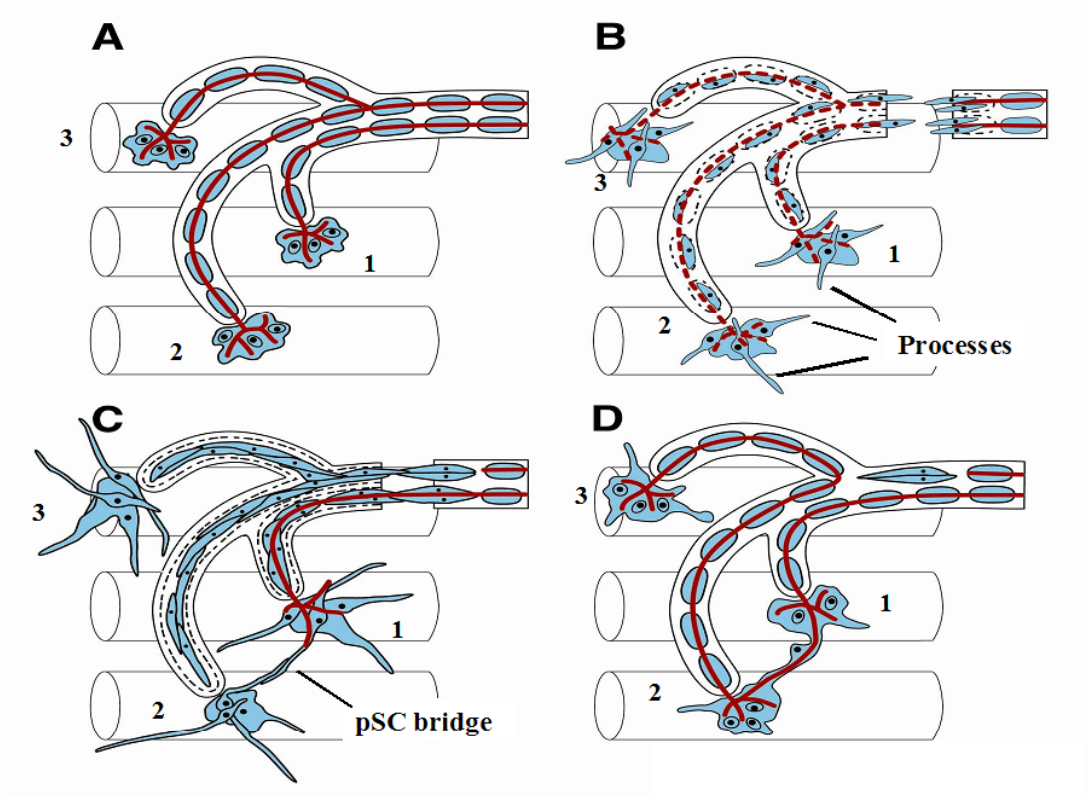

Figure 1.11: Cartoon illustration of changes to TSCs following denervation.

Following denervation, both myelinating and non-myelinating Schwann cells phagocytosed the nerve debris (B). The TSCs also begin to extend processes over the surface of the muscle. These processes can often connect, forming a Schwann cell "bridge" (C). This allows an axon that is reinnervating a single junction to cross this bridge, and innervate the remaining junctions (D). (From Kang *et al*, 2003)

Manipulation of synaptic transmission and muscle function can influence TSC process formation. For example, direct muscle stimulation can inhibit bridge formation between innervated and denervated end plates, as can exercise in extensively denervated muscles (Love *et al*, 2003; Tam *et al*, 2001). This has led the

authors of the latter study to suggest that increased neuromuscular activity is not recommended immediately following motor neurone injury, or early stage motor neurone disease. Inducing a presynaptic blockade with botulinum toxin however results in TSC process formation, but the resulting network is usually less complex and more disorganized than those extended during denervation (Son and Thompson, 1995). When botulinum is applied after denervation, the Schwann cell processes do not form bridges appropriately. Similar effects on process formation are also seen with alpha-bungarotoxin application (a post-synaptic blocker), implying that pre- and post-synaptic function are important in determining successful TSC process formation (Love and Thompson, 1999).

1.4.3.2 Incomplete axotomy

Another method of nerve regrowth facilitated by Schwann cells is known as "terminal sprouting". During incomplete nerve injury (e.g. nerve crush), both intact and denervated terminals coexist. The intact terminals can often extend an axonal outgrowth, called a "terminal sprout" to reinnervate adjacent synaptic sites, and static studies again suggest that Schwann cells facilitate this process. The TSCs from denervated end plates extend cellular processes towards "healthy" end plates, and induce an axonal sprout, which the Schwann cell process then guides to the denervated end plate (figure 1.12). It is thought that this process may be under the control of nitric oxide, generated post-synaptically from muscle fibres (Marques *et al*, 2006).

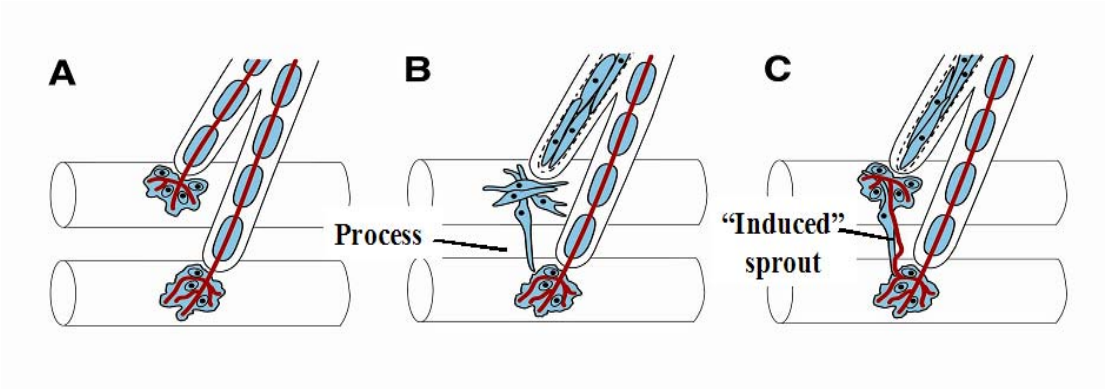

Figure 1.12: Cartoon illustration of TSC response to nerve crush.

In this example, two junctions are seen. Following axon loss from the upper junction, TSCs extend processes across the surface of the muscle (B). A process contacts an adjacent, innervated junction, and induces axon sprouting from this site. The axon sprout travels across the TSC process, and innervates the upper junction (C). (From Love and Thompson, 1999)

This mechanism of sprouting can lead to motor units that are significantly larger than their predecessors, often by as much as 6-8 fold, representing a capacity to compensate for the potential loss of over 85% of all motor units (Thompson and Jansen, 1977; Tam *et al*, 2001). Although functional muscle weakness is only evident when less than 20% of motor units remain intact, this degree of loss can occur in spinal cord injury and conditions such as amyotrophic lateral sclerosis and polio (Rafuse *et al*, 1992). Understanding and controlling Schwann cell function to regulate terminal regeneration may therefore be crucial to improving muscle function in these types of nerve injury.

1.4.3.3 Perisynaptic fibroblasts following axotomy

Ultrastructural analysis of the end plate following axotomy-induced denervation has also demonstrated cellular processes that are not associated with TSCs or axons. These stellate shaped cells, because they lack a basal lamina, and have a rough endoplasmic reticulum on ultrastructural analysis, are thought to be of fibroblast origin (figure 1.13a) (Gatchalian *et al*, 1989). These fibroblasts exist adjacent to the TSC, and produce extracellular matrix components that are considered important in nerve and muscle remodelling following denervation e.g. type I collagen, fibronectin and proteoglycans.

Following denervation, these cells proliferate and extend a network of processes across and around muscle fibres to form a "diaphanous veil" arising from the end plate which is thought to provide trophic support for both the muscle and regenerating nerve immediately following denervation (figure 1.13b) (Connor and McMahan, 1987). The cells arise through local proliferation, although the exact stimulus for this increase is unknown. No clear link has been established between this fibroblast network, and TSCs, but their shared role in axonal regeneration makes an association likely (Gatchalian *et al*, 1989; Reynolds and Woolf, 1992).

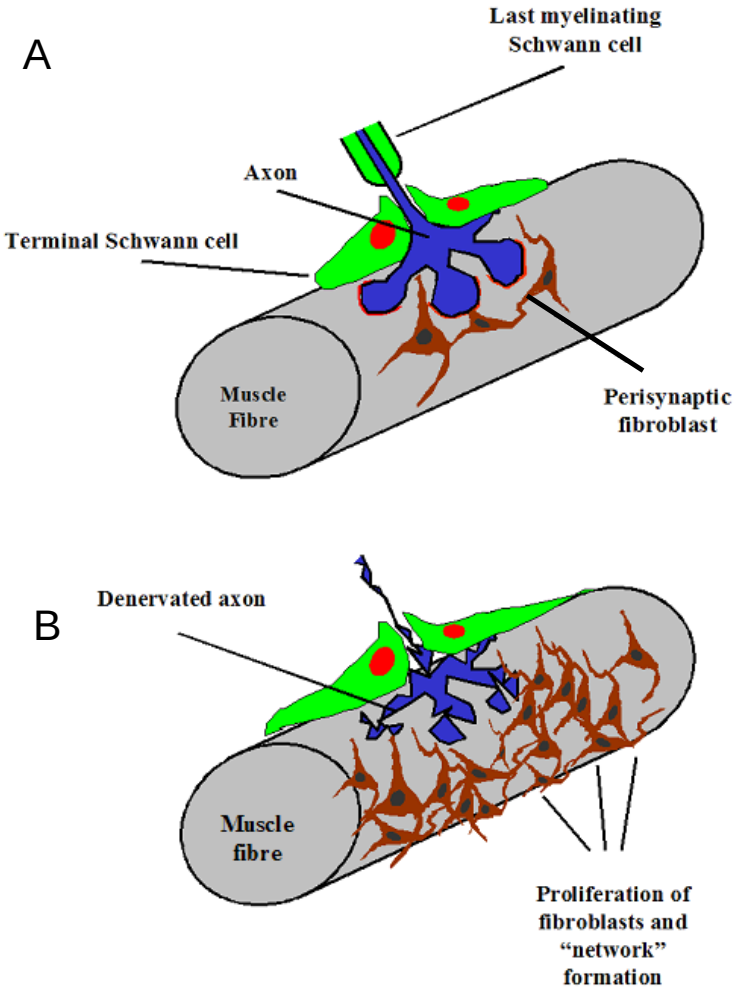

Figure 1.13: Cartoon illustration of fibroblasts at the NMJ.

The NMJ is shown in cross section. Stellate shaped fibroblasts lie over TSCs at the junction (not shown), and over the surface of the muscle around the NMJ (A). Following denervation, these fibroblasts proliferate and extend over the surface of the muscle fibre to form a complex network (B).

1.4.3.4 Synaptic remodelling

Interestingly, TSCs spontaneously extend and retract processes in a manner similar to denervation under normal conditions, although these rarely extend a significant distance beyond the junction or make contact with adjacent junctions. It is thought that these processes can provide trophic support for the axon, and result in subtle changes in end plate morphology over a period of time through competition between active and inactive zones, as described earlier (Lichtman *et al*, 1987). This is supported by *in vivo* studies from the frog, where limited TSC process extension is seen to precede axon growth and eventual remodelling.

1.4.4 Control of Terminal Schwann cell function

Despite learning much about the effects of TSC process formation, little is known about the control mechanisms or signals that result in their production. However, recent work has highlighted possible signalling molecules that may influence both Schwann cell process formation, and nerve terminal guidance.

1.4.4.1 Muscle Factors

Axonal sprouts exist during periods of muscle inactivity, whether induced pre or post synaptically (Pamphlett, 1989; Holland and Brown, 1980). Equally, sprouting is inhibited during periods of muscle activity, or when botulinum toxin induced sprouts are exposed to antibodies from antigens in inactive mouse muscle (Love *et al*, 2003; Grney, 1984). It is thought that sprout formation is the result of local factors released

from muscle, possibly insulin like growth factor II, or neural cell adhesion molecules (Caroni and Grandes, 1990; Gurney *et al*, 1986). A similar effect may exist between TSC processes and muscle derived factors.

1.4.4.2 Neurotrophins and neuregulins

A variety of neuroregulin and neurotrophin receptors also exist on the cellular components of the NMJ, and their distribution changes with different levels of synaptic activity (Auld and Robitaille, 2003). During axotomy-induced denervation, for example, the levels of low-affinity nerve growth factor receptor GAP-43 increase (Reynolds and Woolf, 1992).

Neurotrophins have also been implicated in TSC process formation. Neurotrophins represent a family of molecules that are secreted from a nerve's target area, and are thought to be responsible for promoting nerve survival, possibly by inhibiting axon apoptosis (Arevalo and Wu, 2006).

It is acknowledged that neurotrophin 3 (NT-3) expression, which occurs in muscle, is promoted by neurotransmission during development, allowing ACh receptor clustering (Loeb *et al*, 2002). However, recent work also suggests that NT-3, and its receptor TrkC (which is specific to the TSCs of neonatal and adult mice) may also be important in process extension, since selective inhibition of this signalling interaction can induce sprouting in a fashion similar to denervation. Also, process formation and sprouting were reduced when NT-3 was over expressed in muscle. These data suggest

that reduced NT-3 release from muscle, acting on TSCs via TrkC, may be an important limiting factor in TSC process formation (Auld and Robitaille, 2003).

Recent work suggests that neuregulins, particularly neuregulin-1, are important in the response of the TSC to injury. Neuregulin-1 (Nrg-1) is a series of alternatively spliced growth and differentiation factors that signal through the ErbB receptor tyrosine kinases, and whose levels are extremely concentrated within the synapse, and the synaptic basal lamina (Sandrock *et al*, 1995; Goodearl *et al*, 1995).

Although there are several genes that code for different classes of neuregulin, Nrg-1 is one of the best characterised and has been shown to be involved in cell migration, growth, survival and differentiation (Buonanno and Fischbach, 2001). Various isoforms of Nrg-1 exist, and studies of one variant, glial growth factor II (GGF2) have demonstrated that exogenous application can induce Schwann cell process formation, migration and proliferation in the developing rat (Trachtenberg and Thompson, 1997). This isoform can also protect rat TSCs from undergoing denervation induced apoptosis (Trachtenberg and Thompson, 1996).

However, receptors for Nrg-1 (ErbB) are also present on both the axon and muscle, therefore to confirm that Nrg-1 acts on the TSC, a Tet-On system was used to regulate a mutant constitutively active ErbB-2 receptor expressed on Schwann cells. This demonstrated that activation of the system induced process formation, and migration of the TSCs away from the junction, with associated axonal sprouting in a manner similar to early work with topical application of GGF2 (Hayworth *et al*, 2006). This

suggests strongly that neuregulin-1 is important in the response of Schwann cells to denervation.

1.4.4.3 GFAP

Another hypothesis developed in the frog implicates glial fibrillary acid protein (GFAP) as a TSC regulatory protein, acting via ACh. GFAP is a major glial intermediate filament protein that constitutes part of the glial cell cytoskeleton and is involved in a variety of functions (Galou *et al*, 1997). Approximately 11% of TSCs express GFAP under normal conditions, possibly due to muscarinic receptors on their surface that down regulate GFAP in response to ACh release at the nerve terminal (Georgiou *et al*, 1994; Georgiou and Charlton, 1999).

In the absence of ACh release at the nerve terminal, for example following axotomy, levels of GFAP expression increase to become detectable in 81-91% of all TSCs. This increase may act as a stimulus to process extension. Increase in GFAP expression can be inhibited when the transected nerve is electrically stimulated, and precipitated by blockade of the pre-synaptic calcium channels which govern ACh release. Local release of ACh from adjacent, intact end plates during partial denervation can also limit intracellular GFAP in denervated end plates, and prevent process formation (Tam *et al*, 2001). This interaction is only seen with ACh, and is absent with transmitters ATP, adenosine, and substance P.

1.4.4.4 GAP-43

Although the GFAP work has only been characterised in the amphibian model, changes have also been shown to occur in the TSC's cytoskeleton in the mammal. In particular, levels of growth-associated phosphoprotein (GAP-43) are shown to increase in the TSC following denervation. GAP-43 is associated with neurite production and may be implicated in the TSC process formation following denervation as a result (Woolf *et al*, 1992).

1.4.5 Neuromuscular transmission

1.4.5.1 Detecting synaptic transmission

The TSC appears to be very important in controlling the response to nerve injury, but it is also an active partner in synaptic function (Araque *et al*, 1999). Using marker dyes that become fluorescent in the presence of calcium, it was shown that the concentration of calcium within the TSC derived from intracellular stores increases during high frequency stimulation of the NMJ, but is greatly reduced when transmitter release is blocked. Further, when ACh or muscarinic agonists are applied, similar calcium transients were observed, that diminished in the presence of atropine. Although this represents a muscarinic response, purinergic stimulation with adenosine through A1 (adenosine) receptors can also produce a calcium response. This response is partially blocked by A1 antagonists and therefore suggests that endogenous adenosine may have a limited role in TSC activation.

Interestingly, while ATP can also produce a calcium response in the TSC, possibly via P2x and P2y receptors, A1 receptor antagonists did not impair the effect of ATP, suggesting the involvement of an ATP metabolite other than adenosine in this process. These effects are similar in the more primitive amphibian preparations (Jahromi *et al*, 1992; Georgiou *et al*, 1999; Rochon *et al*, 2001).

1.4.5.2 Altering synaptic transmission

In addition to detecting synaptic transmission, experiments suggest that transient calcium changes within the TSC can influence the nerve terminal itself. In the amphibian model, stimulating calcium release from the intracellular stores of the TSC via thapsigargin (an inhibitor of calcium-ATPase pumps) increased the end plate potential amplitude in response to stimulation, but depression of transmission occurred when calcium chelators were applied (Castonguay and Robitaille, 2001).

Paradoxically however, blocking G-protein signalling pathways, which "activate" the TSC in response to neurotransmitters, can also produce an increase in synaptic activity. This may occur via nitric oxide, a substance that is known to regulate neurotransmitter release (Schuman and Madison, 1994; Robitaille, 1998). It is not clear why blocking this pathway should increase transmission, since it is also crucial for increasing intracellular calcium (and thus potentiating synaptic transmission). Another, as yet undescribed mechanism, may be involved in calcium release however, and be influenced by G-protein signalling. Interestingly, this paradox allows the TSC to exert both positive and negative effects on the synapse, and exert greater control on

the relatively complicated processes that occur during high frequency stimulation (Auld and Robitaille, 2003).

Although these studies were performed in the amphibian preparation, similar mechanisms may exist in the mammal to regulate synaptic transmission and further work in this area is ongoing.

1.4.6 Electrolyte homeostasis

In the mid 1960s, it was demonstrated that astrocytes were permeable to K+, and that a slow inward intake to the glial cells was evident after repeated axonal stimulation (Kuffler and Nicholls, 1966). It was hypothesised that this slow intake of potassium provided a "spatial buffering" mechanism for the axon. Potassium would enter the astrocyte in an area of high concentration, and potassium would then leave the cell in an area where potassium concentrations were lower. This phenomenon is also present in the retina, where it is proposed that Müller cells remove high concentrations of potassium from the retina, by "siphoning" concentrations away from the retina to the vitreous where it will not influence activity (Newman, 1986).

A similar process occurs in the PNS. Myelinating Schwann cells express a high concentration of potassium channels at the ends of internodes in microvilli, and it is thought these channels also provide a buffering mechanism during saltatory propagation (Wilson and Chiu, 1990).

TSCs have been shown to express high concentrations of voltage-dependent sodium channels, and these may also provide a role in buffering. These sodium channels help to maintain the activity of the Na/K ATPase pumps on the cell membrane, by ensuring the entry of sodium into the cell in the resting state and allowing prompt restoration of internal and external ion gradients during depolarisation. It has also been hypothesised that these channels may be synthesised for transfer to the adjacent axon, or are even used for axon-glial communication around the node of Ranvier (Boudier *et al*, 1988; Sontheimer *et al*, 1996). Although glial cells elsewhere in the nervous system have a clear role in ion homeostasis, the exact contribution, if any, of these channels in the TSC remains unclear at this time.

1.5 Current research

1.5.1 Schwann cell ablation using antibodies

To further elucidate the role of TSCs in supporting axonal function and survival at nerve terminals, a TSC-selective monoclonal antibody was developed for use in the frog. This antibody selectively removed all the TSCs in the muscle under study, without damaging other components of the NMJ.

Although there were no acute effects on nerve terminal function within the first week after ablation using this model, synaptic potentials were decreased by approximately half while postsynaptic function remained unchanged one week later. Further, muscle twitch tension was also reduced, growth and addition of additional synapses was

severely limited, and existing synapses underwent widespread withdrawal in developing systems (Reddy *et al*, 2003).

This study offers important insights into the function of the TSC, but the amphibian model is developmentally primitive, and as noted previously, its NMJ is both morphologically and physiologically different to the human and other more complex mammals. For example, human NMJs are 80% smaller than those of frogs, and 50% smaller than those of rats or mice. Since the size of the junction is proportional to the amount of ACh released, fewer quanta of ACh are released in response to direct stimulation in mammals than the amphibian. To maximise transmission, junctions in developmentally more complex animals have deeper junctional folds (Slater *et al*, 1992). Since the monoclonal antibody used by Reddy *et al* is species specific, its application to other species is limited. As a result, mouse antibodies to complex gangliosides developed in the Willison lab will provide a useful tool in the investigation of the role of the TSC in the mammalian system.

1.5.2 Mouse monoclonal antibodies

1.5.2.1 Production of murine anti-ganglioside antibodies

It is difficult to produce a stable cell line that produces sufficient quantities of antibody for experimental use using cells from patients with neurological illness. As a result, studies were directed towards developing a series of anti-ganglioside cell lines, using the mouse as a carrier. These anti-ganglioside antibodies could then be produced in sufficient quantity to study their effect on the nervous system.

In these investigations, mice were inoculated with the LPS core oligosaccharides from the surface of pathogenic strains of *Campylobacter jejuni*. Structural studies have shown that these core oligosaccharides are very similar to gangliosides, and are thus implicated in molecular mimicry (figure 1.14).

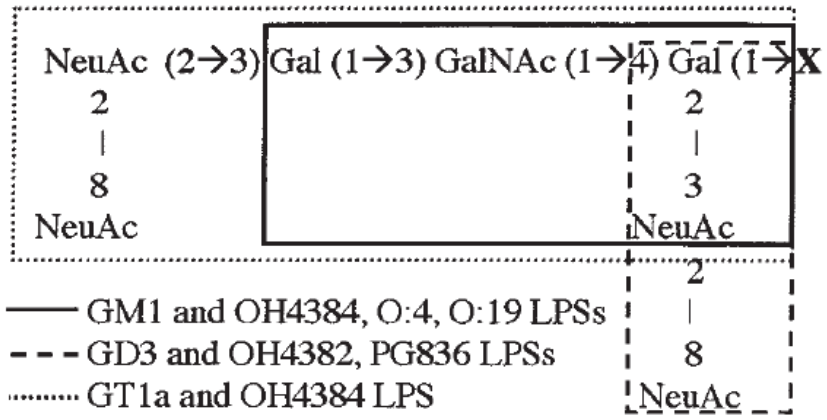

Figure 1.14: Schematic illustration of GQ1b and LPS core OS structures, illustrating the structural similarity between core OS and gangliosides.

The carbohydrate structure for GQ1b is shown, with other gangliosides. The similarities between these ganglioside structures, and the core LPS used to immunise mice to generate an antibody response is highlighted. NeuAc = *N*-acetyl neuraminic acid; Gal = galactose; GalNAc = *N*-acetyl galactosamine; X = Glc (1->1) ceramide (gangliosides) or the remaining core OS/lipid A (LPSs) (adapted from Goodyear, 1999).

Although immunising a mouse with LPS would in itself generate a low level immune response, this effect can be enhanced with the addition of an "adjuvant", which is a substance that enhances the immunogenicity of substances mixed with it. The LPS core oligosaccharides were therefore mixed with both Complete and Incomplete Freund's Adjuvant (CFA and IFA respectively). These adjuvants enhance immunogenicity by converting soluble protein antigens into particulate material, making them more readily ingested by antigen-presenting cells such as macrophages. They also adsorb antigen onto adjuvant particles to enhance immunogenicity, and the presence of mycobacterial products in the CFA in particular, are thought to make the antigen presenting cells more effective. Unlike hapten carriers however, CFA and IFA do not form stable linkages with the immunogen.

Once an immune response was detected, spleen cells were harvested, and fused with myeloma cells to produce a stable cell line of polyreactive antibodies with selective binding to ganglioside like structures. These antibodies, as discussed earlier, appear to arise from a T-cell independent mechanism (Goodyear *et al*, 1999; Boffey *et al*, 2004). Since this study, more cell lines have been established using this technique, and now a large series of antibodies with differing specificities for complex gangliosides on ELISA has been established.

1.5.2.2 Glial specificity of anti-ganglioside antibodies

Early work suggested that the NMJ was a likely target for these newly developed antibodies. Although many shared similar ganglioside binding profiles on ELISA, their behaviour at the NMJ was very different. As a result, it was possible to classify

these new antibodies based on their behaviour *ex vivo*. These studies were performed on *ex vivo* hemidiaphragm preparations, using a combination of immunohistological analysis, electrophysiological assessment and electron microscopy (Halstead *et al*, 2005b).

As described previously, anti-ganglioside antibodies produce their injury by local complement activation, resulting in MAC pore formation and massive influx of calcium across the cell membrane that results in calpain activation and cell death. Ethidium homodimer (EthD-1) was therefore used as a marker of TSC injury, as it is a nuclear impermeant nuclear marker that is taken up into cells in the presence of MAC pores, and has been previously used as a marker of MAC induced cell injury in the TSC (Halstead *et al*, 2004). Disruption to neurofilament over the junction was used as a marker of axonal injury, and complement deposition was assessed to confirm the mechanism of injury. Electrophysiological measurements assessed both the miniature end plate potential frequency, and end plate potential following direct stimulation, as these have previously been shown to be good markers of antibody induced axonal injury (figure 1.15A and B).

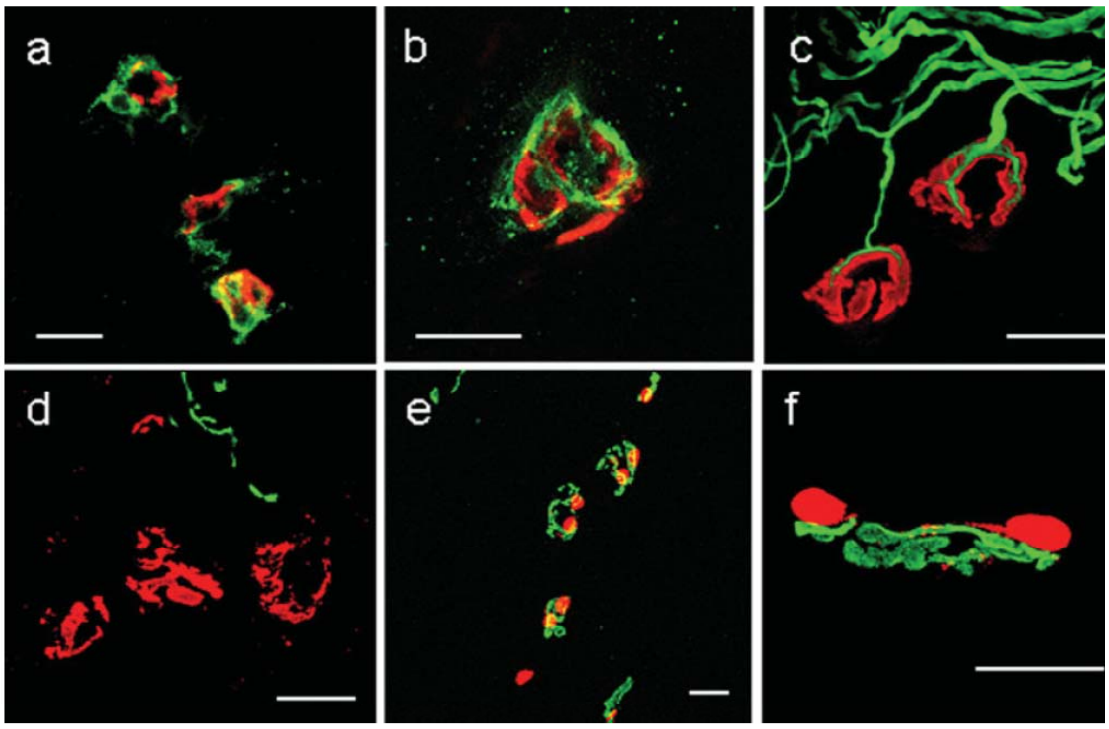

Figure 1.15A: Immunofluorescent staining of hemidiaphragm tissue exposed to anti-ganglioside antibodies with normal human serum as a source of complement.

a,b: All antibodies used in this study produced significant deposits of complement (C3c; green) over the NMJ (BTx staining, red) in the presence of NHS.

c: Normal pattern of nerve terminal NF (green) extended from the distal axon to form an arborization over the NMJ (BTx, red), as seen after exposure to Ringer or Group S antibodies plus NHS.

d: Complete dissolution or fragmentation of the NF signal (green) over the NMJ (BTx, red) or distal intramuscular axons, as seen after exposure to latrotoxin or Group SN and N antibodies plus NHS.

e,f: Abnormal nuclear uptake of EthD-1 (red) by TSCs overlying NMJs (BTx, green) after exposure to Group S and SN antibodies plus NHS. Scale

bars 20μm. (All images taken by Mr. P. Humphreys or Dr. S. Halstead, and published in Halstead *et al,* 2005b).

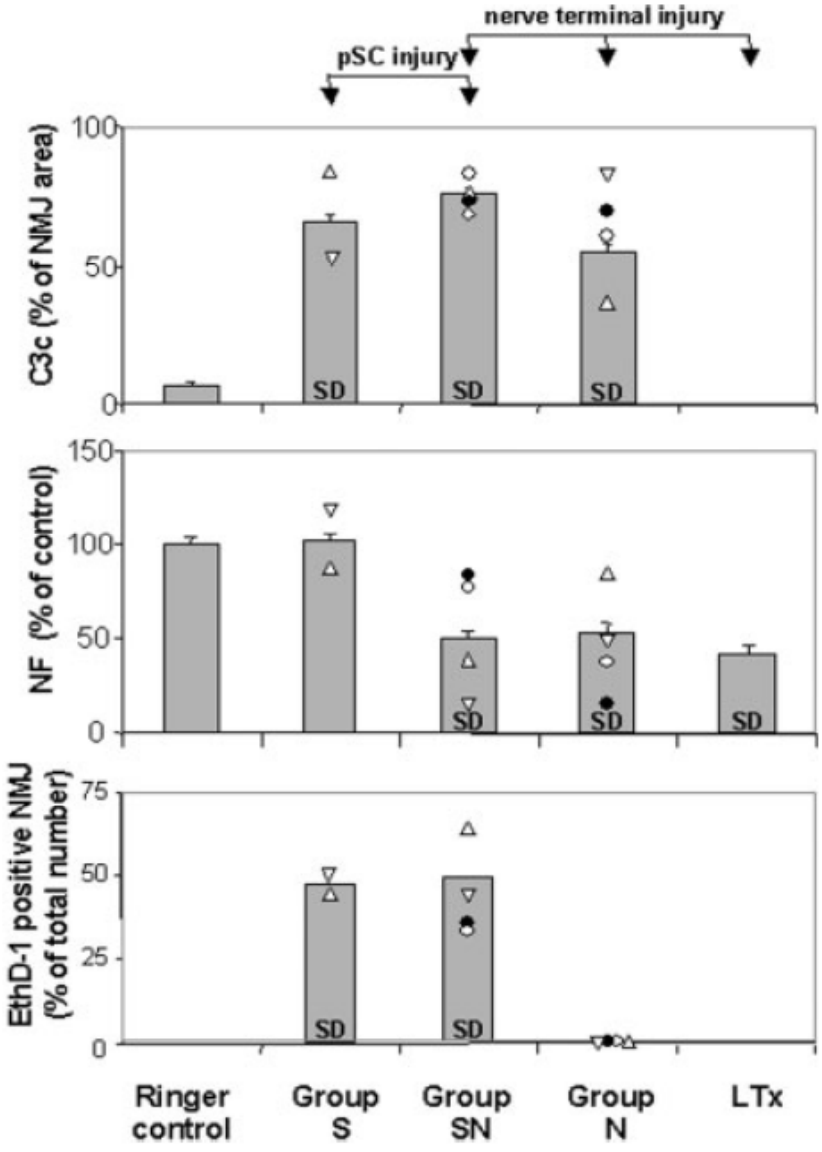

Figure 1.15B: Quantitative analysis of NMJ injury as assessed by immunofluorescent staining for complement product C3c, neurofilament (NF), and abnormal TSC nuclear uptake of ethidium dimer (EthD-1).

According to the distribution of injury, mAbs are segregated into three groups: S (TSC only), N (nerve terminal only), and SN (TSC and nerve terminal).

a: Complement deposits. All antibodies produced significant deposits of C3c over NMJs compared with Ringer controls or LTx exposure.

b: Axonal integrity. NF signal is reduced over the NMJ with antibodies producing a nerve terminal injury (Groups SN, N) and with latrotoxin. NF signal is unaffected by Group S antibodies. For a and b, values represent mean +/- SEM for the pooled data for each group. SD is significantly different from Ringer control (Student's two-tailed t-test $P < 0.01$).

c: TSC injury. EthD-1-positive nuclei were observed over NMJs with Group S and SN antibodies, and not with Group N antibodies or LTx. NMJs with one or more overlying EthD-1-positive nuclei were scored as positive, and counts were pooled from one or more preparations. SD is significantly different from Ringer control (Chi squared test, $P < 0.01$). (Taken from Halstead *et al* 2005b)

Electron microscopy studies identified TSC injury by the presence of cell vacuolation, abnormal cell processes, and electron translucency in the cells. Axonal injury was identified by mitochondrial disruption, loss of ACh vesicles, and the presence of wraps of TSC around the axon itself (figure 1.16).

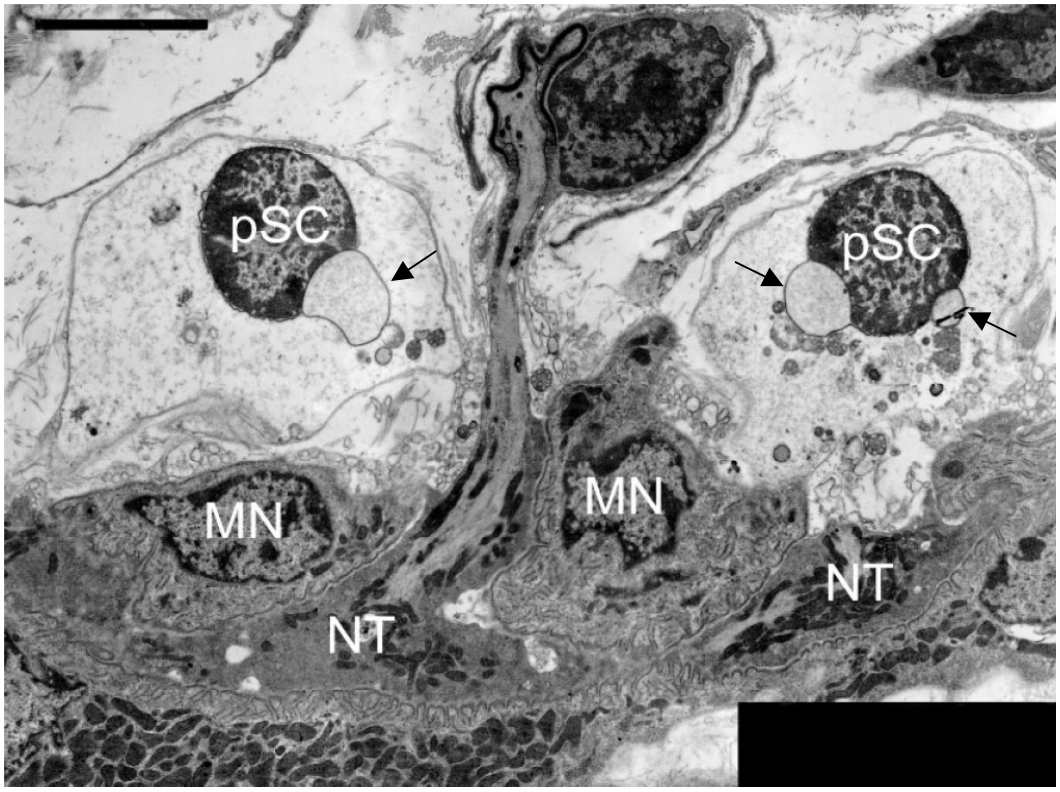

Figure 1.16: Ultrastructural characterization of TSC injury induced by Group S anti-ganglioside antibody, EG-1.

This figure is a low-magnification electron micrograph showing a NMJ in cross section. The axon is wrapped by a myelinating Schwann cell, and forms a synaptic contact with a muscle fibre. Numerous vesicles are seen in the nerve terminal, with electron dense mitochondria. Two damaged TSCs (pSCs) are seen on either side of the nerve terminal, and appear damaged with electron-lucent cytoplasm, damaged organelles, nuclear blebbing and perinuclear bodies (black arrows). The exact function of the perinuclear bodies was not addressed in this study, but they are a feature of TSC injury. Two myonuclei (MN) project from beneath the postsynaptic membrane, and are of normal appearance. Scale bar 5µm. (Taken from Halstead *et al*, 2005b)

Based on these criteria, it was possible to classify the antibodies into:

Group S: Only injure TSCs

Group N: Only injure terminal axons

Group SN: Injure both terminal axons and TSCs.

As expected, antibodies that bound the terminal axon caused massive, uncontrolled exocytosis from the nerve terminal, followed by paralysis. Neurofilament levels over the junction were significantly disrupted, and there were EM changes consistent with axonal injury. These changes are consistent with the "latrotoxin like" effect described previously, and indeed latrotoxin controls performed at the same time showed similar changes (Goodyear *et al*, 1999).

Other antibodies, particularly EG1 (an IgG3 antibody), were shown to selectively damage the TSC whilst leaving the remaining nerve terminal intact. Despite having no TSCs, the junctions did not exhibit any acute electrophysiological changes within the timescale of the experiment, suggesting that TSCs are not required for the acute maintenance of nerve terminal function. This finding supports previous work in the frog, where no short-term electrophysiological disruption was described in the absence of TSCs (figure 1.17) (Reddy *et al*, 2003).

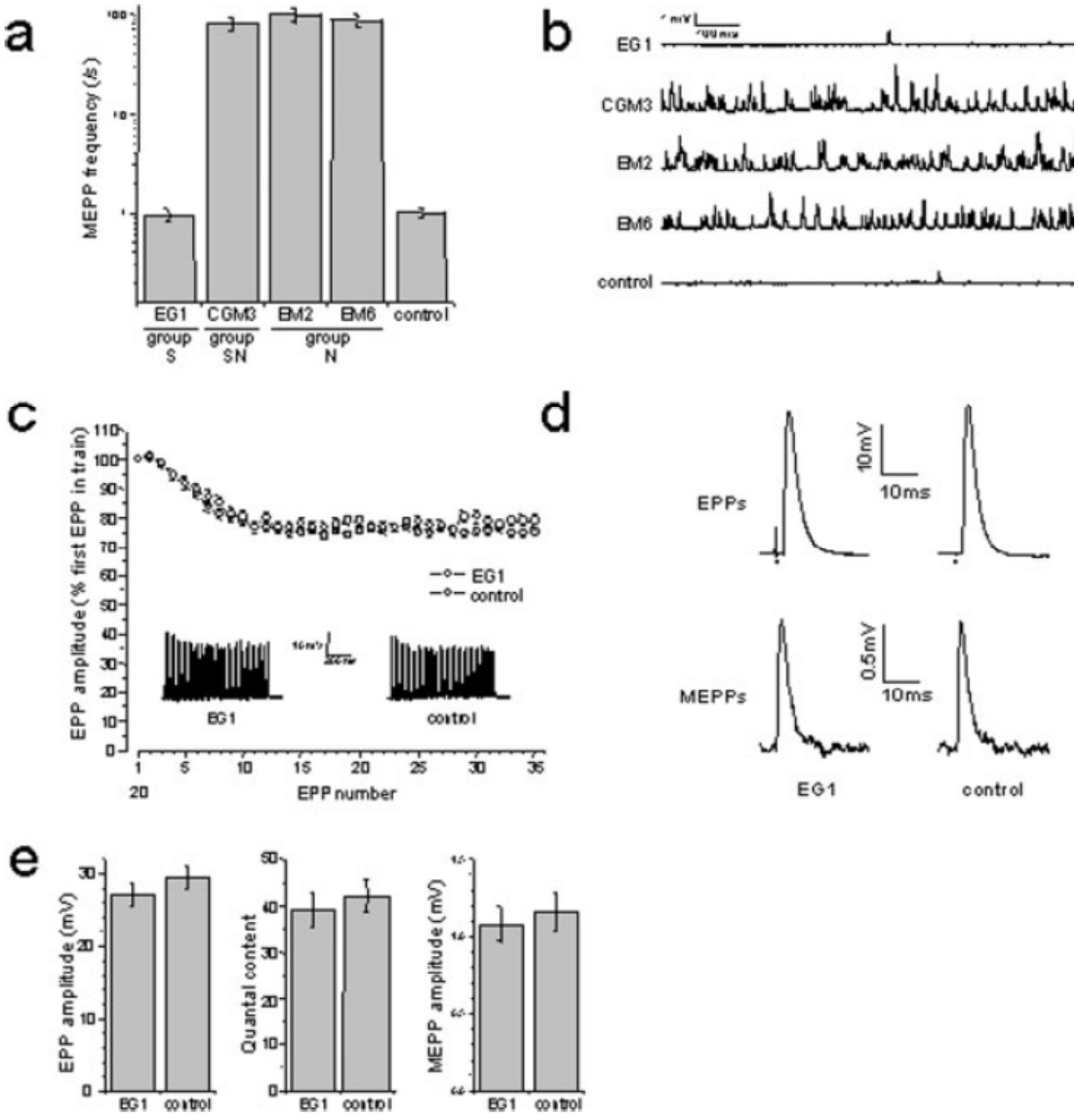

Figure 1.17: Electrophysiological analysis of anti-ganglioside antibody effects on NMJ synaptic function *ex vivo*.

a-b: Hemidiaphragm preparations from BALB/c mice were incubated with anti-ganglioside antibody, and normal human serum. Electrophysiological recordings were made from 7-19 NMJs in each preparation for 1 hour. Antibodies were classified as Groups S (TSC only), N (nerve terminal only), and SN (TSC and nerve terminal) based on previous morphological

studies. Group N and SN induced the latrotoxin-like effect, measured by an increase in miniature endplate potential (MEPP) frequency followed by block of evoked ACh release measured as a reduction in endplate potentials (EPPs).

NMJs that were incubated with Group S antibodies did not show LTx-like effects, with no change in MEPP frequency from the Ringer control.

c–e: Analysis of the effects of the Group S mAbs EG1 on evoked ACh release at either 40-Hz (c) or 0.3-Hz (d,e) nerve stimulation and on spontaneous MEPPs (d) showed no differences from control. This study demonstrates that removal of TSCs does not have any acute effects on neuromuscular function.

Data in a, c, and e are mean values 6 SEM of 16–35 NMJs sampled in two preparations per mAb. Traces in b and d are representative examples of the electrophysiological recordings. Black dot indicates the moment of nerve stimulation. (Taken from Halstead *et al*, 2005b)

The exact reason for this glial specificity is unclear, but may reflect the differing composition of gangliosides across neuronal membranes. This is supported on ELISA studies, where the specificity of TSC specific antibody EG1 was compared to other antibodies which damage either the nerve or both the nerve and TSC. These investigations demonstrate that EG1 appears to have preferential binding to ganglioside GD3 while nerve specific antibodies bind more strongly to gangliosides GQ1b and GT1a. Although the ganglioside composition in different neuronal

membranes is unknown, these localisation studies suggest that gangliosides on nerves are structurally more complex than those on TSCs.

1.5.2.3 Summary

This unique panel of antibodies permits study into the role of anti-ganglioside antibodies in the pathogenesis of autoimmune neuropathy, in addition to studying the contribution made by the glial components at the NMJ. However, these observations were only made one hour after complement exposure, due to the limitations of the *ex vivo* system. To fully study the longer-term effects of TSC injury in the mammalian model, and thus consider the role of the TSC in autoimmune nerve injury, a system was developed that allows repeated imaging over injured NMJs over a prolonged period.

1.5.3 CFP/GFP mouse preparation

Before detailed dynamic studies of the cellular interactions occurring at the NMJ can be undertaken in a mammalian model, a reliable method of vital imaging must be developed which easily distinguishes the various cellular components. However, many of the existing cellular stains used to identify these structures are either toxic to the cell, making recovery impossible, or involve processing that requires sacrifice of the animal, and thus cessation of the experimental time course. However, a new transgenic system has been developed that expresses fluorescent proteins in a site or cell specific manner, allowing repeated imaging of nerves without injuring the cell by immunostaining (Trachtenberg *et al*, 2002; Walsh and Lichtman, 2003).

Green light is produced by the bioluminescent jellyfish, *Aequorea Victoria,* when calcium binds to the photoprotein aequorin, and provides sufficient excitation energy to green fluorescent proten (GFP) to produce green light *in vivo* (Simomura *et al*, 1962; Morin and Hastings, 1971). When aequorin is isolated *ex vivo* without GFP, blue light is produced.

GFP is a stable protein of 238 amino acids, with very specific, and stable fluorescence spectra. The exact mechanism of fluorescence is unclear, but as the protein has a very stable genetic sequence, it is possible to transgenically insert and express GFP in both prokaryotic and eukaryotic cells (Prasher *et al*, 1992; Chalfie *et al*, 1994). Cells can therefore be rendered fluorescent by the introduction of GFP's cDNA, rather than the chromophore itself. As the chromophore is derived entirely from its polypeptide chain, without requiring any additional factors from the cell, this permits imaging with minimal disruption to the cell itself. Using cell-specific promoter sequences, the protein can also be localised to other compartments in the preparation, making specific cell lines fluoresce (Tsien, 1998). As the genetic sequence is stable, the fluorescent properties can be inherited across generations, allowing lines of fluorescent mice to be established. An example of this technique is seen in the Kosmos mouse. In this preparation, GFP is coupled to the promoter sequence of S100 beta, a protein found in Schwann cells. This marker is a small calcium binding protein of uncertain significance found in the cell cytosol, but has a recognised promoter sequence. As a result, a line of mice has been generated whose peripheral Schwann cells are labelled for GFP (Zuo *et al*, 2004).

Another interesting feature of GFP is that its genetic sequence can be easily altered, and thus alter the spectral qualities of the protein, producing chromophores that fluoresce at different wavelengths. Examples of this include the cyan fluorescent protein (CFP), red fluorescent protein (RFP) and yellow fluorescent protein (YFP). These chromophores can then be inserted in differing compartments in the same animal, labelling different cell sub-types (Feng *et al*, 2000).

A mouse line was generated, that expressed cyan fluorescent protein (CFP) in association with the thy 1.1 promotor sequence (Lichtman and Sanes, 2003). Thy 1.1 is an immunoglobulin superfamily member that is expressed by both neuronal, and several non-neuronal cell types including thymocytes (from which it is named) (Gordon *et al*, 1987). However, early work using the sequence demonstrated that altering the genomic elements slightly (by removing selective introns, for example) can abolish the expression of the gene in non-neuronal cells (Vidal *et al*, 1990). This has been used to produce constructs that selectively over-express enzymes and growth-promoting molecules in neurones, but not non-neuronal tissue (Kelley *et al*, 1994; Caroni, 1997). Using this principle, a line of mice was developed that selectively expresses CFP in both motor and sensory neurones in the periphery, in addition to subsets of central neurones. This line was then crossed with S100β-GFP, to produce a mouse whose Schwann cells expressed GFP, and neurones expressed CFP (figure 1.18). This system allows real time visualisation of axon-glial interactions, and has been used to effectively determine the precedence of several processes at the synapse, including the formation of Schwann cell bridges, escape fibres, and sprout formation (Kang and Thompson, 2003).

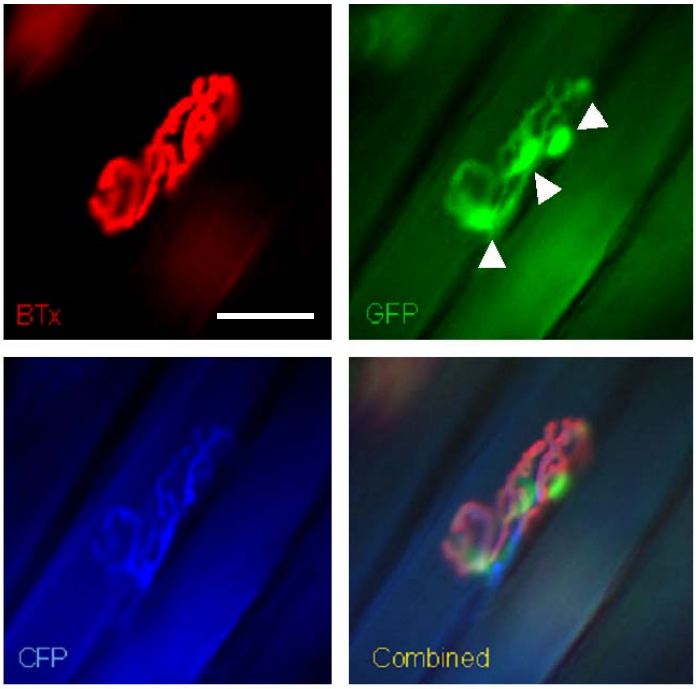

Figure 1.18: *In vivo* image of CK mouse preparation (colourised to reflect actual image through microscope).

S100β-GFP is seen on the TSC bodies (arrow heads) and processes of terminal Schwann cells covering the NMJ. Axon expresses thy 1.1-CFP, and Texas-red bungarotoxin demonstrates post-synaptic specialisation. (Scale bar 10μm) (From pilot studies in Thompson laboratory by Dr. Ian Morrison)

Using our panel of monoclonal antibodies, and a source of exogenous complement, this preparation can be used to investigate the longer-term effects of antibody-mediated injury at the NMJ, and in particular the role of TSCs at this site.

1.6 Research Question

TSCs clearly provide important functional support to the underlying motor nerve terminal, both in the steady state and during regeneration. Although selective ablation of TSCs has been possible in the amphibian model, it has not been achieved at mammalian NMJs. Further, the role of TSCs in autoimmune neuropathy has never been considered in detail. This is a departure from the current emphasis on seeking axonal antigens to account for axonal injury in autoimmune disorders such as GBS, and also has far-reaching implications for understanding the glial contribution to axonal injury and regeneration in other diseases, including multiple sclerosis.

The newly generated panel of antibodies from the Willison laboratory, in conjunction with the GFP/CFP fluorescent mouse model, offers a unique opportunity to study the developmentally advanced mammalian NMJ by selectively attacking and destroying its various components through a complement mediated effect.

These studies will determine the acute and chronic effects of immune mediated TSC depletion at the NMJ. In particular, I will test whether TSC depletion causes motor nerve terminal dysfunction by studying the response of the NMJ to TSC injury in the CK mouse. Human muscle tissue will then be used to examine whether human TSCs are a possible site of injury in autoimmune neuropathy.

Chapter 2: Methods

2.1 Antibody preparation

2.1.1 Tissue Culture

In preparation for these investigations, stocks of pure EG1 antibody were grown from tissue culture. Original hybridoma cell lines were prepared in the laboratory by technical staff, by immunising mice with LOS from a GBS associated *Campylobacter* strain (OH4384) in Complete Freund's adjuvant. Hybridoma cell lines were stabilised in DMSO before freezing in the vapour phase of liquid nitrogen at –196^{o}C for long term storage.

All tissue culture work was performed in a class II sterile hood. The original hybridoma cell line for EG1 was thawed from storage, before being transferred to growth medium (RPMI 1640 with 10% FCS and 5mmol glutamine) to initiate culture. After incubation at 32^{o}C in 95% O_2, 5% CO_2 rich environment for 24 hours, the solution was spun at 1000rpm for 5 minutes in a Beckman GS-6R centrifuge, and the supernatant (containing DMSO) was discarded.

Fresh growth medium was then added, and the cells were incubated for a further 48 hours. A cell count was obtained, and once the cells were confirmed to be growing in the log phase, they were separated into five separate 175ml flasks containing complete RPMI 1640 media, at a concentration of 1-2x10^5 cells/ml.

After 24 hours, the cells were spun again at 1000rpm for 5 minutes, and transferred to FCS rich growth medium (RPMI 1640 with 20% FCS and 5mmol glutamine) at a concentration of $1.5x10^6$ cells/ml. The cells in FCS rich medium were then transferred to an "Integra CL1000". The nutrient medium was exchanged on a twice-weekly basis with RPMI 1640 and 5mmol glutamine. Approximately half the volume of the cell compartment was removed on a weekly basis, and replaced with FCS rich growth medium. The cell compartment solution was frozen at -20^oC until purification.

To assess the viability of the cell line and its ability to produce antibody, twice monthly ganglioside ELISAs were performed on the harvested cell compartment medium.

2.1.2 Antibody purification and concentration

2.1.2.1 Antibody EG1

Once sufficient volumes of nutrient medium were harvested, the solutions were purified using protein A affinity chromatography. Protein A is a surface protein found on the surface of *Staphylococcus aureus*, and is part of the bacterium's defence against immunological attack. The protein binds to the Fc region of immunoglobulins, and mis-orientates any defensive immunoglobulin binding to the surface of the bacterium, preventing opsonization and phagocytosis. This mechanism can be harnessed in the laboratory for purification and concentration of antibody, by creating columns of protein A that bind and remove antibody from its host solution. Antibody can then be eluted at a later stage, resulting in a purified, highly concentrated solution.

Solutions were defrosted to room temperature, before being spun at 10,000rpm for 30 minutes in a Sorval RC5c centrifuge, and filtered using Nalgene 50ml bottle top filters (pore size 0.45μm). The supernatant was dialysed in phosphate buffer solution for 24 hours at $4^{o}C$ (0.1M NaH_2PO_4 at pH7).

A "protein A" affinity column was prepared with 50ml of binding buffer (10 column volumes) at a rate of 5ml/min. Filtered nutrient medium solution, stored on ice, was then passed through the column at 5ml/min and the flow through was collected. The column was washed with a further 50ml of binding buffer solution, and then eluted with 50ml of 0.1M citric acid. One-column volumes of elutant were retained in collecting tubes, and neutralised to pH 7 in an appropriate volume of 1M tris-HCl. The column was again washed with 50ml of binding buffer, and then 50ml of 20% ethanol prior to storage.

Optical densities of the eluted fraction, and final buffer fraction were checked at 280nm to minimise antibody loss. Samples from the elution series with high concentrations of protein were combined, and diluted to concentrations less than 0.5mg/ml to prevent precipitation before being stored at $-70^{o}C$.

A ganglioside ELISA of flow through solutions was also performed from each stage of the purification process, and solutions were run through the column a second time if reactive for GD3, to minimise wastage.

With the assistance of Mr Eric Wagner, the purity of the resulting antibody solution was confirmed using sodium dodecyl sulphate polyacrylamide gel electrophoresis

(SDS page). Antibody solution was diluted in loading buffer to 1/10 and 1/100 concentrations and heated to 99^{o}C for 10 minutes. A 10% polyacrylamide gel was rinsed in distilled water, and coated in running buffer before the antibody dilutions were added with a control (Colorburst pH8 marker). The gel was run at 180V for 1 hour, and transferred to "Coomassie blue" solution for 1 hour to develop.

2.1.2.2 Antibody LB1

Once sufficient volumes of nutrient medium were obtained, solutions were defrosted to room temperature, before being spun at 10,000rpm for 30 minutes in a Sorval RC5c centrifuge, and filtered using Nalgene 50ml bottle top filters (pore size 0.45µm). The supernatant was dialysed in phosphate buffer solution for 24 hours at 4^{o}C (0.1M NaH_2PO_4 at pH7).

Solutions were concentrated before use by spinning through a 10,000MW CO membrane in a "Vivacell 100" at 5000rpm for 10 minutes. Solutions were dialysed overnight at 4^{o}C in Ringers solution (116mM NaCl, 4.5mM KCl, 1mM MgCl, 2mM $CaCl_2$, 1mM NaH_2PO4, 23mM $NaHCO_3$, 11mM glucose at pH 7.4 pre-gassed with 95% O2/5%CO_2).

2.1.3 Quantification of antibody concentration

2.1.3.1 Optical density

For IgG antibodies following purification, the optical density at 280nm was measured, and the concentration was calculated using the following equation:
OD280/1.43 = antibody concentration

2.1.3.2 Quantitative ELISA

IgM samples (LB1) were quantified using quantitative ELISA, and OD measurements using IgG antibodies were also confirmed using this technique. ELISA kits were obtained from Bethyl Laboratories (E90-101 for IgM and E90-131 for IgG)

Capture antibody (anti-mouse IgG or IgM) was diluted to 1:100 in bicarbonate coating buffer, and 25µl was added to each well in a 384 well plate (Immulon 2HB). The plate was left overnight at 4^{o}C, and then washed 3 times in a PBS + 0.05% Tween 20 solution. 50µl of 2% BSA was added to each well, and left for 1 hour at room temperature before being washed again for 3 times in a PBS + 0.05% Tween 20 solution.

Reference antibody was diluted in concentrations from 0ng/ml to 1000ng/ml in 0.1% BSA and added to appropriate wells.

25µl of stock antibody solution was added to each well, and incubated for 2 hours at room temperature before washing 3 times in PBS + 0.05% Tween 20 solution.

Anti-mouse IgG- or IgM-HRP (Bethyl Lab anti-IgG or anti-IgM) was diluted to 1:30000 in 0.1%BSA, and 25µl was added to each well before incubating for 1 hour at room temperature. The plate was then washed 6 times in PBS+ 0.05% Tween 20 solution. 25µl of substrate was added to each well, and incubated for 20 minutes in darkness at room temperature. The reaction was stopped by adding 4M H_2SO_4, and the plate was read at 492nm.

2.1.4 Antibody characterisation

2.1.4.1 Ganglioside ELISA

Alternate rows of an "Immulon IIB ELISA plate" were coated with 100µl per well of 2µg/ml ganglioside GD3, which had been sonicated for 1 minute; and 100µl of methanol for background subtraction. The plate was dried in a fume hood for 2-3 hours until fully dry before being transferred to 4^{o}C for a minimum of 1 hour. The plate was blocked with 2% BSA for 1 hour at 4^{o}C, any excess was discarded, and 100µl of substrate were added to each well for a minimum of 4 hours at 4^{o}C. After washing the plate in PBS, secondary HRP-antibody (Sigma anti-IgG or IgM) at 1:3000 in 0.1%BSA was added for 1 hour at 4^{o}C. After a further PBS wash, 100µl of substrate buffer (0.1M citrate, 0.2M Na_2HPO_4, 1 OPD tablet (Sigma, P4664), 20µl H_20_2) were added to each well, and incubated in the dark for 20 minutes. The reaction was terminated by adding 50µl of 4M H_2SO_4 and the plate was read at 492nm.

2.1.4.2 Ganglioside characterisation

Antibody ganglioside binding profiles were characterised on a multi-ganglioside ELISA plate. Antibodies were tested against a range of gangliosides, sulfatide, and methanol using a standard ganglioside ELISA protocol. Antibodies were then titrated using an ELISA against the positive gangliosides at concentrations ranging from 10^{-2} to 10^{-5}mg/ml. The reciprocal of the Ab concentration that gave half-maximal binding was calculated (1/50%). I am very grateful for the assistance of Ms Dawn Nicholl, who assisted in these characterisation experiments, and described EG1 and R24.

2.1.5 Human antibodies

Human antibodies were obtained from three sources: patients SM, Ha and Ch. Patient SM had multifocal motor neuropathy, and monoclonal antibodies obtained from B cell clones from peripheral blood lymphocytes. Samples of serum from patient Ch were retained during plasmapheresis therapy, and stored at –80^{o}C until further use. Patient Ha has CANOMAD (chronic ataxic neuropathy with ophthalmoplegia, IgM paraprotein, cold agglutinins and disialosyl antibodies) and also undergoes regular plasmapheresis therapy. A red cell eluate was prepared using retained serum samples from this therapy, using established techniques (Willison *et al*, 1993b), and I am very grateful to Mrs Jean Veitch for her assistance in preparing the red cell eluate.

2.2 *Ex vivo* tissue analysis

2.2.1 Animal euthanasia

All animals were male, aged 6 weeks unless otherwise stated, and their strain is identified in the text. Animals were killed by a rising concentration of carbon dioxide, in accordance with Home Office regulations. Other Schedule 1 methods, including terminal anaesthesia, and cervical dislocation were performed as noted in the text.

Euthanasia at the University of Texas in Austin was performed using rising concentrations of carbon dioxide, or intra-peritoneal injections of phenobarbitone, using local and Federal guidelines. These protocols are similar to those established by the Home Office.

2.2.2 Hemidiaphragm preparations

2.2.2.1 Muscle dissection

Ex vivo hemidiaphragm preparations were used to quantify TSC injury, immunoglobulin deposition, complement deposition (C3c and MAC), and neurofilament loss.

Following euthanasia in carbon dioxide, a flap in the anterior wall of the rib cage was reflected, and the phrenic nerves were identified and tied off. The diaphragm was removed from the thoracic cavity with its supporting ribs, and rinsed in Ringer's

solution. The muscle was then pinned onto a sylgard-lined dish, and divided into two halves, each innervated by a single phrenic nerve.

Unless otherwise stated, each hemidiaphragm was described in 3 sections (A-C). Section A (the most anterior part of muscle) was removed immediately after dissection. This section was used as an untreated control for comparative quantification studies. Section B included the section of muscle with the innervating phrenic nerve, and was removed after incubation with antibody/control solutions and complement. This piece of muscle was used for experimental study, including immunoglobulin and complement deposition, and neurofilament loss. Section C was used to quantify TSC injury using ethidium application.

2.2.2.2 Antibody incubation protocols

The following antibody incubation protocol was used to produce injury in the *ex vivo* hemidiaphragm preparation:

1. Anti-ganglioside antibody (100μg/ml unless otherwise stated) dialysed overnight in oxygenated Ringers solution
2. Section A removed from hemidiaphragm and snap frozen
3. Hemidiaphragm preparation incubated in dialysed anti-ganglioside antibody/control solution for 2 hours at 32^{o}C, 30 minutes at 4^{o}C and 15 minutes at room temperature. Washed in Ringers solution
4. 40% normal human serum or control solution for 1 hour at room temperature. Washed in Ringers solution

5. Section B removed and snap frozen
6. Incubated with 1:1000 (2μM) ethidium homodimer (Molecular Probes, Eugene, Oregon, USA) in PBS for 1 hour in dark environment at room temperature. Washed in Ringers solution
7. Section C removed and snap frozen.

Sections of hemidiaphragm muscle were subsequently thawed to –25^{o}C, before mounting on a block of Tissue-Tek OCT embedding matrix. Sections were cut onto 3-aminopropyltriethoxysilane (APES) coated slides using a freezing cryostat. Sections were cut at 8μm for immunoglobulin and complement studies, and 15μm for ethidium and neurofilament quantification, and were then air-dried. Sections were stored at -20^{o}C prior to staining.

Tissue sections were stained and assayed as described in General Staining techniques (section 2.4.2).

2.2.3 Triangularis sterni preparations

Ex vivo preparations of triangularis sterni were used to obtain clear images of the entire NMJ, without sectioning the muscle.

Following euthanasia, the pectoral muscles, and diaphragm were dissected from the rib cage, and the thoracic organs were removed from the chest cavity via the abdomen. The posterior ribs were cut lateral to the thoracic vertebrae, and the entire rib cage was removed, and washed in Ringers solution. The rib cage was then pinned

in a sylgard-lined dish, with the anterior surface uppermost. The intercostal muscles, and their supporting ribs were removed under transverse illumination to reveal a window in the rib cage, showing triangularis sterni underneath.

The following antibody incubation protocol was used to induce a lesion in this muscle:

1. Anti-ganglioside antibody (100μg/ml unless otherwise stated) dialysed overnight in oxygenated Ringers solution
2. Triangularis sterni incubated in dialysed anti-ganglioside antibody/control solution for 2 hours at 32^{o}C, 30 minutes at 4^{o}C and 15 minutes at room temperature. Washed in Ringers solution
3. 40% normal human serum or control solution for 1 hour at room temperature. Washed in Ringers solution
4. 1:500 TxR-BTx (Molecular Probes) for 1 hour at room temperature
5. Fixed in 4% paraformaldehyde for 20 minutes at 4^{o}C then PBS rinse

If neurofilament staining was required in the United States, the following additional steps were performed:

6. Permeabilised in methanol for 8 minutes at –20^{o}C then rinsed in PBS
7. Blocker solution for 30 minutes
8. Incubate anti-SV2 (diluted 1:500; Developmental Studies Hybridoma Bank, Iowa) with anti-2H3 (diluted 1:200; Developmental Studies Hybridoma Bank, Iowa) and TxR-BTx (diluted 1:500) overnight in blocker solution.
9. Rinse in blocker solution for 30 minutes then 1:200 anti-secondary for 1 hour

In certain instances, this incubation protocol was modified:

a) Ethidium – if demonstration of TSC injury is necessary, ethidium homodimer (diluted 1:1000, 2μM, Molecular Probes) in PBS is added for 1 hour in dark environment at room temperature, after incubation with normal human serum. The tissue is then washed in Ringer's solution and FITC bungarotoxin (diluted 1:500, Molecular Probes) was added for 1 hour at room temperature.

b) Sytox – to fully assess the extent of TSC injury, Sytox green (Molecular Probes) was used to co-stain with ethidium, to demonstrate the complete population of TSCs. Sytox green is a membrane impremeant nuclear stain with a distinct wavelength that can be visualised on the laboratory's existing confocal microscope and filter sets. After incubation with ethidium, tissue was stained with 1:500 TxR-BTx for 1 hour at room temperature, and fixed in 4% paraformaldehyde for 20 minutes at 4^{o}C. The tissue was then permeabilised with ethanol as above, and Sytox Green (diluted 1:50000) in blocking solution (1% goat serum, 0.4M l-lysine and 0.5% Triton X-100) was added after a PBS rinse. The tissue was left for a minimum of one hour at room temperature, before mounting.

After staining, the TS muscle was placed on a slide with a supported coverslip, and mounted in citifluor before imaging.

Structural analysis was performed using a Zeiss Pascal confocal microscope with reconstructions performed using Voxx (Indiana Centre for Biological Microscopy) or Volsuite 3.2 (Ohio Supercomputer Center) and Adobe Photoshop Pro 8 (Adobe).

2.3 Topical staining

2.3.1 Murine tissue harvest

All animals were male, aged 6 weeks unless otherwise stated, and their strain is specified in the text. Untreated sections of diaphragm were dissected from mice that were euthanased by approved Schedule 1 methods. These samples were immediately snap frozen following removal, and stored at –80^{o}C until sectioning.

Sections of hemidiaphragm muscle were thawed to –25^{o}C in a freezing cryostat, before mounting on a block of Tissue-Tek OCT embedding matrix. Sections were cut onto 3-aminopropyltriethoxysilane (APES) coated slides using a freezing cryostat. Sections were cut at 8µm for immunoglobulin and complement studies, and 20µm for ethidium and neurofilament quantification, and were then air-dried. Sections were stored at –20^{o}C prior to staining. Unless stated otherwise, experiments were repeated on 3 occasions using tissue from at least 3 different animals. Three non-contiguous sections of muscle were examined on each repeat.

2.3.2 Human tissue harvest

2.3.2.1 Consent

COREC documentation, and local Research and Development Approval forms were completed before human tissue harvests were undertaken. These forms were

submitted to the North and South Glasgow Trusts, in addition to local offices at the Western Infirmary, Glasgow.

Consent was then granted by local hospital ethical committees, to obtain muscle tissue from human volunteers undergoing routine surgery. Subjects were given information sheets and the opportunity to discuss the research before providing written consent (see appendix 3 for information sheet, and consent forms). All tissue would be routinely discarded at operation, and tissue harvest did not affect treatment or outcome of the procedure.

Biobank also sought consent for muscle harvest. Biobank is a commercial branch of the department of Pathology, North Glasgow University NHS Trust, and a fee was paid to them for this service.

Consent was also obtained from relatives of patients undergoing post-mortem examination. Families were given information sheets and the opportunity to discuss the research before providing written consent (see appendix for information sheet, and consent forms).

2.3.2.2 Harvest and processing

A) Intercostal muscle. Sections of this muscle are routinely removed during dissection of the internal mammary artery during coronary artery bypass grafting (CABG). This muscle is dissected from the artery, and routinely discarded.

B) Omohyoid muscles. During radical neck surgery for cancer, complete sections of omohyoid are routinely dissected and discarded without further staging or analysis.

C) Pharyngeal constrictor muscle. During radical neck and oral surgery for cancer, sections of the pharyngeal constrictor muscle are dissected and discarded without further staging or analysis.

D) Biceps muscle. During surgery for tumours of bone and soft tissue, the limb is often amputated. Much of the tissue is discarded without further analysis. Biobank harvest and store surplus muscle, for use in research.

E) Human sciatic nerve. Tissue was obtained from post-mortem examinations, and stored. Samples were also obtained from Biobank and vascular surgery.

F) Peroneus longus, and extensor digitorum longus. Fresh specimens of human leg were obtained from patients having amputations for critical ischaemia of the lower limb, or for tumours of the bone and muscle of the leg. Samples were taken from areas not involved in the primary disease process, and not required by Pathology.

Once removed, muscle was coated in Tissue-Tek OCT embedding matrix before freezing on dry ice.

Muscles were then thawed to –25^{o}C, before mounting on a block of Tissue-Tek OCT embedding matrix. Muscle sections were cut to 20μm thickness onto 3-aminopropyltriethoxysilane (APES) coated slides using a freezing cryostat.

Sections were stored at –20^{o}C prior to staining.

2.4 Staining protocols

2.4.1 Topical primary anti-ganglioside antibody staining

Antibody was applied to untreated sections of human or mouse muscle tissue, to demonstrate binding at the NMJ.

Mouse antibodies, human monoclonals, and human red cell eluate were applied topically overnight at 4^{o}C and a further 15 minutes at room temperature. Dilution series determined optimum binding concentrations, which are specified in the text. Serum samples from patients Ch and Ha was applied at 40% concentration using the same incubation protocol.

Normal human serum at 4% concentration was then applied to sections for a further hour. All antibody and serum samples were diluted in PBS.

2.4.2 General staining protocols

a) C3c - Slides containing 8μm sections of tissue were treated with 1:750 Texas Red bungarotoxin (TxR-BTx) (Molecular Probes) and FITC-Goat anti-human C3c (diluted 1:300; Dako, Ely, UK) for 1 hour at 4^{o}C

b) Immunoglobulin - 8μm sections of tissue were treated with 1:500 Texas Red bungarotoxin (TxR-BTx) (Molecular Probes) and FITC-Goat anti-mouse Ig (diluted 1:300; Southern Biotechnology Associates, inc) for 1 hour at 4C

c) Membrane Attack Complex - 8µm sections were treated with mouse anti-human C5b-9 (diluted 1:50; Dako) for 1 hour at 4^{o}C, followed by 1:500 TxR-BTx and FITC-Goat anti-mouse IgG2a (diluted 1:300, Southern Biotechnology Associates, inc) for 1 hour at 4^{o}C

d) Neurofilament – 20µm sections were treated with TxR-BTx (1:500) for one hour at room temperature. Tissue was permeabilised in ethanol for 8 minutes at –20^{o}C then rinsed. Anti-mouse NF (1211; diluted 1:750; Affinity Bioreagents) was added overnight, then goat anti-rabbit IgG (1:300; Southern Biotechnology Associates, inc) was added for a minimum of 3 hours at 4^{o}C.

e) Ethidium analysis – Section C of hemidiaphragm was cut to 20µm thickness, and stained with FITC bungarotoxin (diluted 1:500; Molecular Probes) for 1 hour at room temperature.

After staining, all slides were mounted in Citifluor antifade (Citifluor Products, Canterbury, UK) before storage at –20^{o}C until viewing. Unless stated otherwise, experiments were repeated on 3 occasions using 3 different animals. Three non-contiguous sections of muscle were examined on each repeat.

2.4.3 Cholera toxin on muscle

FITC-labelled cholera toxin (1mg/ml; Sigma) was applied to sections of mouse and human muscle sections. Cholera toxin was applied at dilutions of 1:500 in the mouse, and 1:3000 on human tissue for one hour. Solutions were diluted with PBS containing 1:500 rhodamine or Texas Red bungarotoxin (Molecular Probes). Where stated, sections were blocked with copper sulphate in ammonium acetate buffer solution for 10 minutes to reduce lipofuscin background.

After staining, all slides were mounted in Citifluor antifade (Citifluor Products, Canterbury, UK) before storage at –20^{o}C until viewing.

2.4.4 Cholera toxin staining on sciatic nerve

A protocol first described by Sheikh and colleagues (Sheikh *et al*, 1999) was modified for cholera toxin staining in sciatic nerve.

Fibres were teased onto 3-aminopropyltriethoxysilane (APES) coated slides under PBS, and air-dried before immediate use. Slides were then fixed with 2% paraformaldehyde solution in PBS for one hour at room temperature. Working buffer (see solutions appendix) was applied for an hour on ice, before incubating with 1:100 FITC labelled cholera toxin with 1:200 anti-Kv1.1 (Abcam, Cambridge UK) diluted in working buffer overnight at 4^{o}C. Samples were washed five times in working buffer the next day, and rhodamine anti-rabbit IgG (1:100; Southern Biotechnology Associates, inc) in PBS was then applied for one hour.

Where specified, slides were stained with 1:50 FITC labelled peanut agglutinin (PNA, L7381, Sigma) and 1:100 FITC labelled cholera toxin diluted in working buffer overnight.

After staining, all slides were mounted in Citifluor antifade (Citifluor Products, Canterbury, UK) before storage at –20^{o}C until viewing.

2.4.5 Neuraminidase treatment

Complex ganglioside distribution was demonstrated by use of neuraminidase (N2876, Neuraminidase from *Clostridium perfringens*, Sigma). Sections of muscle or teased fibre sciatic nerve preparations were first pre-blocked with 20µg/ml unlabelled cholera toxin in PBS (Sigma) in PBS for one hour at room temperature to block any existing GM1 ganglioside. Samples were then incubated with 2 units of neuraminidase in PBS for one hour at room temperature before washing in PBS. Samples were then stained for FITC-cholera toxin, or antibody as described previously.

2.5 *In vivo* studies

2.5.1 Animal preparation

Mice were genotyped elsewhere prior to use, and breeding pairs of animals homozygous for B6CG-TgN(Thy 1.1-CFP) and S100-GFP were established (CK mouse, as discussed in section 1.5.3). Litters were weaned at 4 weeks and screened at week 5, by examination of an ear punch under a Leica MZ FLIII fluorescence stereomicroscope with CFP/GFP filter sets. Animals expressing CFP and GFP were retained, and experiments were started on male animals aged 6 weeks.

Animals from homozygote crosses were crossed onto a DBA background strain to produce "heterozygote" offspring. Where specified, these heterozygotes were paired, and ear punches were screened using a fluorescence stereomicroscope to identify animals that only expressed CFP or GFP.

Unless stated otherwise, antibody studies were paired with an age matched control using sterile Ringer solution.

2.5.2 Anaesthesia

In the USA, animals were anaesthetised using intraperitoneal injections of 0.1 to 0.4ml of ketamine and xylazine according to local and federal protocols (17.4mg/ml of ketamine and 2.6mg/ml of xylazine diluted in 0.9% NaCl solution. Both

anaesthetics were obtained from AJ Buck and Son, MD USA). All anaesthesia was conducted under local and Federal protocols.

In the United Kingdom, animals were anaesthetised using intraperitoneal injections (0.1ml/10g body weight) of Hypnoval/hypnorm (Roche Products Ltd, Welwyn Garden. City, UK). Anaesthesia was selected after consultation with Veterinary staff at the University of Glasgow.

In both the United States and the United Kingdom, depth of anaesthesia was assessed by testing for absence of paw, and whisker reflexes. These were checked frequently during the procedure, and anaesthetic doses were supplemented as required.

During the post-operative recovery phase, animals were maintained on the ventilator until reflexes were returned before prompt extubation.

2.5.3 Surgical Procedure

Following induction of anaesthesia, the animal was transferred to the surgical stage and a depilatory cream was applied to the operative area for 5 minutes, before being removed with a cotton swab. In the UK, the surgical stage was then transferred to a heating pad, and the animal was covered in a thermal space blanket to limit hypothermia. The animal was maintained under a heat lamp in the United States.

The surgical site was cleaned with an alcohol solution, and the animal was covered in sterile drapes, leaving the surgical site exposed.

Under strict aseptic technique, a ventral midline incision in the neck exposed the sternomastoid muscle, and trachea (figure 2.1). Animals were intubated endotracheally under direct vision, and hyper-ventilated using a small rodent ventilator (Harvard rodent ventilator, model 683 set to a respiratory rate of 110 breaths per minute and tidal volume of 1.5ml). Hyper-ventilating the animal is not harmful, and results in a pause in respiratory effort when the ventilator is stopped. This limits respiratory movement, and allows for stable image acquisition from the neck area.

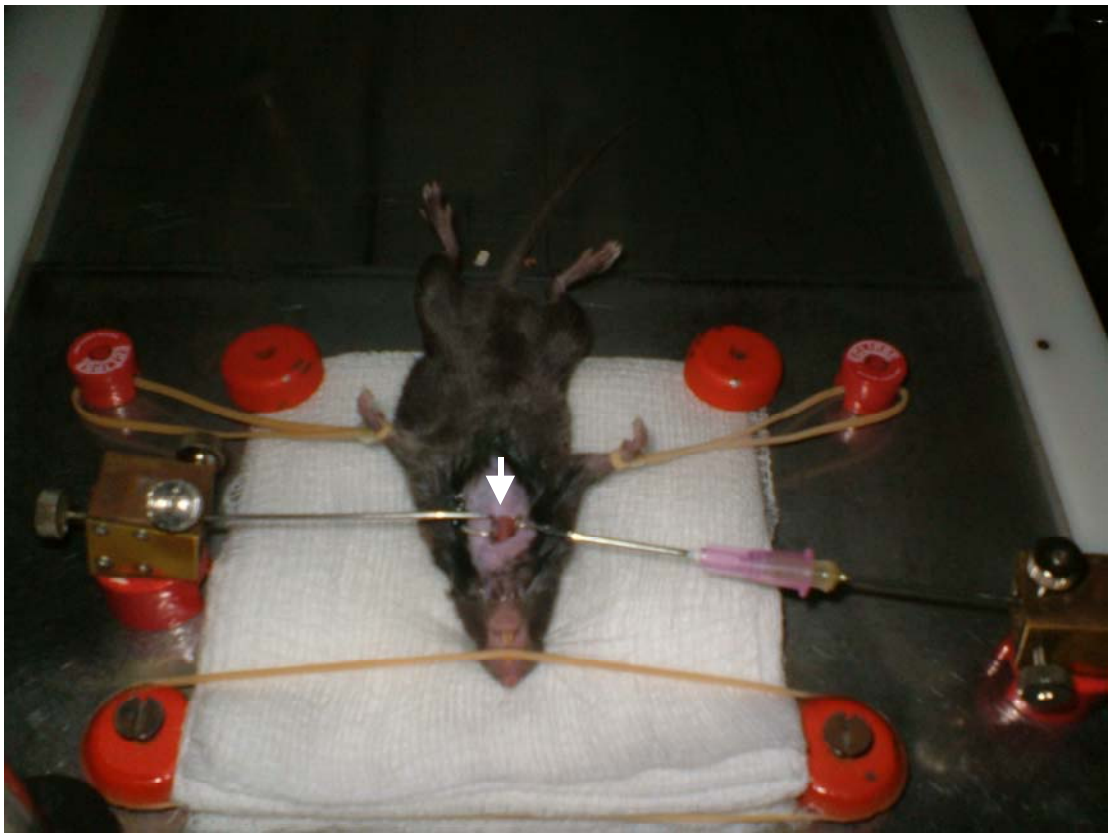

Figure 2.1: Ventral midline incision. Retractors maintain the surgical wound, and the trachea can be visualised directly (arrow) to guide endotracheal intubation.

Under careful blunt dissection, avoiding direct contact with the overlying salivary glands, connective tissue was dissected from the surface of the left sternomastoid muscle. A wire frame was inserted under the muscle to separate connective tissue lying underneath. Care was also taken during this process to avoid any injury to the adjacent carotid artery.

ACh receptors were labelled with either CY5 or rhodamine-conjugated α-bungarotoxin (Molecular Probes, Eugene, OR), in a 5μg/ml solution in sterile Ringers lactate solution (USP, Braun Medical), applied for 5 minutes. Imaging was then performed using the 10x objective to obtain a "map" of BTx labelled end plates, which could then be used to guide repeat imaging in later operations (figure 2.2).

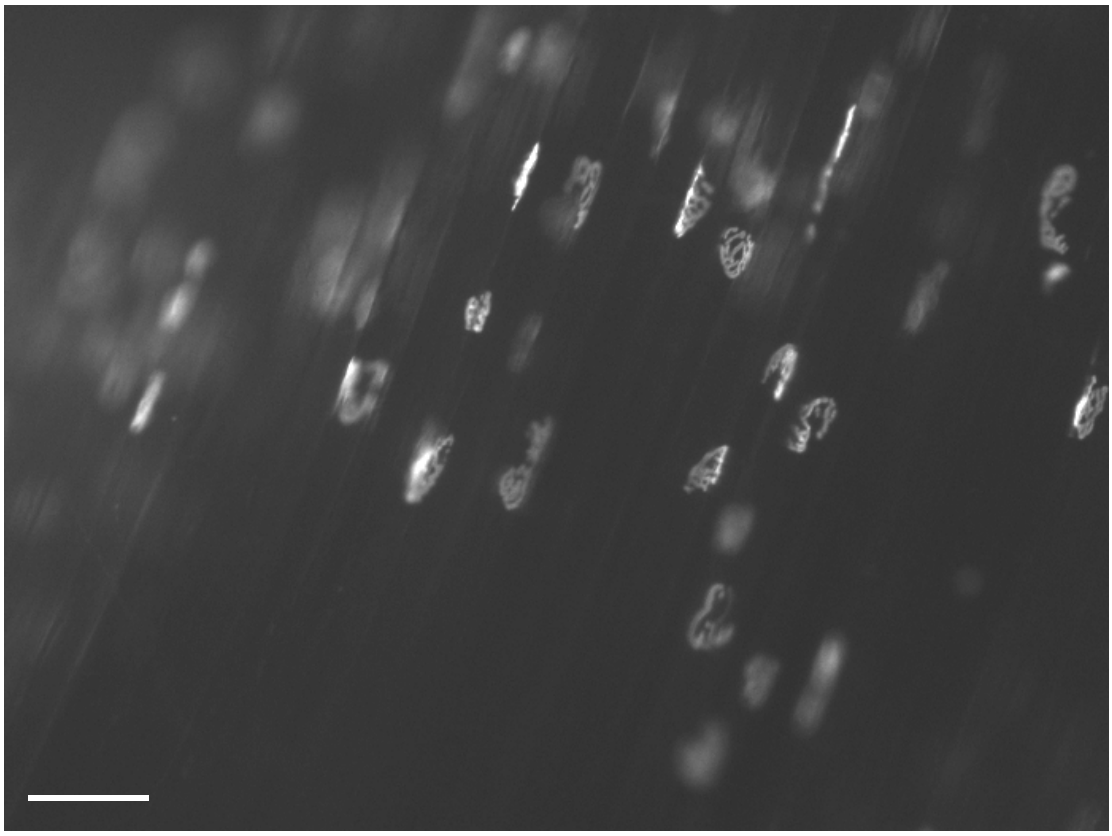

Figure 2.2: Map of sternomastoid after BTx application at 10x. This image was used to locate the same junction during repeat imaging studies (scale bar 50μm).

Antibody EG1 (100μg/ml) or Ringer's lactate (USP, Braun Medical) as control, were applied topically to the sternomastoid muscle for one hour. After washing with Ringer's lactate solution, 40% normal human serum was applied topically for one hour, before a further wash.

When necessary, the nerve to sternomastoid was crushed using standard forceps, at its point of insertion to the muscle, immediately after incubation with antibody and complement. Substances to modify the immune response were applied where specified in the text.

In the United States, the wound was sutured using 6-0 silk, and the animal was recovered under a heat lamp.

In the United Kingdom, the wound was sutured using 6-0 Vicryl, and the animal was recovered by technical staff in a rodent incubator.

Repeat operations were followed using this protocol. Flow charts (appendix 2.1 to 2.6) summarise the incubation protocols used.

Imaging was also performed at the start of each operation using the 10x objective. This allowed a "map" of all NMJs to be taken, which

2.5.4 Whole mount immunostaining

2.5.4.1 Muscle dissection

Under terminal anaesthesia, the animal was perfused with a transcardiac injection of PBS solution. The sternomastoid muscle was dissected, and fixed in 4% paraformaldehyde for 30 minutes, before being washed for 30 min in three changes of PBS. 4,6-diamidino-2-phenylindole (DAPI) (10^{-4}mg/ml) was applied for 7 minutes to demonstrate nuclear staining, and a thin fillet of muscle was then dissected and mounted in anti-fade solution before imaging.

2.5.4.2 Nuclear stains

2.5.4.2.1 Ki-67

Where stated, whole mount sternomastoid was incubated overnight with Ki-67 (AbCam) at 1:200 with 1% triton in PBS following 4% paraformaldehyde fixation. Ki-67 is a monoclonal antibody to the Ki-67 protein, which is detectable in the cell nucleus during the active phases of the cell cycle, but not during the resting phases. The muscle was washed in PBS for 30 minutes before staining with anti-rabbit IgG (1 in 200) for 1 hour with 1:500 rhodamine bungarotoxin. The muscle was then filleted as described earlier.

2.5.4.2.2 BrdU

Where specified, 5-bromo-2-deoxyuridine (BrdU) was used as a marker of cell division (203806; Calbiochem, La Jolla, CA). It was dissolved in sterile Ringer's lactate solution, and injected into the peritoneal cavity (1mg/10g body weight) on a twice-daily basis for 3 days, starting immediately after the first application of antibody. In addition, 1.5mg/ml of BrdU was added to the drinking water of the animals during the same period.

Muscles were fixed in 4% paraformaldehyde as described previously, and permeabilised in methanol at –20^{o}C for 7 minutes before being washed in 3 changes of PBS. Muscles were then denatured in 2N HCl in 0.1M PBS containing 0.3% Triton X-100 for 30 min, before a further PBS wash for 30 minutes. Muscles were incubated overnight in 1:500 rabbit anti-cow S100 (Dako, Carpinteria, CA) and 1:5

mouse monoclonal antibody to BrdU (G3G4, Developmental Studies Hybridoma Bank, Iowa). Following a further PBS wash, 1:400 S-100 rhodamine-conjugated goat F(ab)2 fragment anti-rabbit (Cappel, 55671) and 1:100 fluorescein-conjugated sheep F(ab)2 fragment anti-mouse (Sigma, F-2266) was added for one hour. The muscle was dissected and mounted.

2.5.4.2.3 Ethidium homodimer-1

Ethidium homodimer 1 (EthD-1, Molecular Probes, Eugene, OR) was used as a marker of TSC injury. When required, EthD-1, diluted to 2μM was added to the 40% normal human serum solution for the duration of its incubation, and removed by washing in Ringers lactate before further imaging. Muscle fixation was performed in 4% paraformaldehyde for 15 minutes only, before three, 5 minute washes in Ringers solution otherwise EthD-1 staining was lost. The muscle was then filleted as previously.

2.5.4.3 Schwann cell markers

2.5.4.3.1 Myelin basic protein

Where specified, myelin basic protein (MBP) was used as a marker of myelinating Schwann cells. Muscles were fixed in 4% paraformaldehyde as described previously, and permeabilised in methanol at –20^{o}C for 7 minutes before being washed in 3 changes of PBS. Tissue was then incubated in 1:500 MBP antibody (18-0038, Invitrogen) overnight at room temperature in blocker before being washed 3 times in

blocker over 30 minutes. The muscle was then incubated with a TRITC anti-rabbit IgG (1:250, Southern Biotechnology Associates, inc) for one hour in blocker before being filleted and mounted as previously.

2.5.4.3.2 Nestin

Reactive Schwann cells were labeled using markers for nestin. Nestin is a type VI intermediate filament protein widely used as a marker of proliferating and migrating cells, including those outside the nervous system. Muscles were fixed in 4% paraformaldehyde, and perfused with methanol as described previously. Tissue was incubated in 1:200 anti-nestin (1:200, SCRR-1001; American Type Culture Collection, Manassas, VA) overnight at room temperature in blocker solution before being washed 3 times in blocker. The muscle was then incubated with a TRITC anti-rabbit IgG (1:250, Southern Biotechnology Associates, inc) for one hour in blocker before being filleted and mounted as previously.

2.6 Image acquisition and statistical analysis

2.6.1 Confocal imaging

Quantification of complement and neurofilament deposition of hemidiaphragm preparations was performed on a Zeiss Pascal confocal microscope using standard epifluorescence techniques. Imaging was performed at 40x magnification, with an open pinhole to provide maximum depth of view. Levels were set so no staining was seen on negative controls.

Images were then analysed using either using either Scion Image (Scion Corporation) image analysis software or ImageJ (National Institutes of Health).

Structural analyses of human tissue, hemidiaphragm and triangularis sterni preparations were performed using a Zeiss Pascal confocal microscope with the pinhole set to one Airy unit, and section thickness optimised using existing confocal software. Reconstructions were performed using Voxx (Indiana Centre for Biological Microscopy), or Volsuite 3.2 (Ohio Supercomputer Center) and Adobe Photoshop Pro 8 (Adobe).

2.6.2 Apotome imaging

Other illustrative images were performed at on a Zeiss Axio Imager.Z1 with Apotome. In this system, a grid is used to project stripes of light onto the focal plane of the objective, and shifted laterally in three defined steps relative to the sample. A CCD camera takes images from each step, and computer software reconstructs these images to produce a sharper final image, with out of focus information greatly reduced especially in the z-plane and allowing clearer 3-D imaging (Carl Zeiss website). Reconstructions were performed using Voxx (Indiana Centre for Biological Microscopy), ImageJ (National Institutes for Health) and Adobe Photoshop Pro 8 (Adobe).

2.6.3 In vivo studies

In the United States, images were acquired with a Leica DMRX microscope using both 10x and 40x water immersion objectives, and filter cubes for GFP, CFP, TRITC, and CY5 (Chroma Technology). Neutral density filters were used to reduce the intensity of illumination to the preparation by 50-90%. An integrating CCD camera (Coolsnap HQ, Photometrics, Roper Scientific) was used to capture images that were subsequently processed using IPLab (Scanalytics, Rockville, Maryland USA). Images were taken at various depths in the axial (Z) direction to produce a "manual z stack". The in-focus areas of these images were then combined using Adobe Photoshop (Adobe Systems Inc).

In the United Kingdom, no such *in vivo* imaging facility was available, therefore a new system was developed to comply with Home Office guidelines. Images were acquired with a Leica DM4000 microscope using both 10x and 40x water dipping objectives (HCX APO L 10x/0.3 and HCX APO L 40x/0.8 respectively), and filter cubes for: GFP, CFP, N3, and Y5 (Leica Microsystems). A cooled monochrome camera (Leica DFC350FX) was used to acquire images. The imaging stage was machined from a piece of stainless steel, with holes to allow it to be secured to the existing microscope stage. Magnets secured gauze and intubation equipment to the metal surgical stage.

Reconstructions were performed on Adobe Photoshop (Adobe Systems Inc).

2.6.4 Format of final images

Unless stated otherwise, images are shown in black and white to improve contrast, with a combined colourised image. Text within the figure describes the stain, with the colour of the text corresponding to its colour in the combined image.

2.6.5 Statistical analysis

2.6.5.1 Data accumulation

Unless stated otherwise, all data represents an analysis of 3 separate areas of tissue per experiment, repeated 3 times in different animals.

2.6.5.2 Ethidium analysis

All NMJs stained with bungarotoxin were included in analyses. Junctions with one or more EthD-1 nuclei overlying the bungarotoxin staining were considered positive, and the total was expressed as a percentage of the total number of identified NMJs in the section. Data was compared using Chi-squared tests.

2.6.5.3 Antibody, complement and neurofilament levels

Neurofilament loss was measured as a percentage of bungarotoxin area, and antibody and complement levels were expressed as staining intensity over the bungarotoxin signal using a range from 0 (negative) to 255 (saturation). These values were

calculated using pre-written macros (Peter Humphreys, University of Glasgow) on ImageJ (National Institutes for Health).

Data was compared using the Mann-Whitney mean ranks test. Data was displayed in box-and-whisker plots using Minitab (Minitab Corporation), with outlying data points removed leaving median values, interquartile ranges (box) and 1.5 times the interquartile range (vertical lines).

Chapter 3: Antibody characterisation

3.1 Introduction

Techniques to characterise binding of anti-ganglioside antibodies at the NMJ have been described previously, using both immunofluorescence, and also electron microscopy (Halstead *et al*, 2004; Halstead *et al*, 2005b). These *ex vivo* methods easily identify antibody binding to particular structures within the nervous system, demonstrating the resulting injury to axon and glia, and providing an indication of possible disease pathogenesis.

Neuromuscular morphology was described in these studies by the use of co-staining, to identify both pre- and post-synaptic components of the NMJ and thus localise antibody binding. For example, BTx can be used to identify post-synaptic ACh receptors, while antibodies to neurofilament and S100, found in the nerve and Schwann cells respectively, can be used to demonstrate pre-synaptic morphology. In addition, a reduction in neurofilament co-staining has also been used as a marker of axonal damage, while EthD-1 has been used as a marker of TSC injury (O'Hanlon *et al*, 2003, Halstead *et al*, 2005b).

Using these methods, two IgG3 antibodies were identified that produce selective TSC injury at the NMJ (Halstead *et al*, 2005b). Antibody EG1 was prepared within the Willison laboratory, while R24 is available commercially (American Type Culture Collection (ATCC; Manassas, VA)). Professor Richard Reynolds from Charing Cross Hospital, London, also generously donated a third antibody, LB1. This IgM antibody

is also thought to produce TSC injury, and broadly shares the same ganglioside binding profiles on ELISA as both EG1 and R24 (see table 3.1).

		Disialylated ganglioside specificity		
MAb	**Isotype**	**GT1a**	**GQ1b**	**GD3**
EG1	IgG3	91	$1.8x10^3$	$1x10^2$
R24	IgG3	53	90	$2.5x10^2$
LB1	IgM	N/T	N/B	$5x10^3$

Table 3.1: Antibody specificity on ELISA. Antibodies were titrated in an ELISA against the gangliosides at concentrations ranging from 10^{-2} to 10^{-5} mg/ml, and the reciprocal of the Ab concentration that gave half-maximal binding was calculated (1/50%). Data for EG1 and R24 was kindly supplied by Ms Dawn Nicholl. N/B= no binding on ganglioside ELISA, N/T = not tested.

The aim of this first series of experiments is therefore to identify which antibody is most suitable for producing selective TSC injury at the NMJ, and to characterise its effect at this site.

3.2 Results

3.2.1 Muscle tissue identification for ex vivo *studies*

3.2.1.1 Background

The hemidiaphragm of BALB/c has been used extensively to describe the electrophysiological and structural effects of EG1 and other antibodies at the NMJ (Halstead *et al*, 2005b). In other laboratories, triangularis sterni muscle (a thin thoracic muscle found on the innermost aspect of the rib cage) is used to examine end-plate morphology. Before undertaking more detailed study of antibody effect, hemidiaphragm and TS preparations were compared to identify which would be most suitable for use in later experiments.

3.2.1.2 Muscle comparison

Initial experiments compared the number of NMJs in each muscle preparation to demonstrate which muscle produced the greatest yield of NMJs for statistical analysis. Using *ex vivo* staining protocols described in Methods, end plates were identified using BTx in BALB/c mice, and the number of junctions in each section of muscle tissue was compared.

Three hemidiaphragm preparations were taken from three mice. Each diaphragm yielded 6 areas of muscle. Three distinct sections from the same area of each hemidiaphragm were then examined, giving a total of 9 areas of analysis from 3 mice.

A mean of 93 end plates identified on each cryostat section on the microscope slide (standard deviation of 10.3). In total, at least 558 distinct end plates were available for study across six areas in the diaphragm. However, since these samples were made from 20μm sections of cut diaphragm, they do not include end plates that may lie outwith the sections under study and therefore the total number of available end plates is much higher in this muscle.

Three TS muscles were taken from 3 mice, and the entire muscle was examined. Each TS muscle could be divided into 4 areas, with a mean of 60 end plates in each area (standard deviation of 0.76), yielding an approximate total of 240 end plates across the muscle in total. As the muscle was not sectioned, this represents the total number of end plates available for study in this muscle.

This study shows that hemidiaphragm preparations clearly have a greater number of NMJs, making it more suitable for statistical analysis than TS muscle.

3.2.1.3 Morphological analysis

Hemidiaphragm and TS muscles were then compared using *ex vivo* staining techniques described in Methods, to identify which muscle was most suitable for morphological studies. Both muscles were stained for post-synaptic ACh receptors using BTx as described in Methods. In TS, the majority of junctions were flat, and the morphology was obvious. However, in hemidiaphragm, a number of junctions were sectioned, and it was not possible to visualise the entire junction. The text denotes the

type of stain, and its corresponding colour on the combined image as described in Methods. This is used throughout the thesis, unless stated otherwise (fig 3.1).

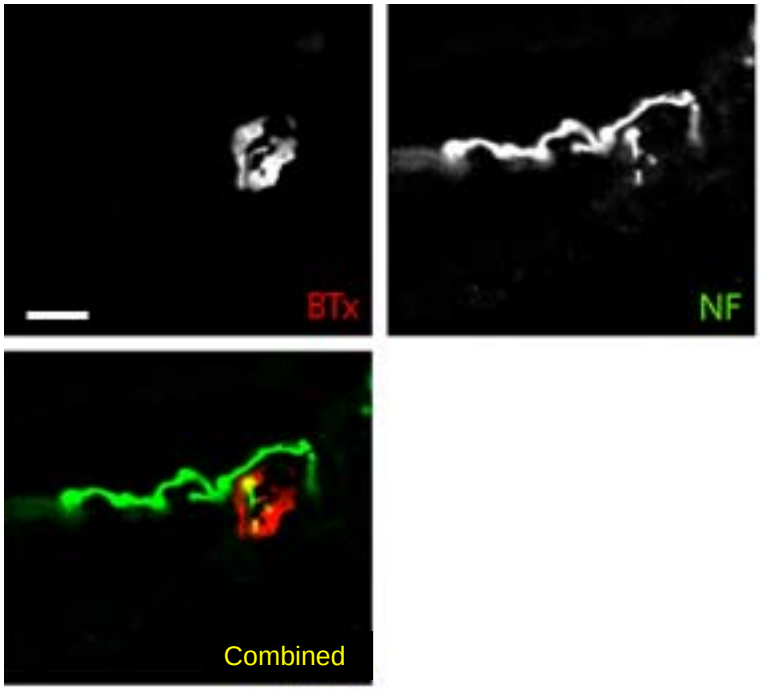

Figure 3.1: Hemidiaphragm sections of BALB/c mouse. Texas red BTx was used to identify end plates, with neurofilament to identify the axon. Although the innervating nerve is seen, its distribution does not exactly correlate with BTx at the NMJ, suggesting that sections of the NMJ are missing from this section. (Scale bar 30µm).

S100 is a common cytosolic marker used to identify Schwann cells, and is useful for studying the morphology of the NMJ. In the TS muscle of BALB/c, an incubation protocol outlined in Methods produced images shown in fig. 3.2. This clearly demonstrates several morphological features of the NMJ. Numerous attempts to stain

the hemidiaphragm of BALB/c using S100 did not produce significant staining, despite different protocols and staining solutions being used. This confirms that TS muscle is more suitable than hemidiaphragm preparations for visualising the NMJ, and performing morphological studies.

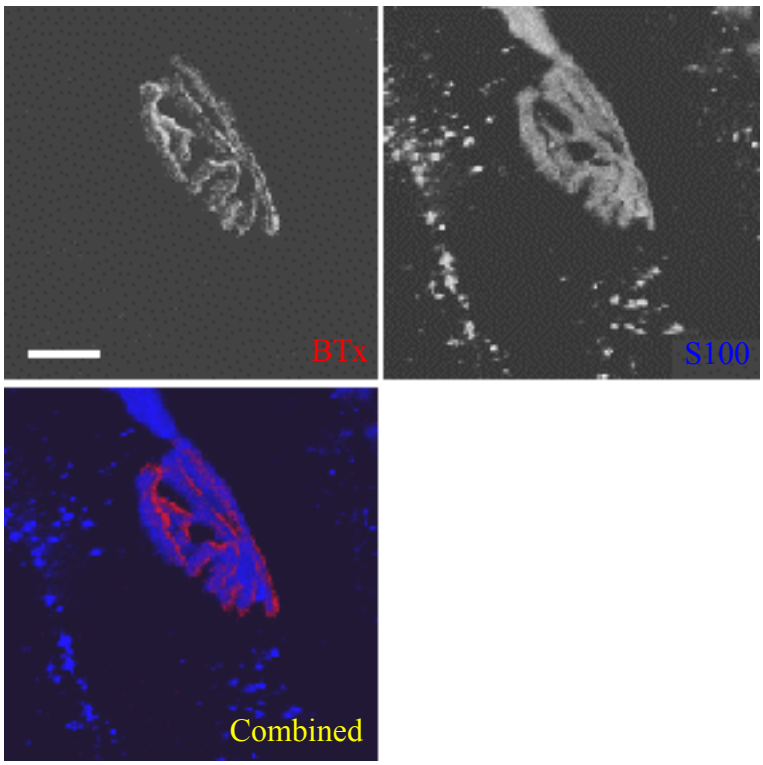

Figure 3.2: Image of single NMJ from the TS muscle in a BALB/c mouse. Texas red BTx demonstrates post-synaptic specialisations. The entire NMJ can be seen in contrast to hemidiaphragm sections. S100 positive cells are stained blue. TSCs overlie the bungarotoxin signal (Scale bar 20µm).

3.2.1.4 Strain comparison

Previous studies using antibodies to complex gangliosides in NIH mice did not describe TSC injury (O'Hanlon *et al*, 2000) while later work using the same antibodies in different mouse strains (BALB/c and C57Bl/6) did describe TSC damage (Halstead *et al,* 2004). To explore this in greater detail, *ex vivo* hemidiaphragm preparations were taken from a series of mouse strains using techniques described in Methods, and the effects of a well characterised antibody to complex gangliosides, which is known to injure both TSCs and axons (CGM3), was studied. This data demonstrates that, while NIH mice do not have obvious TSC injury, damage is evident in the other mouse strains under consideration (figure 3.3). As a result, NIH strains were avoided where possible in later experiments.

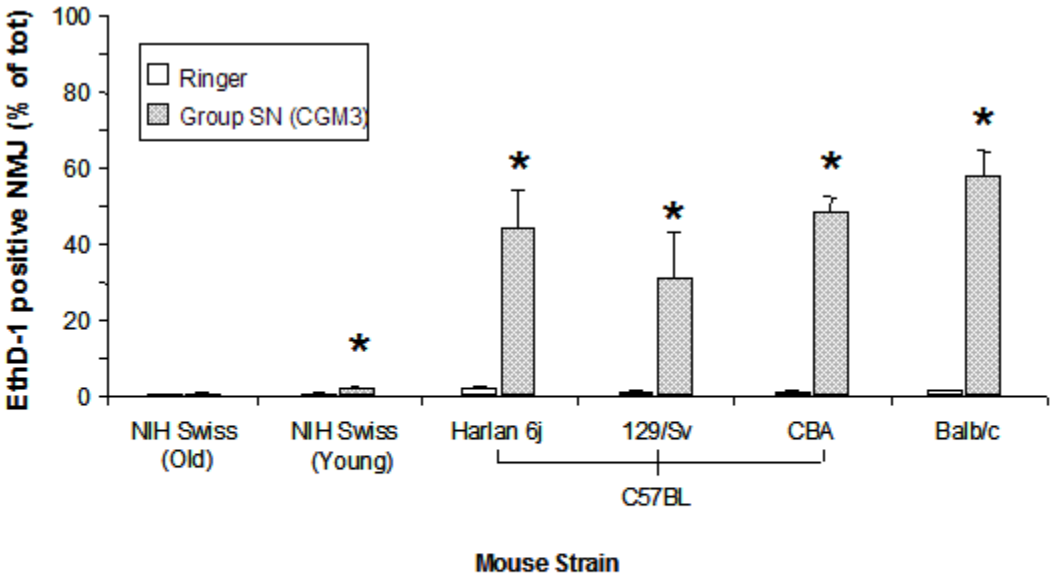

Ringer NMJ	2675	2834	2411	1982	2378	2266
CGM3 NMJ	2994	3355	2214	2134	2224	2755

Figure 3.3: Inter-strain comparison of TSC susceptibility to CGM3 mediated injury. Diaphragms from Harlan, C57Bl/6, 129/Sv and CBA (both crossed onto the C57Bl/6 background); NIH Swiss old and young, and BALB/c mice were exposed to CGM3 and NHS, using EthD-1 uptake to identify TSC injury. Boxed numbers indicate the total number of NMJs assessed per experimental condition. TSC injury is virtually absent from NIH strains (data published in Halstead et al, 2005b).

3.2.2 Antibody selection

The effect of the antibodies at the NMJ was quantified, in an attempt to identify which antibody injures TSCs at the most NMJs. The antibody producing the greatest effect would therefore be most suitable for further study.

3.2.2.1 Antibody growth and purification

Before undertaking *ex vivo* studies, antibodies were first grown, purified and, where possible, concentrated using protocols outlined in Methods. Antibody growth takes place over several weeks, and despite taking place in a sterile environment, was often complicated by infection that resulted in destruction of the hybridoma and antibody.

Twice monthly ganglioside ELISAs were performed on the cell compartment medium, to ensure the continued viability of the cell line as described in Methods. A graphical representation of the resulting dilution series ELISA is shown using Excel in figure 3.4.

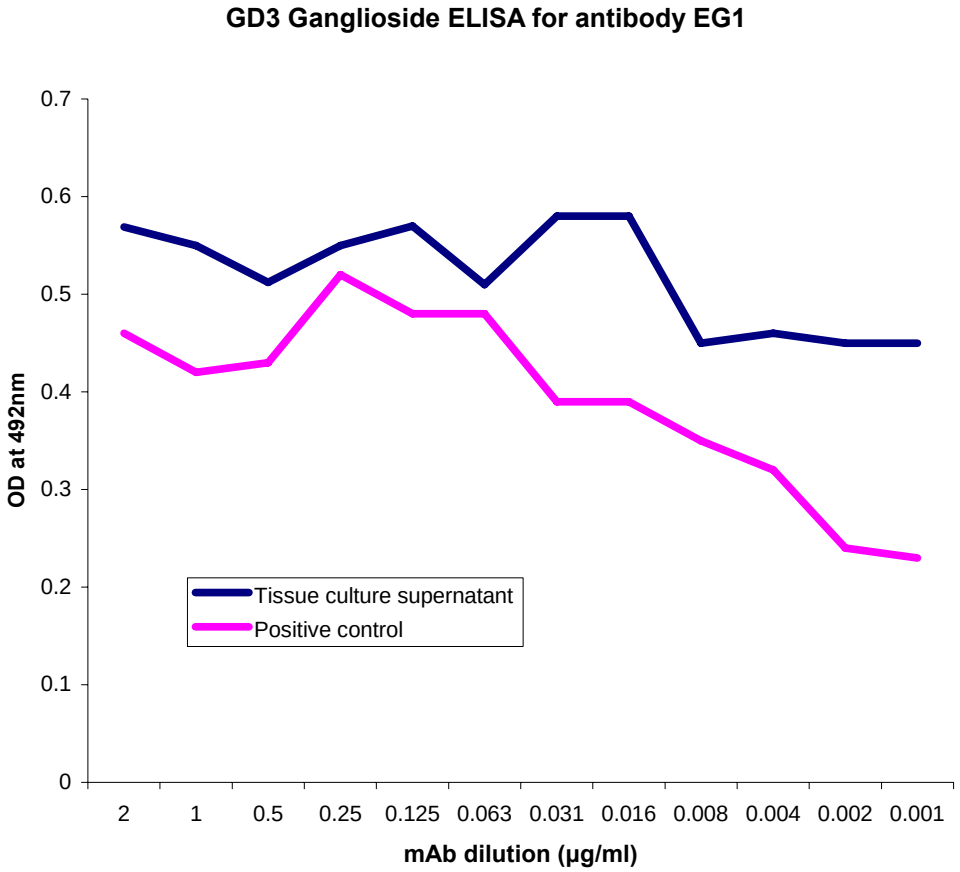

Figure 3.4: Ganglioside ELISA from tissue culture supernatant. The optical density of the tissue culture supernatant is compared against a stock sample of antibody as positive control. The presence of antibody to GD3 ganglioside was used to confirm cell line viability. A similar graph was created for LB1, using GD3 IgM ELISA kit.

Having prepared suitable volumes of antibody over a period of several months in tissue culture, the harvested nutrient medium of EG1 was purified using protein A affinity chromatography as described in Methods (LB1 could not be purified using this technique). Filtered and dialysed nutrient medium solution was passed through the column, and the flow through was collected before the column was washed, and

then eluted. At regular intervals, the resulting solutions were retained, and an OD280nm was performed, to prevent unintentional loss of antibody. The results of these OD measurements are shown in figure 3.5. These data were confirmed using ganglioside ELISA, shown in figure 3.6.

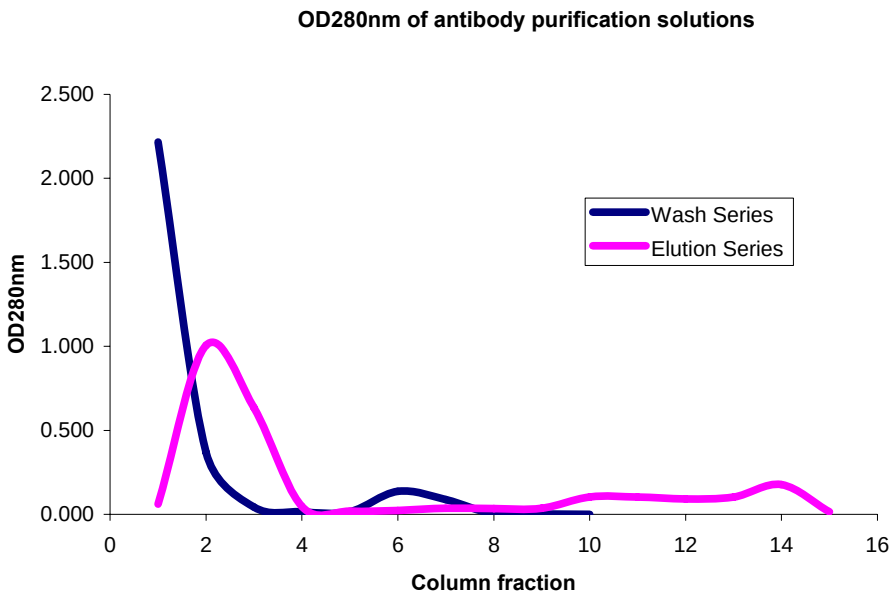

Figure 3.5: OD280nm measurements of antibody purification solutions (flow through not shown). The OD280nm is high for the first column volume in the wash series, this sample did not test positive for antibody on ganglioside ELISA, and represents impurities from the filtered nutrient solution being cleared from the column. In the elution series, the OD280nm peaks between samples 2 and 3, suggesting that the majority of antibody was eluted during these intervals.

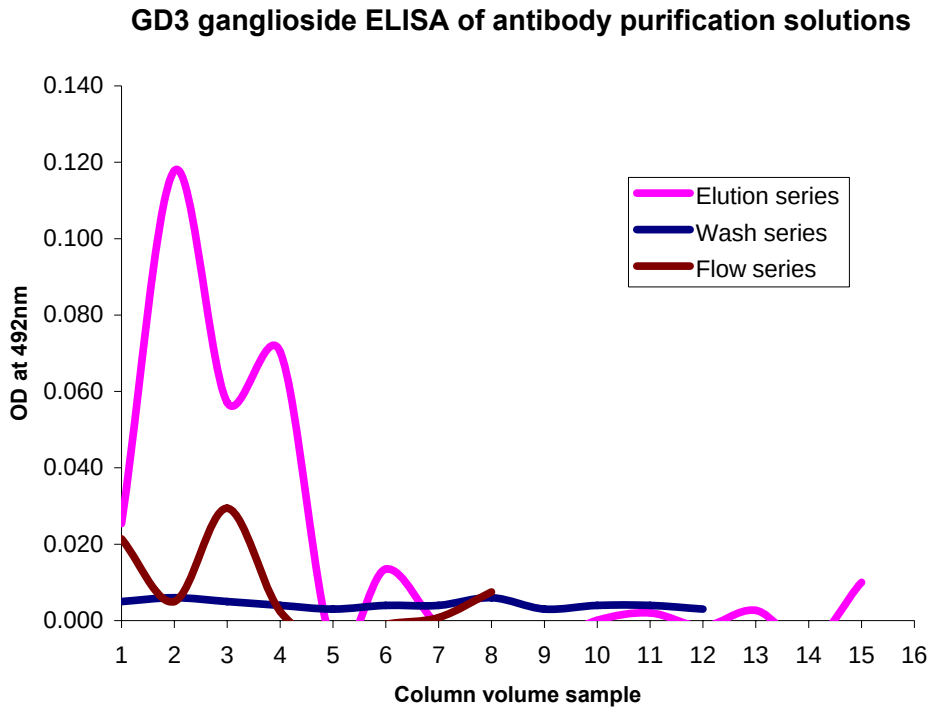

Figure 3.6: Ganglioside ELISA of antibody purification solutions. Antibody to GD3 ganglioside is seen in samples 2-4 in the elution series, but not in the wash series or flow series. This supports observations from the OD280nm study.

Samples 2 to 4 from the elution series were then combined, and the concentration of the resulting antibody solution was measured using quantitative ELISA, as described in Methods, and confirmed using OD280nm to exclude any variability that may result from ELISA. An example of a standard curve for quantitative ELISA is shown in figure 3.7.

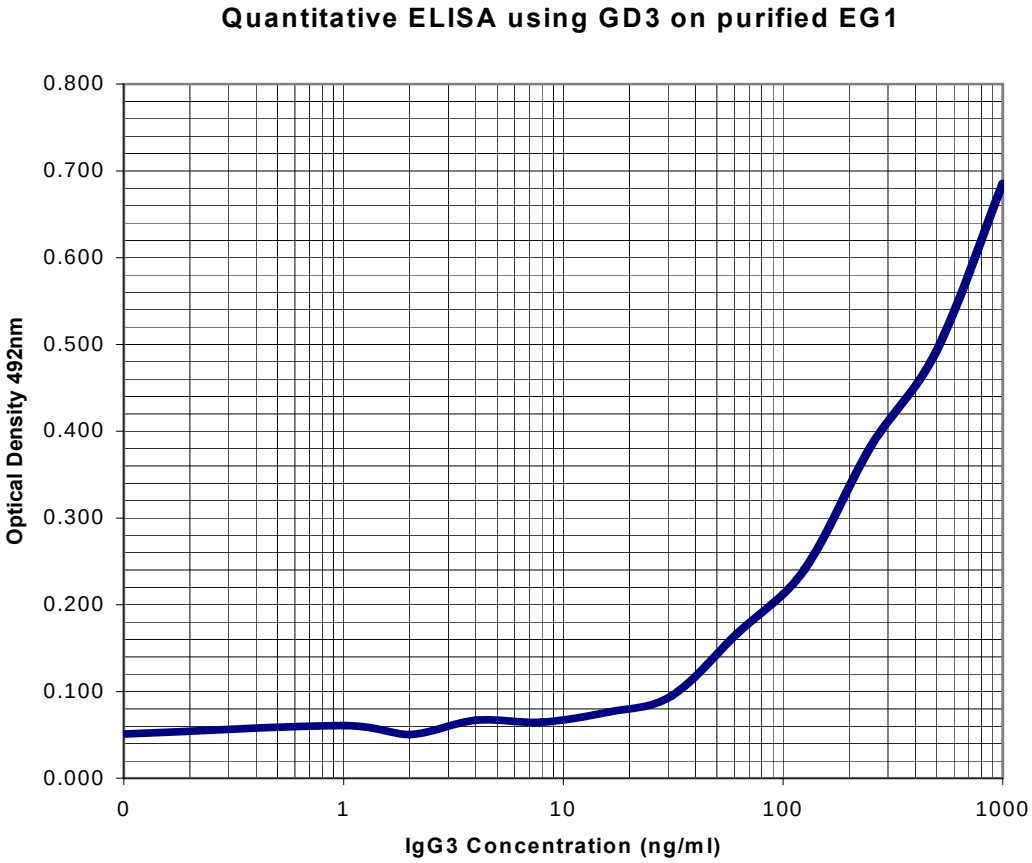

Figure 3.7: Standard curve for quantitative ELISA measurements.

With the assistance of Mr Eric Wagner, the success of the purification process was assessed using an SDS page gel, using techniques outlined in Methods. In this study, samples of purified and quantified antibody solution were run through an SDS page gel, and compared to previously purified samples, as seen in figure 3.8.

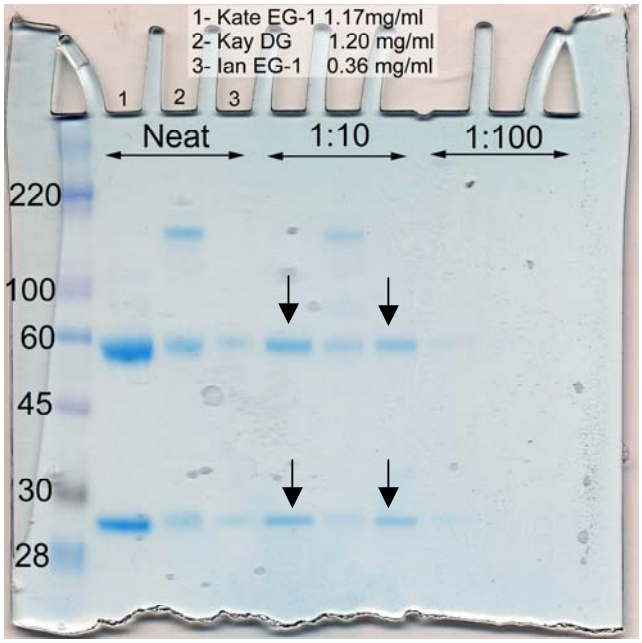

Figure 3.8: SDS PAGE gel of purified antibody EG1 (compared to stock sample – Kate EG-1). The freshly purified sample is comparable to existing stocks, as both show similar heavy and light chain bands on electrophoresis (arrows). A third antibody (Kay DG) is shown, as a control.

3.2.2.2 Terminal Schwann cell injury

Ex vivo hemidiaphragm studies were undertaken using pre-established concentrations of the antibodies under study (100µg/ml for EG1 and R24, and 60µg/ml for LB1), using protocols to measure TSC injury described in Methods with three preparations from 3 mice for each condition. The number of NMJs with TSC damage was determined by using EthD-1 as a marker of TSC injury, and displayed graphically using Excel.

These studies demonstrated that all antibodies produced significant TSC injury at the NMJ, compared to control (fig 3.9). Both EG1 and R24 produced statistically similar effects, and these data are consistent with earlier characterisation studies (Halstead *et al*, 2005b). There is no statistical difference between the mAbs investigated.

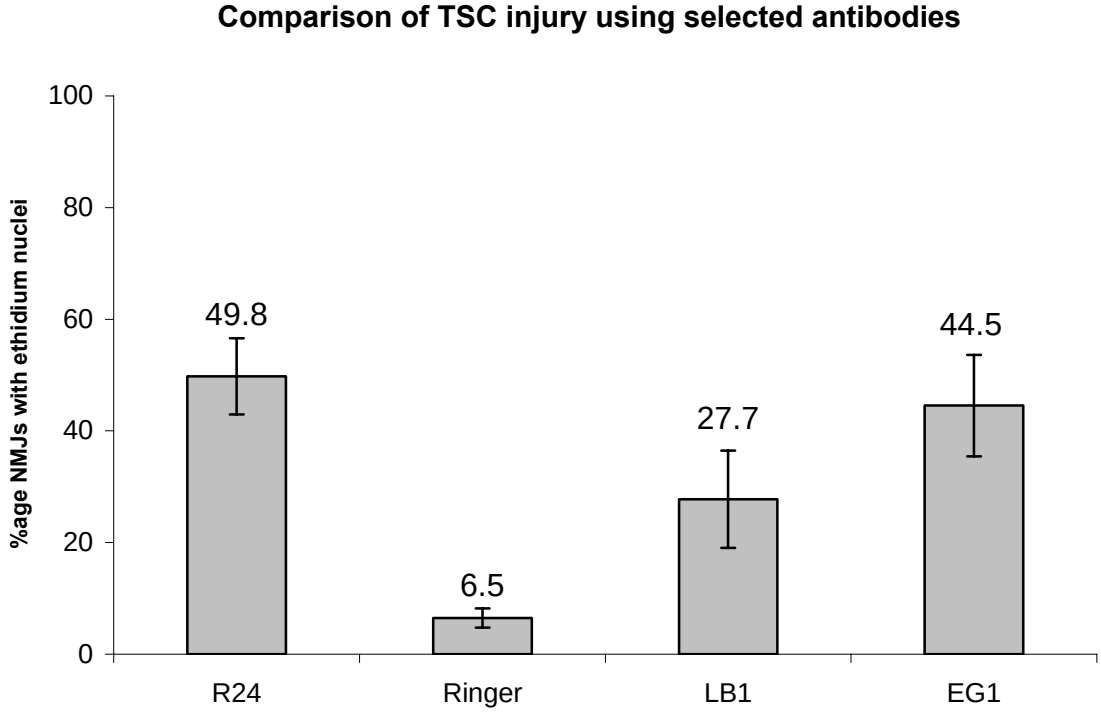

Figure 3.9: Comparison of TSC injury using selected antibodies. These data suggest that EG1 and R24 produce comparable levels of TSC injury (p value=0.652) while LB1 also produces damage, but not to the same extent (p=0.065 for LB1 and R24, and p=0.203 for LB1 and EG1). Mean of 3 hemidiaphragm preparations from 3 mice is shown as a value in the graph, with standard error of mean as error bars.

3.2.2.3 Complement activation products

As damage to TSCs is mediated by complement, measurements of complement activation products C3c and MAC were also made, using *ex vivo* incubation protocols and complement deposition indices described in Methods, and displayed in box-and-whisker format using Minitab. This study further illustrates the extent of antibody-mediated injury, by showing which antibody can activate complement, and thus direct the immune system to the greatest extent. This would also help to clarify data obtained from earlier EthD-1 studies.

Findings from these experiments support data obtained from EthD-1 studies, and show that EG1 and R24 produce similar levels of activation of C3c, while LB1 does not appear to activate complement to the same extent. More MAC is present with antibody EG1 than either R24 or LB1. Data is displayed graphically using Minitab, and represents pooled data from 3 hemidiaphragm preparations from 3 mice as described in Methods (figure 3.10 and 3.11).

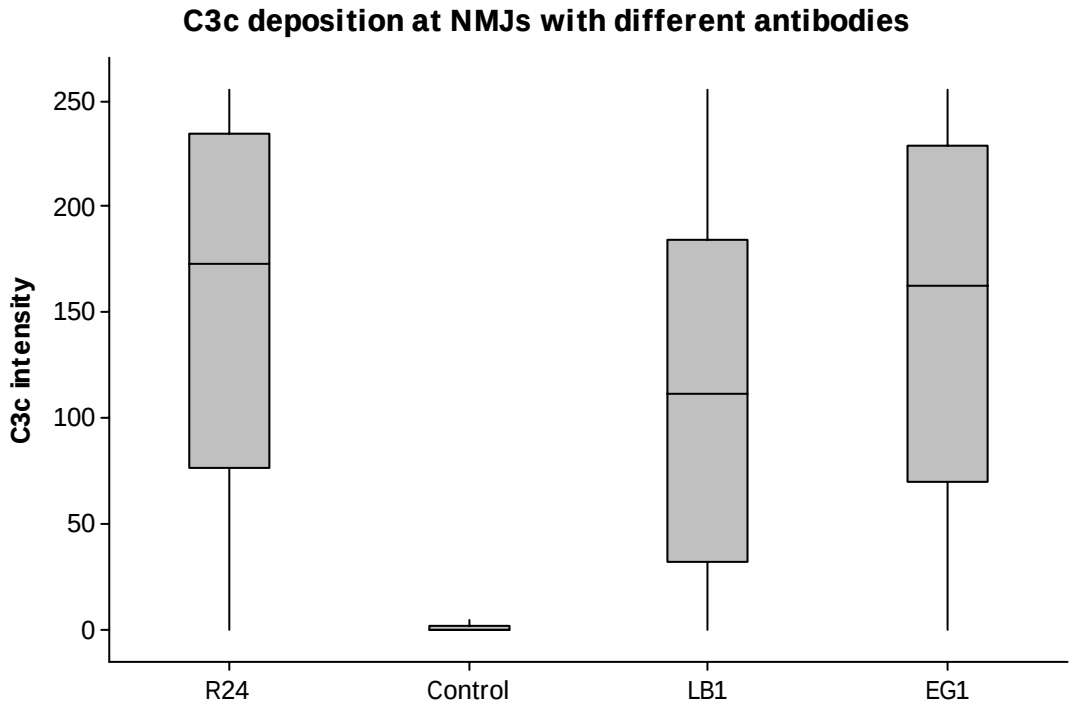

Figure 3.10: C3c deposition at the NMJ with selected antibodies. There is not a significant difference in C3c deposition between EG1 and R24 ($p=0.77$) while LB1 is significantly lower than EG1 or R24 ($p<0.05$). Pooled data from 3 hemidiaphragm preparations from 3 mice is displayed in box-and-whisker plots as intensity of C3c over bungaratoxin staining, measured using ImageJ as described in Methods. Outlying data points are removed, leaving median values, interquartile ranges (box) and 1.5 times the interquartile range (vertical lines).

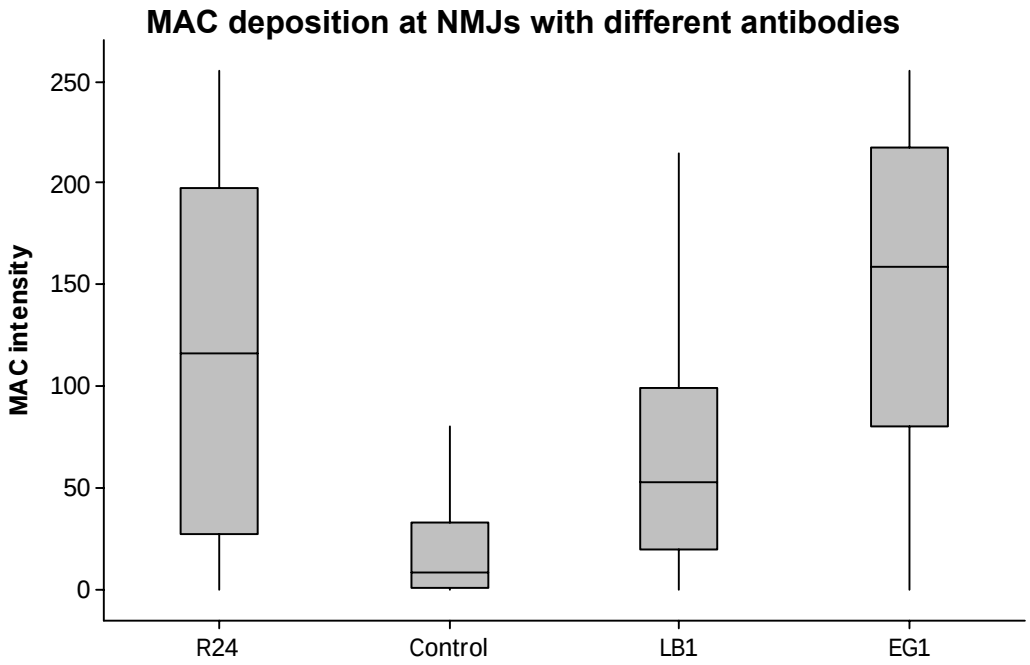

Figure 3.11: MAC deposition using selected antibodies. There is significantly less MAC present on LB1 than either EG1 or R24 ($p<0.01$). There is more MAC deposited on EG1 than R24 ($p=0.01$). Pooled data from 3 hemidiaphragm preparations from 3 mice is displayed in box-and-whisker plots as intensity of MAC over bungaratoxin staining, measured using ImageJ as described in Methods. Outlying data points are removed, leaving median values, interquartile ranges (box) and 1.5 times the interquartile range (vertical lines).

3.2.3 Antibody Characterisation

3.2.3.1 TSC identification

Before undertaking studies to determine the proportion of TSCs injured by the antibody at each NMJ, a reliable cellular marker of TSCs in an *ex vivo* muscle preparation was sought. As shown previously, hemidiaphragm preparations identify a large number of junctions, which is useful for statistical analysis. However, this method does not describe the number of TSCs injured by the antibody, as it is seldom possible to fully visualise NMJ morphology. This prevents hemidiaphragm preparations being used in these experiments.

Although TS can be used for morphological studies, and would be ideal for these characterisation experiments, the marker for TSCs in this muscle (S100) is impractical following antibody-mediated injury as it leaches from TSCs through MAC pores created by complement activation. However, a cell marker (Sytox Green) was identified that does not leach from the cells following antibody-mediated injury. Its suitability for use in these studies was therefore tested in the TS preparation.

Sytox Green is a membrane impermeant nuclear marker, and was used in these studies to stain the TSC nuclei in *ex vivo* TS preparations as described in Methods. The Sytox signal is easy to identify, and co-localises with EthD-1 (figure 3.12) without leaching from the cell following antibody-mediated injury, like S100. Using Triton X-100, the marker can penetrate cell membranes, and label virtually all cell nuclei so the location, and number of cells can be identified at the junction.

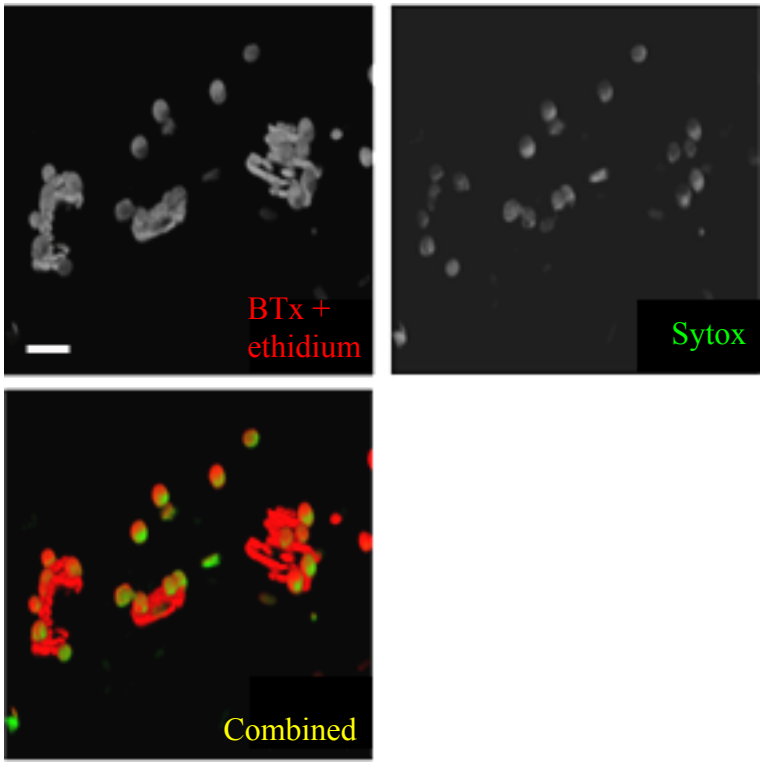

Figure 3.12: Image of staining obtained using Sytox green. Image taken from TS muscle of BALB/c mouse, incubated with EG1 and NHS. Texas red BTx and EthD-1 are shown in red, with Sytox in green. Note the correlation between Sytox and EthD-1 (Scale bar 20µm).

Studies characterising the morphology of the junction were therefore undertaken using Sytox green. Using data from previous experiments with S100 at the NMJ, criteria were developed to identify which nuclei were most likely to correspond to TSCs using confocal microscopy. These criteria were the presence of nuclei lying directly next to the convex surface of BTx, as it overlies the muscle. Nuclei were excluded if they were not immediately adjacent to the BTx signal, or were on the muscle side of the end plate. Other nuclei were not analysed if they did not clearly

meet the criteria for analysis. Unlike S100, however, Sytox is not specific for Schwann cells and labels all nuclei in the TS muscle when used with Triton X-100. Although not formally quantified, no more than 5 NMJs were discarded during each analysis (from 42 junctions) because their associated nuclei did not meet the criteria for inclusion, representing 12% of all junctions in the preparation. Generally, these junctions were excluded as their NMJ morphology made it difficult to identify the convex side easily. This technique was then tested to confirm that it produced results, which supported previously published data on this area.

The number of TSCs at each NMJ was assessed by counting Sytox positive nuclei immediately overlying each end plate from 3 TS preparations taken from 3 different mice. Data was pooled, and displayed graphically as a frequency histogram using Minitab. In these investigations, the number of TSCs at each NMJ follow a normal distribution, with a mean of three TSCs per end plate (figure 3.13).

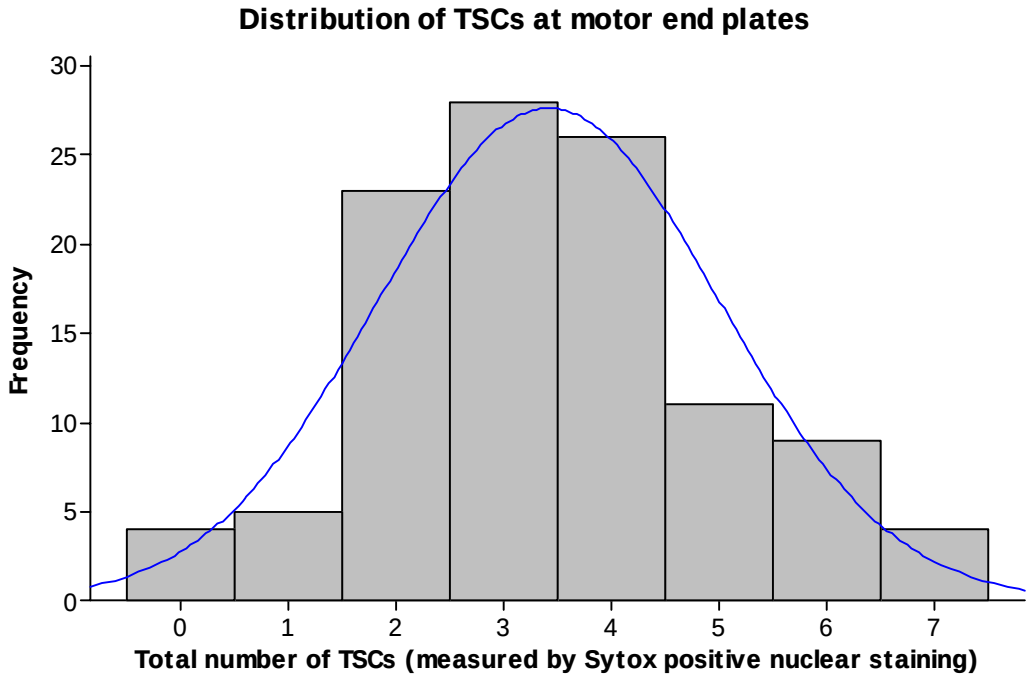

Figure 3.13: Frequency histogram of TSCs at each NMJ using DAF1/CD59a double KO TS preparations, assessed by counting Sytox positive nuclei immediately overlying each end plate. The number of TSCs overlying each end plate follows a normal distribution, with a mean of 3 (standard deviation 1.5).

The long axis of the BTx signal was also measured when counting the number of Sytox nuclei overlying each end plate, and this demonstrated a proportional relationship between the number of TSC nuclei and end plate length, suggesting that larger end plates have more overlying TSCs. This data is displayed graphically using Minitab (figure 3.14).

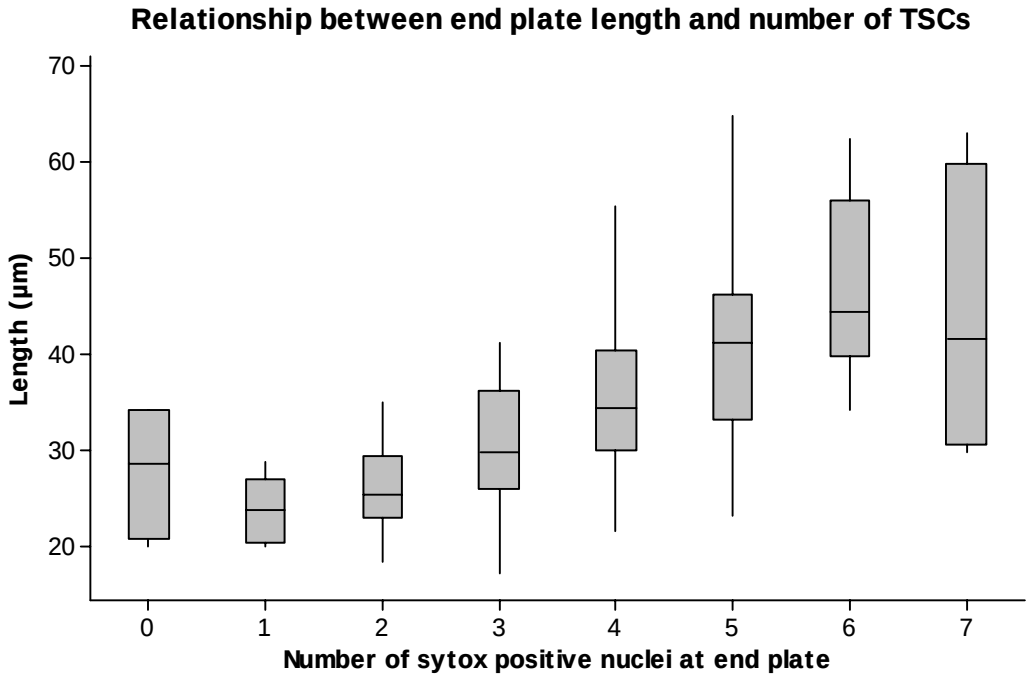

Figure 3.14: Relationship between end plate length and number of TSCs. Using DAF1/CD59a double KO TS muscle preparations, a proportional relationship between end plate length and number of TSC nuclei is demonstrated (R^2=78.3%). When NMJs with no Sytox staining are removed from the regression, the relationship is more significant (R^2=86.8%). Data is displayed in box-and-whisker format using Minitab. Outlying data points are removed, leaving median values, interquartile ranges (box) and 1.5 times the interquartile range (vertical lines).

3.2.3.2 Antibody effect

Using this new Sytox technique, the effect of the antibody was further characterised by studying the proportion of TSCs that were injured at each junction in the TS muscle preparation by antibody EG1. Three TS muscles from 3 BALB/c mice were

incubated with antibody, NHS and EthD-1, and were then treated with Sytox following fixation as described in Methods. The nuclei of TSCs binding Sytox was compared to EthD-1 nuclei at each junction, providing an indication of the proportion of TSCs damaged at each NMJ.

This study demonstrated that a mean of 86% of NMJs from the 3 TS preparations (SEM = 4.3) had evidence of TSC injury (150 from 174 junctions in 3 animals). A median quartile of 75% of TSCs were damaged at each NMJ (Q1=50%).

3.3 Discussion

3.3.1 Muscle tissue identification

Although *in vivo* studies would be performed using the sternomastoid muscle in the CK mouse, it was not possible to use this preparation during the early stages of this investigation for a number of reasons. In particular, the animal strain was not available at the time in the United Kingdom, permission was not available for animal surgery, and it is difficult to maintain the sternomastoid muscle *ex vivo* during incubation protocols without causing muscle fibre damage. Unlike the hemidiaphragm or triangularis sterni muscles, it is not possible to remove sternomastoid with its supporting bone or tendon sheaths intact and therefore it is difficult to maintain appropriate tension on the muscle for the period required for antibody incubation. As a result, alternative muscles were sought that would allow testing of antibodies.

Two commonly used muscles in anti-ganglioside antibody binding studies in the Willison laboratory are hemidiaphragm muscle and TS. Both muscles are located in the thoracic cavity, and are easily dissected with supporting bone to maintain muscle tension *ex vivo*. A comparison study was therefore undertaken to determine which would be most suitable for antibody studies.

TS muscle was selected to investigate the morphological effects of the antibody on the NMJ *ex vivo* as it offered the best images and did not require sectioning to image NMJs. Although the hemidiaphragm had a large number of NMJs, it was not possible to stain for S100, a key morphological marker at this site. Unlike the TS muscle, which is a whole mount preparation, the hemidiaphragm is sectioned prior to analysis and this often results in sectioning through NMJs. This can damage the TSCs, producing leaching of the cytosolic contents into the extracellular space, preventing staining with S100. Although it would be possible to stain the hemidiaphragm muscle as a whole mount, the thickness of the muscle limits the quality of image obtained, and therefore TS was used for morphological analysis.

However, sectioning the hemi-diaphragm does yield a large number of NMJs that can be used for analysis of neurofilament injury, and complement and immunoglobulin deposition, using established techniques for analysis (O'Hanlon *et al*, 2003). The number of available NMJs can therefore maximise the statistical significance of any data, while reducing the number of animals required for each study in compliance with Home Office guidelines. As a result, the hemidiaphragm was used to screen antibodies, measure the effect of the antibody on the components of the nerve terminal, and establish staining protocols.

It is also interesting to note that NIH mouse strain TSCs are insensitive to the effects of antibody CGM3, despite axonal sensitivity. Preliminary work by colleagues in the laboratory suggests that ganglioside composition is different between BALB/c and NIH, as immunoglobulin deposits of CGM3 are lower at the NMJs of NIH mice than BALB/c (Dr Sue Halstead, personal communication). Although further study of this area was outwith the scope of this investigation, it would be interesting to explore this in greater detail.

3.3.2 Antibody selection

A series of antibodies with similar binding properties on ELISA were previously identified for their ability to selectively injure TSCs. These antibodies were either commercially available (R24), or grown in the laboratory, from hybridomas developed in the Willison laboratory (EG1) or from the Reynolds laboratory (LB1). Both R24 and EG1 are IgG antibodies, while LB1 is an IgM antibody.

Experiments show that the TSC killing effects of both R24 and EG1 are broadly similar. Although LB1 injures fewer TSCs, this difference does not reach statistical significance. The reduced effect of LB1 is also seen when examining complement activation products at the junction, with both R24 and EG1 activating more C3c and MAC than LB1.

This is an unexpected result, as LB1 is an IgM antibody with a pentameric structure that has more potential binding sites than a corresponding IgG antibody. However, it was used at a lower concentration than both R24 and LB1, and this may explain the

difference in effect. It was not possible to compare LB1, R24 and EG1 at the same concentration as it was impossible to concentrate LB1 beyond 60μg/ml. IgG antibodies can be purified and concentrated using a protein A column, but this technique cannot be used for IgM antibodies. Protein A binds to the Fc of IgG, but the pentameric structure and disulfide bonds of IgM antibodies mask the Fc site. As a result, LB1 cannot bind to protein A columns and other less effective methods e.g. Vivacell concentration columns, must be used instead. These methods only concentrate, rather than purify the antibody. LB1, despite being easily grown in the laboratory, was not considered for further use.

Interestingly, EG1 appears to activate more MAC at the NMJ than other antibodies, despite having similar levels of C3c and EthD-1 injury as antibody R24. MAC is the final common pathway of complement activation, and is responsible for the injury with antibody EG1. It is not clear why more MAC should be present with EG1, but it suggests that it is more capable of activating the complement cascade to produce TSC injury.

Although the effects of R24 and EG1 on TSCs were not statistically different, EG1 was selected for use in later experiments, as it was developed in the Willison laboratory, it activated MAC more efficiently than other antibodies, it could be easily grown from existing hybridoma lines, and the resulting antibody could be purified through a protein A column for further use.

3.3.3 Antibody Characterisation

Previous work characterising the effect of EG1 used *ex vivo* hemidiaphragm preparations to identify the number of NMJs with evidence of TSC injury. Although this data is statistically very robust, and a strong method for identifying, and comparing antibody effect, it does not consider the number of TSCs injured at each junction. However, this information would be very useful, as removing all the TSCs from a junction would permit observation of the NMJ in their absence, giving an important insight into TSC biology, and also the junction's response to this form of injury, which may occur in MFS. As a result, experiments were conducted to identify the proportion of TSCs damaged by the antibody at each junction, using antibody EG1.

Before these studies could be performed, an accurate method of identifying TSCs at the NMJ had to be developed. Unfortunately, it was not possible to obtain the CK mouse model at the time of these studies, and other methods were therefore devised to identify these cells. A reliable Schwann cell stain is S100, which is a low molecular weight calcium binding protein of uncertain significance. It was hoped that staining with this marker would demonstrate all the TSCs at the NMJ of TS, and this could then be correlated with EthD-1 nuclei showing TSC injury. However, early studies with antibody EG1 showed that S100 staining was lost following antibody-mediated injury. Following antibody injury, pores are formed in the membrane of the cell, causing loss of cytoplasmic contents (including S100) into the extracellular compartment, at the same time as calcium ingress. As a result, S100 staining was not reliable, and it was not felt to be an appropriate co-stain for these studies.

It is known that the TSC nucleus remains intact for at least the first hour following injury, as staining using the nuclear marker EthD-1 persists, and is used as a marker for TSC injury. Nuclear stains other than EthD-1 were therefore considered as possible co-stains. Early studies used DAPI, but it was difficult to correlate DAPI staining accurately with structural markers at the NMJ, as it was not possible to confocal this stain, and analysis had to be performed under epifluorescence microscopy.

Sytox green was identified as an alternative. This nuclear stain has been used extensively for studies of the cellular apoptosis in a similar manner to EthD-1, but has a distinct absorption and emission spectrum from EthD-1, and unlike DAPI can be examined under the laboratory's confocal microscope with existing filters. Sytox also has an emission peak at 523nm, and can be examined through the FITC filter set of the confocal microscope, while EthD-1, with its emission wavelength of 617nm can be examined using a TRITC filter set. By using laser stimulation to take z stacks through each junction, images can be constructed of TSC nuclei, and correlated with EthD-1 staining.

Like EthD-1, Sytox green is a membrane impermeant dye, so that protocol was devised to facilitate cell penetration during tissue processing, using Triton X-100 as a permeabilising agent. The detergent disrupted the cell membranes in previously fixed tissue, allowing access and binding of the dye to the cell nucleus. This method however, resulted in very non-specific nuclear staining and identified nuclei belonging to many other tissue types, including myonuclei and fibroblasts. Previous

experiments in the laboratory identified strict criteria for describing TSC nuclei in TS muscle, by staining with S100. These criteria were applied to the Sytox Green method, and in most examples, offered a reliable method of identifying TSC nuclei using confocal microscopy.

Early characterisation studies using this technique confirmed previous data that the size of the junction correlates closely with the number of TSCs (Love *et al*, 1998). This confirms that the Sytox technique produces data that is consistent with previous findings.

However, during the analysis, several end plates appeared to have no overlying Sytox positive nuclei, and by implication, no TSCs. The pattern of nuclear staining adjacent to these end plates, representing adjacent end plates or muscle nuclei, appeared normal, and suggests that this was not an issue of dye penetration. Equally, there was no correlation between end plate size and location with these end plates. These junctions may therefore represent the latter stages of synaptic elimination or denervation and if followed over a period of time, the NMJ may eventually degenerate. If these end plates are removed from the correlation analysis as being unrepresentative, the relationship between the number of TSCs and the length of the end plate becomes more significant.

Having established this technique, studies were then undertaken to describe the number of TSCs at each junction injured by antibody EG1. These investigations showed that 87% of junctions in triangularis sterni had evidence of TSC injury. Although no direct comparison studies were performed, the proportion of injured

junctions in TS appears to be higher than hemidiaphragm (figure 3.9). TS is significantly thinner than the diaphragm, and therefore this discrepancy may be the result of muscle thickness, and tissue penetration. However the hemidiaphragm sections were cut on a cryostat, and it is likely that measurements of injury using this muscle are underestimated. It would be interesting to directly compare antibody effects between these muscles, to identify if the antibody effect, and therefore by implication, ganglioside composition, is different between the two muscles. All the junctions in the hemidiaphragm preparation would be assayed to ensure a fair comparison. If the ganglioside composition were different between the muscles, this would support the hypothesis in humans that complex gangliosides are mainly located in the head and neck, which is an explanation for the symptoms of MFS being confined to this site (Chiba *et al*, 1997).

It was also shown that a mean of 75% of TSCs are injured at each junction by antibody EG1 in the timescale under consideration, although a number of junctions have complete TSC loss. While it is difficult to extrapolate these *ex vivo* findings to the human disease, these results suggest that certain TSCs at the NMJ may be insensitive to the effects of anti-ganglioside antibodies, while others at the same junction experience injury. A number of possibilities may account for this observation, including differing ganglioside composition or complement regulator expression on individual TSCs at the junction. The NMJ is not a static junction, and the morphology (including TSC number and distribution) does change with age (Lubischer and Bebinger, 1999). The difference in ganglioside or complement regulator expression may be related to the age of the cell, and it would therefore be interesting to see if the antibody's effect is only confined to cells at a particular level

of maturity for this reason. It may also provide insight into the human disease, and whether certain age groups would be more susceptible to certain types of immune mediated injury.

The study also demonstrates that many junctions had complete loss of all TSCs after antibody exposure. This proves that EG1 can be used to remove all TSCs from certain junctions, and study the longer-term effects of their absence at these sites. Although it would be interesting to remove all the TSCs from a preparation and examine the consequences, having a range of injury across a series of junctions (from no damage to complete loss of TSCs), will provide a series of different scenarios that can be observed. Further, having some junctions with no damage may provide an internal control in the muscle, which would be useful for comparison.

Although it is not possible to directly extrapolate these findings to the sternomastoid due to strain and muscle differences, these studies provide a likely indication of antibody effect with the *in vivo* system.

3.4 Conclusion

This study sought to identify an antibody that would produce a significant injury to TSCs in *ex vivo* preparations that could then be used for later work in *in vivo* animal models. The most appropriate testing system for antibody comparison studies was identified as the hemidiaphragm preparation, due to the yield and established techniques for antibody testing in this system; while the TS muscle was shown to be the most suitable for structural, and morphological studies.

Using the hemidiaphragm technique, 3 antibodies with similar binding profiles to GQ1b and GD3 on ganglioside ELISA were compared, and EG1 was selected as the most suitable for use in later experiments as it produced TSC injury at a large number of junctions. Also, because this IgG antibody was prepared from laboratory stocks, large amounts could be grown and purified for regular use.

Finally, the effect of this antibody was quantified in TS muscle, and it was shown that 75% of TSCs at each junction were damaged by antibody EG1, but some junctions had complete TSC loss. This antibody would therefore provide a range of injury across the muscle that could be directly observed using the *in vivo* imaging system, to compare the effects of varying degrees of TSC injury at the NMJ.

In summary, antibody EG1 was selected as the most suitable antibody for use in later experiments.

Chapter 4: Effect of DAF1/CD59a regulators on complement-mediated antibody effect

4.1 Introduction

TSC injury caused by antibody EG1 is a complement dependent process that involves the formation of MAC, via activation of the classical pathway of the complement cascade. The MAC molecule renders the cell membrane permeant, and disrupts the cell's osmotic balance leading to cell lysis. Although a single MAC pore is sufficient to produce lysis in an erythrocyte, nucleated cells utilise a number of systems to minimise the effects of MAC, including ion pumps to regulate any osmotic disruption, and vesicular mechanisms to remove MAC from the cellular membrane (Morgan, 1989; Scolding *et al*, 1989). This prevents cell death in response to low level MAC formation, as part of a non-specific immune response.

In addition, regulator proteins exist which can disrupt the formation of MAC. These proteins can exist in the serum, or on the surface of cells. One of the cellular membrane bound proteins, CD59a acts by inhibiting insertion of C9 into the membrane itself, to directly reduce the efficacy of MAC by preventing the formation of the molecule (Meri *et al*, 1990). Another protein on the cell surface, decay accelerating factor (DAF) also known as CD55, binds C3 and C5 convertases. Both C3 and C5 convertases are important in generating MAC, and DAF acts to increase the breakdown of these enzymes, and thus inhibit subsequent MAC formation (Fujita *et al*, 1987).

These regulator mechanisms, in conjunction with other systems that control complement activity, mean that more complex, nucleated cells are relatively resistant to the action of MAC, and a significant number of MAC pores are therefore required to produce injury in these cell types.

The expression of these regulator proteins can be manipulated genetically to study the effects of these inhibitors directly, and gain an understanding of their contribution to complement function (Miwa *et al*, 2002). Much of this work was developed to study the pathogenesis of paroxysmal nocturnal haemoglobinuria, a complement dependent process causing haemolysis of erythrocytes. In this disease, patients have a defect in the gene that codes for phosphatidylinositol glycan A (PIGA) which makes the membrane anchor protein called glycosylphosphatidylinositol (GPI). These GPI structures "anchor" a number of complement regulators to the cell membrane, including CD59 and DAF. Without these regulators on the surface of their red blood cells, patients experience complement-induced haemolysis of their erythrocytes (Nangaku, 2003). Mouse strains were developed with deficiencies in CD59a and DAF1, which are similar regulators of complement function in mice, to understand the contribution of GPI anchored complement regulators at the cell surface.

The purpose of this study was therefore to determine whether removing regulators of complement function would increase the effect of EG1. These studies were undertaken using a mouse strain deficient in complement regulators DAF1 and CD59a (double KO), and this was compared to the C57Bl/6 background strain (DAF WT). BALB/c mice were used as a positive control, as the antibodies have previously

been described in this strain. Complement regulator knockout lines were kindly donated by Dr P Morgan (Cardiff University, Wales).

4.2 Results

4.2.1 Image acquisition

Before undertaking *ex vivo* and topical assays of complement and immunoglobulin deposition, experiments were conducted to optimise the image acquisition settings using the confocal microscope. Three settings on the confocal software could be altered to influence the resulting image: detector gain, amplifier offset (representing background levels) and amplifier gain (amplification factor). Incorrect settings on the acquisition software could either mask any staining that is present over the end plate, or over-saturate the image to a false positive signal as shown in figure 4.1 (a-c).

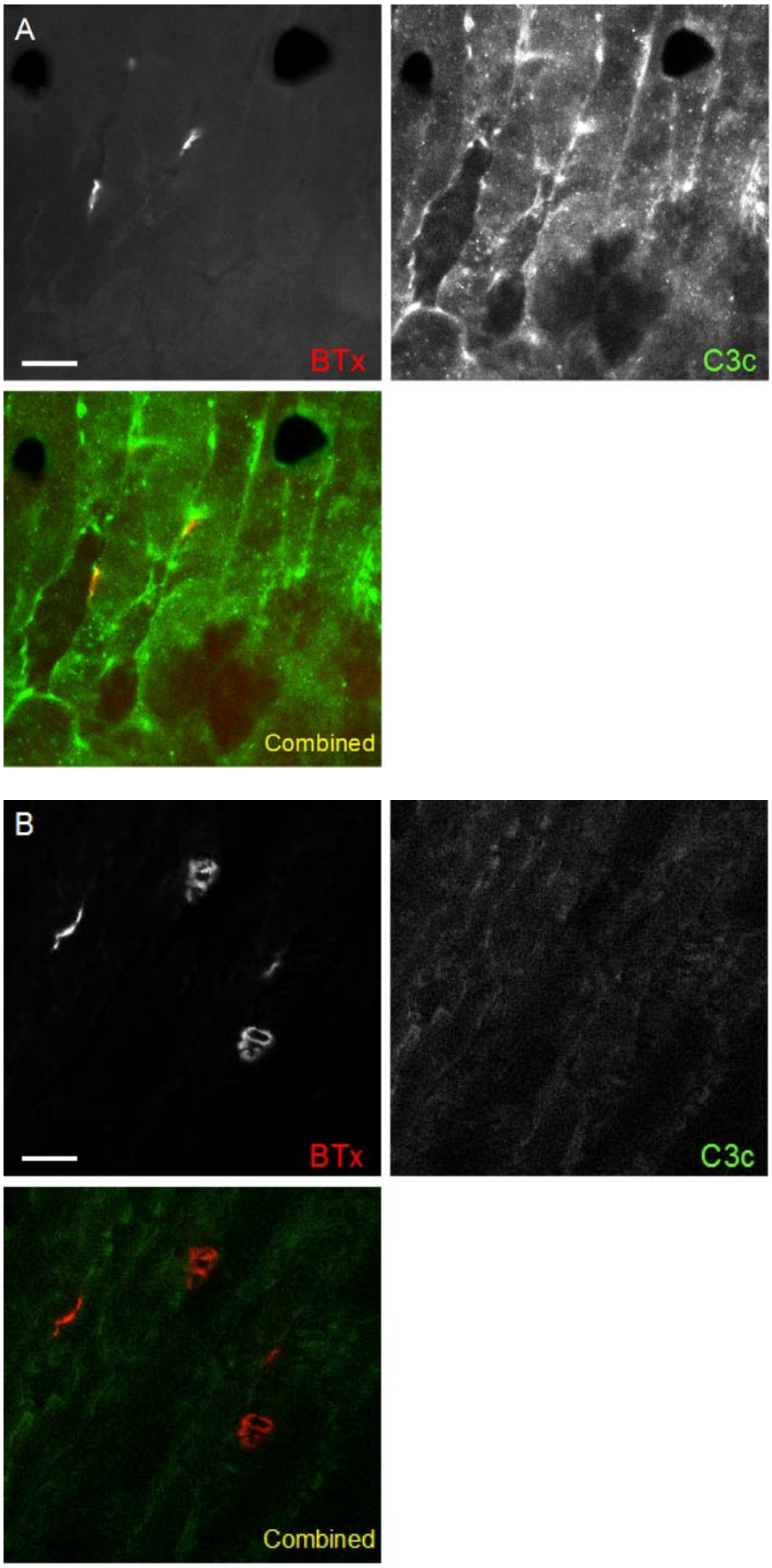
A
BTx
C3c
Combined
B
BTx
C3c
Combined

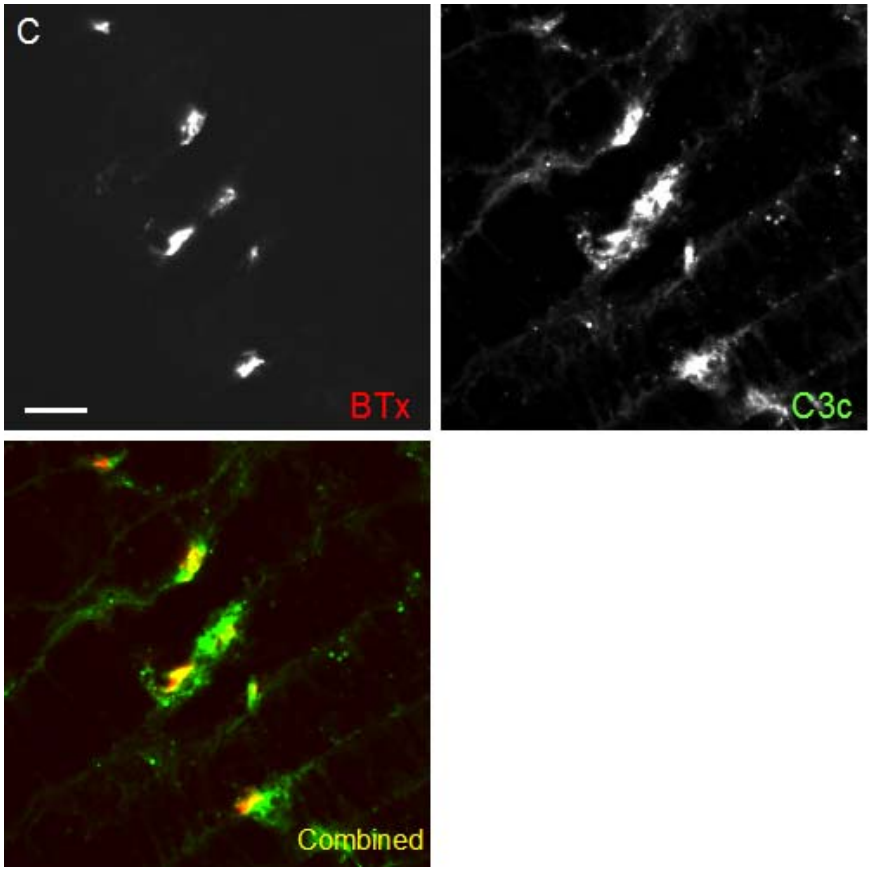

Figure 4.1: A-C. In these figures, sections from the same *ex vivo* BALB/c hemidiaphragm muscle are imaged using different acquisition settings on the imaging software. The muscle was incubated with EG1 and NHS, and stained for C3c using protocols outlined in Methods. Although the pattern of staining should be the same between samples, the effect of altering the image acquisition software settings is clearly seen. In (A), the image is oversaturated by increasing amplifier gain, and offset, and detector gain to produce a false positive signal. In (B), the levels are decreased and no staining is apparent. However, by setting the acquisition levels correctly (C), the image is a more accurate representation of actual staining patterns as visualised through the microscope (Scale bar 15μm).

The effects of altering the settings is also seen when the data is represented graphically, using Minitab (figure 4.2).

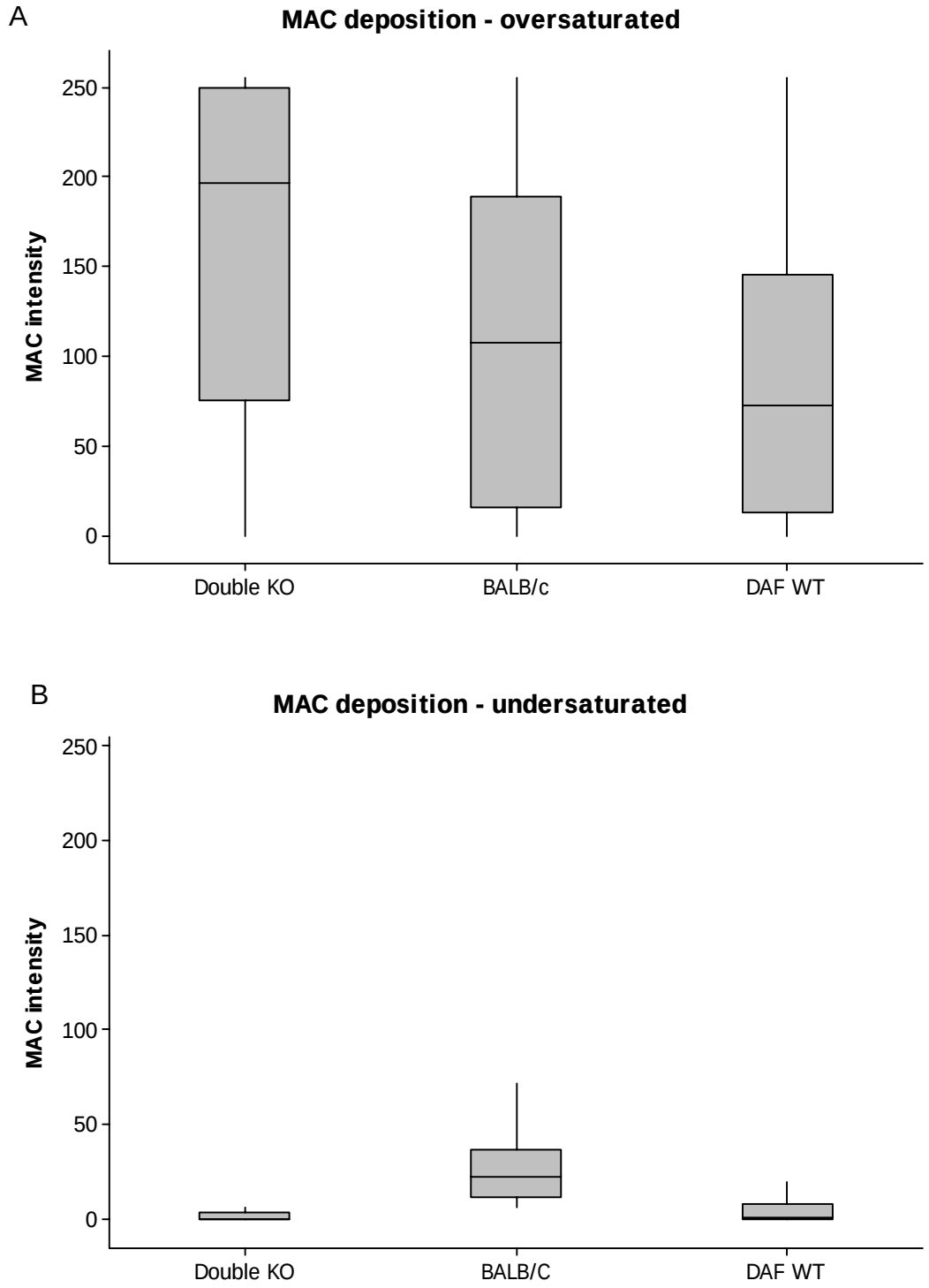

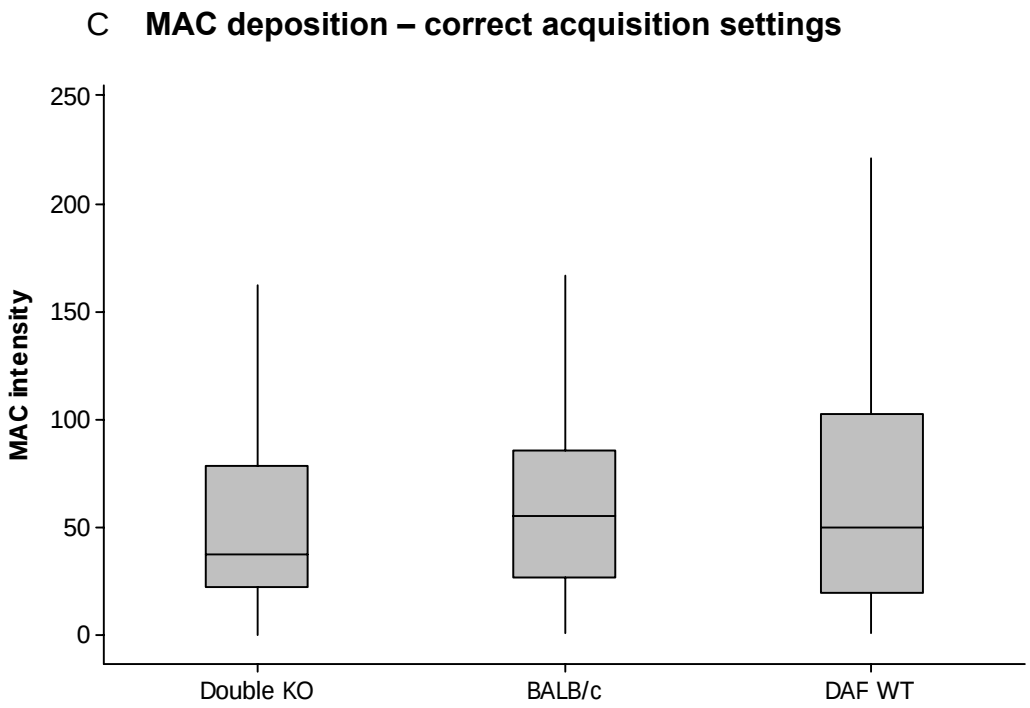

Figure 4.2: *Ex vivo* hemidiaphragm preparations of EG1 and normal human serum, stained for BTx and MAC as described in Methods. Despite the same muscle being used, altering the settings can drastically alter the appearance of the data. In graph A, the data range is broad whilst in B, the data sets are very small. In both, it is difficult to establish any clear trends and the data is inconsistent. In C, the correct settings are used giving consistent, reproducible data sets. Pooled data from 3 hemidiaphragm preparations from 3 mice for each stain is displayed in box-and-whisker plots as intensity of MAC over bungaratoxin staining, measured using ImageJ as described in Methods. Outlying data points are removed, leaving median values, interquartile ranges (box) and 1.5 times the interquartile range (vertical lines).

To ensure the accuracy of image acquisition settings, *ex vivo* experiments were often conducted in parallel with Mr Peter Humphreys to ensure that the resulting data was comparable. Also, images acquired for analysis were often reviewed by laboratory colleagues, and compared with images viewed directly through the microscope to ensure their accuracy.

4.2.2 Topical staining

4.2.2.1 Tissue preparation

Sections of untreated hemidiaphragm were obtained from the mouse strains under study, and were stained topically with antibody and a source of complement as described in Methods. Intensities of immunoglobulin and MAC were measured using a confocal microscope, and ImageJ analysis software as described in Methods. Non-parametric data is displayed in "box and whisker" format, and represents pooled data of muscle tissue from 3 mice, as outlined in Methods.

4.2.2.2 Immunoglobulin deposition

Before undertaking detailed comparison studies of the effect of antibody EG1 in different strains, topical deposition of immunoglobulin was measured on sections of hemidiaphragm tissue from the selected mouse strains. This study would identify whether the ganglioside composition of each strain was different, and may account for differences in complement activation, or TSC injury.

The results show that the strains under examination had measurable levels of antibody EG1. There is a statistically significant difference in immunoglobulin deposition between the strains (figure 4.3), with less immunoglobulin binding to BALB/c than the complement regulator knockout, or its wild type. Further, the knockout preparation has more intense binding than its wild type.

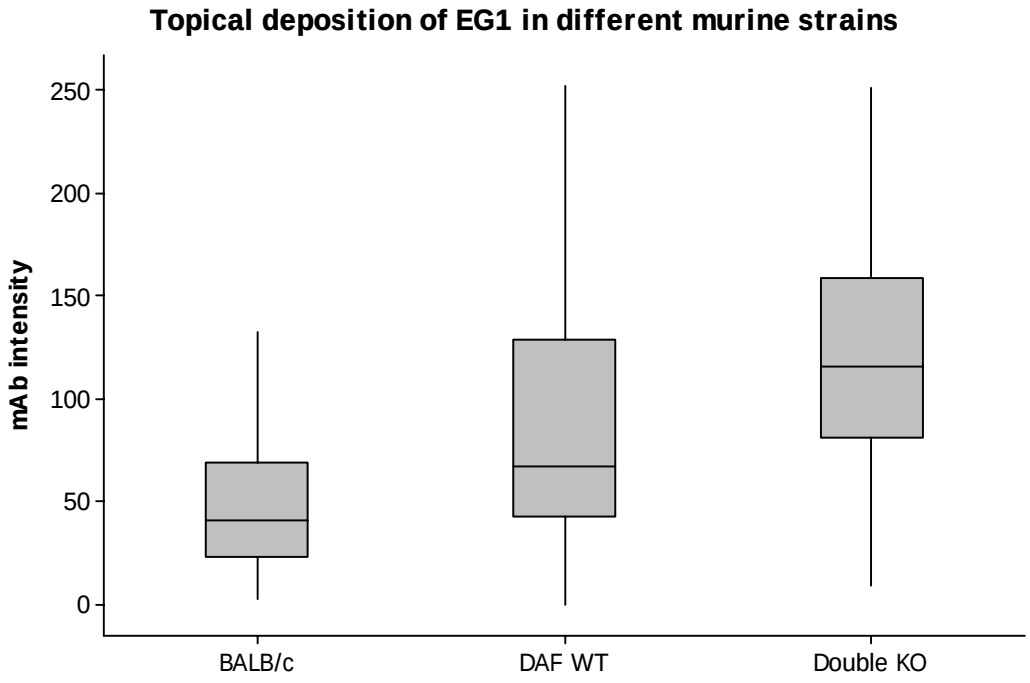

Figure 4.3: Topical deposition of antibody EG1 in different mouse strains. There is a statistically significant difference between deposition of antibody in BALB/c and DAF WT ($p<0.01$), or the DAF1/CD59a double knockout preparation ($p<0.01$); and also between the DAF1/CD59a knockout preparation, and its wild type ($p<0.01$). Pooled data from 3 hemidiaphragm preparations from 3 mice for each stain is displayed in box-and-whisker plots as intensity of mAb over bungaratoxin staining, measured using ImageJ as described in Methods. Outlying data points are removed, leaving

median values, interquartile ranges (box) and 1.5 times the interquartile range (vertical lines).

4.2.2.3 Complement deposition

The ability of antibody EG1 to activate complement at the NMJs of different mouse strains was then measured, using the complement activation product MAC. In this study, a well-described antibody that binds both the TSCs and nerve terminal (CGM3) was used as a positive control.

All mouse strains had detectable levels of MAC overlying the end plate with both antibodies (figure 4.4). There was a statistically significant difference in intensity of MAC deposition between BALB/c, and both the complement regulator knockout preparation and its wild type, using EG1 and CGM3. However, there was no statistical difference in complement deposition between the complement regulator strains (fig 4.4). This demonstrates that complement deposition due to EG1 or CGM3 in BALB/c is lower than the DAF1/CD59a knockout mouse, or its wild type.

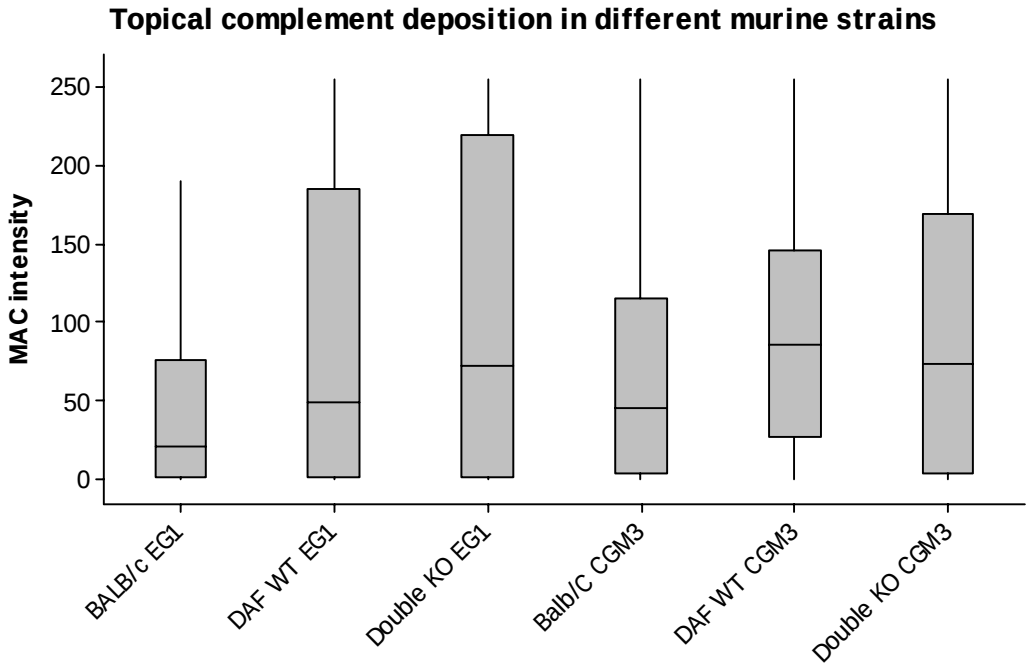

Figure 4.4: Topical complement deposition in different mouse strains. MAC deposition with both antibodies was lower in BALB/c than DAF WT ($p<0.01$) and DAF1/CD59a double knockout preparations ($p<0.01$). There was no difference between DAF WT and DAF1/CD59a double knockout preparations for both antibodies ($p=0.07$ for EG1 and $p=0.49$ for CGM3). Pooled data from 3 hemidiaphragm preparations from 3 mice for each condition is displayed in box-and-whisker plots as intensity of MAC over bungaratoxin staining, measured using ImageJ as described in Methods. Outlying data points are removed, leaving median values, interquartile ranges (box) and 1.5 times the interquartile range (vertical lines).

4.2.3 Ex vivo hemidiaphragm preparations

4.2.3.1 Pathological effects of antibodies

Although topical staining provides a useful indication of antibody binding to tissues and subsequent complement activation, it does not describe the pathological effects of the antibody on live tissue. Experiments were therefore undertaken using *ex vivo* hemidiaphragm preparations, which provide a better model for effects *in vivo* than topical sections. Hemidiaphragm sections were harvested, and treated with antibody EG1 and normal human serum as described in Methods. Tissue was retained for measurement of MAC deposition, and remaining sections of hemidiaphragm were exposed to EthD-1 as a marker of TSC injury. Results are pooled data from 3 hemidiaphragm preparations from 3 mice, as described in Methods.

4.2.3.2 Terminal Schwann cell injury

To investigate whether removing complement regulators enhanced the effect of EG1, the number of NMJs with EthD-1 positive nuclei, (suggesting TSC injury), were measured in BALB/c, C57Bl/6, and DAF1/CD59a deficient preparations.

No statistically significant difference in the number of end plates with EthD-1 nuclei was seen across any of the mouse strains, suggesting that removing complement regulators DAF1/CD59a do not enhance the Schwann cell damaging effect of EG1. Data is displayed graphically using Excel (fig 4.5).

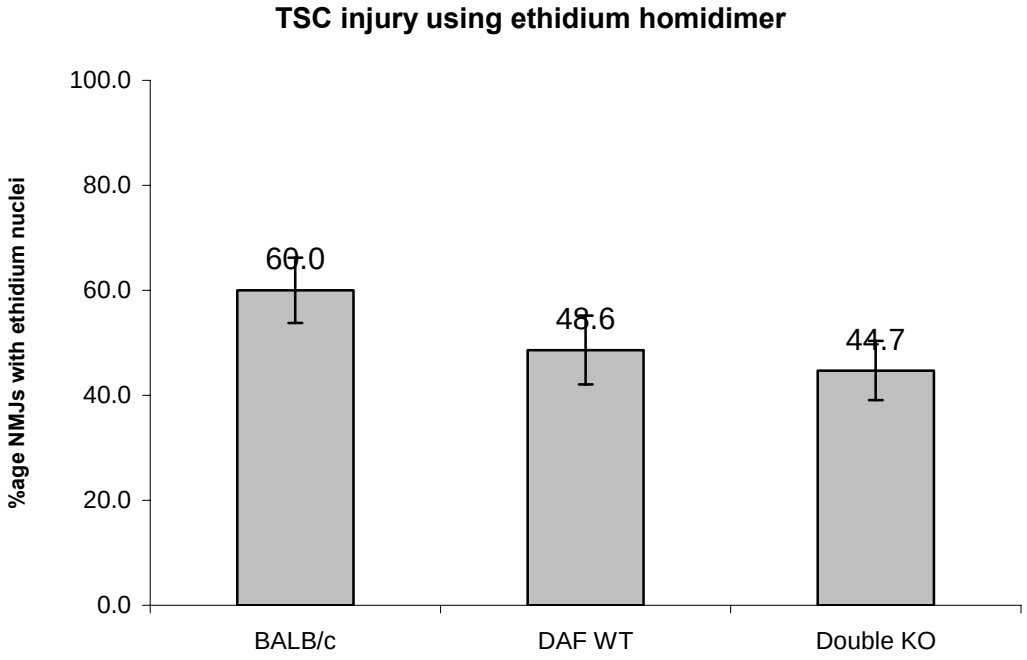

Figure 4.5: TSC injury using EthD-1 as marker of TSC injury *ex vivo*. There is no statistical difference between mouse strains using antibody EG1 (p=0.22 for DAF vs BALB/c, p=0.73 for Double KO vs DAF WT and p=0.12 for BALB/c vs Double KO). Pooled data from 3 hemidiaphragm preparations from 3 mice is shown for each strain, with mean displayed as a value in the graph, with standard error of mean as error bars.

4.2.3.3 Complement product deposition

As with earlier topical investigations, MAC immunostaining was used to study whether removing complement regulators would enhance the complement activating effect of antibody EG1.

No statistically significant difference was present with MAC deposition (fig 4.6) across any of the strains under study, suggesting that removing complement regulators DAF1/CD59a do not enhance complement activation mediated by EG1.

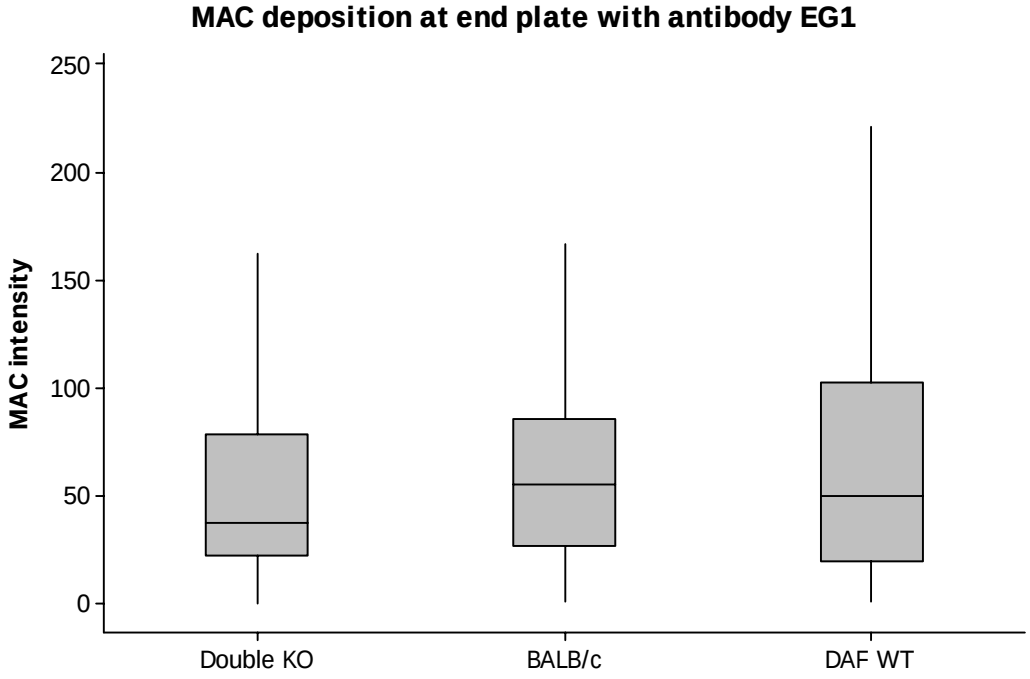

Figure 4.6: MAC deposition at NMJ across mouse strains with antibody EG1. No statistical difference was evident in complement deposition product C3c in *ex vivo* preparations with antibody EG1 (p=0.06 for Double KO vs BALB/c; p=0.26 for Double KO vs DAF WT; and p=0.8 for BALB/c vs DAF WT). Pooled data from 3 hemidiaphragm preparations from 3 mice for each strain is displayed in box-and-whisker plots as intensity of MAC over bungaratoxin staining, measured using ImageJ as described in Methods. Outlying data points are removed, leaving median values, interquartile ranges (box) and 1.5 times the interquartile range (vertical lines).

4.3 Discussion

4.3.1 Topical Staining

4.3.1.1 Immunoglobulin staining

Before starting *in vivo* studies using antibody EG1, experiments were undertaken to examine whether removing complement regulators could enhance the effect of antibody EG1, and if it would be worthwhile to establish a transgenic fluorescent complement regulator knockout mouse model for *in vivo* imaging. Although mouse strains are available which are separately deficient in DAF1 and CD59a, the "double knockout" model was used in these studies. If a difference in effect were identified, the mice deficient in either CD59a or DAF1 would then be used to determine which regulator made the greatest contribution.

Early experiments considered the effects of antibody binding topically to sections of hemidiaphragm muscle tissue, and its ability to fix complement. This type of study is a useful screening tool: by using small quantities of muscle and antibody to determine immunoglobulin deposition, a large number of strains can be screened rapidly while reducing the number of animals required for each investigation. However, the system is relatively artificial because sectioning muscle reveals epitopes that are normally masked by connective tissue or other structures, and this may influence antibody binding. Also, the morphology of the junction is largely lost during sectioning, and detailed co-localisation is therefore virtually impossible. Despite these minor limitations, the method is useful as a screening tool and was therefore used early in

these regulator studies to show if the mouse strains under study could actually bind antibody, and fix complement.

Topical immunoglobulin deposition demonstrated a statistically significant difference in antibody deposition across the three muscle strains under consideration. The difference between BALB/c and the complement regulator mice could be the result of strain differences in ganglioside composition. Other work has suggested that ganglioside composition can vary between mouse strains, and this difference can influence anti-ganglioside antibody binding (Halstead *et al*, 2005b). Although it is not directly related to this study, it would be interesting to examine the binding characteristics of other anti-ganglioside antibodies in these mouse strains, in an attempt to elucidate the different ganglioside compositions between strains.

Interestingly however, the topical study also identified a difference in antibody binding between the DAF1/CD59a knockout mouse, and its wild type. This is an unexpected finding, as the DAF1/CD59a mouse should have the same ganglioside backgrounds as its wild type. As both DAF1 and CD59a exist on the cell membrane surface, and both are GPI-anchored, they may be associated with gangliosides through lipid rafts (Simons and Ikonen, 1997; Fukinaga *et al*, 2003). It is conceivable that their absence may influence ganglioside composition in the cell membrane and influence antibody binding. If this hypothesis were correct, it would identify a new aspect of cell membrane glycobiology, and the interaction of molecules on lipid rafts.

However, the breeding programme to create the DAF1/CD59a knockout mouse may have unintentionally bred animals selectively with a different ganglioside composition

to their background stain, and this may also account for the difference. It would again be interesting to examine other anti-ganglioside antibodies in these strains, to further elucidate the differences in ganglioside composition. Comparing antibody binding in the single knockout preparations, deficient in either DAF1 or CD59a may also help to identify which molecule may be influencing ganglioside composition.

4.3.1.2 Topical complement activation

These experiments also show that levels of complement deposition after incubation with antibody and complement were significantly lower in BALB/c mice than either DAF1/CD59a preparations, or their corresponding wild type. However, levels of immunoglobulin deposition are different in between these strains, and it is possible that differences in complement deposition may be the result of differences in antibody deposition between the strains. Equally, as the tissue is sectioned, and effectively "dead", complement regulators may not be able to function within this model. Finally, it is possible that the amount of antibody present, and concentration of heterologous serum, overwhelms the regulators DAF1 and CD59a, making it impossible to identify any difference between the knockout, and its wild type. To investigate these hypotheses, a dose response experiment could be undertaken where different amounts of antibody and serum were applied, and the intensity of MAC and immunoglobulin were measured. If the regulator system was overwhelmed, a difference in MAC deposition may become apparent at lower concentration of serum or antibody. If not, this would suggest that differences in deposition may be due to regulator inactivity in "dead" tissue.

In summary, this study demonstrates that the antibody can bind, and fix complement to the mouse strains under study, and they are suitable for further investigation. It also suggests that there is a significant difference in immunoglobulin deposition between DAF1/CD59a knockout preparations and its wild type, there is no difference in MAC deposition between these strains suggesting that removing DAF1/CD59a does not enhance the human complement activating effects of antibody EG1 on topical sections of tissue. These experiments were continued using *ex vivo* models, using whole mount hemidiaphragm preparations to provide a more accurate experimental paradigm that is comparable to *in vivo* models.

4.3.2 Ex vivo hemidiaphragm preparations

Comparison studies were therefore made using *ex vivo* hemidiaphragm preparations taken from BALB/c, DAF1/CD59a knockout and DAF wild type mice, to investigate whether there was a difference in TSC injury between these mouse strains *ex vivo*, and in particular whether removing complement regulators would enhance TSC injury. In contrast to topical studies, these *ex vivo* preparations provide a more accurate model for *in vivo* tissue damage.

The results suggest that removing complement regulators DAF1/CD59a do not enhance the TSC injury of antibody EG1 when compared to their corresponding wild type. There is also no difference in TSC injury between BALB/c mice, and other mouse strains under consideration. In addition to TSC injury, there is also no difference in MAC deposition between mouse strains on *ex vivo* preparations.

This presents an interesting contrast with data from the topical sections, where less antibody and MAC was present on BALB/c than either of the complement regulator knockout strains, although it is obviously not possible to directly compare topical sections to *ex vivo* preparations for reasons outlined previously.

As the *ex vivo* preparation is a more accurate model, which identifies injury rather than passive antibody binding, these experiments suggest that removing complement regulators do not increase the antibody effect on TSCs, or alter MAC activation at the NMJ. This is surprising, as both DAF1 and CD59a influence the formation of MAC, and their removal should increase MAC deposition and possibly injury. As discussed with topical sections, the expression of complement regulators may be tissue specific, and DAF1 and CD59a may not be expressed at sufficient concentration to demonstrate an effect in diaphragm muscle. This may also account for the lack of difference in complement deposition, or TSC injury in this model. However, the concentration of serum used in the *ex vivo* experimental protocol is very high (40%), and this may instead overwhelm the complement regulatory system, rendering both DAF1 and CD59a ineffective. This hypothesis could be confirmed by repeating the *ex vivo* experiments in the same strains, using differing concentrations of human serum. A difference in effect would be expected at lower concentrations if the hypothesis were correct.

Additionally, as human serum is used on mouse tissue, it is possible that cross-species complement regulation is not possible in this system. This hypothesis could be tested by applying mouse serum to the preparation under similar conditions, which may demonstrate a difference in effect between complement regulator strains.

4.4 Conclusion

The aim of this study was to identify whether removing complement regulators DAF1 and CD59a would enhance the effect of antibody EG1 in the hemidiaphragm.

Using topical sections of mouse diaphragm, it was shown that complement deposition is lower in BALB/c mice than either DAF/CD59a knockout preparations, or their corresponding wild types. This effect may be due to differences in antibody deposition between the strains.

The investigation also demonstrated that there was no statistically significant difference in TSC injury between any of the mouse strains under investigation *ex vivo*, and that removing DAF/CD59a did not enhance the effect of antibody EG1. Instead, it is possible that the high concentration of human serum used in the experimental protocol overwhelms the regulator system, and the effect has been maximised using this current system; or that normal human serum can bypass mouse complement regulator systems.

Chapter 5: TSC injury and recovery using an *in vivo* fluorescent system

5.1 Introduction

One of the major difficulties encountered during histological analysis of the PNS is the difficulty in staining tissue *in vivo*. Most stains are either cytotoxic, or bind to the cell and alter its normal behaviour, making serial morphological studies impossible. This is particularly problematic when studying the effect of injury and recovery at the NMJ. Although junctions share the same gross morphology – axon, TSCs, and post-synaptic specialisation, there are important differences that make each junction unique, including the pattern of axon distribution, the number and position of TSCs, and the pattern of bungarotoxin (and hence, ACh receptor) distribution. Current *ex vivo* studies of injury only state whether any gross change occurs at the junction (i.e. absence of axon, or TSC) as a result. Potentially important, more subtle observations that will influence nerve terminal function may not be identified using current methods e.g. change in TSC number, alteration in bungarotoxin area or axonal distribution, etc.

Equally, these practical difficulties prevent accurate description of longer-term changes at the NMJ. In the human, the effects of immune mediated nerve injury can last from weeks to months, and to produce an accurate rodent model of disease, it is important to describe changes that occur following injury over a comparable period of time. Again, it is only possible to describe gross changes using current methods. To

produce an accurate rodent model of disease, and describe disease pathogenesis, it is crucial to derive a suitable system for repetitive *in vivo* imaging.

It has recently become possible to transgenically insert fluorescent protein derivatives from the bioluminescent jellyfish, *Aequorea victoria* in a cell specific manner in the mouse (CK mouse model). These green and cyan fluorescent proteins (GFP and CFP) act as vital stains, which permit visualisation of the nervous system without causing cellular injury. By using existing techniques that allow repetitive imaging of the sternomastoid muscle of the mouse under recovery anaesthesia (Lichtman *et al*, 1987), it is now possible to repeatedly image NMJs in these fluorescent mouse preparations. By combining this technique with anti-ganglioside antibody and an exogenous source of complement, this mouse model could be used to study both the immediate, and long-term sequelae of immune mediated injury at the NMJ.

The purpose of this study therefore is to establish and characterise an *in vivo* system for immune mediated injury at the NMJ of the CK mouse, in sternomastoid muscle. Using this system, the immediate effects of selective glial cell injury at this site will be confirmed, using antibody EG1 and human serum. The longer-term sequelae to selective TSC injury will also be examined, by reviewing injured junctions over time.

These experiments will also support *ex vivo* studies in the mouse (Halstead *et al*, 2005b) that illustrate another possible mechanism of immune mediated injury at the NMJ, where antibodies to complex gangliosides injure the TSCs independently of the terminal axon.

5.2 Results

5.2.1 In vivo terminal Schwann cell injury using antibody EG1

5.2.1.1 Identifying antibody effect in CK mouse model

Initial studies of the sternomastoid muscle demonstrated that the fluorescence of GFP was lost from TSCs following incubation with antibody EG1 and 40% normal human serum (NHS) (Fig. 5.1A). This was evident immediately after the incubation with NHS. Since the GFP is expressed as a soluble cytoplasmic protein, its loss suggests a lack of membrane integrity in the Schwann cells. Such a conclusion is supported by the application of ethidium homodimer (EthD-1), a membrane impermeable nuclear dye, to the Ringers solution bathing the muscle. The ethidium labelled the nuclei of the same cells that lost GFP (Fig. 5.1B). On the other hand, the CFP expressed in the terminals of the motor axons was unaffected in the majority of junctions (Fig. 5.1C), suggesting that the effect of the EG1 was confined to the TSCs. A small proportion of axons (see below) did display evidence of damage in addition to Schwann cell loss; this consisted of swelling, and fragmentation with eventual loss of CFP fluorescence. These junctions were easily identifiable following antibody and NHS incubation, and were excluded from studies of isolated TSC injury.

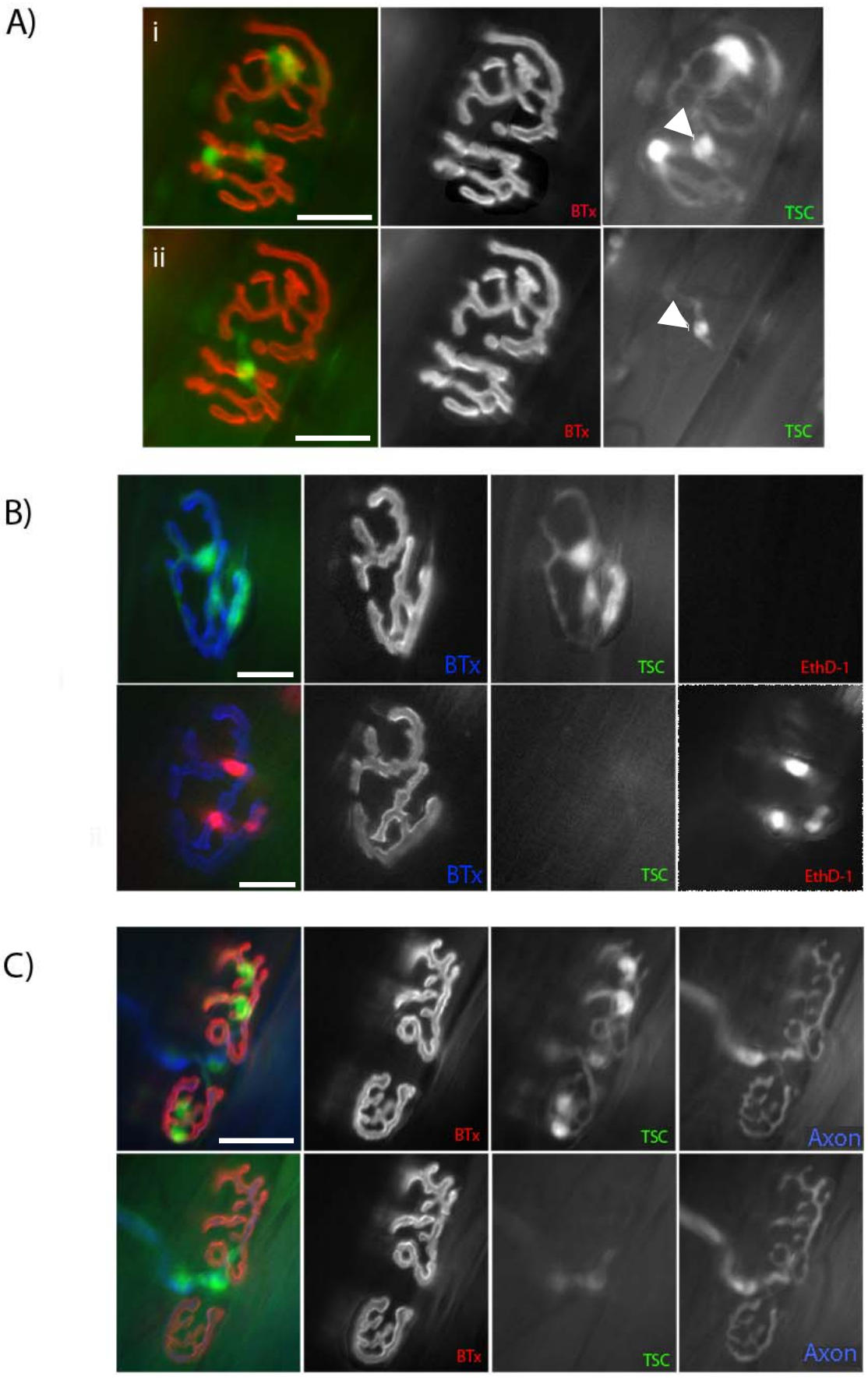
A)
i
BTx
TSC
ii
BTx
TSC
B)
BTx
TSC
EthD-1
BTx
TSC
EthD-1
C)
BTx
TSC
Axon
BTx
TSC
Axon

Figure 5.1: Acute terminal Schwann cell injury

A) Acute effect of antibody exposure in mouse that only expresses S100β-GFP, before (i) and after (ii) application of antibody and NHS, thus avoiding bleed-through from the CFP channel. Rhodamine bungarotoxin is added to identify post-synaptic ACh receptors. Complete loss of GFP staining is seen in TSCs after antibody application. The last myelinating Schwann cell does not lose GFP (arrow)

B) Ethidium uptake before (i) and after (ii) antibody-mediated injury, with Cy-5 bungarotoxin in mouse that only expressed S100β-GFP. There is complete loss of GFP staining following antibody and NHS exposure. Ethidium homodimer localises to the areas previously occupied by the TSC bodies.

C) Effect of antibody and NHS before (i) and after (ii) incubation in CK mouse. Loss of GFP from the TSC bodies is seen. The axonal expression of CFP appears unchanged. Bleed-through from the CFP channel into the GFP channel is seen after loss of GFP staining.

(Scale bar: 30μm)

5.2.1.2 Addressing issues of bleed through of CFP into GFP

One complication in these pilot studies was the presence of bleed-through of CFP fluorescence into the GFP channel. While such bleed-through is not obvious in the images taken from control material, it becomes more evident when the GFP is lost from the TSCs, and junctions were viewed through the GFP filter at longer exposure

times (not shown). An additional complication is the increase in background fluorescence in the GFP channel resulting from exposure to complement. To present an accurate reflection of the fluorescence seen, the images are presented at the same camera gain and exposure time as the images obtained prior to application of antibody and complement. In addition, a series of experiments were undertaken where animals expressing GFP in Schwann cells but no CFP in axons were exposed to the antibody and complement. In these experiments, there was no complication of bleed-through and the results of these experiments confirmed the conclusion that the SCs at the junction lost their GFP label as a result of the procedure (figure 5.1A). These cells were reviewed over a 48-hour period following this initial loss of GFP, and they did not appear to recover their GFP fluorescence during this time (as illustrated in figure 5.4).

5.2.1.3 Issues with repetitive imaging

One of the major considerations in repetitive *in vivo* imaging is minimising trauma to the animal. On all occasions, the induction of anaesthetic was conducted in a controlled environment to minimise distress and anxiety to the animal. An unsatisfactory depth of anaesthesia was achieved if the animal was stimulated during induction, and this occasionally resulted in early termination of the experiment.

Another significant complication of repetitive imaging is the requirement for intubation. If the animal is not intubated quickly, unnecessary trauma would be induced at the back of the oropharynx, causing localised inflammation which would affect feeding and animal welfare in the longer term. The process of intubation is

technically difficult, and experiments were often terminated early due to complicated intubation.

Finally, the other significant issue was minimising trauma to the muscle surface itself, which could result from either direct injury through the dissection process, or indirect injury to surrounding structures. In particular, the sternomastoid muscle lies next to major blood vessels, and inappropriate dissection could injure these structures leading to exsanguination, and euthanasia of the animal. The salivary glands lie on the surface of the sternomastoid muscle, and their associated connective tissue has to be carefully removed during the dissection process otherwise the glands themselves can be damaged, causing localised inflammation to the muscle surface. This inflammation can impair imaging, by disrupting both CFP and GFP fluorescence (figure 5.2) and animals exhibiting these changes were euthanased.

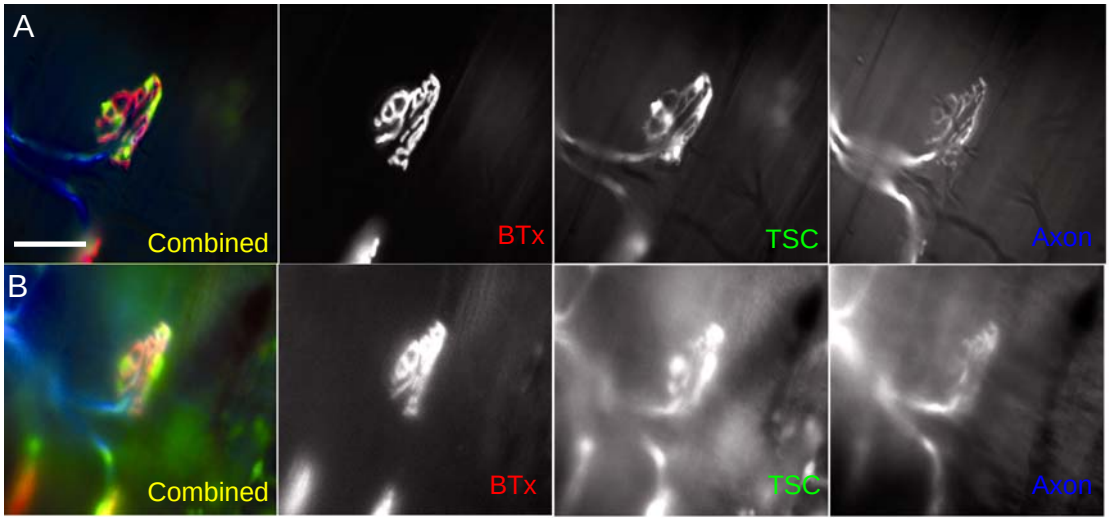

Figure 5.2: Effects of inflammation on imaging quality. This *in vivo* control preparation was incubated with sterile Ringers solution and NHS as described in Methods. The junction is visualised before incubation with Ringers solution and NHS (A). During the initial dissection process, the salivary glands were inadvertently damaged. When the junctions were imaged again at 3 days (B), the fluorescence is poor due to overlying inflammatory tissue, making it difficult to focus on structures at the NMJ. (Scale bar 40µm)

5.2.1.4 Quantification of antibody effect

To obtain an estimate of the percentage of junctions affected by the application of antibody and complement, 6 sternomastoid muscles from 6 animals were treated, identifying 746 junctions. Of these, data from 3 animals exposed to antibody were pooled to give 405 junctions, while data from 3 animals exposed to a ringer control solution were pooled to give 341 junctions. Immediately after incubation, the muscles were exposed to ethidium in situ. Muscles were dissected from freshly euthanized animals, and fixed with paraformaldehyde. A layer of muscle fibres was dissected

from each side of the muscle for examination. Junctions labelled with bungarotoxin were scored for the presence of ethidium label as a marker of TSC injury, and CFP. A mean of 23% of junctions (SEM 5.1) so scored (93 junctions from 405) had TSCs that took up EthD-1 in the muscle exposed to antibody (figure 5.3a). These junctions were located on the muscle surface in direct contact with the incubating solutions and were absent from the side of the muscle that was not directly exposed to the solutions. Control preparations were exposed to Ringers solution without antibody, and 40% NHS. EthD-1 positive nuclei were present in a mean of 1.8% of junctions (SEM=0.8) (6 junctions from 341) imaged under the same conditions, a significant difference from muscles that received antibody ($p<0.01$, Chi-squared test). These few ethidium positive cells in the control muscle could not be localized to any distinct area of the muscle. 6% of junctions (SEM=1.8) in experimental tissue (24 junctions from 405) had evidence of axonal injury (figure 5.3b), defined by swelling, fragmentation or loss of CFP fluorescence in the antibody preparation compared to 3% (SEM=2.4) in the control tissue (10 junctions from 341) ($p = 0.084$). It was not possible to localize this injury to an area in the control muscle although in the antibody preparation, a number of injured axons (less than 3%) were seen in association with TSC injury.

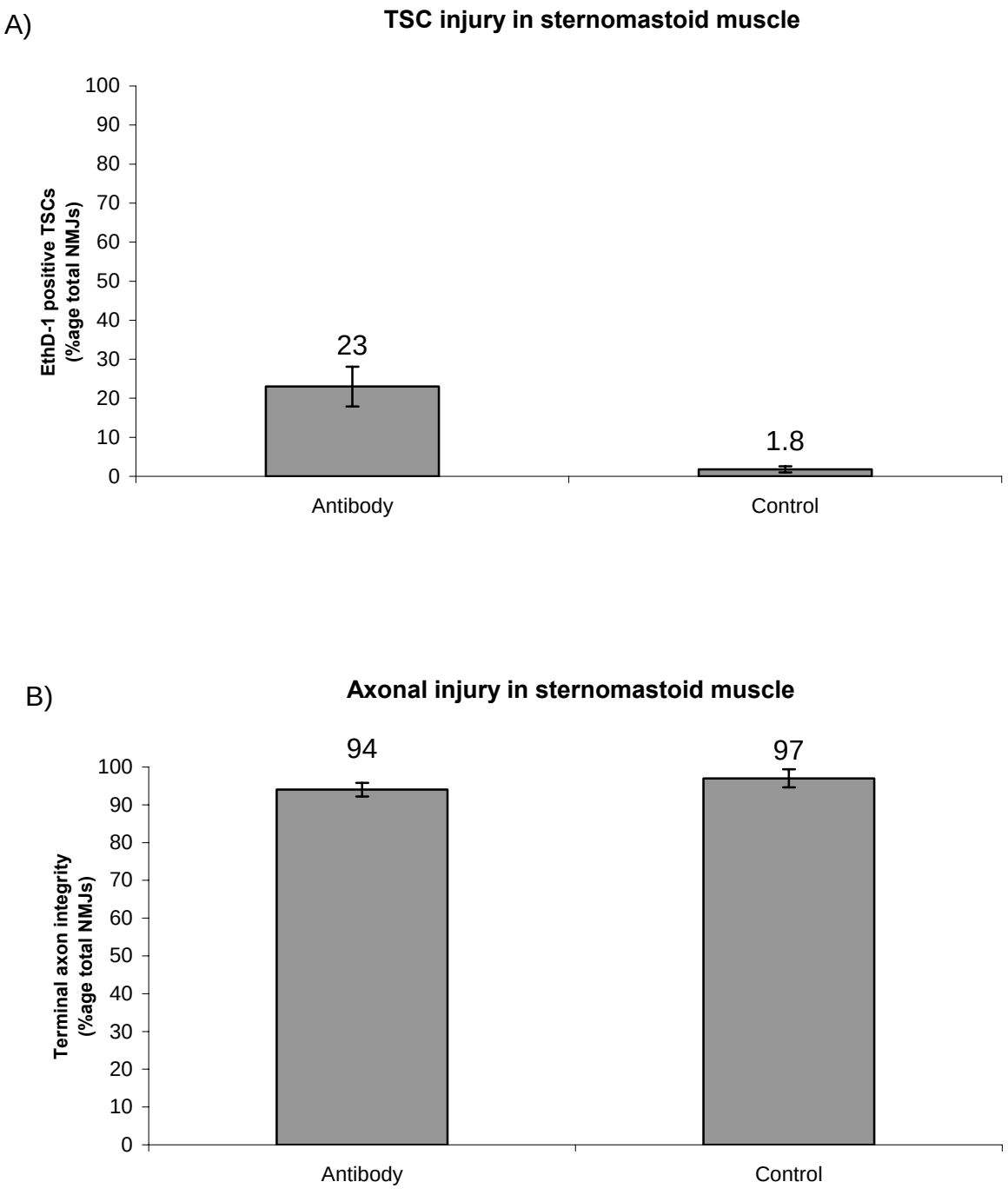

Figure 5.3: Quantification of TSC and axonal injury in sternomastoid muscle.

A) 23% of junctions across sternomastoid muscle had evidence of TSC injury as demonstrated by ethidium uptake. Less than 2% of junctions had ethidium nuclei in control muscles, representing a statistically significant difference between the two preparations ($p<0.01$).

B) 6% of junctions had evidence of axonal injury in the antibody preparation, compared to 3% in the control muscle. This difference is statistically significant (p=0.084).

Mean of 3 muscles from 3 mice with each condition is shown as a value in the graph, with standard error of mean as error bars as described in Methods.

5.2.2 Nerve terminal morphology following acute injury

A series of experiments examining a total of 9 junctions from 3 different animals were then undertaken to study whether the TSCs were required for the maintenance of the nerve terminal, using protocols outlined in Methods. For a one day period following the ablation, no GFP processes could be detected at the NMJs whose TSCs were ablated during the initial procedure. As there were no acute changes in the distribution of AChR at the TSC ablated junctions, nerve terminals that remained in apposition to the AChR were quantified. In 9 junctions from 3 animals, the apposition remained perfect (figure 5.4). Not only did nerve terminals remain in apposition to the receptors sites, there were no terminal sprouts that formed during this period.

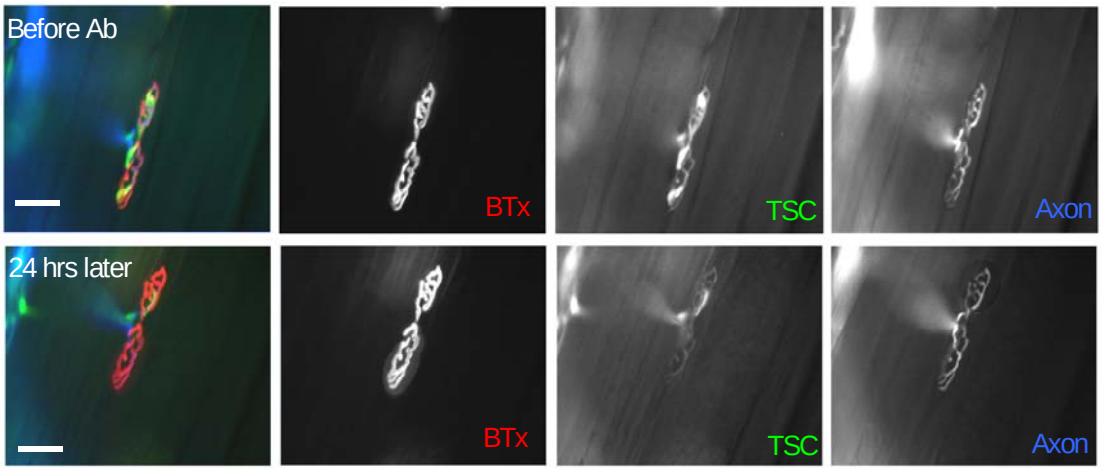

Figure 5.4: Nerve terminal apposition following TSC injury. 24 hours after selective TSC injury, the axon is seen in perfect apposition to the bungarotoxin. Some bleed through from the axon is seen in the GFP channel at this time point. (Scale bar: 30µm)

These observations support previous findings from the mouse hemidiaphragm using this antibody. In these acute studies over the first hour following injury, immunofluorescence studies and electron microscopy demonstrated selective SC injury at the NMJ, with no apparent injury to the terminal axon. In addition, no electrophysiological changes were seen in junctions with selective SC injury in previous studies, with no changes to the miniature end plate potential (MEPP) frequency, or end plate potential (EPP) immediately after antibody and NHS incubation (Halstead *et al*, 2005b). This suggests that TSCs are not required for nerve terminal maintenance over the first hour.

5.2.3 Schwann cell recovery following acute TSC injury

At 30 hours following the ablation of the TSCs, GFP labelled processes were observed with the junctions (figure 5.5C). These processes were always connected to the site where the pre-terminal axon entered the junction, suggesting that these processes were extended by cells located somewhere along this axon. Initially, these processes covered only a portion of the NMJ; however, with a very short period, the entire junction was covered. Within 3 days, new SC bodies were observed with the synaptic site (figure 5.5D). These cell bodies were obvious as swellings along the GFP positive processes that were usually brighter in their labelling than the processes. Application of DAPI to such preparations showed that these sites contained nuclei (not shown).

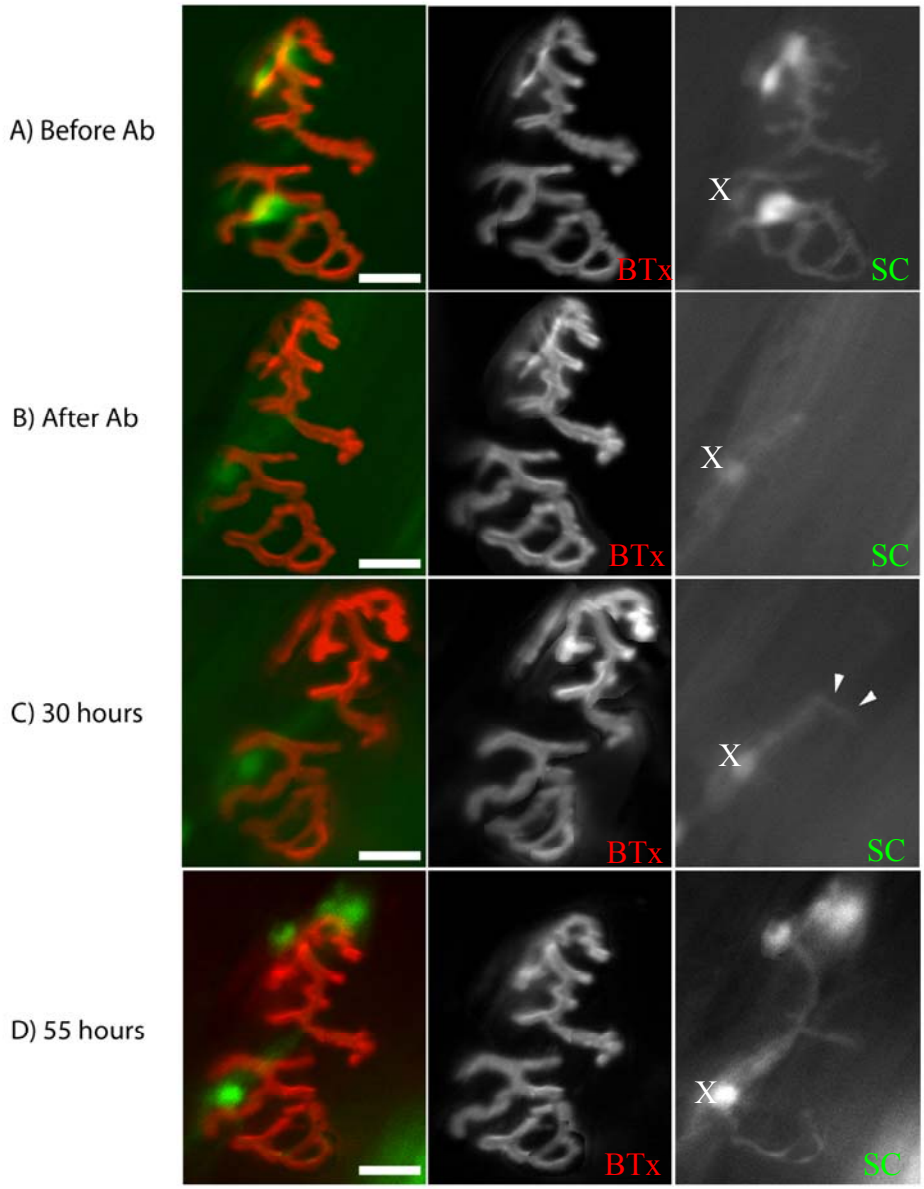

Figure 5.5: Acute effect of antibody exposure in mouse that only expresses S100-GFP to avoid bleed-through from the CFP channel. Rhodamine bungarotoxin is added to identify post-synaptic ACh receptors. Complete loss of GFP staining is seen in TSCs after antibody application. The last myelinating Schwann cell (X) does not lose GFP. Processes extend from the pre-terminal nerve over the junction at 30 hours (arrows) with more extensive coverage at 55 hours. In addition, GFP positive structures

are seen at the periphery at 55 hours, which stain for DAPI (not shown), and most likely represent new TSC cell bodies.
(Scale bar: 15μm)

The number of these Schwann cell bodies increased over the following week, with the consequence that these junctions had more Schwann cell bodies than were present prior to ablation (figure 5.6). Repeated imaging over the course of the next few months showed that these cell bodies persisted, although they occasionally changed their locations within the junctions (figure 5.7).

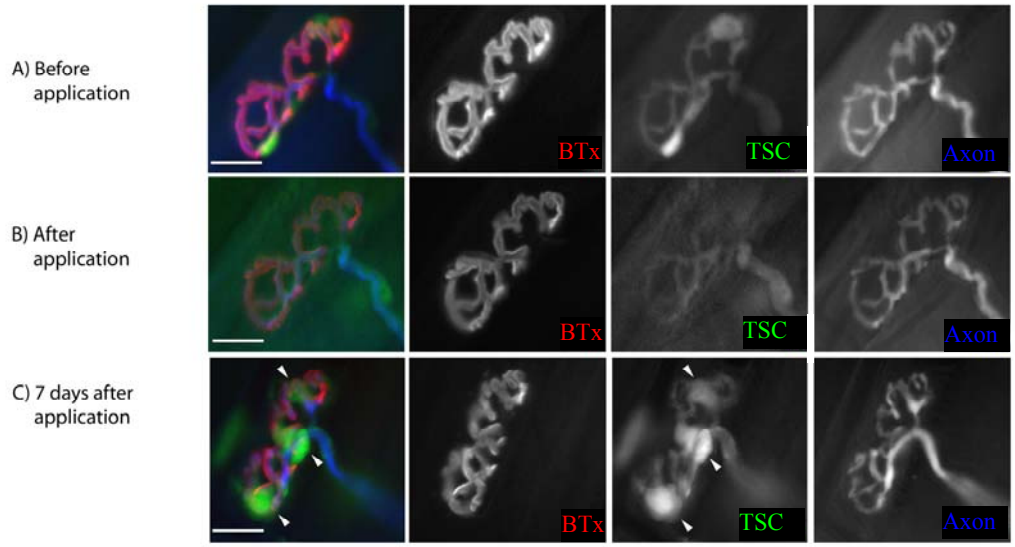

Figure 5.6: TSC repopulation. After the TSC processes extend over the junction, the dense areas of GFP appear to differentiate to form numerous GFP positive cell bodies (figure 5.4C - arrow) that migrate over junctional area, and also stain for DAPI (not shown). They are more numerous, and do not share the same location, or morphology as those present before antibody and NHS exposure. (Scale bar: 20µm)

5.2.4 Long-term review of neuromuscular junction following injury

Junctions were also examined at 3 months from the experimental animals (3 animals, 8 junctions), and controls (2 animals, 6 junctions). The number of Schwann cell bodies remained unchanged from one week, and only occasionally changed their position within the junction. At 3 months, changes in bungarotoxin distribution were also evident. Small areas of bungarotoxin were added around the junction, but these

were also seen in the control preparations and are consistent with remodelling in the ageing animal. Four junctions exposed to antibody also had areas of significant localised bungarotoxin loss (figure 5.7, arrows), but this was also seen in control preparations.

Subtle changes in the axon were evident at 3 months in 3 junctions under study. In these examples, CFP distribution gave the axon a "fragile" appearance with an irregular edge. However, these junctions did not undergo further remodelling, and their appearance remained constant at 6 months.

Although a comparative control was not available, one mouse treated with mAb and NHS (3 junctions) was imaged at one year (figure 5.5D). The junction appeared morphologically stable, with an intact axon. Further, the number of TSCs was unchanged from 3 months, occupying similar territories. Changes to bungarotoxin distribution represented a continuation of changes seen at 3 months. It would therefore appear that the NMJ remains morphologically stable after repopulation with TSCs (table 5.1).

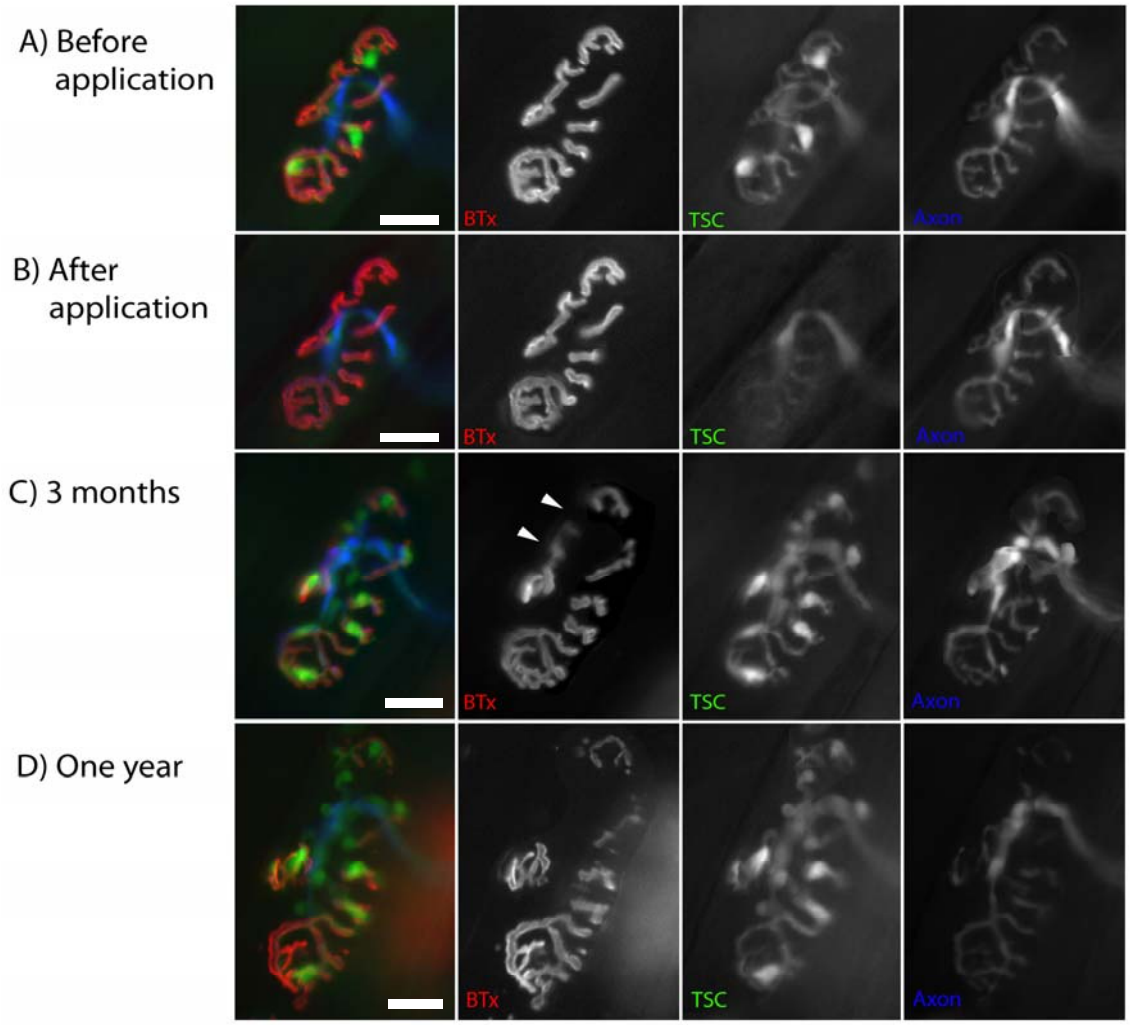

Figure 5.7: Long term effects of TSC loss. Junctions were also examined at 3 months. These examples had changes in bungarotoxin distribution (arrowhead), and axon morphology that were consistent with ageing. These included areas of addition and deletion of ACh receptors as imaged by bungarotoxin. The number of GFP positive cell bodies at the junction was unchanged from day 7. (Scale bar: 15µm)

Time	NMJ changes
0-60 minutes	Loss of GFP from TSCs Ethidium uptake
24 hours	No axonal changes
2 days	GFP positive processes extend from pre-terminal area
2-3 days	GFP positive cell bodies become evident at terminal
7 days	Large number of GFP positive cell bodies over junction Axon unchanged
3 months	GFP cell bodies remain Subtle changes in bungarotoxin distribution
6 months to 1 year	Bungarotoxin/axon changes more pronounced

Table 5.1: Summary of changes following antibody-mediated injury.

5.2.5 Effect of denervation following TSC injury

The stimulus for TSC repopulation was unclear from these early studies, therefore an experiment was undertaken to determine if the axon was important in this process. During these studies, the nerve to sternomastoid was crushed immediately after incubation with antibody and NHS. The animal was recovered, and re-examined at 3 and 7 days.

These experiments show that terminal Schwann processes and cell bodies had returned to the junction by 3 days as expected, without a terminal axon being present

(3 animals, 9 junctions). Although covering the bungarotoxin label, the pattern of process coverage was different to that present prior to mAb-mediated ablation (figure 5.8).

When the junctions were re-examined at 7 days, the axon returned to the junction, apparently following the TSC processes. In addition, extra-junctional TSC processes were seen in association with axonal sprouts (see figure 5.8).

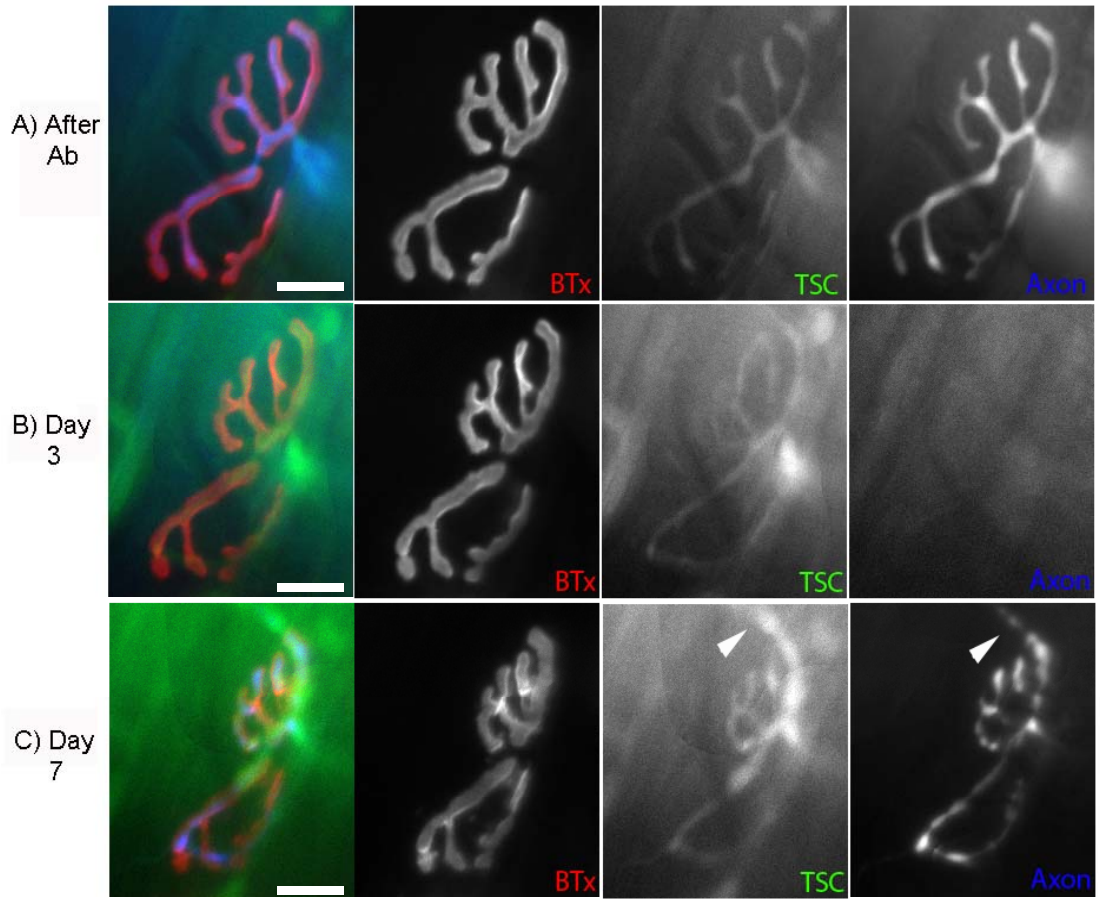

Figure 5.8: Effect of denervation on TSC repopulation. The nerve to sternomastoid was crushed following TSC injury. Repopulation occurs as expected by day 3 in the absence of an axon. However, TSC processes with associated axon sprouts extend beyond the junction at 7 days (arrowhead). (Scale bar: 10µm). Images courtesy of Dr Yue Li, University of Texas.

5.2.6 Origin of returning terminal Schwann cells

5.2.6.1 Nestin and myelin basic protein

In an attempt to identify the origin of returning TSCs, two markers of Schwann cell activity (nestin, and myelin basic protein) were considered.

5.2.6.1.1 Nestin staining

Nestin is an intermediate filament protein, which is synthesised by synaptic myonuclei at mouse NMJs (Kang *et al*, 2007). Although it is also weakly expressed by myelinating Schwann cells but not TSCs, it is upregulated in response to muscle denervation (Kang *et al*, 2003). As a result of this observation, nestin has since been used as a marker of Schwann cell reactivity (Hayworth *et al*, 2006). Staining for nestin was therefore undertaken following TSC injury, in an attempt to identify reactive glia in the pre-terminal area, which may represent the source of returning TSCs and their processes. However, despite using established protocols under the guidance of experienced investigators (Dr. C. Hayworth), repeated attempts did not demonstrate upregulation of nestin along the pre-terminal nerve area at time points: 24 hours, 55 hours, and 72 hours after mAb injury, or convincing TSC expression of nestin in positive controls (figure 5.9). The process of nestin staining is technically very challenging, and the failure of repeatable staining in the positive control suggests this was most likely a technical issue. However, time constraints prevented further investigation into this area, although it would be interesting to explore this technique again at a later stage

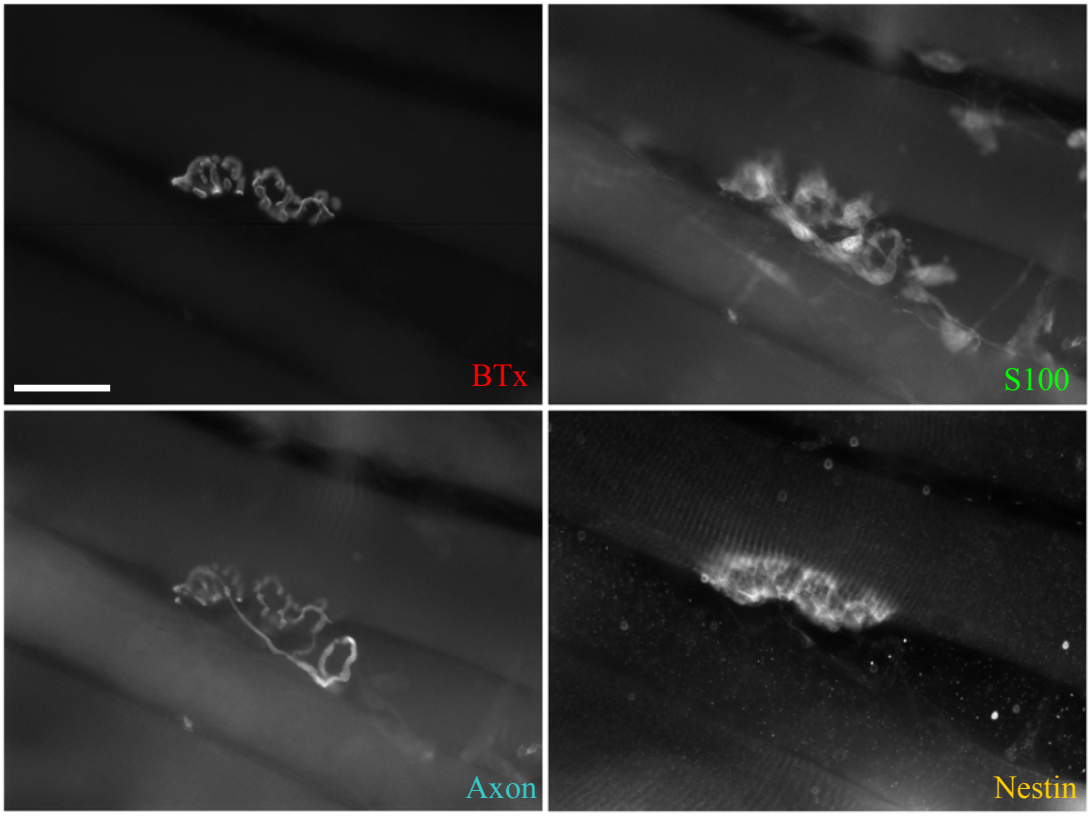

Figure 5.9: Nestin staining from mAb and NHS treated animal at 72 hours. In this junction, the axon is present, and a large number of TSCs are seen at the NMJ as would be expected at this time point. Post-synaptic nestin staining is seen at the junction, which may represent synaptic myonuclear staining. This staining was typical at other time points, and also in control animals. (Scale bar 40µm)

5.2.6.1.2 Myelin basic protein

Myelin basic protein (MBP) is a key component of compact myelin (Martini and Schachner, 1986), and is not therefore present in TSCs. If the returning TSCs arose from the pre-existing myelinating Schwann cells surrounding the innervating axon, it was hypothesised that these "parent cells" would be unable to lose their compact myelin

within 55 hours, and their processes extending into the junction would express myelin basic protein. Staining was therefore undertaken at 55 hours, when processes first appeared over the junction using protocols outlined in Methods.

However, staining for MBP over the junction was very non-specific, and it was not possible to localise MBP to returning processes at the junction (figure 5.10). Again, this may be a technical issue, or it could represent a problem with detection, due to the size of the processes in relation to the rest of the junction. It would be useful to repeat these studies at the electron microscope level to clarify staining in more detail.

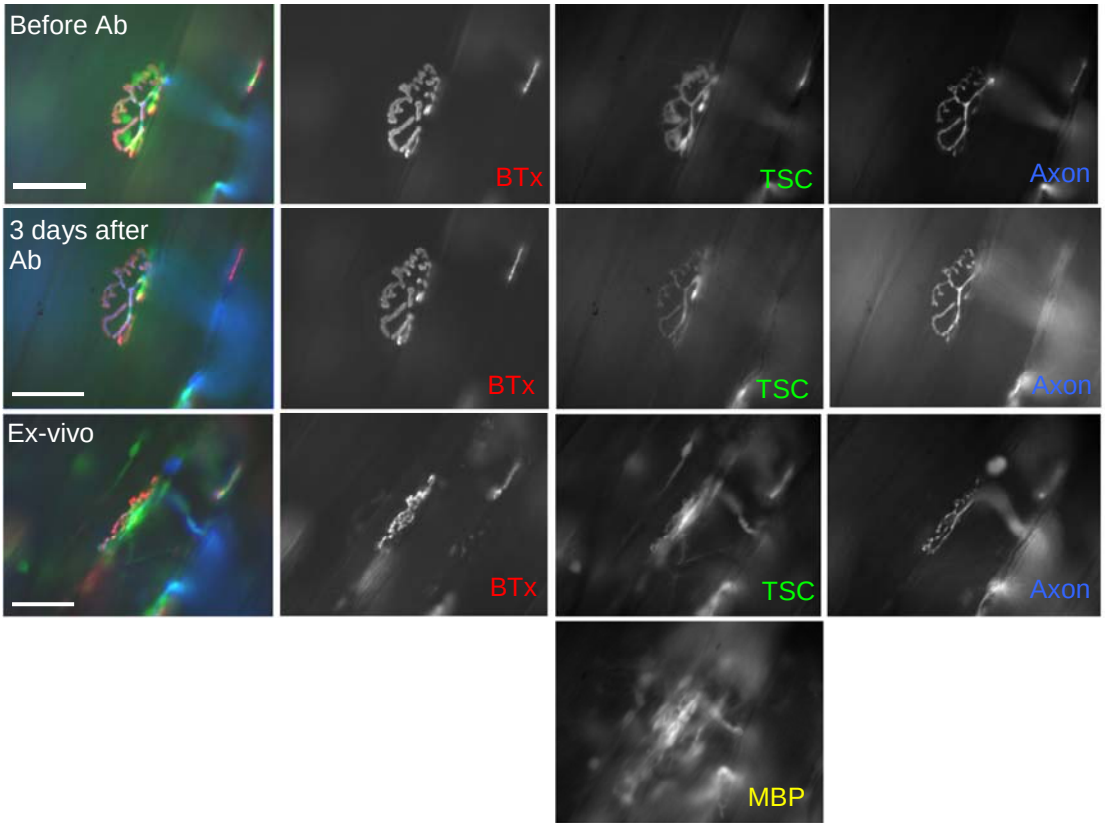

Figure 5.10: Myelin basic protein staining. In this junction, process formation is seen over the junction as expected at 3 days after mAb and NHS exposure. *Ex vivo* staining at this time-point for MBP shows a non-specific MBP stain over the junction, which is difficult to localise to any structure (Scale bar 30µm).

5.2.6.2 Nuclear marker stains

Having conducted unsuccessful experiments using both MBP and nestin, experiments were then conducted using nuclear stains that indicate cell division and activity. It was hypothesised that the source of the returning cells would be undergoing cellular division to provide "daughter" cells to repopulate the NMJ, and nuclear markers of

cell division would identify these cells. The nerve to the contralateral sternomastoid was crushed, and used as a positive control.

Antibodies to Ki-67 were considered in the first instance. Ki-67 is expressed by proliferating cells in all phases of the active cell cycle (G1, S, G2 and M phase) while being absent in resting (G0) cells (AbCam data sheet). This technique as described in Methods, is relatively uncomplicated but despite numerous attempts at staining, it was not possible to identify nuclear staining in nerve bundles with evidence of TSC injury at time points: 24 hours, 55 hours, and 72 hours after mAb injury.

Experiments were also made using another nuclear stain, bromodeoxyuridine (5-bromo-2-deoxyuridine, BrdU), which is an analogue of thymidine, and is incorporated into nuclei during the S-phase of the cell cycle. In one animal, the last myelinating Schwann cell stained positive for BrdU in one junction, suggesting that the cell is undergoing cellular division at the same time as TSC repopulation (figure 5.11). However, it was not possible to repeat this result in other animals, and this finding was not supported by findings using Ki-67.

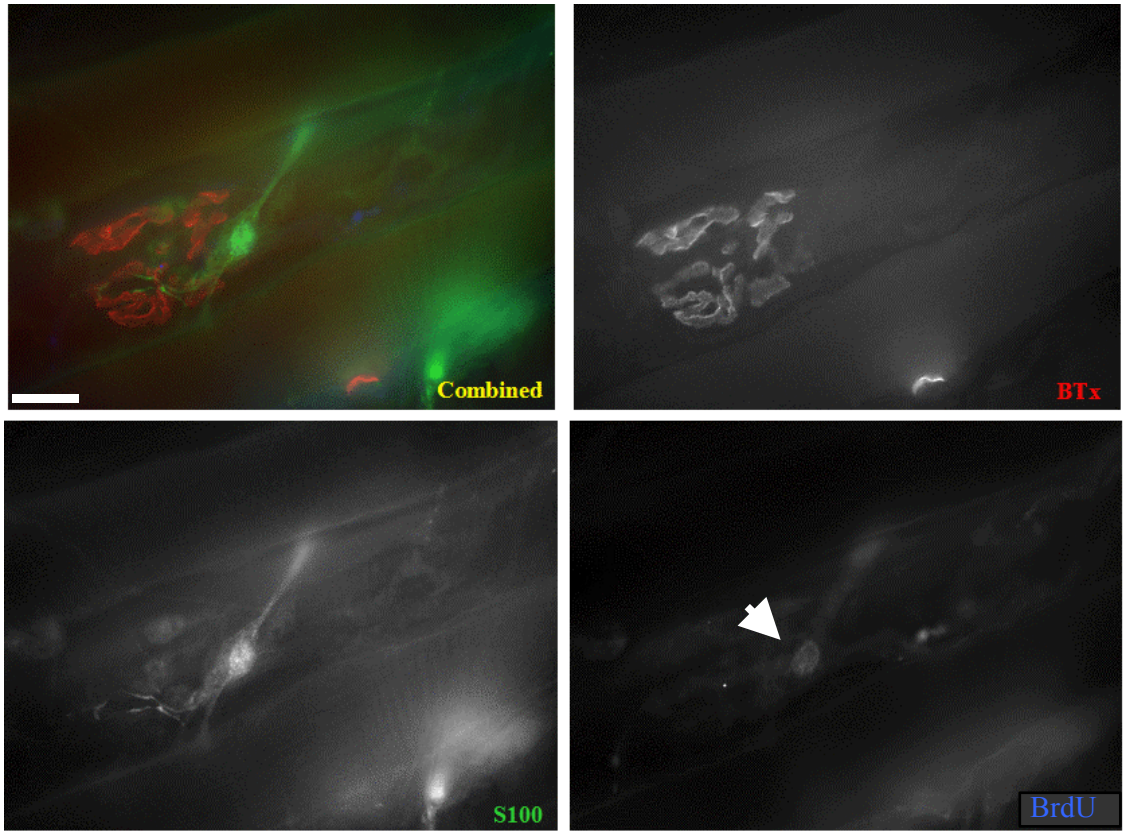

Figure 5.11: BrdU staining during repopulation. Fluorescence from the junction is lost during the staining process, and S100 is used as a marker of Schwann cell morphology. The nucleus of the last myelinating Schwann cell incorporates BrdU at 3 days (arrow). (Scale bar: 30μm)

5.2.7 Repeat application of antibody, and associated changes

To model the effect of chronic antibody titres that are present in human immune mediated disease, and also to investigate the long-term effects of TSC ablation at the NMJ, an attempt was made to stop the repopulation of the junction by TSCs. A second dose of antibody and NHS was applied 48 hours after the first exposure in an attempt to injure returning TSCs, with a third at 72 hours. In total, 3 animals, with 9 junctions were examined.

Unexpectedly, there was no obvious damage to these processes after the second or third applications of antibody and NHS, with GFP fluorescence remaining over the terminal axon (figure 5.12B and C). Processes continued to cover the junction over the following day (figure 5.12C), and also extended beyond the junction itself. Axon sprouts were closely related to these processes and travelled a short distance from the junction at 11 days, where they were associated with new areas of bungarotoxin (figure 5.12 – 11 days).

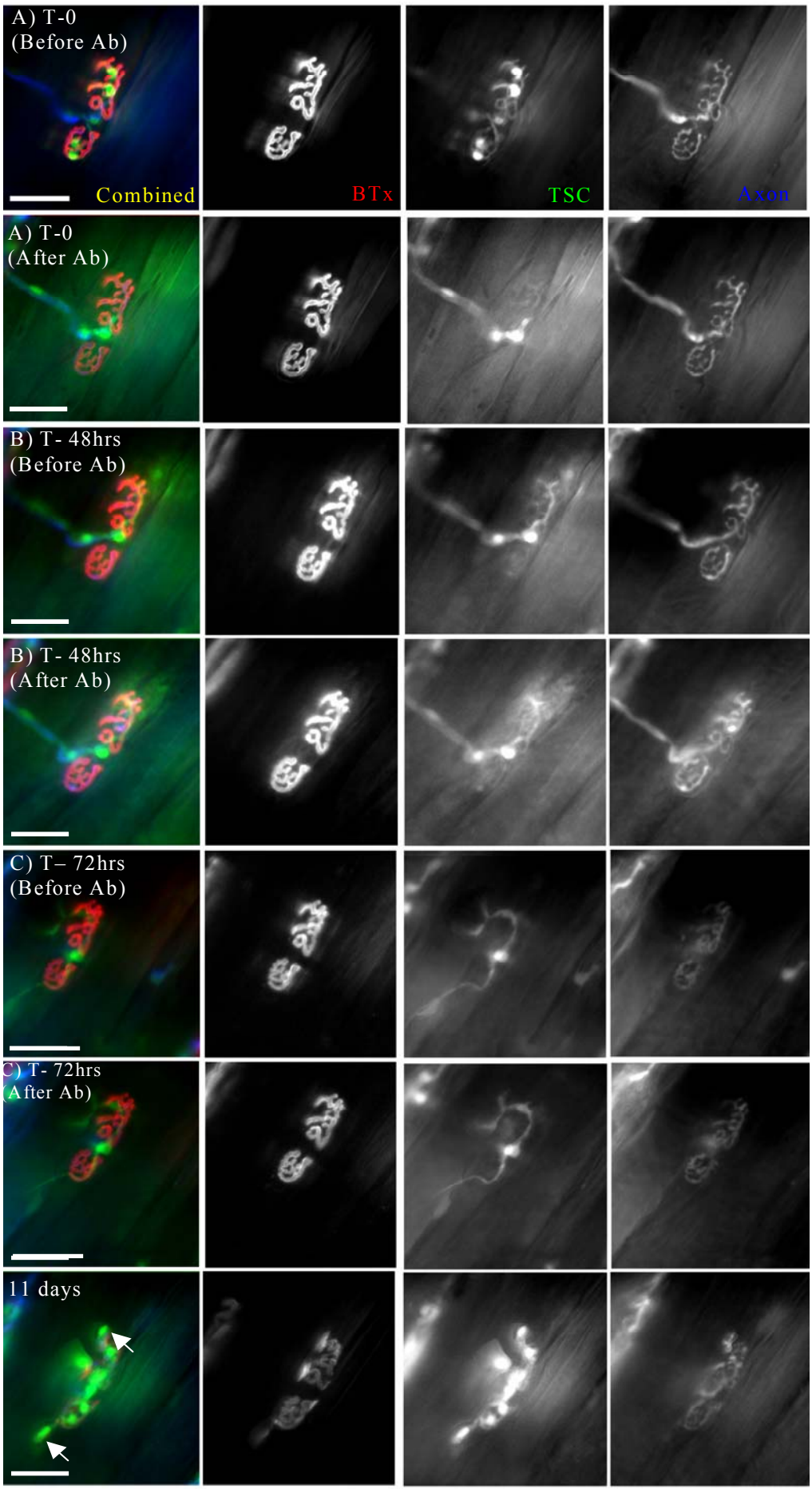
A) T-0
(Before Ab)
Combined
BTx
TSC
Axon
A) T-0
(After Ab)
B) T- 48hrs
(Before Ab)
B) T- 48hrs
(After Ab)
C) T– 72hrs
(Before Ab)
C) T- 72hrs
(After Ab)
11 days

Figure 5.12: Repeat application of antibody. A: Before and after the initial application of mAb and NHS. B: Before and after mAb and NHS application at 48 hours. C: Before and after mAb and NHS at 72 hours. Returning processes, or the underlying axon did not appear to be injured by the second or third application of antibody. However at one week, TSC processes were seen to extend beyond the NMJ. Axon sprouts were also seen in association with TSC processes at 11 days, extending beyond the junction (arrow) and were associated with new areas of bungarotoxin. (Scale bar: 30μm)

To determine if the differences seen with repeat antibody application were the result of antibody binding to the processes, or newly exposed antigenic sites on the axon, a pilot study was performed with a second application of antibody at 12 hours following the initial mAb and NHS incubation, before processes returned to the junction. In this study of a single animal, and 3 junctions, TSC processes did not extend from the junction, and the pattern of repopulation was similar to a single application of antibody. Although more data is required to achieve significance, this study suggests that changes seen when antibody is applied at 48 hours likely result from antibody binding to the newly returning processes without causing cell death, rather than exposed sites on the axon.

5.2.8 Selective injury is dependent on antibody concentration

Under normal circumstances, approximately 6% of NMJs had evidence of axonal injury following antibody exposure. During the course of the study, it became clear that altering the concentration of the antibody would also alter its behaviour. When increased concentrations of EG1 were applied topically to sternomastoid muscle, the antibody also caused axonal injury at the nerve terminal, characterised by axonal fragmentation and degradation in addition to TSC injury. It was not possible to identify any NMJs that had selective TSC loss at concentrations of antibody greater than 200µg/ml (figure 5.13), with all junctions displaying both axonal and TSC loss. Between 100-150µg/ml, a range of injury was visible with both selective TSC injury, and mixed axonal and TSC loss. The axon loss was localised to the terminal axon only, and no disruption to axon structure was seen more proximally.

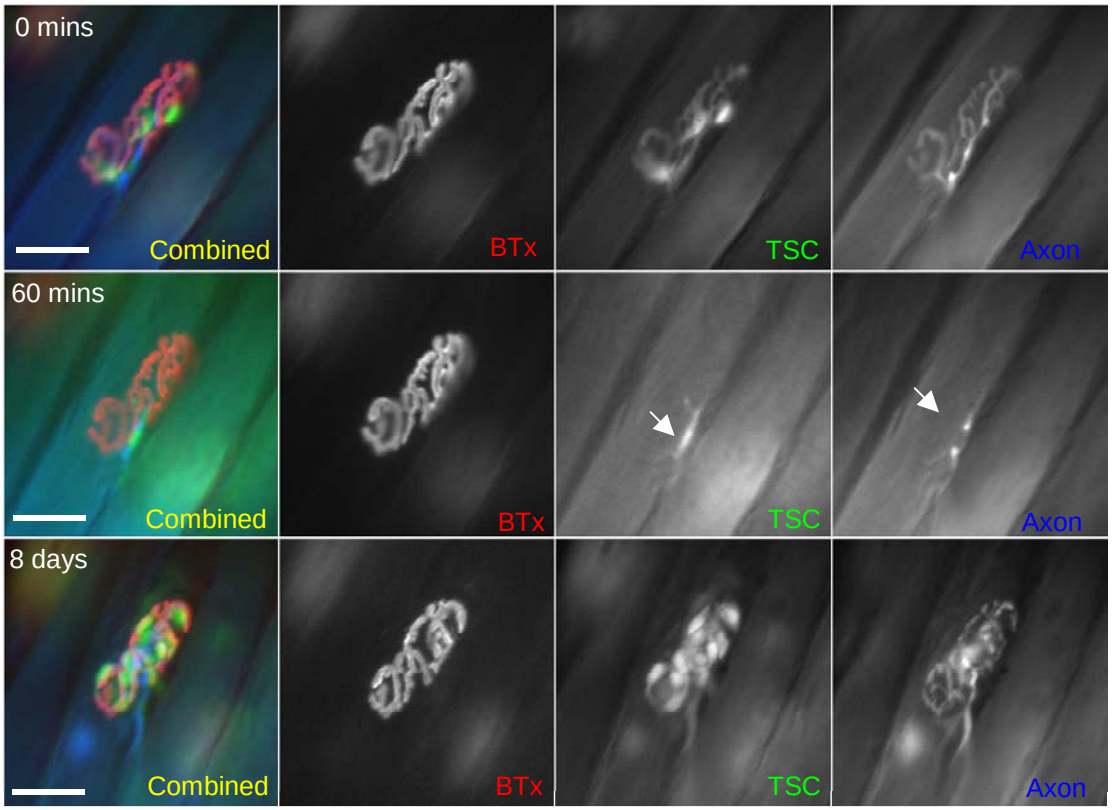

Figure 5.13: Axon and TSC injury following EG1 application at 200µg/ml with NHS. Before antibody application, TSCs and axon are seen over the motor end plate. Following antibody application (60 mins), both TSCs and the terminal axon are absent. However, the last myelinating Schwann cell, and the pre-terminal axon remain intact (arrows). TSC proliferation is seen at 8 days as expected (Scale bar 15µm)

Interestingly, the axon recovered promptly following injury (3 animals, 3 junctions per animal). As can be seen in figure 5.13 and 5.14, the terminal axon is present 8 days after injury, and there is associated TSC proliferation. Although not shown here, the axon was seen to return to the junction within 3 days. Only one animal (3 junctions) was followed beyond 8 days, and the axon remained present over the motor end plate for the duration of this study (28 days). Although its appearance was more irregular than prior to injury,

no change in junction morphology was seen in this animal during the timescale of this investigation (figure 5.14).

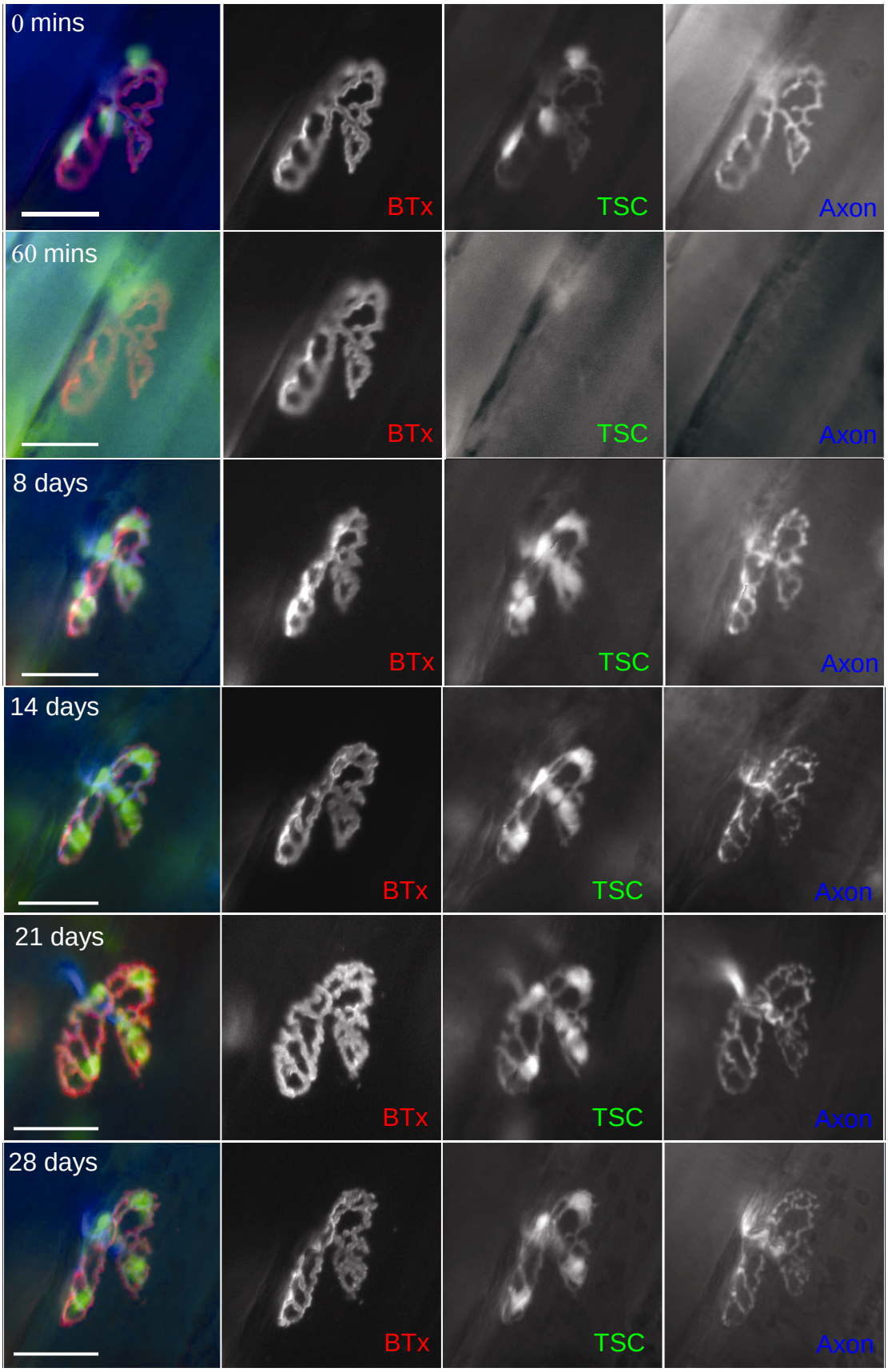
0 mins
BTx
TSC
Axon
60 mins
BTx
TSC
Axon
8 days
BTx
TSC
Axon
14 days
BTx
TSC
Axon
21 days
BTx
TSC
Axon
28 days
BTx
TSC
Axon

Figure 5.14: Long term effects of axon and TSC injury. In this preparation, both the terminal axon and Schwann cells are injured, but demonstrate recovery at 8 days. TSC proliferation is seen at 8 days, in association with axon recovery. Although the axon appearance is more irregular than prior to injury, the end plate appearance remains unchanged up to 28 days after axon injury. (Scale bar 30μm)

5.3 Discussion

5.3.1 Antibody effect in CK mouse

Characterising the antibody effect on sternomastoid muscle confirms TSC injury, using ethidium uptake into TSC nuclei as a marker of damage. The presence of ethidium nuclei also correlate very closely with loss of GFP expression from TSCs, most likely through formation of membrane attack complex, rendering the cell membrane permeant which allows access of ethidium to the cell nucleus in addition to loss of GFP.

Unsurprisingly, NMJs with evidence of damage lie most superficially on the sternomastoid muscle, in direct contact with incubating solutions of antibody and complement. Junctions lying deeper within the muscle are unaffected, most likely due to the muscle thickness with associated connective tissue acting as a barrier for antibody and complement penetration to deeper junctions.

Interestingly, a proportion of junctions also displayed evidence of axonal injury, characterised by swelling and breakdown of the axon. This pattern of change is consistent with an antibody-mediated injury at this site, and was enhanced when higher concentrations of antibody were applied. It is possible that EG1 is binding to axons at these junctions under normal circumstances, and may be activating complement in a small minority to cause injury. When the concentration of antibody is increased, more is available to bind to the axon and produce a greater injury as a consequence.

5.3.2 Short-term changes following selective terminal Schwann cell injury

This study also suggests that the nerve terminal can survive for at least 48 hours without TSCs. There was no gross morphological change to the axon or nAChR up to 48 hours without TSCs, suggesting that the TSC does not provide significant trophic support for the axon or post-synaptic apparatus over this time. Further studies examining the electrophysiology of damaged junctions just prior to repopulation would be interesting, to determine whether any physiological, rather than anatomical disturbance was evident at this time. This would confirm the the conclusions of Ko and colleagues who suggest that frog TSCs are not necessary for the acute maintenance of the NMJ (Reddy *et al*, 2003).

5.3.3 Terminal Schwann cell recovery

5.3.3.1 Terminal Schwann cells proliferate following injury, and occupy new sites at the NMJ causing long-term synaptic remodelling in the mammal

In contrast to studies in the frog, all visualised junctions with TSC injury exhibited TSC recovery in the mouse, beginning around 48 hours after initial injury. A number of factors may account for this difference between the two studies. In particular, different species were used: the amphibian NMJ is developmentally less complex than the mammal, and therefore its capacity to regenerate may be different to the mouse. Additionally, the method of antibody delivery was different between the two systems. In the mouse model, muscle was incubated for an hour with antibody and then complement, before both were washed off with Ringer's solution. However, Ko and colleagues administered antibody between muscle layers, presumably maintaining antibody levels for a longer period. This prolonged dosing may inhibit the return of TSCs in the frog, and prevent any recovery that was shown in our system. This difference allowed us to characterise the process of TSC recovery in greater detail, rather than examine effects of chronic TSC depletion that has been described previously.

Prior to TSC return to the NMJ, GFP expressing processes were seen to extend from the pre-terminal nerve to cover the terminal axon. The appearance of these processes was very similar to those seen following denervation (Son and Thompson, 1995a,b; Son *et al*, 1996; Trachtenberg and Thompson, 1996; Trachtenberg and Thompson, 1997). Unlike the changes seen following denervation however, these processes did

not extend beyond the NMJ, and were also present over an intact axon. Myelinating Schwann cells have been shown to migrate along intact axons following demyelination (Griffin *et al*, 1987) and nerve graft repair (Hall, 1986; Hall, 1989); and also possibly during development (Reithmacher *et al*, 1997). This was highlighted by Asbury in his original review in 1969 (Asbury, 1969).

Within 72 hours of the original TSC injury, GFP positive cell bodies were evident at the junction. Over the following week, these cells multiplied to exceed the number present before injury. An increase in myelinating Schwann cell number is often seen after axonal injury and demyelination elsewhere in the PNS (Pellegrino and Spencer, 1985; Griffin *et al*, 1987; Griffin *et al*, 1990; Murinson *et al*, 2005), although the stimulus for this proliferation is not known (Pellegrino *et al*, 1986; Oaklander *et al*, 1987). Proliferation of TSCs is also seen following axonal injury, although the stimulus for repopulation in these examples is renervation, rather than the initial injury (Love and Thompson, 1998; Connor and McMahan, 1987). However, it is also known that complement, and in particular membrane attack complex, can cause cell proliferation (Dashiell *et al*, 2000; Cole and Morgan, 2003). Although it is unlikely that residual levels of MAC would be present at the NMJ after 3 days and then cause significant cell division, it is possible that the presence of MAC at the time of the initial injury is a sufficient signal to initiate repopulation.

5.3.3.2 Response of junction is similar following TSC and axon injury

Interestingly, junctions with evidence of axon damage behaved in a very similar fashion to those with TSC injury alone. In these junctions, both axons and TSCs would return to

the NMJ by 72 hours after initial mAb and NHS exposure. Proliferation of TSCs would follow over the next week, and the structure of the junction would remain remarkably constant up to 28 days later. This suggests that the process of recovery following localised injury to the motor nerve terminal is very rapid, and does not appear to cause significant disruption to terminal morphology. It would be interesting to perform electrophysiological measurements during this recovery process, to identify whether any functional deficit is evident following this injury as both axon and TSC injury have been implicated as a possible method of disease pathogenesis in MFS.

5.3.3.3 TSC repopulation is not axon dependent

Another interesting finding suggests that an intact axon is not required to achieve TSC repopulation of the junction. Although the stimulus for repopulation is not entirely clear from our studies, a number of possibilities may cause the return of TSCs. The stimulus may arise from loss or alteration of contact between the last myelinating Schwann cell and the TSCs, causing the last myelinating Schwann cell to undergo morphological change, permitting repopulation. The stimulus may also arise post-synaptically, either from the muscle fibre, or junction itself.

Interestingly, returning TSC processes do not appear to follow the same pattern of axonal distribution that was seen prior to denervation, and these processes appear to alter the location of the returning axon at 7 days. This contrasts with antibody induced axon and TSC injury, where there was no gross morphological disruption to the motor nerve terminal.

However, axon recovery was much more rapid following antibody-mediated injury, as only the terminal axon was disrupted. It is possible that the rapid recovery of the axon in this circumstance provided a framework for TSC regrowth over the junction, which was not present following nerve crush. It is possible that the synaptic basal lamina may act as a guide for the returning processes in the absence of an axon following nerve crush, but further work is required to investigate this more fully.

5.3.4 Origin of returning cells

TSCs returned to the NMJ relatively quickly, within approximately 55 hours, and the pattern of process return appears to suggest that the cells arise from the pre-terminal nerve bundle. One possible source of these repopulating cells could therefore be the last myelinating Schwann cell, which would de-differentiate to lose its myelinating phenotype, and repopulate the junction. TSCs share many proteins associated with myelinating Schwann cells, including MAG, 2',3'-cyclic nucleotide 3'-phosphodiesterace (CNPase), myelin galactolipid and galactocerebroside (GalC) (Georgio, 1999), and this suggests that both cell types are closely related. Additionally, demyelination and nerve injury can cause SCs to alter their phenotype (Aguayo, 1976; Cheng 2002), and illustrates how established Schwann cells can alter their behaviour depending on local circumstances.

To investigate this hypothesis, staining was undertaken using both BrdU, and Ki-67 which are separate markers of cell division. Despite extensive studies, only one animal showed BrdU uptake into the last myelinating Schwann cell in a "recovering" junction, while no uptake was seen using Ki-67. As a result, it is impossible to

conclude that returning TSCs arise from the last myelinating Schwann cell. This observation is supported by other studies which demonstrate that myelinating Schwann cells do not normally undergo cell division, while non-myelinating SCs undergo division relatively infrequently (Griffin *et al* 1987, 1990). While demyelination and nerve injury can cause SCs to undergo mitosis (Pellegrino and Spencer, 1985; Oaklander *et al*, 1987) and also alter their phenotype (Aguayo *et al*, 1976; Cheng and Zochodne, 2002), it is conceptually difficult to accept that the last myelinating Schwann cell could demyelinate, extend processes, and undergo mitosis within the timescale.

Another possible source of these cells may be the non-myelinating Schwann cell pool, which lies more proximally in nerve bundles. These cells have been shown to multiply and migrate (Murenson et al, 2005) following nerve injury but two main reasons preclude this mechanism in the TSC ablation model. Firstly, the cells would have to move to the NMJ rapidly, and possibly undergo mitosis prior to this migration, which may not be possible within the timeframe of this model. Equally, this mechanism would most likely require a myelinating nerve bundle to signal to a non-myelinating nerve bundle, and there is little evidence that such a signalling pathway exists. As a result, although this hypothesis is possible, it is not likely.

Another hypothesis suggests that cells may migrate from outwith the nervous system to proliferate and produce new TSCs. Although processes are seen to extend from the pre-terminal nerve bundle, the majority of the cell bodies, when present, are usually seen to the outside of the junction (figure 5.5). While this could simply be the cells migrating to the tips of the newly formed processes, it may also represent cells

entering from outwith the junction, and associating with processes from the pre-terminal nerve. One source of these cells could be the latent pool of primitive stem cells that are present in muscle (Seale et al, 2001). Several populations of multipotent stem cells are thought to exist in the muscle (Qu et al, 1998; Gussoni et al, 1999; Jackson et al, 1999; Lee et al, 2000), and while none have been shown to differentiate into Schwann cells as yet, it is thought that these multipotent stem cells in the muscle only commit to a lineage in response to a differentiation inducing signal (Wada et al, 2002). This "stock options" model may allow early stage multipotent stem cells to differentiate into TSCs in response to injury.

5.3.5 Repeat antibody application

Experiments were also undertaken to examine whether the axon can survive without TSCs. A second dose of antibody was applied when processes returned to the junction, in an attempt to injure the returning processes and stop repopulation. However, this second dose of antibody did not produce any obvious injury to the cells, with no loss of GFP or interruption to the process of repopulation. It is possible that the returning TSC processes become less sensitive to the effects of the antibody and complement, either by altering complement regulators on the cell surface or changing the ganglioside composition of the membrane. Both of these mechanisms would allow recovery, without any further antibody-mediated injury to the cell.

However, it is likely that the antibody had some effect, because the returning processes extended beyond the junctional area, and induced limited axon sprouts with associated bungarotoxin changes within 2 weeks. This effect was not seen when a

second dose of antibody was applied before processes returned to the junction at 12 hours (1 animal, 3 junctions), which suggests that these changes are not the result of cryptic ganglioside binding sites being exposed on the surface of the axon following TSC removal.

It was not possible to replicate chronic exposure to antibody, as occurs in disease, in this model system within the timescale of the study. However, these early pilot experiments suggest that significant changes may occur to the junction during this type of exposure, which may influence both NMJ structure and function.

It would be interesting to perform both passive transfer models of disease to maintain an antibody titre, and studies involving inhibitors of cellular mitosis (to prevent TSC repopulation). These models would provide a more accurate model of chronic TSC injury, and study the effects of their absence in the mammalian NMJ.

5.4 Conclusion

The purpose of this study was to illustrate the changes that occur at the mammalian NMJ following selective TSC injury, and to compare this with previous studies in the frog.

This study shows that selective TSC injury can be achieved in the sternomastoid muscle of the CK mouse preparation, with the effect being seen in junctions lying most superficially. Morphological data also supports previous *ex vivo* findings that an axon can survive without TSCs in the short term, and can maintain its morphology in

their absence. However, the results contrast with a previous study in the frog, by demonstrating TSC recovery following an acute injury, and subsequent repopulation of the junction. Despite the increase in TSC number, the junction remains remarkably stable over this time. Although the stimulus for this recovery is not apparent from this investigation, it is clear that recovery can take place in the absence of the terminal axon.

Remodelling is seen following a second application of antibody, and suggests that the returning TSC distribution is altered following repeat antibody exposure. This interesting finding offers a possible insight into human disease, where antibodies may selectively injure TSCs at the NMJ.

Chapter 6: Human tissue

6.1 Introduction

Antibodies to complex gangliosides have been implicated in a number of diseases of the PNS, including GBS and its variants (Yuki *et al*, 1990; Ropper, 1992; Willison *et al*, 1993a). Although a substantial body of both clinical and epidemiological evidence exists to support the possible pathogenic role of anti-ganglioside antibodies in PNS disease (Kornberg and Pestronk 1991, 1995), it has been difficult to confirm this unequivocally in humans.

Antibodies to GM1 ganglioside have been used extensively in human disease modelling, due to its close association with AMAN/AMSAN variant of GBS (Yuki *et al*, 1990; Pestronk and Li, 1991; Ogino *et al*, 1995). Anti-GM1 antibodies have been shown to bind to human nerve tissue (Kusunoki *et al*, 1997; Gong *et al*, 2002), and also mouse preparations (O'Hanlon *et al*, 1996; Molander *et al*, 1997). However, studies examining the pathogenicity of these antibodies are often contradictory. For example, certain studies have shown that anti-GM1 antibodies can produce demyelination and electrophysiological disturbance in *ex vivo* nerve fibre preparations (Santoro *et al*, 1992), while others have not shown such a lesion (Harvey *et al*, 1995). Despite this contradictory work, it has been shown that injecting rabbits with a bovine brain ganglioside mixture or isolated GM1 causes high titres of antibodies to GM1, flaccid limb weakness and pathological changes consistent with an axonal neuropathy. This has provided researchers with an animal model of GM1 mediated

GBS (Yuki *et al*, 2001), and supports other models using the GD1b ganglioside (Kusonoki *et al*, 1996).

Antibodies to the complex ganglioside GQ1b have been closely associated with cases of MFS, and other immune-mediated diseases associated with ophthalmoplegia (Chiba *et al*, 1993; Willison *et al*, 1993a, Yuki *et al*, 1993c). Considerable work has been undertaken using antibodies to these gangliosides, in an attempt to elucidate disease pathogenesis (as discussed in chapter 1). Many of these experiments have been performed in mouse *ex vivo* preparations, where both monoclonal antibodies to complex gangliosides, and also sera from patients have been shown to induce electrophysiological disruptions, particularly at the NMJ (Roberts *et al*, 1994, Willison *et al*, 1996; Plomp *et al*, 1999). This supports neurophysiology measurements made from patients who are in the acute phase of MFS, and also from patients with CANOMAD (chronic ataxic neuropathy with ophthalmoplegia, IgM paraprotein, cold agglutinins and disialosyl antibodies) (Willison *et al*, 1993b; Sartucci *et al*, 2005).

Although much of the work using antibodies to complex gangliosides has been performed in mouse tissue, there have only been limited studies in human nerve and muscle preparations. An interesting publication by Chiba and colleagues in 1993 described an association between symptoms of ophthalmoplegia, and antibodies to complex gangliosides demonstrated from patient sera. In addition, they also used a separate monoclonal antibody to GQ1b to map the distribution of this ganglioside in human cranial nerves, and highlighted its distribution in the nodes of Ranvier, particularly in oculomotor nerves. However, they did not demonstrate significant

binding of their patient serum to these sites. Another study from the same laboratory also examined the distribution of GQ1b alpha and GT1a alpha (minor gangliosides) in human tissue, and mapped these to lamina I and III of dorsal horn and lateral horn of human thoracic cord, but not to motor neurones (Kusunoki *et al*, 1993).

Despite antibodies to complex gangliosides causing injury at the mouse NMJ, no experiments have been performed that demonstrate antibody binding at this site in the human. Additionally, although the TSC has been shown to be an antibody target in the mouse model, it is important to clarify whether this is also a target in human disease. This would bridge the gap between animal and human studies, while also identifying glia, as possible disease targets at human NMJs.

The purpose of these experiments is therefore to demonstrate whether the human NMJ is a likely target for antibodies to complex gangliosides, and in particular whether human TSCs are a disease target.

6.2 Results

6.2.1 TSC injury using human serum

6.2.1.1 Introduction

A technique for studying the effects of antibodies to complex gangliosides is well established using mouse *ex vivo* hemidiaphragm muscle preparations. Before examining antibody binding in human tissue, human serum was first tested in mouse

hemidiaphragm preparations using this established technique. This experiment would demonstrate whether human serum is capable of producing TSC injury in an established experimental model, and would also show if any special conditions are required for using human antibodies in *ex vivo* preparations.

Samples of serum were taken from a patient in the acute phase of MFS (sample Ch), who had elevated titres of antibodies to complex gangliosides (see table 6.1, Ch). Samples of serum, and also red cell eluate from a patient with CANOMAD who had antibodies to complex gangliosides (table 6.1, Ha) were also studied. A serum sample from a healthy volunteer with no anti-ganglioside antibodies (table 6.1, Col) was used as a negative control.

Glycolipid	IgG			IgM			Normal Ranges (IgG & IgM)
	Ch	Ha	Col	Ch	Ha	Col	
GM1	NEG	NEG	NEG	NEG	NEG	NEG	1/500
GM2	NEG	NEG	NEG	NEG	NEG	NEG	1/500
GM3	NEG	NEG	NEG	NEG	NEG	NEG	1/500
GA1	NEG	NEG	NEG	1/300	NEG	NEG	1/5000
GD1a	1/450	NEG	NEG	1/200	NEG	NEG	1/500
GD1b	NEG	NEG	NEG	NEG	>1/12500	NEG	1/500
GT1b	1/420	NEG	NEG	NEG	>1/12500	NEG	1/500
GQ1b	>1/12500	NEG	NEG	NEG	>1/12500	NEG	1/500
GD3	1/500	NEG	NEG	NEG	>1/12500	NEG	1/500
Sulphatides	NEG	1/3200	NEG	NEG	>1/15000	NEG	<1/10000
Globoside	NEG	NEG	NEG	NEG	NEG	NEG	1/500

Table 6.1: Anti-glycolipid antibody titres for patient Ch, Ha and Col (data supplied by Mrs. J. Veitch).

Hemidiaphragm preparations from 3 BALB/c mice were incubated with samples of human serum as described in Methods. TSC injury was measured by EthD-1 uptake. Intensities of immunoglobulin and membrane attack complex (MAC) were measured using a confocal microscope, and ImageJ analysis software as described in Methods.

6.2.1.2 *Ex vivo* analysis of sample Ch

The results show that immunoglobulin was present over the junctions with samples Ch (figure 6.1), but not Col. There was also evidence of TSC injury with sample Ch, in association with elevated levels of MAC (figures 6.2a and 6.2b). There was associated neurofilament loss with human serum (figure 6.2c), suggesting that the effect was not entirely TSC selective.

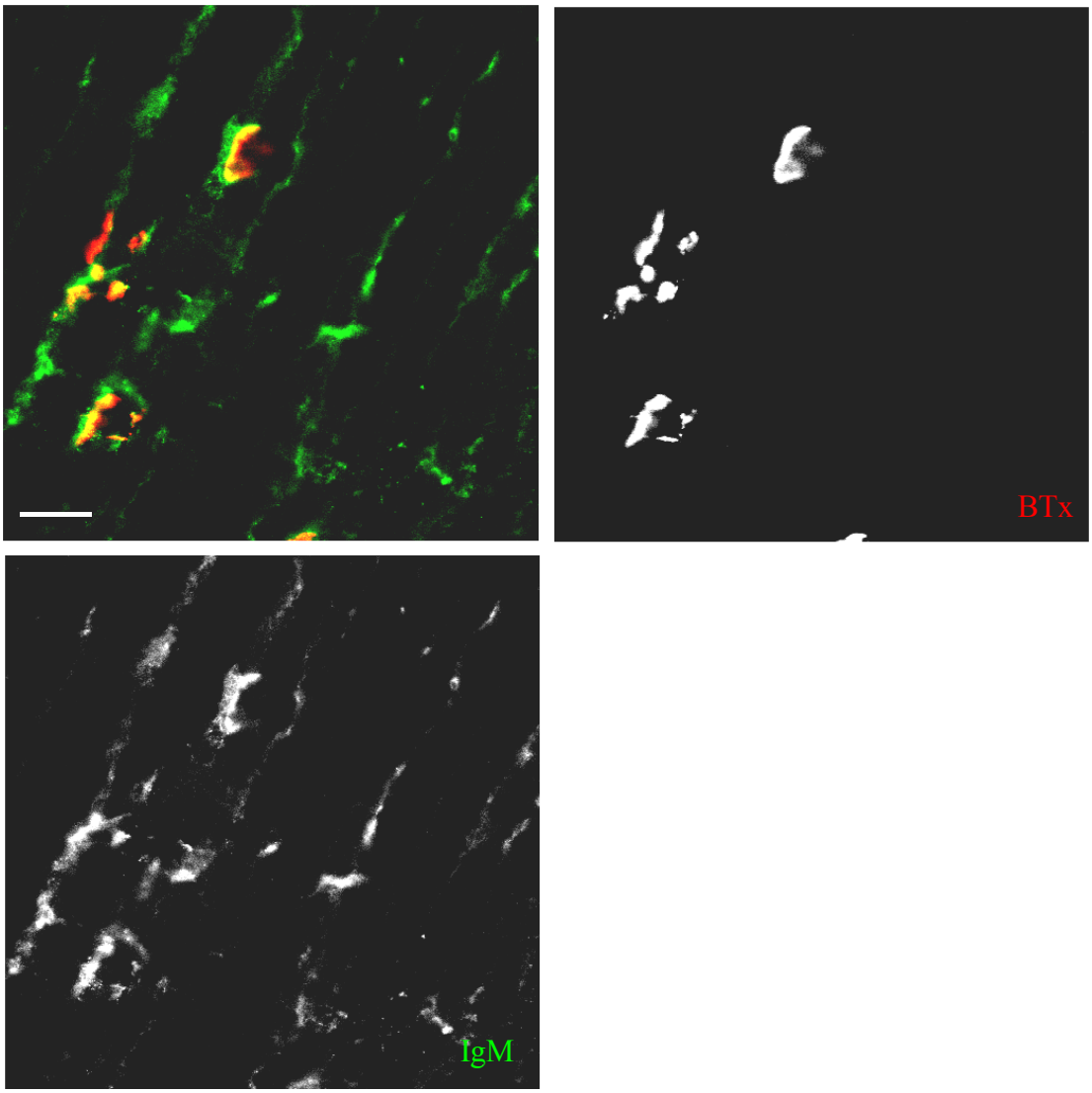

Figure 6.1: Immunoglobulin deposition using serum from patient Ch in *ex vivo* hemidiaphragm preparations from BALB/c mice (Scale bar 30µm).

A

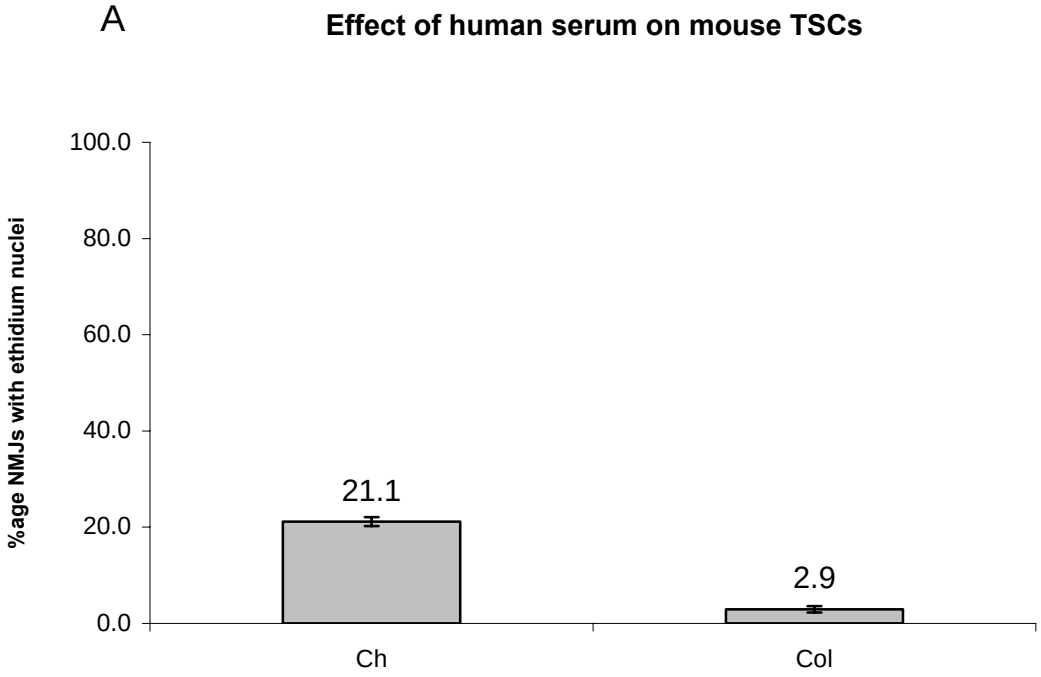
Effect of human serum on mouse TSCs
%age NMJs with ethidium nuclei
100.0
80.0
60.0
40.0
20.0
0.0
21.1
2.9
Ch
Col

B

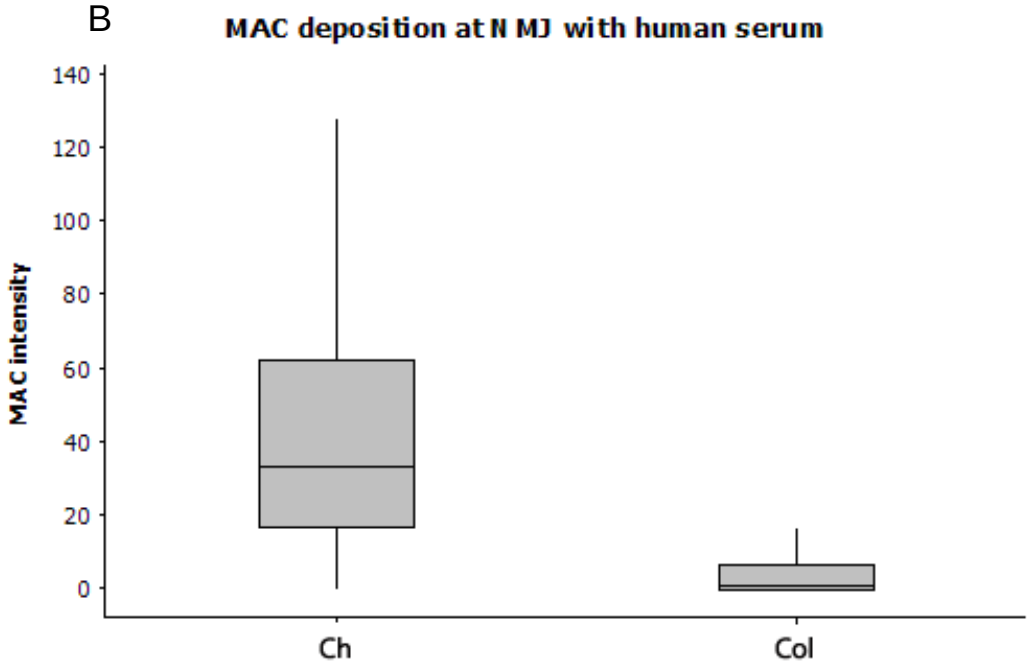
MAC deposition at N MJ with human serum
MAC intensity
140
120
100
80
60
40
20
0
Ch
Col

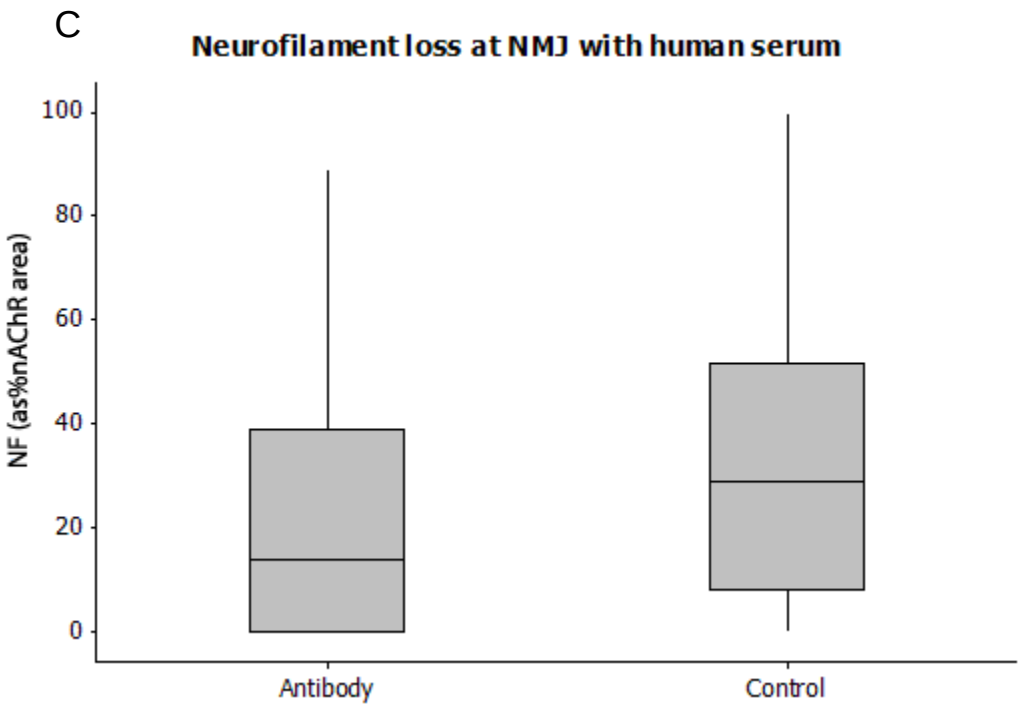

Figure 6.2: Quantitative analysis of NMJ injury as assessed by immunofluorescent staining for membrane attack complex (MAC), neurofilament (NF), and abnormal TSC nuclear uptake of EthD-1.

A - TSC injury. NMJs with one or more overlying EthD-1-positive nuclei were scored as positive, and counts were pooled from 3 preparations from 3 mice. Human serum is significantly different from control ($p < 0.01$), with a mean of 21.1 (SEM=0.9) compared with a mean of 2.9 in control (SEM=0.7).

B - MAC deposits. Patient serum Ch produced significant deposits of MAC over NMJs compared with controls ($p < 0.01$).

C - Axonal integrity. NF signal is reduced over the NMJ with human serum. Human serum preparations are significantly different from control ($p < 0.01$).

In figure A, the mean is shown as a value in the graph, with standard error of mean as error bars. In figures B+C, outlying data points are removed, leaving median values, interquartile ranges (box) and 1.5 times the interquartile range (vertical lines). MAC intensity or NF is measured using ImageJ as described in Methods. Data is pooled from 3 hemidiaphragm preparations from 3 mice for each condition, using techniques outlined in Methods.

6.2.1.3 *Ex vivo* analysis of sample Ha

Samples from patient Ha were initially considered for use as a positive control, as it has been previously characterised *ex vivo* (Willison *et al*, 1993b; Willison *et al*, 1996). Samples of serum and red cell eluate were studied on BALB/c and NIH hemidiaphragm preparations, but despite using previously established *ex vivo* protocols, it was not possible to reproduce either the electrophysiological or morphological changes described previously even using different concentrations of antibody during the initial incubation. Although immunoglobulin was present over the end plate, this was not associated with C3c deposition. The results of 3 preparations taken from 3 mice is shown in figure 6.3. These findings were supported by ganglioside ELISAs that confirmed the presence of antibody in both serum and red cell eluate (not shown).

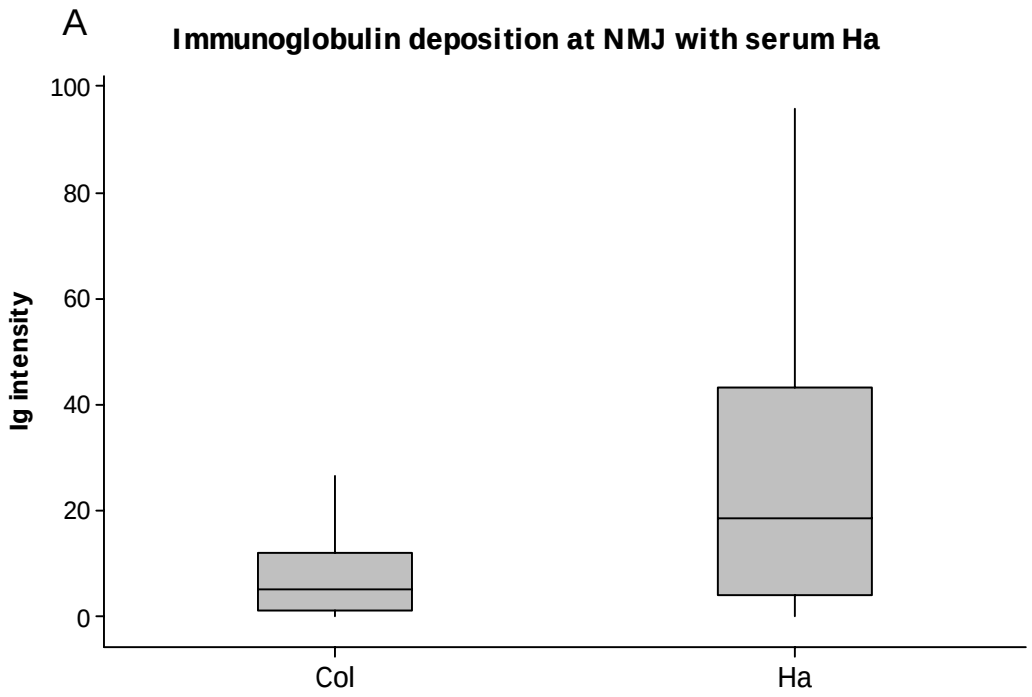
A
Immunoglobulin deposition at NMJ with serum Ha
Ig intensity
100
80
60
40
20
0
Col
Ha

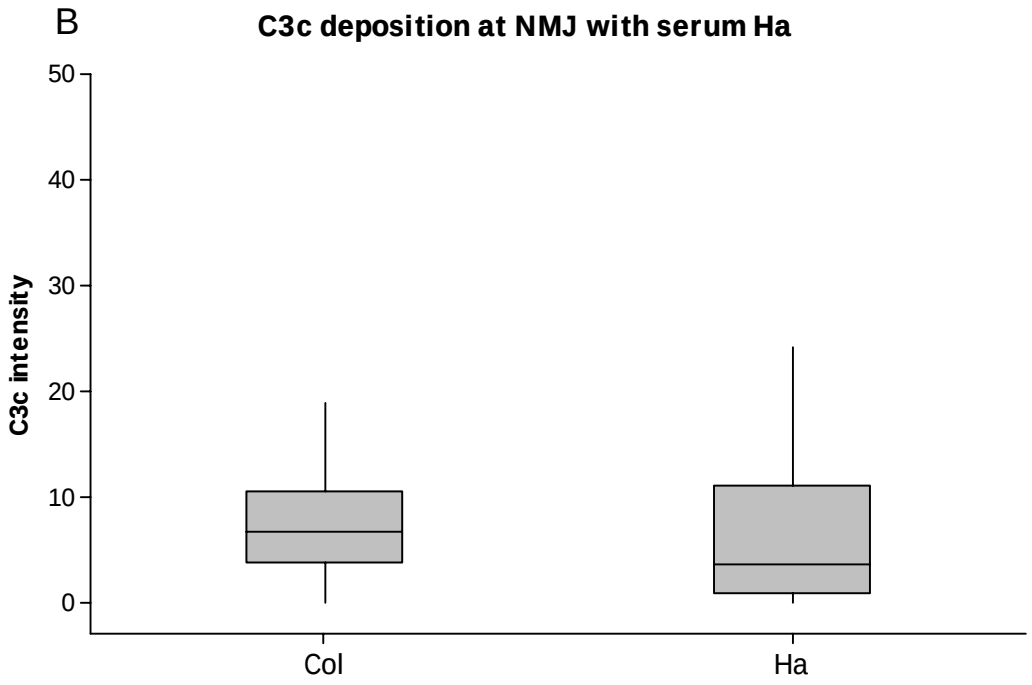
B
C3c deposition at NMJ with serum Ha
C3c intensity
50
40
30
20
10
0
Col
Ha

Figure 6.3: Quantitative analysis of NMJ injury using serum Ha as assessed by immunofluorescent staining for immunoglobulin and C3c deposition using ImageJ as described in Methods, from 3 hemidiaphragm preparations taken from 3 mice for each condition. Outlying data points are removed, leaving median values, interquartile ranges (box) and 1.5 times the interquartile range (vertical lines).

A – Immunoglobulin deposition. Patient serum Ha produced significant deposits of immunoglobulin over NMJs compared with controls ($p = 0.03$)

B – C3c deposits. There was no difference in C3c intensity overlying the junction between serum from patient Ha and control ($p>0.13$)

6.2.2 Human muscle tissue

6.2.2.1 Characterisation of human muscle tissue

Several muscle groups were considered for these experiments, including: innermost intercostal muscle, omohyoid muscle, pharyngeal constrictor muscle, extra-ocular muscle (EOM) and biceps. These muscles were either routinely discarded during intra-operative dissection for a variety of procedures, or were obtained from post-mortem tissue banks. Table 6.2 shows the number of samples for each muscle group, the type of operation, and the patient diagnoses. A summary of the tissue harvest is included in Methods.

Human tissue	Number of samples	Operation	Time to freeze	Diagnosis
Intercostal muscle	1	Coronary artery bypass graft	Immediate	IHD
Omohyoid muscle	3	Neck dissection	Immediate	Neoplasia
Pharyngeal constrictor muscle	3	Oro-pharyngeal dissection	Immediate	Neoplasia
Peroneus longus	1	Amputation	One hour	Neoplasia
Extensor digitorum brevis	1	Amputation	One hour	Neoplasia
Extra-ocular muscle	1	Post mortem harvest	Not known	Unknown (non-neoplastic)
Sciatic nerve	1	Post mortem harvest	Not known	Unknown (non-neoplastic)
Lumbar spine	1	Post mortem harvest	Not known	Unknown (non-neoplastic)

Table 6.2: Summary of human tissue samples. "Time to freeze" is the time from removal of the muscle to snap freezing.

Although studies on the morphology of human NMJs have been performed previously (Slater *et al*, 1992), no comparison studies have been made using the muscles in this investigation. Before undertaking more detailed studies, the number of available junctions in each muscle was measured. Junctions were identified by post-synaptic bungarotoxin labelling from each muscle group, from at least 3 different sections of each muscle block as described in Methods.

These studies showed that there was a significant difference in the number of junctions available per sample between human and mouse muscle. Additionally, there were more junctions in EOM, and omohyoid than other human muscles under study (figure 6.4). Although it is not possible to draw a meaningful conclusion from the absolute values obtained from this study, it does demonstrate the differences in the number of junctions available for further study.

The size of junctions were also measured in each muscle tissue. Junctions were identified by bungarotoxin labelling, and the long axis of each junction was measured using existing scaling software (Axiovision, Zeiss). Data from three repeats using three non-contiguous muscle sections in each experiment were pooled.

In this study, there does not appear to be a statistically significant difference in end plate size between the different muscles under consideration, and in particular, there was no difference between human or mouse muscle (figure 6.4).

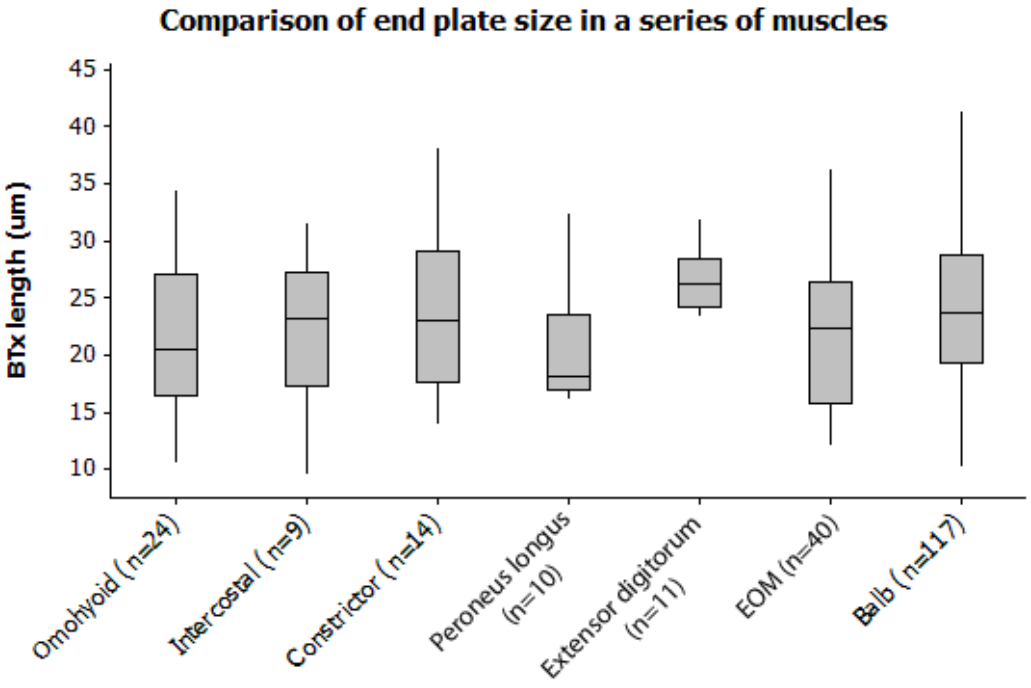

Figure 6.4: End plate size, and number of junctions in 20µm muscle sections. Muscle sections were stained with bungarotoxin, and the long axis of this signal was measured. No statistically significant difference in junction length was evident between muscle groups, although the sample numbers are low for all muscles except EOM and BALB/c. Outlying data points are removed, leaving median values, interquartile ranges (box) and 1.5 times the interquartile range (vertical lines).

.

6.2.2.2 Anti-ganglioside antibody binding

Having characterised the human muscles, the binding patterns of anti-ganglioside antibodies was examined. Cryostat sections of human muscles were first incubated with antibodies that are known to bind to the mouse NMJ, and produce TSC injury (EG1, R24, LB1, and CGM3) using protocols outlined in Methods. Human lumbar

spine (figure 6.5) and mouse hemi-diaphragm sections were used as a positive control. Imaging was performed using Zeiss AxioImager with Apotome microscopy, as described in Methods.

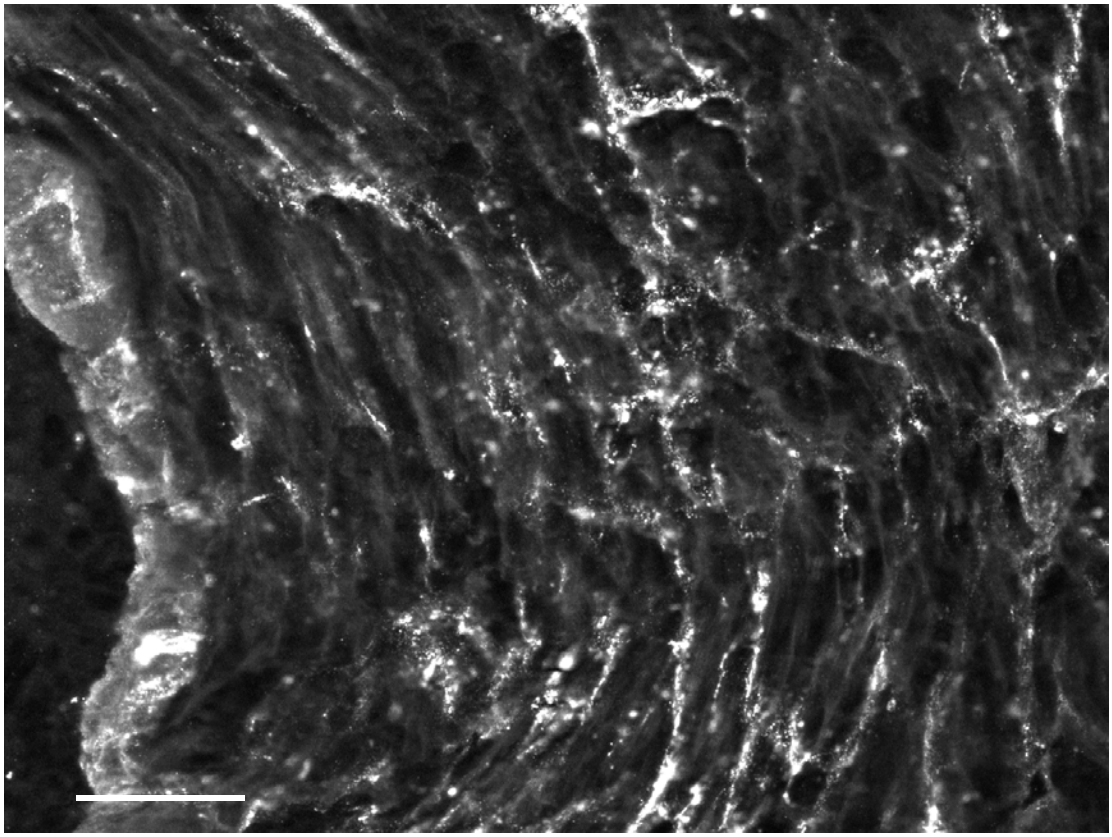

Figure 6.5: Binding of antibody CGM3 to human lumbar spinal cord as positive control. (Scale bar 60μm). Staining was absent from control tissues.

Despite various incubation protocols being used, and a series of dose-response experiments with differing concentrations of antibody, it was not possible to identify any selective binding of these antibodies to any of the human NMJs. Unfortunately, it was not possible to examine patient sample Ch on these tissues due to limited stocks of this serum being available.

Antibodies to GM1 were also examined in an attempt to identify binding to the human NMJ. One antibody, DG2, is raised in the mouse while SM1 is a human monoclonal antibody. In these experiments, DG2 was shown to bind strongly to 60% of NMJs (15 of 25) in human peroneus longus samples, and also to intramuscular nerve bundles (figure 6.6a, b); while SM1 was shown to bind to human intramuscular nerve bundles (figure 6.7), but not NMJs in peroneus longus. Binding pattern data is summarised in table 6.3.

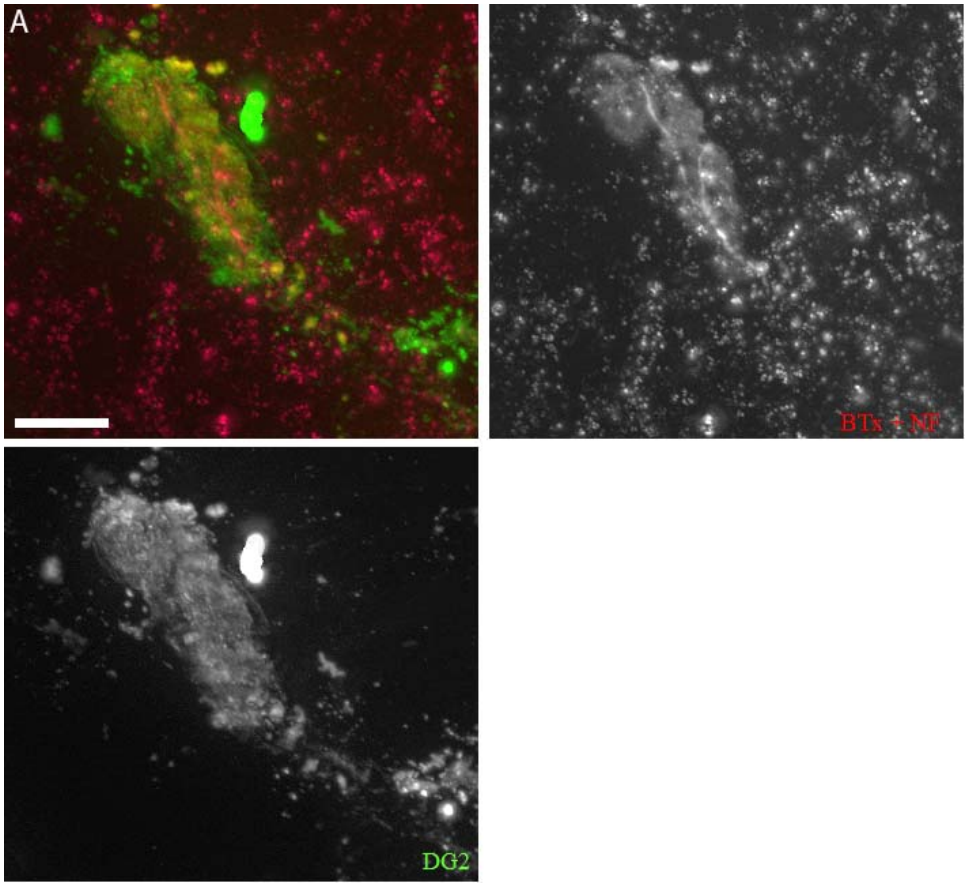
A
BTx + NF
DG2
B
NF
DG2

Figure 6.6: Binding of mouse antibody DG2 to peroneus longus muscle. Sections of peroneus longus muscle were incubated with antibody DG2.

A – A NMJ is shown, with innervating nerve. DG2 is shown overlying the junction. This could represent binding to TSCs or perisynaptic fibroblasts. 60% of junctions exhibited this binding.

B – Intramuscular nerve bundles are identified with neurofilament. Antibody DG2 binds extensively to these bundles, although it was not possible to localise this to either Schwann cells or axon.

(Scale bar 15μm)

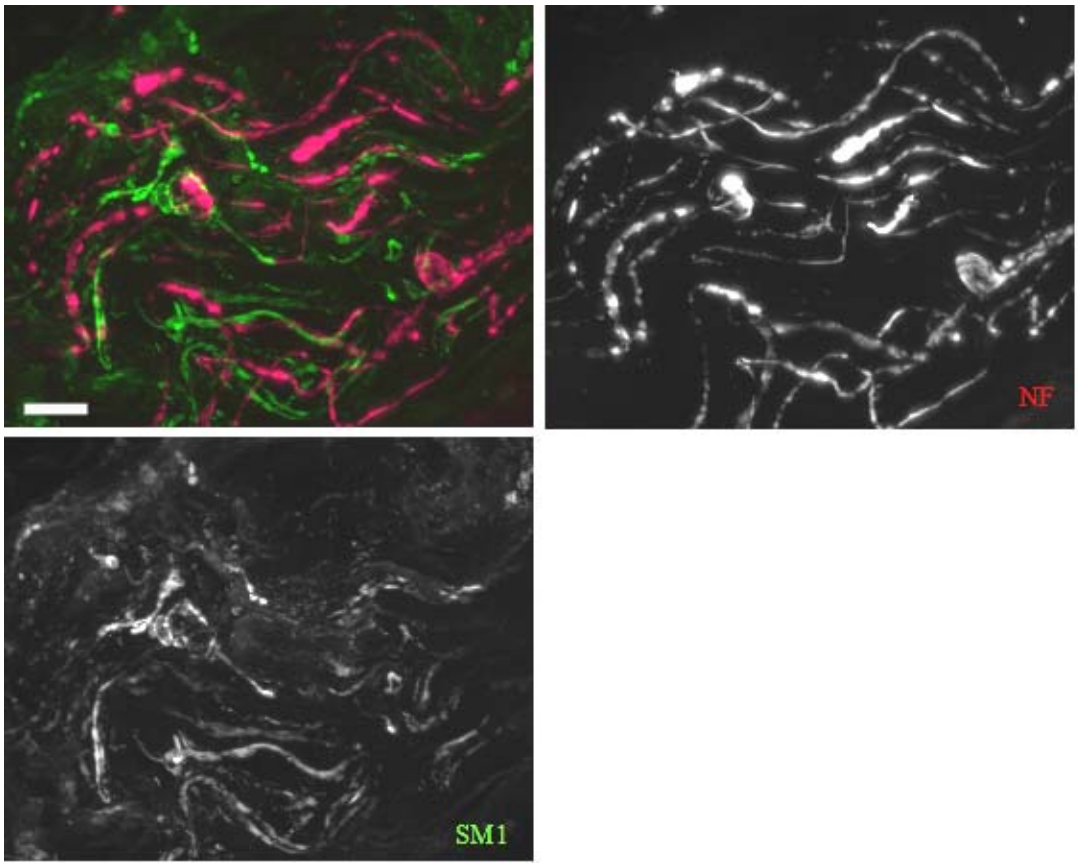

Figure 6.7: Binding of SM1 to peroneus longus intramuscular nerve bundles. Intramuscular nerve bundles are shown with neurofilament. (Scale bar 15μm)

	Anti-disialosyl antibodies			
Muscle	**EG1/LB1/R24**	**CGM3**	**DG2**	**SM1**
Intercostal	0	0	N/T	N/T
Omohyoid	0	0	N/T	N/T
Pharyngeal Constrictor	0	0	N/T	N/T
Peroneus longus	0	0	NMJ, Nerve bundles	Nerve bundles
Extensor digitorum brevis	0	0	0	0
Extra-ocular muscle	0	0	0	0

Table 6.3: Ganglioside binding patterns of anti-disialosyl antibodies. 0 = no binding, N/T = not tested.

6.2.3 Ganglioside distribution in human tissues

The surprising failure of antibody binding to human muscle tissue was then examined in greater detail. The next study examined the distribution of gangliosides in various human tissue samples, to determine which gangliosides were present at human NMJs, or other locations. This would determine whether gangliosides were available to bind antibody at the NMJs.

6.2.3.1 Sciatic nerve GM1 distribution

Before examining ganglioside distribution in human muscle tissue, staining protocols and distribution assays were first explored in human sciatic nerve samples. Previous work examined the distribution of cholera toxin at the nodes of Ranvier in human sciatic nerves when studying the pathogenesis of AMAN/AMSAN (Sheikh *et al*, 1999).

Using techniques described in Methods, samples of human sciatic nerve were stained for cholera toxin and markers of the node of Ranvier, peanut agglutinin (PNA) or the juxtaparanode (Kv1.1). Imaging was performed using Apotome microscopy, as described in Methods.

These studies confirm the findings of Sheikh and colleagues, who show that ganglioside GM1 is present around the nodes of Ranvier in human sciatic nerves (figures 6.8a and 6.8b). This binding appeared to be most evident on the para-nodal myelin, but is also present at the nodes also.

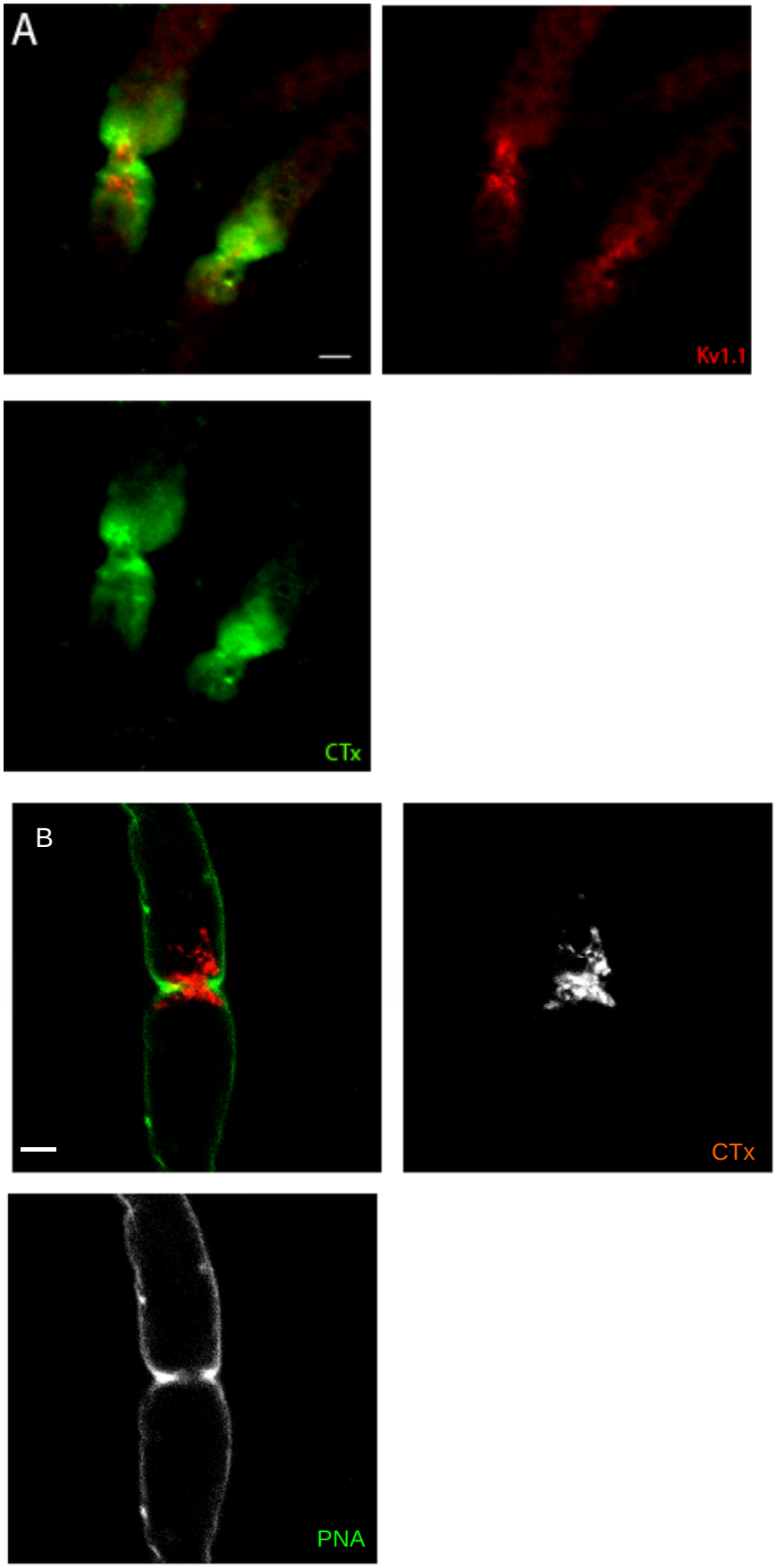
A
Kv1.1
CTx
B
CTx
PNA

Figure 6.8: Cholera toxin deposition at human nodes of Ranvier in sciatic nerve. Two methods are shown for identifying nodes at this site – Kv1.1 (A) and peanut agglutinin (B). Cholera toxin is shown prominently in the perinodal area in both examples, but is also present at the node. (Scale bar: 5μm)

6.2.3.2 Sciatic nerve complex ganglioside distribution

Using techniques described in Methods, cholera toxin and neuraminidase were then used to demonstrate complex ganglioside distribution in various tissues. Neuraminidase cleaves complex gangliosides to GM1 by removing terminal sialic acid residues from glycoconjugates, while leaving GM1 relatively spared. This technique has been used successfully by colleagues in the laboratory in mouse tissue (Kay Greenshields, personal communication). Imaging was performed using Apotome microscopy, as described in Methods. Three conditions were used in these studies:

1) Cholera toxin alone – demonstrates existing GM1 distribution
2) Block with high concentration unlabelled cholera toxin then 2U neuraminidase– existing GM1 is blocked, and neuraminidase is used to identify complex gangliosides
3) Block with high concentration unlabelled cholera toxin, then no neuraminidase- negative control

A study was first performed in an *ex vivo* hemidiaphragm preparation taken from BALB/c mice to illustrate the technique. This muscle has been used extensively to study the effects of monoclonal antibodies to a variety of gangliosides, and their

distribution is therefore well known. By using neuraminidase and cholera toxin, the difference between GM1 and complex gangliosides deposition at the NMJ and the innervating axon was shown (figure 6.9). In particular, GM1 can be seen to localise along the pre-terminal nerve bundles in this preparation, while complex gangliosides are present both on, and around the NMJ, supporting previous work using monoclonal antibodies.

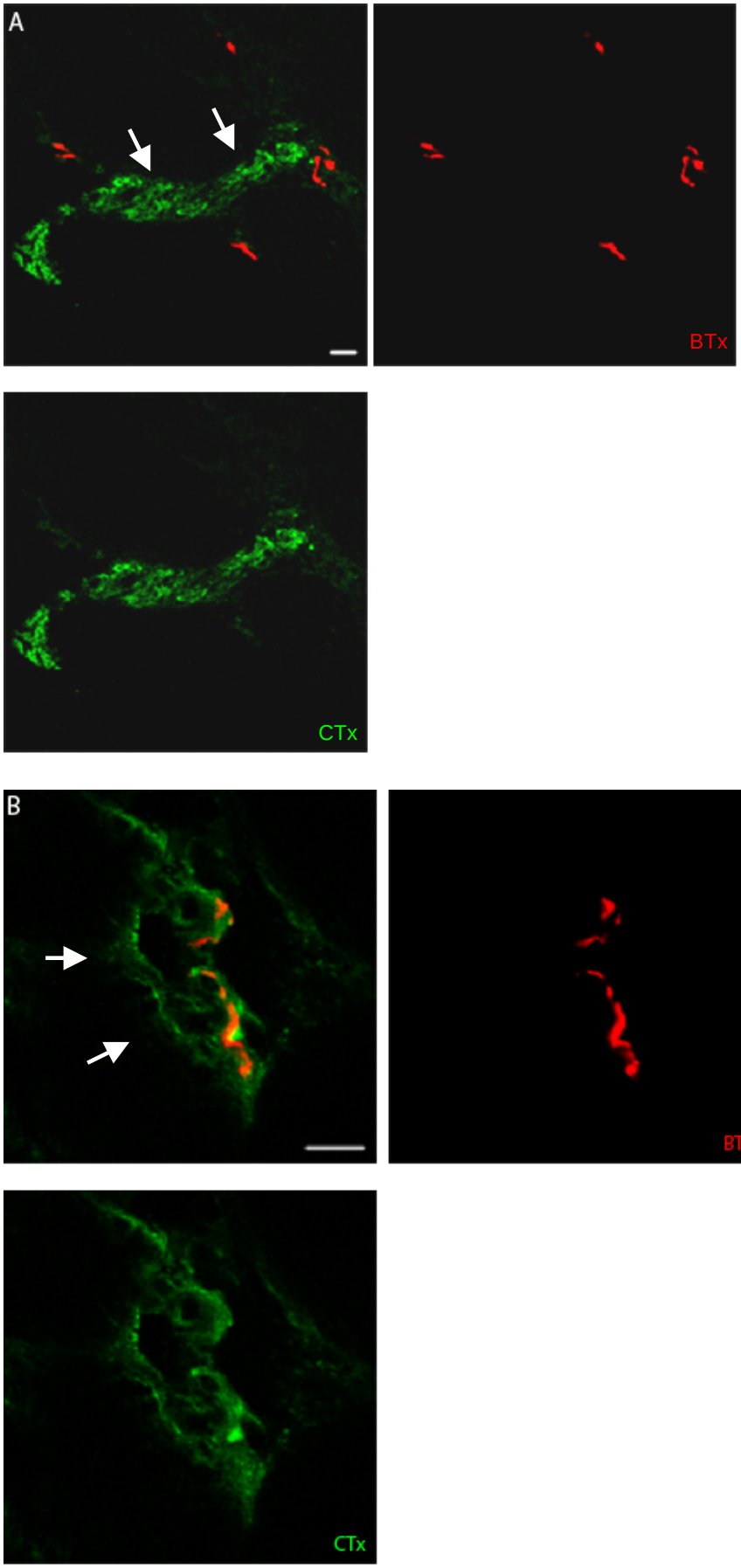
A
BTx
CTx
B
BTx
CTx

Figure 6.9: Effect of neuraminidase on BALB/c hemidiaphragm sections.

A - Before neuraminidase treatment, cholera toxin is shown in nerve bundles (arrows), demonstrating GM1 at this site. Virtually no cholera toxin staining is demonstrated over the end plate.

B – Following neuraminidase treatment, cholera toxin staining in nerve bundles is much reduced, and staining over the NMJ becomes more apparent suggesting complex gangliosides are located at this site. Arrows demonstrate cholera toxin "around" the NMJ, possibly binding to TSCs and terminal axon.

(Scale bar 10μm)

Having reproduced the neuraminidase technique successfully in the mouse, the method was then used in 3 human sciatic nerves from different patients, using 3 mouse hemidiaphragm preparations from 3 separate mice as a positive control in the absence of suitable human tissue at the time of the study.

These studies showed that cholera toxin was present at the nodes of Ranvier in human sciatic nerves (figures 6.10). This data was quantified by randomly identifying nodes of Ranvier by PNA, and counting the number that had evidence of cholera toxin staining. More nodes scored positive for both GM1 and complex gangliosides in mouse sciatic nerve than human but saturating levels of cholera toxin were not achieved in the mouse therefore it would be difficult to draw direct comparisons between the tissues. These data are displayed graphically using Excel in figure 6.11.

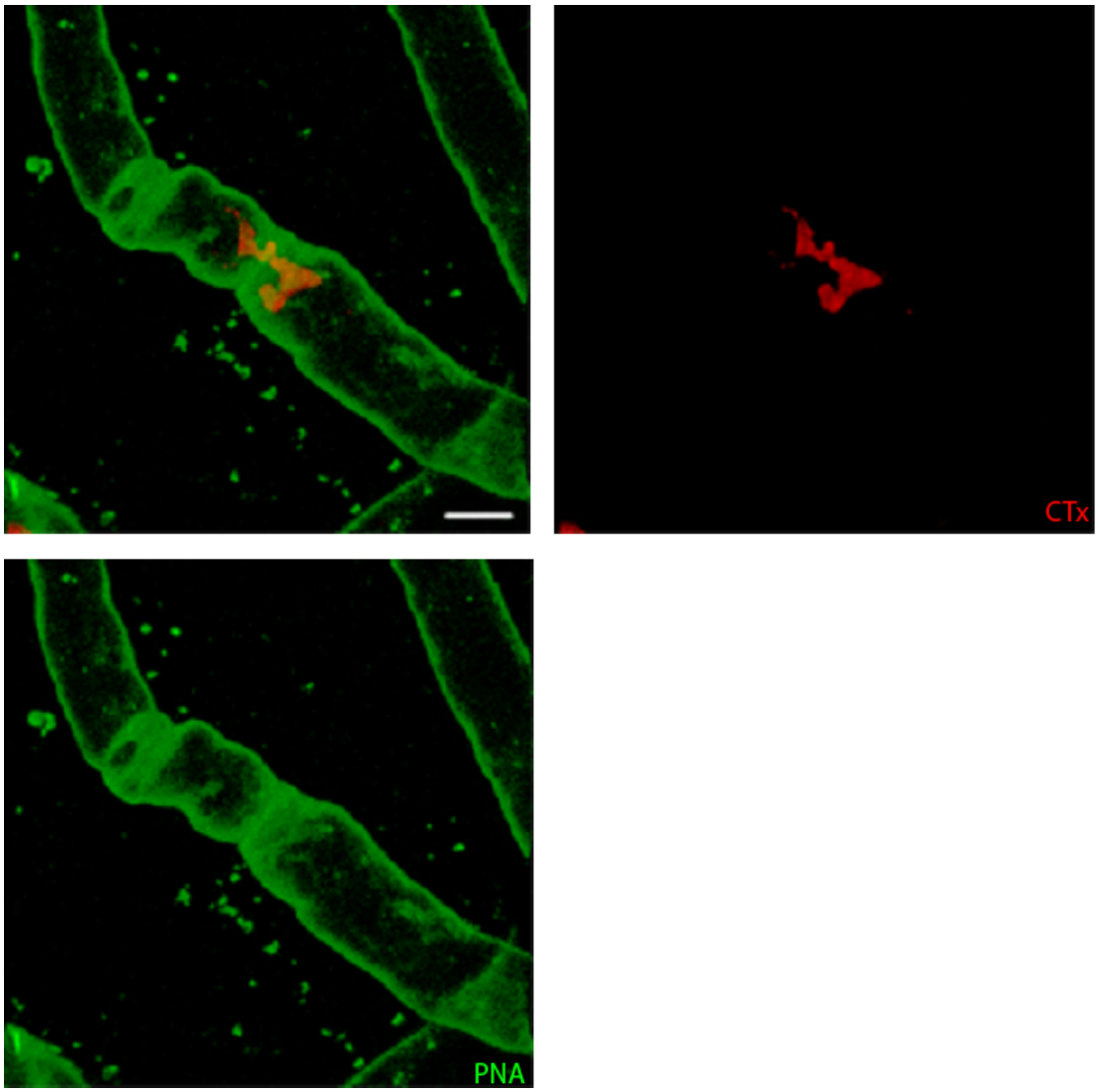

Figure 6.10: Complex ganglioside deposition at human sciatic nerve shown after neuraminidase treatment (confocal reconstruction). Following neuraminidase treatment, cholera toxin is shown at the node of Ranvier suggesting that complex gangliosides are located at this site. (Scale bar 5µm)

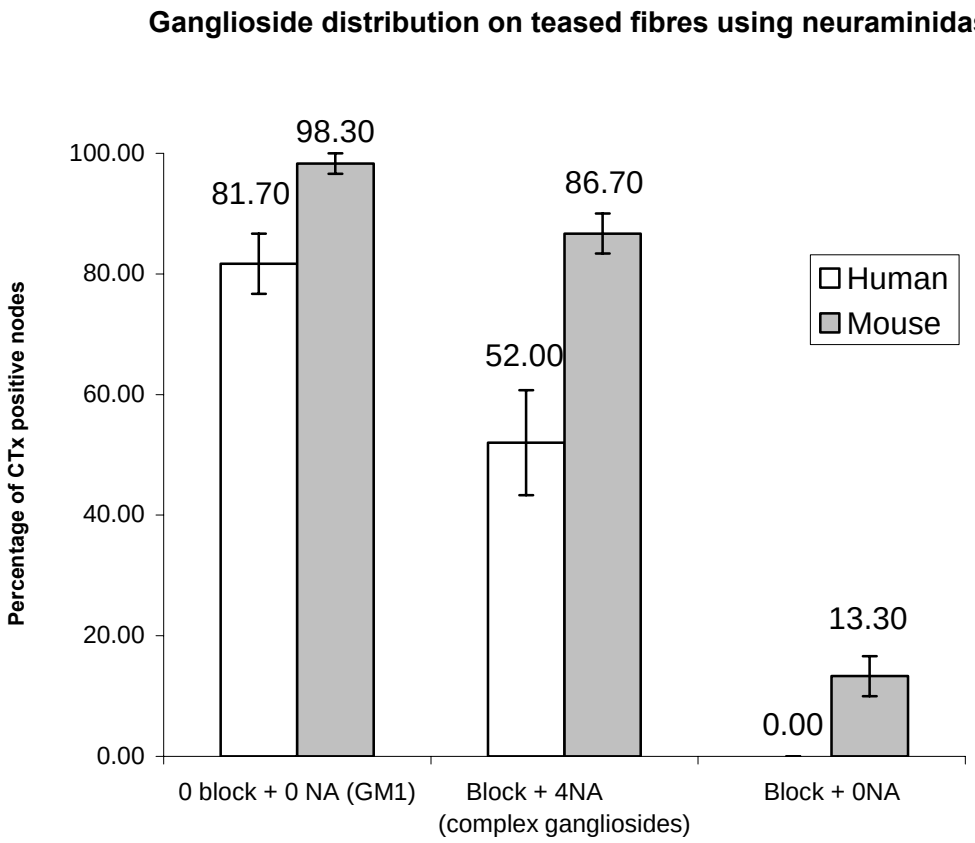

Figure 6.11: Ganglioside distribution on sciatic nerves. Nodes of Ranvier were identified by PNA staining in sciatic nerve teased fibre preparations, and scored as positive if cholera toxin was present at the node. 81% of human, and 98% of mouse nodes were positive when cholera toxin was applied alone. When background GM1 was blocked, and neuraminidase was added, over 52% of human and 86% of mouse nodes scored positive for cholera toxin. In samples that were blocked, but not treated with neuraminidase, no human nodes scored positive while less than 13% of mouse nodes had evidence of cholera toxin suggesting that a saturating

concentration of cholera toxin was not achieved in the mouse. Mean is shown as a value in the graph, with standard error of mean as error bars.

6.2.3.3 Human muscle GM1 distribution

Studies were undertaken to map the distribution of gangliosides in human muscle samples using techniques established from the sciatic nerve, and described in Methods. This protocol demonstrated cholera toxin binding strongly to a number of sites in the muscle sections, including across and between muscle fibres, nerve bundles, and also at the NMJ. It was therefore difficult to distinguish staining patterns as a result. Dose response experiments using lower concentrations of cholera toxin did not clarify the staining further. These studies were further complicated by lipofuscin deposition across the tissue.

Another protocol used to illustrate cholera toxin deposition in human muscle tissue, (described in O'Hanlon *et al*., 1998) was then attempted but staining was similar to that seen using protocols developed in the sciatic nerve. Again lower dilutions of cholera toxin using the O'Hanlon protocol, ranging from 1 in 500 to 1 in 6000 did not clarify staining.

Eventually, the protocol outlined in Methods was devised. Using this method, peroneus longus showed evidence of concentrated cholera toxin staining at some NMJs (figure 6.12), and also in nerve bundles throughout the muscle. However, it was not possible to demonstrate specific NMJ staining in other muscles, or in

intramuscular nerve bundles (where present). This supports the binding patterns seen with antibodies to GM1 gangliosides (DG2 and SM1).

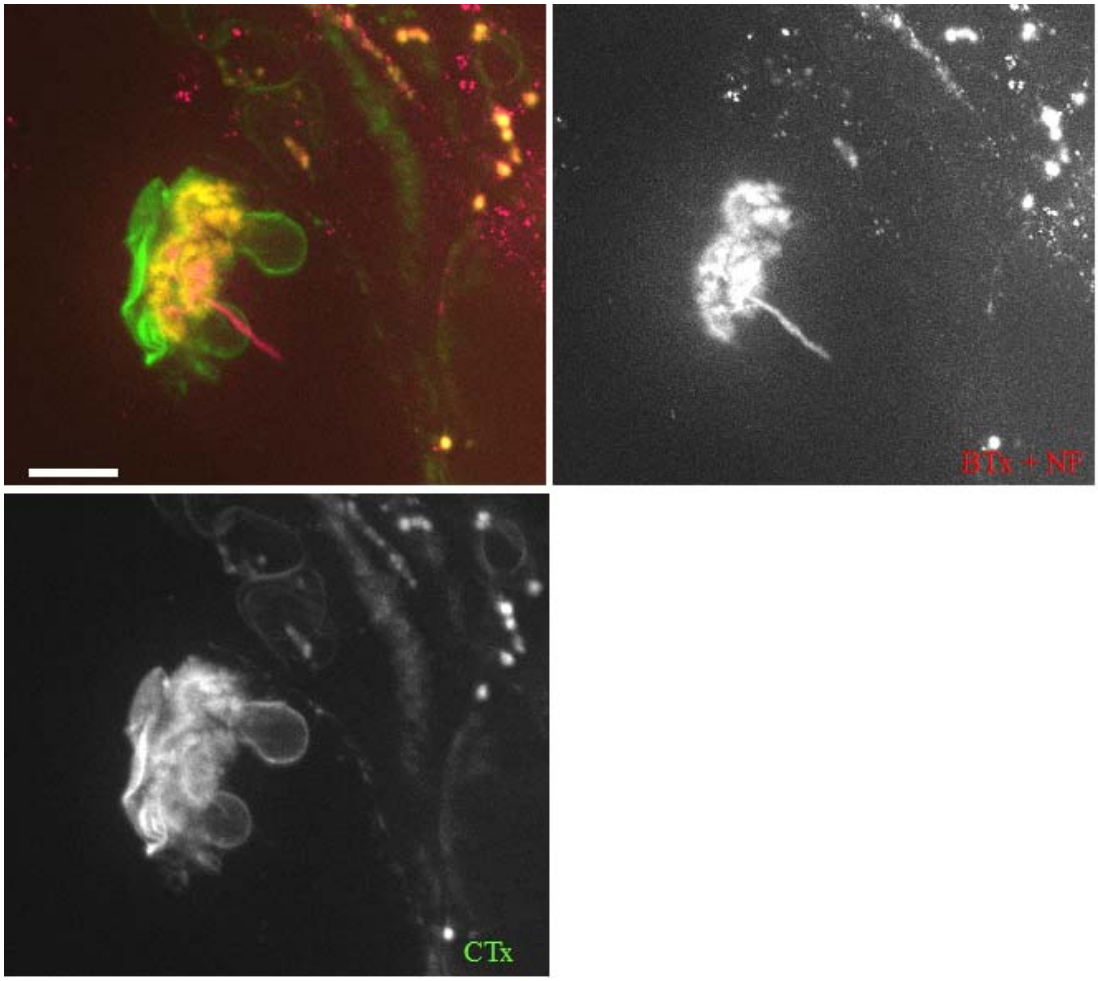

Figure 6.12: Cholera toxin at human NMJs. A NMJ is identified by bungarotoxin staining, and its innervating nerve is shown with neurofilament. Cholera toxin is seen to cover the junction, and adjacent DAPI positive nuclei (not shown). It is not clear if these nuclei are muscle nuclei, or TSCs. This staining was present in 60% of junctions, and correlates with antibody staining described previously. (Scale bar 10μm)

Colleagues in the laboratory have since modified this protocol to include a copper sulphate based blocking step (see Methods). In addition to further reducing the concentration of cholera toxin, this produced a startling reduction in the level of staining secondary to lipofuscin deposits staining across the muscle, in particular across and between muscle fibres. This new protocol confirmed cholera toxin deposition at the junction in peroneus longus, and also demonstrated cholera toxin at junctions in the intercostal muscle (figure 6.13). Other muscles have yet to be tested using this new protocol.

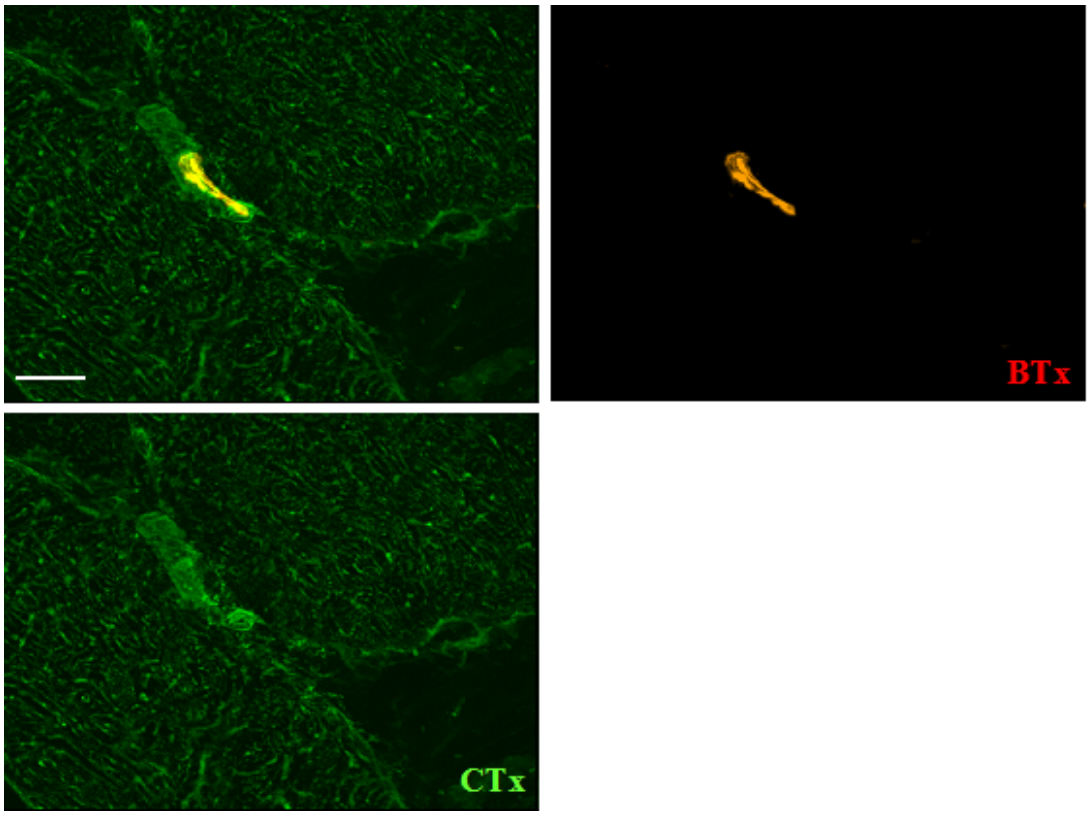

Figure 6.13: Cholera toxin deposition in human intercostal muscle following copper sulphate blocking. Cholera toxin staining in intercostal muscle was greatly improved when copper sulphate is used. In this example, cholera toxin is seen around the NMJ at a dilution of 1 in 8000 (125ng/ml) when copper sulphate is used. (reproduced with permission from Dr Sue Halstead) (Scale bar 15 µm)

6.2.3.4 Human muscle complex ganglioside distribution

Using the protocol outlined in Methods, the neuraminidase technique was then used to identify the distribution of complex gangliosides in human muscle tissue. However, the distribution of cholera toxin following neuraminidase treatment was again generalised across the tissue, and was not particularly concentrated at the NMJ or

other structure in any muscle tested. This supports studies using antibodies to complex gangliosides.

6.3 Discussion

6.3.1 Human serum produces TSC injury in mouse hemidiaphragm preparations

To determine whether the TSC could be a disease target in human immune-mediated neuromuscular disease, it is important to show that patient serum can produce TSC injury. It was not possible to obtain biopsy samples of human muscle tissue from patients with acute MFS, as this is not a routine investigation, and obtaining samples would be technically challenging, with a high complication rate. It would not be ethically justified to obtain samples in this manner.

However, the *ex vivo* hemidiaphragm muscle preparation from the mouse is a robust method of studying glial injury at the NMJ, and was used as an alternative model. Serum was obtained from a patient in the acute phase of MFS (patient Ch), and was shown to have high antibody titres to complex gangliosides, in particular GQ1b as expected in the acute phase of MFS (Chiba *et al*, 1993; Willison *et al*, 1993a). Interestingly, serum from patient Ch produced a very similar effect to antibodies to complex gangliosides raised in the mouse, by producing both axonal and TSC injury at the mouse NMJ. This suggests that mouse antibodies raised in the laboratory have an effect that is broadly similar to pathogenic human antibodies, supporting previous findings (Plomp *et al*. 1999).

Additionally, this study also illustrates for the first time that a human serum with antibodies to complex gangliosides can produce TSC injury in the mouse when compared to human serum without antibodies to gangliosides. However, it is difficult to extrapolate results obtained from animal tissue to humans, because glycolipid expression is highly species specific. Despite this, the study does illustrate the potential for human antibodies to produce complement-mediated injury at sites with high concentrations of complex gangliosides. If it were possible to demonstrate binding of anti-ganglioside antibodies to human tissue, this would suggest that complement dependent injury could potentially occur at the binding site, in a manner similar to mouse NMJs.

Interestingly, it was not possible to reproduce previously published data using either red cell eluate, or serum from a patient with CANOMAD in either BALB/c or NIH mouse strains. It would appear from both immunoglobulin staining, and ganglioside ELISA that antibody was present in the incubating solutions, and was capable of binding to the NMJ, but could not activate complement. Protocols, and methods were checked with colleagues in the laboratory who have also experienced similar problems with the antibody recently (Mr Peter Humphreys, personal communication). It would be interesting to explore this area further, in an attempt to determine the reason for this failure, and also to examine other human sera to determine whether they can also produce a TSC injury in this model.

6.3.2 Characterisation of human muscle tissue

In an attempt to demonstrate anti-ganglioside antibody binding at human NMJs, a series of topical staining experiments were undertaken using a panel of antibodies with different specificities to identify potential binding sites in human samples.

6.3.2.1 Obtaining human muscle tissue

Basic characterisation studies were first performed on human muscle tissue to gain a better understanding of the tissue, and any special staining conditions that may be required. These studies described the number, and size of junctions on each section of muscle. Although the symptoms of MFS are usually restricted to the head and neck, it was only possible to obtain muscle for use in the study if it was routinely discarded in operation, due to ethical constraints. Although samples became available from post mortem tissue banks latterly, the types of muscles available for this study were restricted, and hence sites outwith the head and neck were also considered.

6.3.2.2 Differences in number of junctions between muscles

Early studies described the number of junctions visualised in each muscle. This demonstrated that the number of available NMJs identified by bungarotoxin staining in each human muscle sample was significantly lower than similar muscle sections from BALB/c hemidiaphragm. Within the human muscle samples, there was also a significant difference between muscles, with extra-ocular muscle having more NMJs

than omohyoid, and both EOM and omohyoid having more NMJs than other muscles under examination.

The difference in the number of available NMJs reflects the size of muscle involved, pattern of innervation in the muscle, and also the sampling area. For example, it is relatively easy to identify a large number of junctions in EOM, as it is a small muscle, and NMJs are localised in a small area. However, in muscles such as intercostal, or omohyoid, the muscle is much larger, and although attempts were made to sample at the point of nerve innervation, junctions were still scattered throughout the muscle making it difficult to localise large numbers of NMJs. In contrast, BALB/c hemidiaphragm muscle is very small and thin, with junctions localised to a particular area within the muscle, making it easy to identify and access areas with a large number of junctions.

As a consequence, observations in most muscles were based on observations on a small number of NMJs taken from either one or two patients. The statistical significance of the data is reduced as a consequence, and it is therefore difficult to extrapolate this data to a whole population.

6.3.2.3 Junction size between muscles

Studies were also made to examine if the size of each junction varies between muscle samples. Surprisingly, there was no statistical difference between any of the sampled human muscles, or BALB/c mouse tissue. In contrast, work from human vastus lateralis biopsy samples suggests that human NMJs are smaller than those in the

mouse (Slater *et al,* 1992; Wood and Slater, 2001). This interesting study compared muscle biopsy samples from patients with myopathy to healthy controls, and also noted that while human NMJs were smaller and their quantal content was lower, the post-synaptic folds were deeper and overall this enhanced neuromuscular transmission.

However, the study by Slater and colleagues used teased fibre preparations and measured junction length and area using EM techniques that were not available in my study. The limited number of samples, and the small amounts of muscle available made it difficult to perform teased fibre studies, and cryostating was selected as an alternate method for analysis due to the high tissue yield.

The limitations of this method are shown when examining junction size between muscle fibres. The median length of the samples is around 20µm, which corresponds with the thickness of cryostat section. Work by Slater and colleagues using vastus lateralis suggest that human junctions are at least 30µm in length, and junctions are even larger in the mouse. This study illustrates that sections of both human and BALB/c NMJs are missing from cryostat sections, and potential binding sites may not be included in the morphological analysis as a result.

6.3.3 Anti-ganglioside antibody binding was seen in peroneus longus muscle

Although these experiments used mouse antibodies, it was not possible to use serum from patients with MFS due to insufficient volumes being available. However, using mouse anti-ganglioside monoclonals ensures that any binding to tissue is not the result

of binding due to the immunoreactivity within mixed human serum to other antigens in the tissue.

In contrast to studies in the mouse hemidiaphragm preparation (Halstead *et al*, 2005b), antibodies to complex gangliosides did not appear to bind to the NMJs in any of the human muscles under examination. In particular, no binding was seen in pharyngeal constrictor or extra-ocular muscles, both of which are likely targets for weakness in MFS due to their location in the head and neck. However, positive control samples from human lumbar spine (Graus *et al*, 1984), and also mouse hemidiaphragm muscle confirmed that antibody solutions were binding successfully to other sites.

Complex gangliosides have not been shown directly at human NMJs. However, botulinum toxin binds to complex gangliosides (Kamata *et al,* 1986; Kozaki *et al*, 1998), is known to produce paralysis at human NMJs (Willison and Kennedy, 1993), and has been shown to exert its effect via complex gangliosides at the mouse NMJ (Bullens *et al,* 2002). By implication therefore, complex gangliosides, and in particular GT1b and GQ1b, are present in human NMJs. Although this binding failure could be the result of a species difference in antibody, this is improbable. Both the mouse antibodies, and human serum shared similar binding profiles on ELISA, and also produced similar types of injury in mouse *ex vivo* hemidiaphragm preparations. The antibodies therefore recognise similar targets, and it is unlikely that a species difference in antibody exists.

As discussed previously, the antigenic targets in the mouse may be presented differently to human muscles. The glycolipid repertoire between species does vary (Kusunoki *et al*, 1997), and therefore the presentation of gangliosides between the two species could result in different antibody binding patterns. Further work using other antibodies with different specificities could demonstrate this effect.

It is also possible that the limited sample of this study may not accurately represent the general population, and these results are atypical. Indeed, with the exception of pharyngeal constrictor and omohyoid, these studies were conducted on samples obtained from a single patient per muscle group. It may be possible that the ganglioside profile of these patients is not consistent with the population, or patients with immune mediated nerve injury. If this is the case, this finding may explain geographical variation in disease, and the diversity of illness presentation. Obtaining more samples from a broad range of patients is clearly very important to continue these studies.

Despite the binding failure of antibodies to complex gangliosides, two antibodies to GM1 ganglioside did bind to human peroneus longus muscle. Two antibodies were examined: DG2, which is a mouse monoclonal, and SM1, which is a human monoclonal antibody. Only DG2 bound convincingly to the NMJ and intramuscular nerve bundles, while SM1 only bound to nerve bundles. Antibodies to GM1 are strongly implicated in the pathogenesis of AMAN, and this study supports the observation that a likely source of injury in anti-GM1 disease is the innervating nerve (Hafer-Macko *et al*, 1996a, Sheikh *et al*, 1999, Willison and Yuki, 2002). However,

the difference between the patterns of binding between the two antibodies is interesting, particularly when comparing their similarity on ganglioside ELISA.

It is now widely recognised that gangliosides can form "complexes" with surrounding structures, and these interactions can influence antibody-binding patterns (Kaida *et al*, 2004; Willison, 2005). Current clinical practice identifies anti-ganglioside antibodies by ELISA, using single purified ganglioside in individual wells as antigens. However, gangliosides do not exist in isolation in the cell membrane, and many are clustered in "lipid rafts" on the surface, in close association with other gangliosides or membrane components (Hakomori, 2002). It may be possible in human tissue that these ganglioside complexes influence the presentation of the ganglioside to the antibody, and alter subsequent binding. Examining antibody binding profile on ELISA using mixed ganglioside wells may demonstrate which complexes are present at each site to account for the binding differences.

This study also demonstrates that anti-GM1 antibodies can bind to the NMJ. While it was not possible to identify the structures to which the antibody bound, it is clear that these structures were overlying the NMJ, and could be either TSCs or supporting fibroblasts. This supports the hypothesis that the TSC could be a disease target in anti-ganglioside antibody-mediated disease, although clearly further confirmatory work should be undertaken to fully identify which structures are involved. In the first instance, teased fibre preparations could be undertaken, and whole mount imaging performed in a similar manner to TS preparations in the mouse. This method would fully retain the structure of the junction, and allow detailed confocal microscopy to determine which sites bound antibody. Additionally, the number of patient samples

should be increased, to increase diversity, and remove any variation that may result from the pre-existing disease.

However, it is also interesting to note that only 60% of junctions in each muscle displayed significant antibody binding. Although it was outwith the scope of this study, these junctions could be innervating different muscle fibre types (Wood and Slater, 2001) and may suggest that ganglioside profiles may change depending on the muscle fibre type. This important finding would provide interesting insights into basic ganglioside glycobiology and manufacture, in addition to demonstrating variations in disease, and onset of symptoms.

6.3.4 GM1 and complex gangliosides are present in human sciatic nerves

To clarify staining patterns seen with anti-ganglioside antibodies, cholera toxin was used to demonstrate ganglioside deposition in a variety of tissues. Before undertaking these studies, pilot investigations using human teased fibre sciatic nerve preparations were conducted to clarify protocols, using a tissue whose ganglioside composition has been described previously (Sheikh *et al*, 1999). In this experiment, cholera toxin deposition was shown at the nodes of Ranvier in human sciatic nerve, suggesting GM1 localisation to this site and confirming findings from other workers examining this area (Ganser *et al*, 1983; Corbo *et al*, 1993; Kusunoki *et al*, 1993, O'Hanlon *et al*, 1998).

Having established a reliable staining technique to illustrate GM1 deposition on human tissue, the technique was adapted to demonstrate the localisation of complex

gangliosides. The enzyme neuraminidase, from *Clostridium perfringens* has been shown to cleave complex gangliosides to GM1 by removing terminal sialic acid residues from gangliosides. As the sialic acid of GM1 is relatively resistant to this enzyme, more complex gangliosides can be converted to GM1 by its action (Holmgren et al, 1980; Ganser *et al*, 1983; Brennan *et al*, 1988). Blocking existing GM1 with unlabelled cholera toxin before treatment clearly identifies any new GM1 created by the action of the enzyme.

Using this technique, complex gangliosides were demonstrated across the myelin in human sciatic nerve, but were especially concentrated at the nodes of Ranvier. Although it is not possible to identify which gangliosides are located at this site, these results support biochemical studies that have shown high concentrations of complex gangliosides in the axonal fraction of human peripheral nerve (Svennerholm *et al*, 1994). It is difficult to correlate this finding with human pathology, as almost all cases of disease caused by antibodies to complex ganglioside have symptoms confined to the head and neck. However, there have been descriptions of patients with variants of MFS having limb involvement, and while this may be the result of co-existing anti-GM1 antibodies (Odaka *et al*, 2001), it is possible that the peripheral nodes of Ranvier could also be injured by antibodies to GQ1b.

6.3.5 GM1 but not complex gangliosides are present in human NMJs from peroneus longus muscle

The neuraminidase technique was then used on human muscles. Although GM1 was present over the surface of all the muscles under examination, GM1 appears to be particularly concentrated at the NMJs and intramuscular nerve bundles of peroneus longus and intercostal muscle. The neuraminidase technique did not demonstrate the presence of complex gangliosides, and these findings support earlier antibody work. In particular, the extra-ocular muscle, and pharyngeal constrictor muscles did not have any evidence of concentrated areas of complex gangliosides at NMJs.

However, in the latter stages of this study, a blocking step using copper sulphate was developed, which reduced background lipofuscin. By reducing the concentration of cholera toxin, GM1 was shown to be present at the NMJ. Other blocking steps using BSA did not produce a comparable reduction in background staining, although this technique did not specifically reduce autofluorescence. Colleagues in the laboratory have used this copper sulphate blocking step on intercostal muscle, and have shown cholera toxin deposition at human NMJs. It is possible that repeating the neuraminidase study on human muscle, using this step to reduce autofluorescence, may demonstrate new areas of ganglioside localisation that were not evident previously as occurred in intercostal muscle.

6.4 Conclusions

The purpose of this study was to determine if the NMJ, and in particular TSCs, could be a site of disease injury in MFS.

These studies show that human serum from a patient in the acute phase of MFS produce TSC injury in mouse models, and this injury is similar to damage caused by mouse anti-ganglioside antibodies. This illustrates the similarity in effect between human serum, and antibodies raised in the laboratory.

Although antibodies to complex gangliosides were not shown to bind to the NMJ in any of the muscles in this study, the limited sample size makes it difficult to extrapolate this data to the general population. However, anti-ganglioside antibodies were shown to bind to human NMJs in peroneus longus muscle, suggesting that structures in the NMJ, including TSCs, may be a disease target in anti-ganglioside antibody-mediated disease.

Chapter 7: Conclusions

7.1 Antibody characterisation

Before conducting experiments on the chronic effects of TSC injury, I sought to identify the most suitable antibody for use in these investigations. However, the CK mouse was not available in the early stages of the study, and restrictions on animal surgery made it difficult to examine sternomastoid muscle, which would be used in the longer term *in vivo* experiments. Early studies therefore identified the most suitable muscle for later antibody characterisation studies.

Two different muscle preparations that are widely used in the laboratory were compared, to examine which would be most suitable for *ex vivo* experiments. These studies demonstrated that triangularis sterni (TS) muscle was most suitable for morphological studies requiring detailed imaging of synaptic structures, in addition to demonstrating antibody and complement deposition. TS is a thin, sheet like muscle which can be dissected as a whole mount from an animal, and maintained for several hours *ex vivo*. It can also be imaged without sectioning and can therefore be used to stain intracellular components, such as S100. This muscle was later used with Sytox green to illustrate the proportion of TSCs injured by antibody EG1 at each NMJ, which would not have been possible using a standard hemidiaphragm preparation.

Although it was not suitable for detailed morphological studies, the large number of available NMJs in the hemidiaphragm preparation made it very suitable for statistical analysis. Neurofilament measurements, complement and immunoglobulin deposition

studies can also be performed on hemidiaphragm muscle sections, and then quantified using computer analysis software to provide numerical measurement. Additionally, the EthD-1 protocol on hemidiaphragm provides a strong method for quantifying antibody-mediated TSC injury, and was used extensively throughout this study.

A series of antibodies with similar ganglioside binding profiles on ELISA were compared on the *ex vivo* hemidiaphragm preparation, and antibody EG1 was identified as most suitable for use in later experiments. EG1 was considered most suitable as it produced TSC injury in a high number of NMJs, in addition to activating MAC and C3c at this site more efficiently than other antibodies. Further, this antibody has been previously shown to be TSC selective, it does not need to be purchased from a commercial supplier, and it is very easy to purify and concentrate IgG class antibodies.

It was important to identify the proportion of TSCs killed by antibody EG1 at each NMJ, to fully characterise its effect. However, this was not possible with hemidiaphragm sections, as cryostating would often leave junctions incomplete. Although entire junctions were visible with TS muscle, antibody injury rendered the cell permeant, and reliable Schwann cell intracellular markers (e.g. S100) were often lost making morphological analysis difficult. As a result, a nuclear stain was used (Sytox green) with confocal microscopy to identify nuclei overlying the junction that were most likely TSCs. This method proved robust, and confirmed previously published data showing that end plate size correlates with the number of TSC nuclei overlying the junction (Love and Thompson, 1998).

This Sytox method also demonstrated that antibody EG1 did not produce a uniform pattern of TSC injury at each NMJ, with a range of injury from no apparent damage to complete TSC loss. This provides a useful range of conditions in which to study TSC injury, and recovery in the mammal.

7.2 Effect of complement regulators on antibody injury

A large number of junctions were injured by the antibody in both hemidiaphragm and TS preparations, and a range of TSC injury was present at each junction. Many NMJs were spared, therefore experiments were undertaken in an attempt to enhance the antibody effect and produce greater TSC injury. If this could be achieved, an animal model could be created which exhibits complete TSC loss in response to antibody exposure.

Antibody EG1 produces its effect via complement activation and subsequent MAC production causing failure of membrane integrity. Experiments were conducted to examine whether removing regulators of complement activity (DAF1 and CD59a) could enhance antibody effect at the NMJ and produce greater TSC injury. Although it may be possible to increase complement activation by removing other complement regulators, these were not available for this investigation and were not examined.

As part of these investigations, early topical studies demonstrated differences in antibody binding between the mouse strains. This difference in antibody binding suggests different ganglioside expression at the NMJ between the mouse strains, and has implications for researchers examining the role of other antibodies to gangliosides

at this site. For example, a lack of injury in one mouse strain does not necessarily exclude an antibody from having a pathological effect in another. This emphasises the importance of fully understanding target gangliosides present at each binding site before stating a lack of effect, and is particularly important for human studies, which are discussed later.

Topical complement studies also demonstrated differences in complement activation products between mouse strains. Although this could be the result of complement regulator expression, it is not known if complement regulators are active in cut tissue, and if so, to what extent. It is more likely therefore that the differences in complement activation product deposition could be explained by different levels of immunoglobulin deposition at the junction shown earlier.

Despite differences in immunoglobulin deposition on topical staining studies, *ex vivo* hemidiaphragm preparations measuring TSC injury using EthD-1 and complement activation products did not show any difference between BALB/c or the wild type of the DAF1/CD59a knockout strain. Although topical staining is useful for screening purposes, *ex vivo* preparations provide a more accurate experimental model. These data suggest that removing complement regulators DAF1 and CD59a do not increase the effect of antibody EG1 in this system, suggesting that within the current experimental model, the effect of the antibody has been maximised.

A number of possibilities could explain why complement regulators had no apparent effect: the regulator system may be "overwhelmed" with complement from exogenous human serum that is applied or that these complement regulators are

unable to efficiently regulate NHS. Although the purpose of this study was not to examine complement regulators directly at the NMJ, it would be interesting to repeat these studies using different concentrations of human serum, and also antibody, to examine whether complement regulators are expressed at the NMJ. This could also be confirmed by immunostaining or in-situ hybridisation studies. These studies may identify whether particular cell types have increased levels of complement regulator, and are "protected" from antibody-mediated injury. Defects in this expression may explain why certain individuals are more susceptible to this form of injury than others in the population.

7.3 Terminal Schwann cell recovery following antibody-mediated injury

It has been very difficult to examine the long-term effects of antibody-mediated injury at the mouse NMJ. Passive transfer studies, where the antibody is introduced intra-peritoneally, can provide both functional, and morphological data. However, motor paralysis can affect diaphragmatic function and this can limit the duration of the study.

The CK mouse has been shown previously to provide a stable method for repeated *in vivo* imaging of the PNS using sternomastoid muscle. This technique was adapted to demonstrate the acute and chronic changes at the NMJ following immune-mediated injury caused by anti-ganglioside antibodies. Since the injury was localised to junctions on the surface of the muscle, there was no significant functional deficit that impairs the animal's quality of life. As a consequence, experiments could continue without the requirement for early euthanasia.

Although isolated TSC injury was examined exclusively in this study, the system could easily be adapted to examine the effects of immune-mediated injury to other structures at the NMJ, including the terminal axon, ACh receptors, fibroblasts and the pre-terminal nerve bundle. This versatile technique could therefore provide new insights into antibody-mediated nerve injury, and subsequent recovery in the PNS. Although not described in detail in this study, other muscles in the CK mouse, for example soleus, can also be used in addition to sternomastoid muscle to examine chronic functional and electrophysiological changes.

Previous studies examining the chronic effects of TSC injury in the frog (Reddy *et al*, 2003) did not consider in detail the recovery of TSCs in response to injury. In contrast, recovery was seen in all mouse NMJs within 48 hours following injury. Initially, processes were shown to extend from the pre-terminal nerve bundle to cover the existing terminal axon, before DAPI-positive cell bodies were seen at the periphery of the junction at 72 hours post-injury. Over the next 4 days, the processes continued to cover the junction, and the new cell bodies occupied new sites within the junction.

Surprisingly, this process of recovery was not axon dependent and suggests that the stimulus for repopulation arises from another source. Colleagues in the United States have recently shown that TSC recovery can occur even in the absence of an intact muscle fibre (Yue Li, personal communication) suggesting that a stimulus from the muscle fibre itself is also unlikely. A number of structures exist around the junction that could produce the signal for repopulation however. For example, the stimulus

may arise from a direct glial-glial interaction, between the last myelinating Schwann cell, and the TSCs. Signals could also arise from the supporting fibroblasts that overlie the junction, or other muscle fibres or junctions in the vicinity of the injured NMJ could signal recovery. Although it was not addressed in this study, it would be interesting to identify these signals, as it would offer important insights into Schwann cell signalling at the NMJ.

The origin of the returning TSCs is also unclear from this study. The last myelinating Schwann cell was thought to be the most likely source of returning Schwann cells, as processes were initially seen to emerge from the pre-terminal nerve bundle. However, only one experiment from several using BrdU identified nuclear division at the last myelinating Schwann cell in one junction. Other markers of cell division (Ki-67) did not show any evidence of mitosis in this cell either, and stains to identify if these returning cells arose from myelinating Schwann cells were also unhelpful.

Since it was not possible to demonstrate that returning cells arise from the pre-terminal nerve bundle, it is possible that TSCs may originate from another source. One exciting hypothesis suggests that these cells may arise from the latent pool of muscle stem cells, which have been previously documented. Cell bodies normally appear to the periphery of the junction, and it is possible that they are arising from sources outwith the junction, before differentiating into TSCs once they reach the NMJ. If this is correct, it would be the first time that these stem cells have been shown to differentiate into TSCs, and may offer new insights into nerve recovery. However, it would not explain why processes emerge from the pre-terminal nerve bundle prior to the appearance of the cell bodies.

Following recovery, the junction remained relatively unchanged over the following few months. Although more TSCs were present at the junction following injury, their number remained remarkably stable for the following 12 months, and the structure of the junction did not undergo significant changes. This confirms the stability of the junction following TSC injury, and that the process of recovery is very successful.

One of the aims of this study was to develop a disease model of immune mediated injury at the NMJ, where chronic antibody exposure caused constant TSC injury as may occur in conditions such as CANOMAD. In this system, it was thought that TSC return to the junction would be inhibited, and the effects of chronic depletion could be identified. However, repeat application of antibody during TSC recovery did not inhibit repopulation. Instead, the junction behaved as if the axon had been injured, with TSC process formation, and remodelling despite the axon appearing morphologically unchanged. It is possible that returning TSCs do not have the same ganglioside, or complement regulator phenotype as their predecessors, and this could alter their behaviour in response to antibody exposure. If this were the case, it would illustrate the protective mechanisms that exist to limit immune-mediated injury in the PNS. In the actual disease however, constant antibody exposure may overwhelm, or exhaust these protective mechanisms. The returning TSCs may not be damaged, but the junction could experience significant disruption by the protective process. Further experiments looking at different repetitive dosing regimes may elucidate this further.

However, it is unlikely that this study would illustrate the effects of chronic TSC depletion at the mammalian NMJ (as was shown in the frog by Reddy and

colleagues). This could be described by using inhibitors of cell division to prevent cells returning to the NMJ, and would offer insights into basic mammalian physiology, and the role of TSCs in neuromuscular function.

7.4 Human tissue as a disease target in anti-ganglioside antibody-mediated disease

After it was shown that mouse NMJs are susceptible to anti-ganglioside antibody-mediated injury, experiments were conducted on human tissue to identify if human NMJs were also a potential site of injury. These studies would bridge the gap between the animal models and human disease, in addition to offering TSCs as a new disease target at the NMJ.

It was shown that serum from patients with MFS behaves in a very similar way to antibodies to complex gangliosides raised in the mouse, and that TSCs can also be injured by human serum. This study supports previous data that mouse antibodies to complex gangliosides are very similar to human antibodies, and can be used as an alternative to human serum in animal models. It also shows that human antibodies can produce TSC injury, albeit in the mouse NMJ, and suggests that the TSC could potentially be a disease target in MFS.

However, species differences in ganglioside composition make it difficult to correlate findings in the mouse with human. As a result, a series of human muscles were obtained intra-operatively, and the binding patterns of anti-ganglioside antibodies were compared on these tissues.

These experiments show that antibodies to complex gangliosides did not bind to human NMJs, although anti-GM1 antibodies do bind to NMJs in peroneus longus, and also intramuscular nerve bundles. To investigate this further, ganglioside distribution was mapped using cholera toxin and neuraminidase. These experiments supported the anti-ganglioside antibody work, by identifying concentrations of GM1 at the NMJ and nerve bundles of peroneus longus, and the NMJ of intercostals, but not other muscles. Complex gangliosides were not concentrated in any site in the muscles under examination.

This result is very surprising, since it would suggest that human NMJs do not have significant levels of complex gangliosides. This is unlikely as both botulinum and tetanus toxins both exert their effects at the NMJ via complex gangliosides. However, sample size in this study was limited due to practical difficulties, with only one or two muscles being harvested from each patient group. This very small sample size makes it difficult to extrapolate the data to a whole population. Also, despite numerous staining protocols using different blocking solutions, it was not possible to reduce background staining. However, colleagues in Glasgow have since implimented a new method using copper sulphate to reduce autofluorescence, and these technical modifications may well identify new staining patterns that were not evident previously.

Despite these difficulties, these studies cannot exclude the possibility that human NMJs may be a source of injury in anti-ganglioside mediated disease, and that TSCs may be involved in injury at this site.

7.5 Future directions

A number of options for further experiments arise from the results of this series of experiments.

Firstly, there is a need for clarification and extension of a number of issues arising from these studies:

1) Although the role of anti-ganglioside antibodies is widely acknowledged in the pathogenesis of MFS, the mechanism of injury appears to be complement dependent and an understanding of the mechanisms behind this aspect of the injury are crucial for fully understanding disease pathogenesis. The role of complement regulators at the mouse NMJ has not, however been fully explored, and this model would provide a useful paradigm for further studies in this area. In particular, it would be interesting to repeat these experiments with different concentrations of human serum to see if a difference in antibody effect is evident between different complement regulator knockout strains. This study could then be expanded to include other knockout strains and may offer important insights into the mechanisms that protect the mouse junction from injury. Although it is not possible to directly compare mouse and human tissue directly, these insights into complement regulator function in the mouse could be used to guide further studies in the human.
2) The CK mouse model presents an ideal method for studying the response of the PNS to immune mediated injury, and it would be interesting to examine

the effects of other anti-ganglioside antibodies at this site. The effects of injuring the terminal axon would be of particular interest, especially comparing the changes of isolated terminal axon injury with more proximal damage, for example following nerve crush. This may offer insights into axonal regeneration, and understanding recovery in MFS. However, the system could also be adapted to examine other antibodies that may exert their action elsewhere, for example at nodes of Ranvier in models of AMAN. It could also be used to test the effects of patient sera.

3) Axon integrity during TSC repopulation in the CK mouse model was assessed by CFP fluorescence in these studies. However, this data could be greatly strengthened by more detailed studies of axon structure and function. For example, electron microscopy studies of the NMJ at various time points during TSC recovery would illustrate more subtle changes to axon structure that may not be evident at the light microscope level. Additionally, electrophysiological measurements of the junction during the recovery phase would also illustrate if the axon were functionally intact. This would identify whether the axon function was maintained in the absence of TSCs. Both of these experiments would be impractical in sternomastoid due to practical intra-operative difficulties, and other muscles should therefore be considered, for example soleus. Animal surgery restrictions prevented more detailed consideration of this area within this study.

4) Despite using several markers of cell division, the origin of returning TSCs was not identified in this study. Clearly this is very important to understand the response of the NMJ to injury, and its subsequent recovery. One of the most helpful investigations may be electron microscopy, to visualise the

returning processes, and their associated cells. Their location, and morphology at EM level may provide an indication of their source. Immunofluorescence markers may also help to discriminate the origin of the returning cells, but clearly further work needs to be conducted in this important area.

5) The stimulus for TSC repopulation was not demonstrated in these experiments. Again, it was not possible to study this in greater detail, but it would be interesting to identify the stimulus to gain a greater understanding of the mechanisms of NMJ recovery following injury.
6) The effects of chronic TSC depletion were not addressed specifically in this investigation, as it was not possible to injure returning Schwann cells with the antibody. To gain a better understanding of disease, it is important to understand why these returning cells were not injured, and why the junction behaved as if it were denervated. To examine this further, TSC recovery could be prevented by using mitosis inhibitors to inhibit repopulation, but again these experiments were not possible within the timescale of the study
7) A significant limitation of work using human tissue was the small number of samples obtained for each muscle group. Unfortunately, it was not possible to expand these sample populations due to time constraints, but it is crucial to continue these studies using samples obtained from different patients, with differing pathologies, to increase the significance of the data. This data could be used to map the distribution of gangliosides in human tissue, which is crucial for examination of antibodies at this site, and fully understanding the pathogenesis of MFS.

In a broader context, this information could be brought together to eventually establish an accurate mouse model of both MFS and CANOMAD. Mouse and human anti-ganglioside antibodies could be tested using *in vivo* methods to examine injury and subsequent recovery in the PNS. This could specifically address several hypotheses surrounding injury in MFS:

a) The true pathological role of anti-ganglioside antibodies in the PNS could be established by demonstrating whether damage mediated by these antibodies actually causes clinical motor and sensory deficits.
b) The response of the immune system to antibody-mediated injury could be described in more detail, by possibly showing macrophage recruitment to the NMJ to remove cellular debris for example.
c) Recovering Schwann cells could offer insights into protective mechanisms that prevent further immune mediated injury. These may be relevant when developing new therapies, in addition to understanding basic Schwann cell biology.

7.6 Summary

The aim of my study was to identify whether the TSC was a disease target in anti-ganglioside antibody-mediated injury, and these experiments provide evidence to support this hypothesis. In particular, these experiments illustrate the susceptibility of mouse TSCs to anti-ganglioside antibodies, and also describe the response of the NMJ to this injury. The study uses a new mouse model system to show that TSC recovery

alters the behaviour of the NMJ in response to antibody injury, which may have significant implications for disease progression and long-term recovery.

It was also shown for the first time that serum from a patient with MFS can produce acute TSC injury in the mouse model, and highlights the similarity between human anti-ganglioside antibodies, and those raised in the mouse confirming the latter's suitability for experimental use.

Finally, the study examines the distribution of gangliosides for the first time in a series of human muscle tissues, in an attempt to identify new disease targets. The study also shows binding of anti-ganglioside antibodies to human NMJs for the first time, suggesting that the NMJ, and in particular TSCs, may be implicated in disease pathogenesis.

Appendix 1: Commonly Used Solutions

A1.1 10x PBS

NaCl	80g
KH_2PO_4	2g
$Na_2HPO_4.12H_2O$	29g
KCl	2g

Dilute in dH_20 to a final volume of 1 litre, pH 7.4. Dilute 1:10 in dH_20 for use.

A1.2 10x Ringer's solution

NaCl	66g
KCl	3.36g
$NaHCO_3$	21g
NaH_2PO_4	1.38g
Glucose	21.86g
$MgCl_2$	10ml

Dilute in dH_20 to a final volume of 1 litre, pH 7.4.

Dilute 1:10 in dH_20 for use.

Bubble with O_2 for 5 minutes, and add 2ml/litre 1M $CaCl_2$ before use.

A1.3 0.1M glycine

Glycine	0.375g

Make up to 50ml in PBS

A1.4 ELISA

A1.4.1 Substrate solution

0.1M Citrate	14ml
0.2M Na_2PO_4	16ml
dH_20	30ml
15mg O-Phenylenediamine tablet	1
30% hydrogen peroxide	20µl

A1.4.2 Bicarbonate coating buffer

Na_2CO_3	0.79g
$NaHCO_3$	1.46g

dH_20 to a final volume 500ml, pH 9.6

A1.5 Antibody purification buffers

A1.5.1 Binding buffer

0.1M sodium phosphate buffer with 0.15M NaCl, adjusted to pH 7.4

A1.5.2 Tris-HCl

1M (12.1g) Tris base in 100ml H_20 made up to pH9 with HCl

A1.5.3 Elution buffer (0.1M citric acid)

1.92g anhydrous citric acid in 100ml H_20, pH 3-6.

A1.5.4 Phosphate buffer solution (0.1M NaH_2PO_4)

19ml of 0.2M $NaH_2PO_4.2H_20$ and 81ml of 0.2M $Na_2H_2PO_4$ diluted to 200ml in dH_20.

A1.6 Standard antibody blocker

Triton X-100	0.3g
10% sodium azide	1ml
Bovine serum albumin	0.2g

dH_20 to a final volume of 100ml.

To make final concentration of 0.3% Triton X-100, 0.2% BSA and 0.1% sodium azide.

A1.7 Copper sulphate buffer

Copper sulphate	10mM
Ammonium acetate	50mM

In dH_20 to pH5.0

A1.8 Coomassie blue

Coomassie Brilliant Blue R	2.5g
Ethanol	455ml
dH_20	455ml
Glacial acetic acid	90ml

Appendix 2: Animal surgery protocols

Appendix 2.1

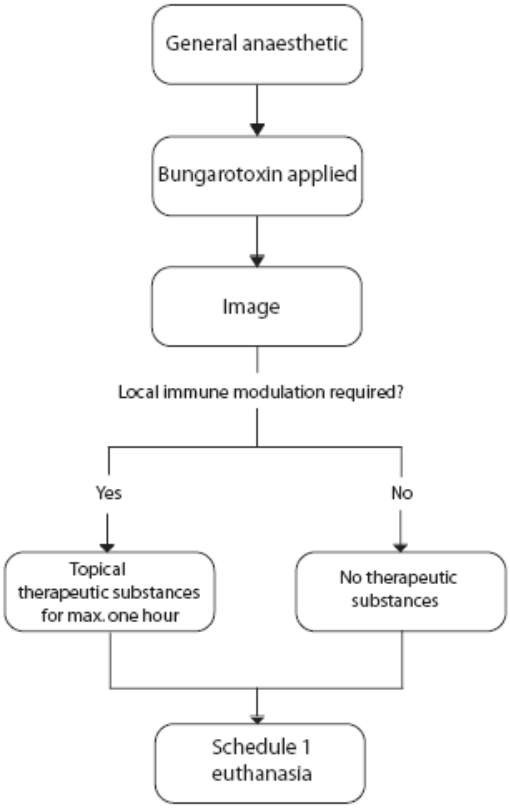

Appendix 2.2

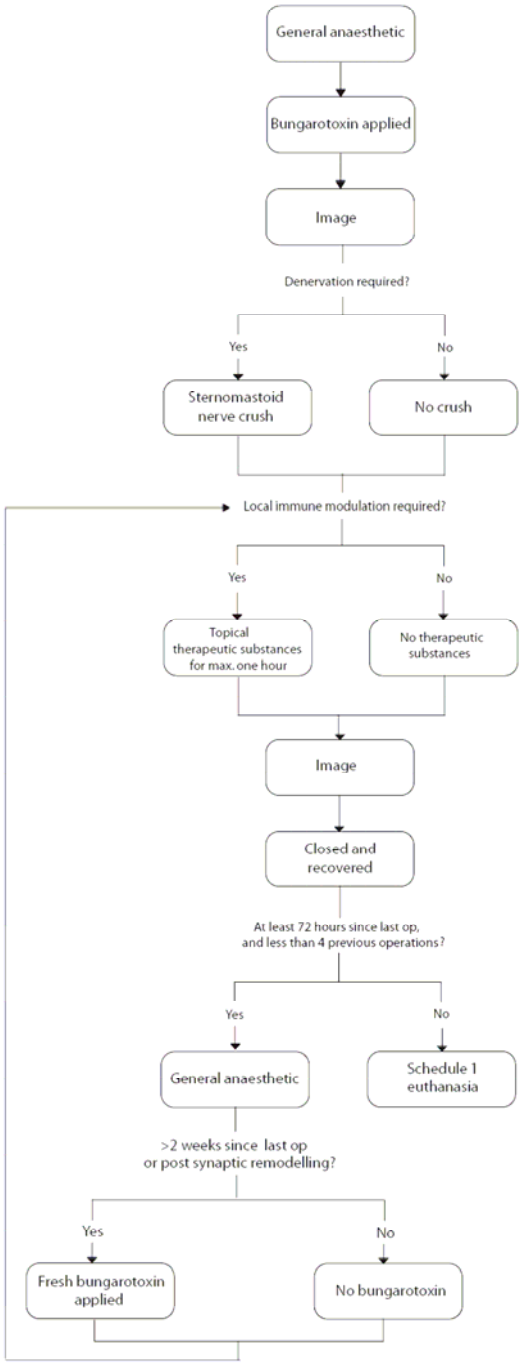
General anaesthetic
Bungarotoxin applied
Image
Denervation required?
Yes
No
Sternomastoid nerve crush
No crush
Local immune modulation required?
Yes
No
Topical therapeutic substances for max. one hour
No therapeutic substances
Image
Closed and recovered
At least 72 hours since last op, and less than 4 previous operations?
Yes
No
General anaesthetic
Schedule 1 euthanasia
>2 weeks since last op or post synaptic remodelling?
Yes
No
Fresh bungarotoxin applied
No bungarotoxin

Appendix 2.3

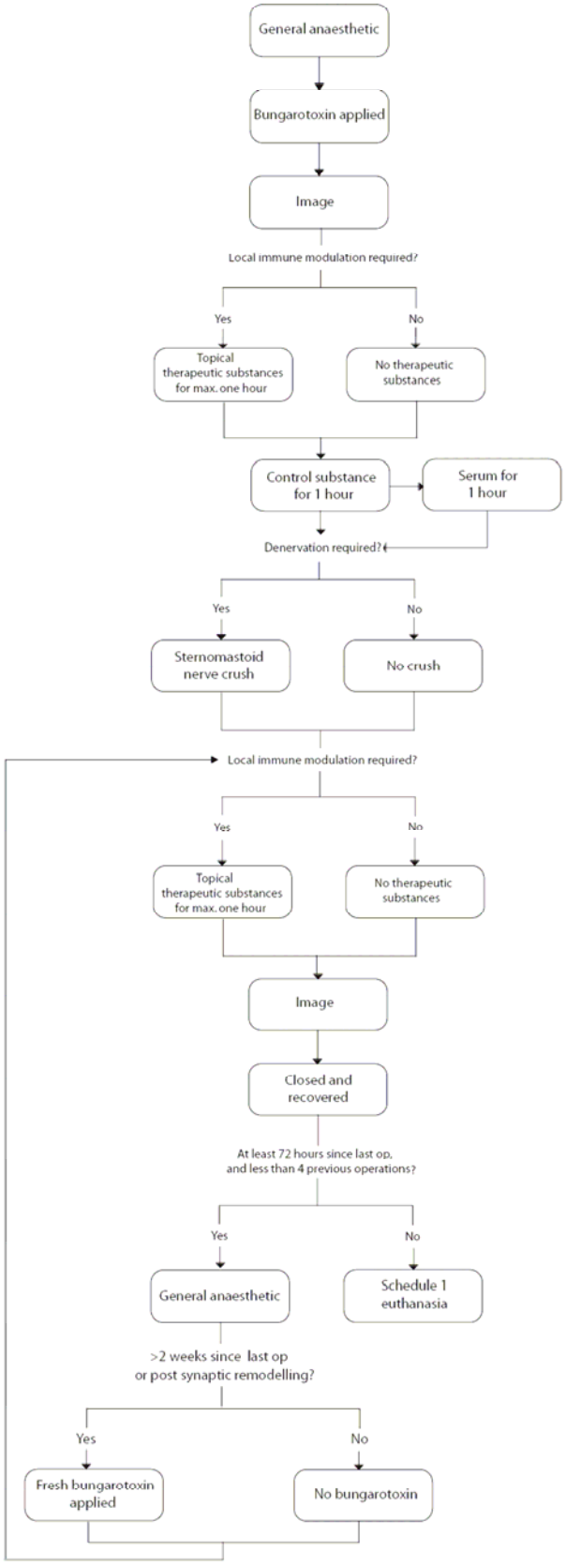
General anaesthetic
Bungarotoxin applied
Image
Local immune modulation required?
Yes
No
Topical therapeutic substances for max. one hour
No therapeutic substances
Control substance for 1 hour
Serum for 1 hour
Denervation required?
Yes
No
Sternomastoid nerve crush
No crush
Local immune modulation required?
Yes
No
Topical therapeutic substances for max. one hour
No therapeutic substances
Image
Closed and recovered
At least 72 hours since last op. and less than 4 previous operations?
Yes
No
General anaesthetic
Schedule 1 euthanasia
>2 weeks since last op or post synaptic remodelling?
Yes
No
Fresh bungarotoxin applied
No bungarotoxin

Appendix 2.4

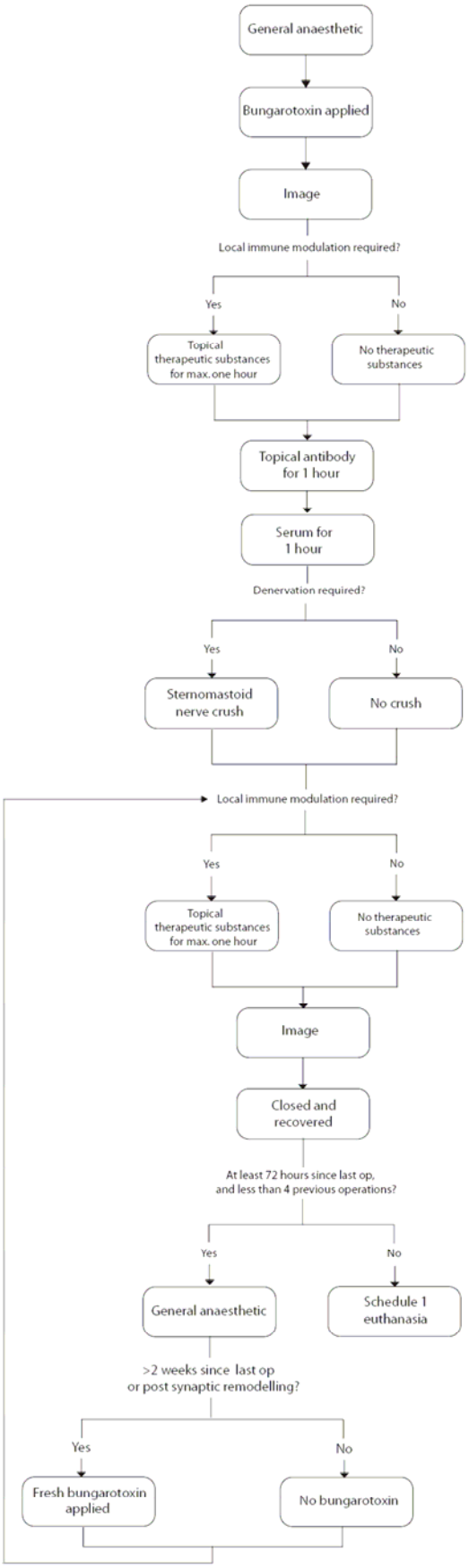
General anaesthetic
Bungarotoxin applied
Image
Local immune modulation required?
Yes
No
Topical therapeutic substances for max. one hour
No therapeutic substances
Topical antibody for 1 hour
Serum for 1 hour
Denervation required?
Yes
No
Sternomastoid nerve crush
No crush
Local immune modulation required?
Yes
No
Topical therapeutic substances for max. one hour
No therapeutic substances
Image
Closed and recovered
At least 72 hours since last op, and less than 4 previous operations?
Yes
No
General anaesthetic
Schedule 1 euthanasia
>2 weeks since last op or post synaptic remodelling?
Yes
No
Fresh bungarotoxin applied
No bungarotoxin

Appendix 2.5

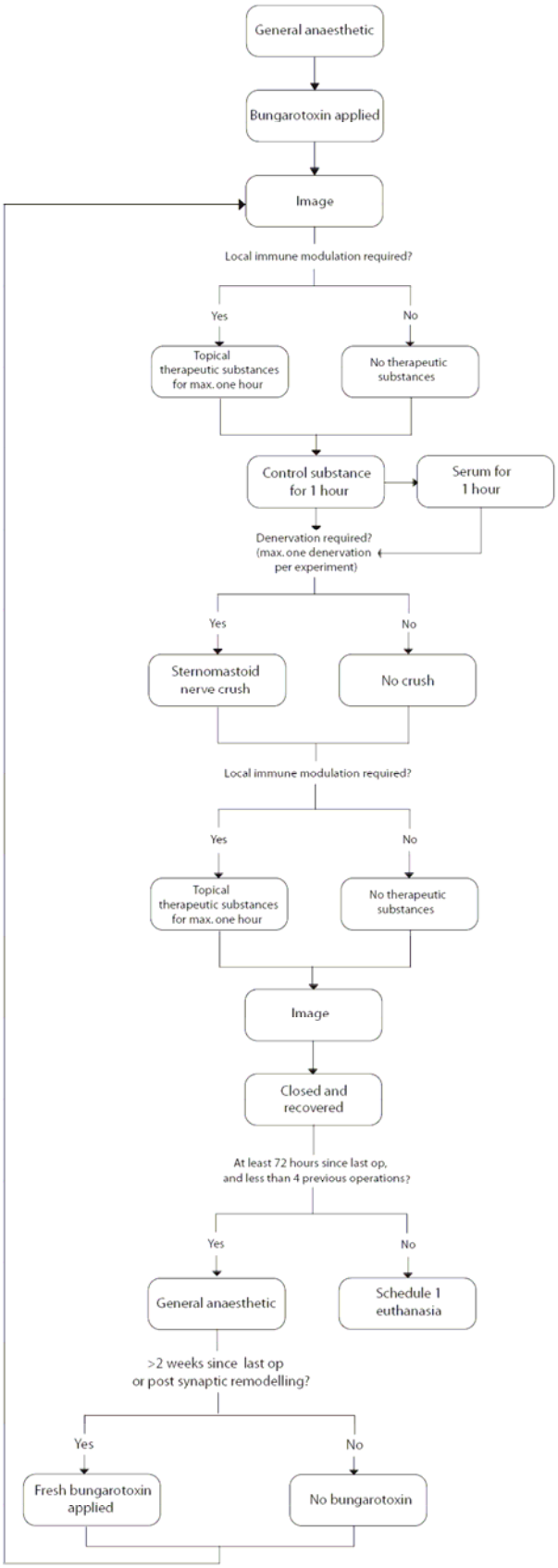
General anaesthetic
Bungarotoxin applied
Image
Local immune modulation required?
Yes
No
Topical therapeutic substances for max. one hour
No therapeutic substances
Control substance for 1 hour
Serum for 1 hour
Denervation required? (max. one denervation per experiment)
Yes
No
Sternomastoid nerve crush
No crush
Local immune modulation required?
Yes
No
Topical therapeutic substances for max. one hour
No therapeutic substances
Image
Closed and recovered
At least 72 hours since last op, and less than 4 previous operations?
Yes
No
General anaesthetic
Schedule 1 euthanasia
>2 weeks since last op or post synaptic remodelling?
Yes
No
Fresh bungarotoxin applied
No bungarotoxin

Appendix 2.6

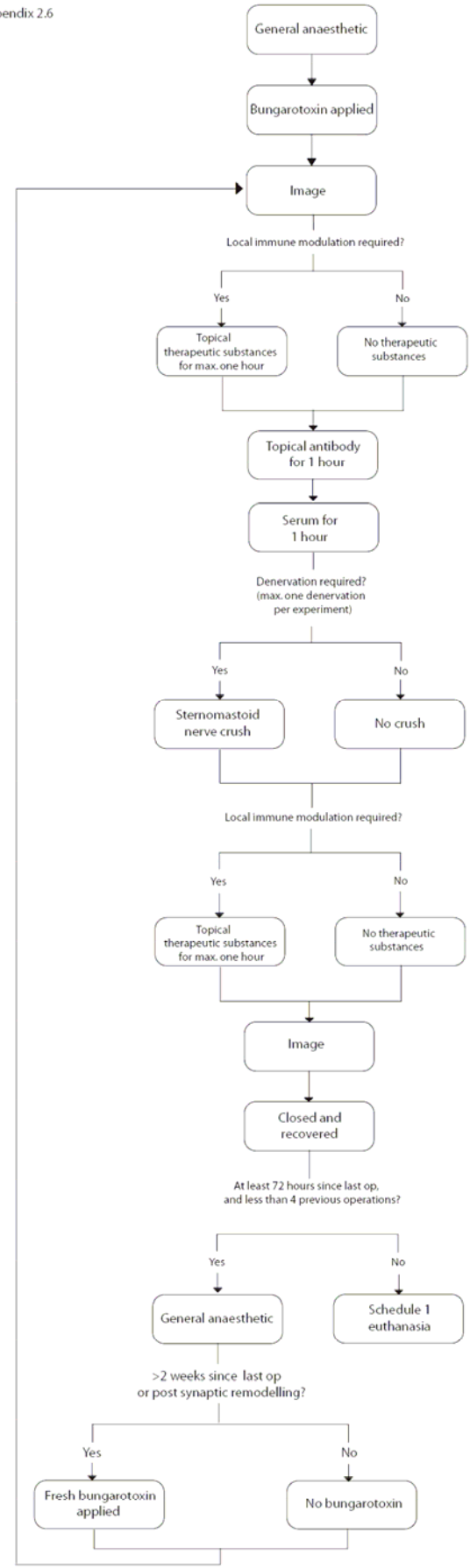
General anaesthetic
Bungarotoxin applied
Image
Local immune modulation required?
Yes
No
Topical therapeutic substances for max. one hour
No therapeutic substances
Topical antibody for 1 hour
Serum for 1 hour
Denervation required? (max. one denervation per experiment)
Yes
No
Sternomastoid nerve crush
No crush
Local immune modulation required?
Yes
No
Topical therapeutic substances for max. one hour
No therapeutic substances
Image
Closed and recovered
At least 72 hours since last op, and less than 4 previous operations?
Yes
No
General anaesthetic
Schedule 1 euthanasia
>2 weeks since last op or post synaptic remodelling?
Yes
No
Fresh bungarotoxin applied
No bungarotoxin

Appendix 3: Patient consent documentation

SOUTHERN GENERAL HOSPITAL NHS TRUST

CONSENT FOR RETENTION OF NERVE AND MUSCLE TISSUES

PATIENT INFORMATION SHEET

You are being asked to give permission for small amounts of the nerve or muscle tissue that is being removed during the course of your biopsy to be retained for research purposes.

- Diseases of the nerves, called 'peripheral neuropathy' are an important cause of paralysis, sensory loss, disability and death, affecting many millions of people worldwide in a wide variety of ways. In most cases, detailed scientific information about the causes are unknown and research is needed to understand this and thereby develop new treatments.
- Many cases of peripheral neuropathy have an 'autoimmune' basis, in which the body's own immune mistakenly attacks the nerves, causing tissue damage and nerve malfunction. The research your nerve or muscle will be used for aims to identify the cause of autoimmune neuropathy by examining tissue samples from affected subjects and control groups in whom the nerves are normal, and thereby identifying the key factors that lead to the disease.
- All research projects are approved and monitored under the guidance of the SGH NHS Trust Ethics Committee.

What we wish to do

You are about to undergo an operation in which nerve or muscle tissue will be removed. The tissue that will be removed from you will be examined by pathologists to provide information about your condition. From these specimens, small amounts that are not required for diagnostic purposes will be set aside for our research on the nerves in the tissues.

What are the risks and benefits to you? There are no risks to you over and above the surgery you already require to treat your condition. No extra tissue will be removed from you that is not already part of your treatment. There will be no benefit to you directly.

Can you refuse? You are free to refuse to take part in the study. You do not have to give any reason. All of you routine treatment will continue as usual. ***(Consent overleaf)***

SOUTHERN GENERAL HOSPITAL NHS TRUST

CONSENT FOR RETENTION OF NERVE AND MUSCLE TISSUES

SHEET FOR SIGNATURE

	Please circle	
Have you read the information sheet overleaf?	**Yes**	**No**
Have you had an opportunity to ask questions and discuss this study?	**Yes**	**No**
Have you received satisfactory answers to all your questions?	**Yes**	**No**
Have you received enough information about the study?	**Yes**	**No**

Who have you spoken to concerning the study?

Dr/Mr/Ms

Do you understand that you are free to withdraw from the study -

	Please circle	
at any time?	**Yes**	**No**
without having to give a reason	**Yes**	**No**
and without affecting your future medical care?	**Yes**	**No**
Do you agree to participate in this study?	**Yes**	**No**

Signed..... Date.....

Name in Block Letters..... Date.....

Signature of Witness..... Date.....

Name in Block Letters..... Date.....

This investigation aims to study human nerve and muscle tissue in surgical specimens in order to understand the causes of peripheral neuropathy and related disorders.

(Patient information overleaf)

North Glasgow University Hospitals NHS Trust
Bio Bank Services

NHS
Greater Glasgow

CONSENT TO DONATION OF RESIDUAL TISSUE FOR MEDICAL RESEARCH & TEACHING

Patient ID Label	DATE	
	Proposed procedure (block capitals)	

I agree to give any residual (left-over) tissue removed during my operation or treatment to the North Glasgow University Hospitals NHS Trust for medical research and teaching purposes. I agree that the tissue may be provided to a research institution or pharmaceutical company for regulated medical research. This work could help researchers understand disease, develop new diagnostic tests and produce better and safer drugs.

I understand that:

- You may remove tissue as part of my treatment. You will examine this, and use any residual material for medical research and teaching purposes. My doctor will not take more tissue than is needed for my care.
- You will make sure that all my donated tissue is anonymised (in other words I cannot be identified by the researcher).
- You may give some information from my medical records (that will not identify me) to the researcher.
- You will not sell my tissue but costs will be recovered on a non-profit making basis.
- I will not benefit financially or be entitled to a share of any profit that might arise from the research.
- It may be appropriate for genetic tests to be carried out in order to determine whether genetic makeup has any connection with disease.
- I will not receive results of any research carried out on my tissue.

Staff gave me a patient information leaflet on the use of residual tissue. I've had the opportunity to discuss the information with a qualified member of staff.

Patient's Name (block capitals)	Patient's Signature
Date	
Clinical Practitioner	**Grade/Designation**

Copies: Top – Patient's notes, Middle – Bio Bank, Lower – Patient
Bio Bank Services, Glasgow Royal Infirmary, Castle St, Glasgow G4 0SF Tel: 0141 211 4531 ~ www.ngt.org.biobank

GRI 07674/1

Appendix 4: Publication

GLIA 52:177–189 (2005)

Anti-Disialosyl Antibodies Mediate Selective Neuronal or Schwann Cell Injury at Mouse Neuromuscular Junctions

SUSAN K. HALSTEAD,[1] IAN MORRISON,[1] GRAHAM M. O'HANLON,[1] PETER D. HUMPHREYS,[1] JOHN A. GOODFELLOW,[1] JAAP J. PLOMP,[2,3] AND HUGH J. WILLISON[1]*
[1]*Department of Neurology, Division of Clinical Neurosciences, University of Glasgow, Southern General Hospital, Glasgow, Scotland*
[2]*Departments of Neurology, Leiden University Medical Centre, The Netherlands*
[3]*Department of Neurophysiology, Leiden University Medical Centre, The Netherlands*

KEY WORDS
ganglioside; autoantibody; synapse; glia

ABSTRACT
The human paralytic neuropathy, Miller Fisher syndrome (MFS) is associated with autoantibodies specific for disialosyl epitopes on gangliosides GQ1b, GT1a, and GD3. Since these gangliosides are enriched in synaptic membranes, anti-ganglioside antibodies may target neuromuscular junctions (NMJs), thereby contributing to disease symptoms. We have shown previously that at murine NMJs, anti-disialosyl antibodies induce an α-latrotoxin-like effect, electrophysiologically characterized by transient massive increase of spontaneous neurotransmitter release followed by block of evoked release, resulting in paralysis of the muscle preparation. Morphologically, motor nerve terminal damage, as well as perisynaptic Schwann cell (pSC) death is observed. The relative contributions of neuronal and pSC injury to the paralytic effect and subsequent repair are unknown. In this study, we have examined the ability of subsets of anti-disialosyl antibodies to discriminate between the neuronal and glial elements of the NMJ and thereby induce either neuronal injury or pSC death. Most antibodies reactive with GD3 induced pSC death, whereas antibody reactivity with GT1a correlated with the extent of nerve terminal injury. Motor nerve terminal injury resulted in massive uncontrolled exocytosis with paralysis. However, pSC ablation induced no acute (within 1 h) electrophysiological or morphological changes to the underlying nerve terminal. These data suggest that at mammalian NMJs, acute pSC injury or ablation has no major deleterious influence on synapse function. Our studies provide evidence for highly selective targeting of mammalian NMJ membranes, based on ganglioside composition, that can be exploited for examining axonal–glial interactions both in disease states and in normal NMJ homeostasis.

INTRODUCTION

Anti-disialylated ganglioside autoantibodies are the specific serological marker for the Miller-Fisher syndrome (MFS) variant of the paralytic neuropathy, Guillain-Barré syndrome (Chiba et al., 1992; Willison and O'Hanlon, 1999). MFS autoantibodies principally react with NeuAc(α2–8)NeuAc "disialosyl" epitopes that are (α2–3) linked to the terminal galactose of b-series gangliosides including GQ1b, GT1a, and GD3. Gangliosides are glycosphingolipids embedded in the outer leaflets of cell membranes, and are enriched in neurons. The fine specificity of anti-disialosyl antibodies found in MFS is heterogeneous, with some antibodies showing a preference for binding GQ1b, GT1a, or GD3, and others binding more promiscuously to terminally or internally disialylated gangliosides, the latter including GD1b and GT1b (Table 1). These differences in antibody specificity correlate with the clinical patterns of disease and reflect differences in ganglioside composition within different regions of the human peripheral nervous system (O'Leary et al., 1996; Susuki et al., 2001; Willison and Yuki, 2002; Koga et al., 2002).

The pathophysiological pathways underlying MFS are incompletely understood. In mouse studies, using a range of human and mouse anti-disialosyl antisera and monoclonal antibodies (mAbs), we have previously identified the motor nerve terminal at neuromuscular junctions (NMJ) as one of several potential sites of antibody mediated injury (Roberts et al., 1994; Willison et al., 1996; Goodyear et al., 1999; Plomp et al., 1999; O'Hanlon et al., 2001; Bullens et al., 2002; O'Hanlon et al., 2002; Halstead et al., 2004). MFS sera, MFS IgG, monoclonal IgM, and a prototypic anti-disialosyl mouse mAb, CGM3, that reacts with all terminally disialylated gangliosides (i.e., GD3, GT1a, and GQ1b) induce a paralytic effect at the mouse NMJ in vitro that is electrophysiologically similar to that of α-latrotoxin (LTx), i.e., transient massive, spontaneous, asynchronous release of acetylcholine (ACh) manifested as elevated miniature endplate potential (MEPP) frequencies, rapidly followed by failure of evoked release (Goodyear et al., 1999; Plomp et al., 1999; Bullens et al., 2000). This effect is dependent on antibody-mediated activation of the complement cascade that culminates in the deposition of the pore forming membrane attack complex (MAC) in the pre-synaptic NMJ membranes (Halstead et al., 2004). Morphological analy-

Grant sponsor: Wellcome Trust; Grant sponsor: Guillain-Barré Syndrome Support Group UK; Grant sponsor: KNAW Van Leersumfonds; Grant sponsor: Prinses Beatrix Fonds; Grant number: MAR04-0213.

*Correspondence to: Hugh J. Willison, Department of Neurology, Division of Clinical Neurosciences, University of Glasgow, Southern General Hospital, Glasgow G51 4TF, Scotland. E-mail: h.j.willison@clinmed.gla.ac.uk

Received 7 January 2005; Accepted 8 March 2005

DOI 10.1002/glia.20228

Published online 20 June 2005 in Wiley InterScience (www.interscience.wiley.com).

TABLE 1. Ganglioside Binding Patterns of Anti-Disialosyl mAbs

MAb	Isotype	Disialylated ganglioside specificity[a]			MAb group[b]
		GT1a	GQ1b	GD3	
CGM1	IgM	2.5×10^3	2.9×10^3	2.3×10^3	SN
CGM2	IgM	5.0×10^3	1.1×10^3	7.7×10^3	SN
CGM3	IgM	6.7×10^3	8.3×10^4	3.3×10^4	SN
EM1	IgM	3.6×10^4	2.5×10^5	8.3×10^4	SN
EM2	IgM	1.3×10^4	3.3×10^5	3.3×10^2	N
EM3	IgM	2.0×10^4	2.5×10^4	5.0×10^3	N
EM6	IgM	1.7×10^3	1.3×10^3	1	N
EG1	IgG3	91	1.8×10^3	1×10^2	S
EG2	IgG3	2.9×10^2	8.3×10^2	1	N
R24	IgG3	53	90	2.5×10^2	S

[a]Antibodies were titrated in an ELISA against the relevant gangliosides at Ab concentrations ranging from 10^{-2} to 10^{-5} mg/mL, and the reciprocal of the Ab concentration that gave half-maximal binding was calculated (1/50%).
[b]MAbs are referred according to site of tissue injury as follows: Group SN, pSC and nerve terminal; Group N, nerve terminal only; Group S, pSC only. Ganglioside structures: GT1a: Neu5Acα8Neu5Acα3Galβ3GalNAcβ4(Neu5Acα3)Galβ4GlcCer; GQ1b: Neu5Acα8Neu5Acα3Galβ3GalNAcβ4(Neu5Acα8Neu5Acα3)Galβ4GlcCer; GD3: Neu5Acα8Neu5Acα3Galβ4GlcCer.

sis of NMJs exposed to CGM3 reveals extensive deposits of anti-disialosyl antibody and complement products, localized to both the nerve terminal and the overlying perisynaptic Schwann cells (pSCs) (Bullens et al., 2002; Halstead et al., 2004). At physiological extracellular calcium concentrations, there is a severe loss of cytoskeletal proteins that can be attenuated by calpain inhibition (O'Hanlon et al., 2003), accompanied by major physical disruption of the terminal axon, including vesicle depletion and complete separation of the axon from the postsynaptic membrane, i.e., denervation (Duchen et al., 1981; Willison and O'Hanlon, 1999; O'Hanlon et al., 2001). Using nuclear ethidium homodimer (EthD-1) uptake as an index of disrupted plasma membrane permeability (by MAC pores) and cell death (Reddy et al., 2003; Halstead et al., 2004), we have also observed concurrent pSC death at a high proportion of NMJs (Halstead et al., 2004). The precise nature of the disialosyl targets within the membranes of the different NMJ compartments is unknown, although for the nerve terminal at least, they are proved to be epitopes displayed on gangliosides (Bullens et al., 2002).

The interactions between neuronal elements and their pSC glial partners at NMJs are extensive (Castonguay et al., 2001; Auld and Robitaille, 2003a). Recent data from frog studies indicates a pivotal role for pSCs in maintaining synaptic structure and function (Reddy et al., 2003). From a human disease perspective, pSC injury or loss may have an important influence on neuromuscular function. In this study we have sought to establish whether subtypes of anti-disialosyl mAbs with preferred reactivities with particular gangliosides might selectively target either the neuronal or glial elements of the NMJ, and thereby identify the ganglioside specificities responsible. To this end, we have used a panel of recently cloned anti-disialosyl mouse mAbs with varying degrees of reactivity for GD3, GD1b, GT1b, GQ1b, and GT1a to explore this (Boffey et al., 2004). We report the identification of groups of mAbs that can selectively injure either neuronal or pSC membranes, or both.

MATERIALS AND METHODS

Antibodies and Serum

An array of anti-ganglioside mAbs were generated as described in previous studies (Goodyear et al., 1999). Seven IgM and three IgG3 anti-ganglioside mAbs were identified following a wider screen of anti-disialosyl ganglioside antibodies that assessed their ability to induce complement deposition and tissue injury at the mouse NMJ. Isotype and ganglioside reactivities were determined by enzyme-linked immunosorbent assay (ELISA) and expressed as half-maximal binding values, as summarized in Table 1 and as previously reported (Boffey et al., 2004). Ganglioside structures and nomenclature follows IUPAC-IUB 1997 recommendations: http://www.chem.qmul.ac.uk/iupac/misc/glylp.html. The anti-GD3 mAb, R24 (that also binds GQ1b) was obtained from American Type Culture Collection (ATCC; Manassas, VA) (Dippold et al., 1980; Chapman et al., 1990). In both morphological and electrophysiological studies, mAbs were screened in in vitro hemi-diaphragm assays (see below) at 100 μg/ml, except for CGM3 that has previously been found to be active at 50 μg/ml. All mAbs and the normal human serum (NHS) used as a complement source were dialyzed against physiological Ringer's solution (see below) for 24 h. NHS was taken from a single donor stock that was freshly frozen and stored in aliquots at −70°C to preserve complement activity (Plomp et al., 1999).

Mice

Male Balb/c mice (4–7 weeks old, Harlan, UK) were used for all studies unless stated otherwise. For interstrain comparison studies, male C57BL/6j (5–7 weeks old), NIH(s) (Swiss, young: 4–6 weeks; old: 11–13 weeks), both from Harlan (UK), C57BL/6 × 129/Sv (3–6 weeks) (Holt et al., 2001), and C57BL/6 × CBA (4–8 weeks) (Takamiya et al., 1996) were studied.

Hemi-Diaphragm Preparations

Left and right hemi-diaphragms with their phrenic nerve attached were pinned out in a dish containing Ringer's solution (116 mM NaCl, 4.5 mM KCl, 1 mM $MgCl_2$, 2 mM $CaCl_2$, 1 mM NaH_2PO_4, 23 mM $NaHCO_3$, 11 mM glucose, pH 7.4) at room temperature (RT; 20–22°C), pregassed with 95% O_2/5% CO_2. Tissue was incubated with an anti-ganglioside mAb for 2 h at 32°C, followed by 30 min at 4°C to facilitate binding (Plomp et al., 1999). The preparations were rinsed briefly in Ringer at RT, then incubated with diluted NHS for 1 h at RT. Preparations were monitored to determine if they underwent spontaneous asynchronous contractile activity, indicating that the LTx-like effect was taking place (Jacobs et al., 2002). In control experiments, tissue was incubated with either LTx (4 nM) in Ringer as a positive control, provided by Dr. Yuri Ushkaryov (Ashton et al., 2000), or Ringer alone as a negative control. Muscle fiber twitching was observed only in the positive control.

Analysis of Perisynaptic Schwann Cell Integrity

Ethidium homodimer 1 (EthD-1; Molecular Probes, Eugene, OR), a membrane-impermeant dye that labels with red fluorescence the nucleic acids of membrane-compromised cells was used to monitor pSC viability as previously reported (Halstead et al., 2004). A 2 mM stock solution of EthD-1, stored at −20°C was diluted to 2 μM in fresh oxygenated Ringer. In preparations used for fluorescent analysis of pSC integrity, each hemi-diaphragm was halved, giving a total of four muscle preparations to be studied in parallel. After mAb and complement exposure (or LTx incubations as above), the tissue was rinsed in fresh Ringer, and the bath volume was then replaced with 2 mM EthD-1. The tissue was incubated in the dark at RT for 1 h, fixed in the dark in 0.1% formaldehyde for 1 h, then rinsed in Ringer and frozen for histological analysis; 15-μm cryostat sections were cut onto 3-aminopropyltriethoxysilane (APES)-coated glass slides, stored at −20°C before analysis. NMJs were identified by staining with bodipy-labeled α-bungarotoxin (bodipy-BTx; diluted 1:500; Molecular Probes), which binds to postsynaptic ACh receptors, and the frequency distribution of EthD-1-positive nuclei at NMJs was calculated.

Tissue Preparation for Complement and Neurofilament Immunohistology, and Ultrastructural Quantification

Before the addition of test reagents, the ventralmost quarter of each hemi-diaphragm was removed, and immediately processed for baseline immunohistology. Tissue samples were mounted in Lipshaw's M-1 mounting medium (Pittsburgh, PA, USA), and longitudinal cryostat sections (8 μm) were cut onto APES coated slides, allowed to air-dry and stored at −20°C. This tissue constituted the untreated standard to which other results were subsequently ratiometrically compared, thus enabling the pooling of results from separate staining runs.

After incubation, one-half of the remaining hemi-diaphragm was processed for immunohistology. Samples consisting of the pre-incubation standard and corresponding experimentally treated tissues were mounted together on the same slide. The remaining portion of the hemi-diaphragm was fixed in situ for electron microscopy (EM) analysis with 4% formaldehyde for 2 min, after which the tissue was removed for overnight immersion in 2% formaldehyde, 2.5% glutaraldehyde, and then stored in phosphate-buffered saline (PBS) at 4°C before resin embedding.

Immunostaining

Complement activation at the NMJ was quantified by C3c immunostaining as reported (O'Hanlon et al., 2001). C3c is common to all complement pathways, and correlates well with MAC levels (S.K. Halstead and G.M. O'Hanlon, unpublished observations). Unfixed tissue sections were incubated with FITC labeled anti-complement C3c (diluted 1:300; Dako, Ely, UK) in PBS containing 10% goat serum. To localize NMJs, Texas red-labeled α-BTx (Tx-BTx; diluted 1:2,000; Molecular Probes) was also included. The sections were incubated for 1 h at 4°C, rinsed, and mounted in Citifluor antifade (Citifluor Products, Canterbury, UK).

Nerve injury as manifested by loss of neurofilament (NF) immunoreactivity at the NMJ was monitored as reported using rabbit polyclonal anti-phosphorylated 200 kDa NF antibody (1211, diluted 1:750; Affiniti Research Products Ltd., Exeter, UK) (O'Hanlon et al., 2001). Sections of unfixed tissue were pre-incubated for 1 h at RT with Tx-BTx (1:1,000), rinsed, immersed in ethanol at −20°C for 20 min, then incubated at RT overnight with anti-NF antibody in a staining solution of PBS containing 10% goat serum and 0.1% Triton X-100. The sections were then rinsed, incubated for 1 h at 4°C with FITC-conjugated goat anti-rabbit IgG (1:300; Southern Biotechnology Associates, Birmingham, AL), and mounted in Citifluor antifade. A minimum of two staining runs of each marker was performed on tissue from individual hemi-diaphragm preparations.

Image Acquisition

Digital images were captured by a Zeiss Pascal confocal microscope. Image-analysis measurements were made using Scion Image (Scion) image analysis software. Bitmap processing and annotation were conducted on Adobe Photoshop (Adobe Systems) and Powerpoint (Microsoft).

Ultrastructural Quantification

Tissue samples were prepared for EM analysis using standard procedures (O'Hanlon et al., 2001). NMJs were identified by the presence of postsynaptic junctional folds, and images recorded at 10,000× and 30,000× magnification were used for morphological assessment. On average, 10 NMJs were photographed from a single hemi-diaphragm preparation, and in most cases two or more repeats of each preparations were performed. Quantitative analysis was as previously described with minor modification (O'Hanlon et al., 2001). Morphological comparisons were made with reference control data from Balb/c NMJs exposed in vitro either to Ringer or to Ringer plus NHS. Additional control data were collected during the current study and did not differ significantly from the reference data set (Student's two-tailed t-test; $P < 0.01$). Individual NMJs were composed of one or more separate nerve terminal profiles, presented in a range of orientations, and for each profile a series of measurements and counts were made. EM analysis of normal control NMJs demonstrates regions of dense synaptic vesicles adjacent to the pre-synaptic membrane.

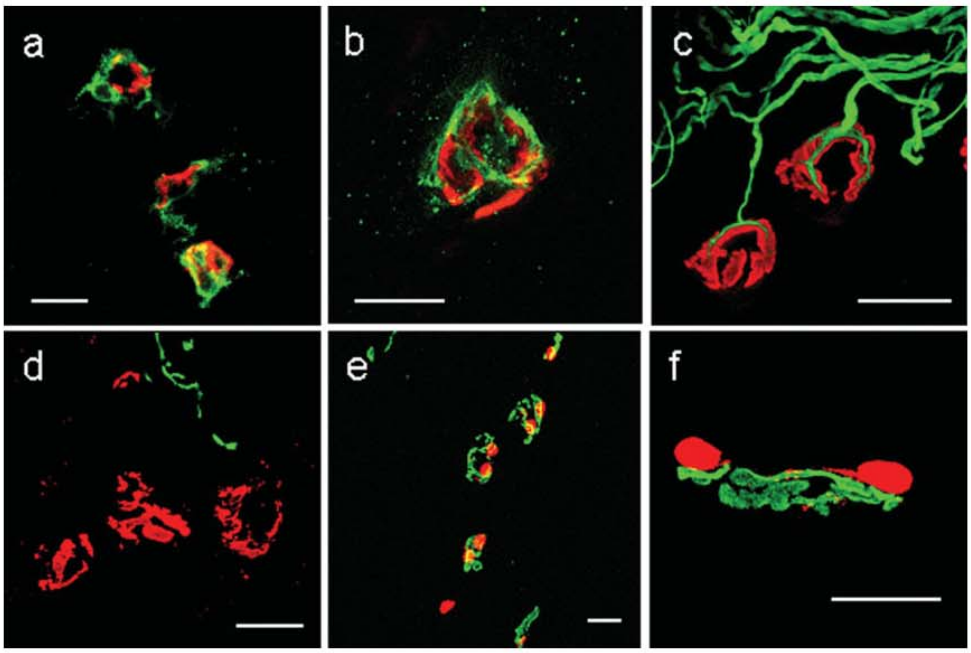

Fig. 1. Immunofluorescent staining of hemidiaphragm tissue exposed to anti-disialosyl mAbs plus NHS as a source of complement. **a,b:** All mAbs used in this study produced significant deposits of complement (C3c; green) over the NMJ (BTx staining, red) in the presence of NHS. **c:** Normal pattern of nerve terminal NF (green) extended from the distal axon to form an arborization over the NMJ (BTx, red), as seen after exposure to Ringer or Group S mAbs plus NHS. **d:** Complete dissolution or fragmentation of the NF signal (green) over the NMJ (BTx, red) or distal intramuscular axons, as seen after exposure to Iatrotoxin or Group SN and N mAbs plus NHS. **e,f:** Abnormal nuclear uptake of EthD-1 (red) by perisynaptic Schwann cells overlying NMJs (BTx, green) after exposure to Group S and SN mAbs plus NHS. Scale bars 20 μm. (This figure is available in color, online at www.interscience.wiley.com).

Typically set back behind the vesicle region, the mitochondria appeared electron dense with well-defined cristae. The pSCs appear as compact cells overlying the nerve terminal profiles with electron-dense processes that extended to the edges of the synaptic cleft but rarely separate the pre-synaptic membrane from a post-synaptic junctional fold (see Fig. 3a–c).

Four ultrastructural parameters that represent the pathological features induced by the anti-disialosyl mAbs were analyzed: (1) percentage of mitochondria showing breakdown of internal structures; (2) vesicle depletion assessed as the number of vesicles per 200 × 200-nm grid placed over the pre-synaptic nerve terminal opposite the opening of a junctional fold, a position considered to coincide with the active zone; (3) the presence of pSC processes forming a "full wrap" defined as Schwann cell processes that completely separates a nerve profile from the muscle (scored 1 or 0); and (4) the presence of one or more injured pSCs (scored 1 or 0) defined by the presence of swollen and electron-lucent pSC cytoplasm and processes, often containing multiple circular figures, mitochondrial damage, nuclear fragmentation with membrane blebs.

In Vitro Electrophysiological Measurements

For in vitro electrophysiological NMJ analysis, male Balb/c mice (~4 weeks old) were killed by CO_2 inhalation, subject to Leiden University guidelines and Dutch law (DEC 01055). Hemi-diaphragms with attached phrenic nerve were dissected and pinned out onto the silicone rubber lined base of a dish containing Ringer's solution at room temperature (20–22°C), pre-gassed with 95% O_2/5% CO_2. Muscles were incubated with 50 μg/ml (mAb CGM3) or 100 μg/ml (all other mAbs tested) of the mAb for 3 h at 32°C. Thereafter, NHS (1:2 diluted with Ringer's solution) was added and intracellular recordings of MEPPs (the small postsynaptic depolarizations resulting from spontaneous pre-synaptic release of single quanta of ACh packaged in a single vesicle) and end-plate potentials (EPPs), upon nerve stimulation, were

made using standard recording equipment at 20–22°C for a period of 1 h. The peptide μ-conotoxin-GIIIB (3 μM, Scientific Marketing Associates, Barnet, UK) was added to block muscle Na^+ channels selectively, to eliminate muscle action potentials. Randomly within the preparation, muscle fibers were impaled near the NMJ with a 10–20 M glass microelectrode filled with 3 M KCl. Signals were digitized and stored for later, off-line analysis of MEPP and EPPs and calculation of quantal content, i.e., the number of ACh quanta released pre nerve impulse. For details on the recording and analysis procedure, see Bullens et al. (2002). As negative control, the whole test procedure was performed with Ringer preincubation without included mAb. All measurements were performed with the experimenter blinded for the identity of the mAbs tested.

RESULTS

Identification of Anti-Disialosyl Antibodies That Fix Complement at Motor Nerve Terminals

In a preliminary screening study, 10 anti-disialosyl mAbs, including R24 were identified that produced a significant deposition of C3c over the NMJ in the presence of NHS as complement source, compared with Ringer-treated controls (117–228 NMJ analyzed from five to nine separate preparations per group; Student's two-tailed *t*-test; $P < 0.01$) (Figs. 1a,b and 2a). These 10 mAbs were then assigned to one of three groups according to their ability to damage either the pSC or the nerve terminal, or both. Allocation to each group was defined as follows: Group S (pSC injury), ultrastructurally damaged pSCs and EthD-1-stained nuclei; Group N (nerve terminal injury), reduction in neurofilament signal over the end-plate region (O'Hanlon et al., 2001), damaged mitochondria and depletion of synaptic vesicles; Group SN (nerve terminal and pSC injury), all features of both. Group assignments were made after data analysis, and for clarity of presentation the mAbs have been segregated into their appropriate group retrospectively, as shown in Figures 2 and 6. mAbs segregated as follows: Group S: EG1, R24; Group N: EM2, EM3, EM6, EG2; Group SN: CGM1, CGM2, CGM3, EM1.

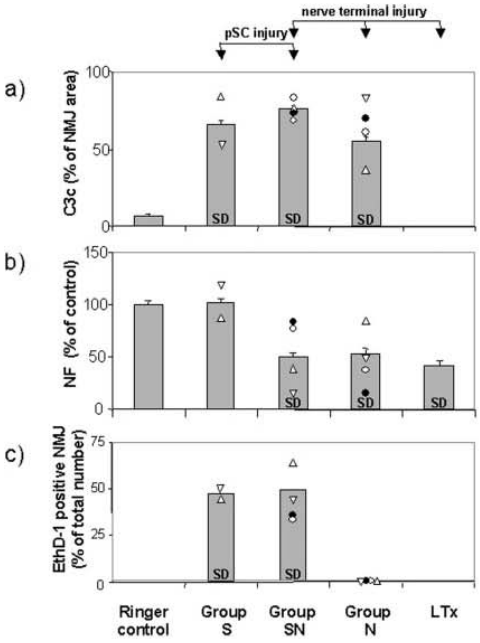

Fig. 2. Quantitative analysis of NMJ injury as assessed by immunofluorescent staining for complement product C3c, neurofilament (NF), and abnormal pSC nuclear uptake of ethidium dimer (EthD-1). According to the distribution of injury, mAbs are segregated into three groups: S (pSC only), N (nerve terminal only), and SN (pSC and nerve terminal). **a:** Complement deposits. All antibodies produced significant deposits of C3c over NMJs compared with Ringer controls or LTx exposure. **b:** Axonal integrity. NF signal is reduced over the NMJ with mAbs producing a nerve terminal injury (Groups SN, N) and with latrotoxin. NF signal is unaffected by Group S mAbs. For a and b, values represent mean ± SEM for the pooled data for each Group. SD is significantly different from Ringer control (Student's two-tailed *t*-test $P < 0.01$). **c:** pSC injury. EthD-1-positive nuclei were observed over NMJs with Group S and SN mAbs, and not with Group N mAbs or LTx. NMJs with one or more overlying EthD-1-positive nuclei were scored as positive, and counts were pooled from one or more preparations. SD is significantly different from Ringer control (Chi squared test, $P < 0.01$). The values obtained for individual mAbs within each group in a c are marked as follows. Group S: EG1 (▽ R24 (△); Group SN: CGM1 (●); CGM2 (▽); CGM3 (△); EM1 (○); Group N: EM2 (●); EM3 (▽); EM6 (▲); EG2 (○).

Characteristics of Perisynaptic Schwann Cell Injury and Death

Nuclear EthD-1 uptake was used to identify membrane permeabilized, dead pSCs at NMJs (127–1,168 NMJs per group from 1–7 preparations) following in vitro exposure to anti-disialosyl mAbs plus NHS (the source of complement). EthD-1-positive nuclei were not observed at the NMJ in control tissue exposed to normal Ringer plus NHS (Fig. 2c, column 1, 127 NMJs analyzed). The 10 mAbs clearly segregated into two groups comprising those that resulted in EthD-1 uptake into one or more pSCs per NMJ (n = 6, Groups S and SN, 578, and 1168 NMJs, respectively) and those that did not (n = 4, Group N, 499 NMJs). Chi squared, $P < 0.01$; Figs. 1e,f and 2c.

EM analysis was performed on 14–155 NMJs from 1–16 preparations per group. Group S and SN mAbs produced a characteristic pSC appearance with swollen cell bodies, fragmented processes, and pSC nuclear membrane blebs. For Group S mAbs, the underlying nerve terminals were unaffected, appearing as described for control tissue (Figs. 3d,e and 4). The presence of pSCs with ultrastructural damage correlated with the EthD-1 uptake measure of pSC injury (Spearman's rank correlation coefficient

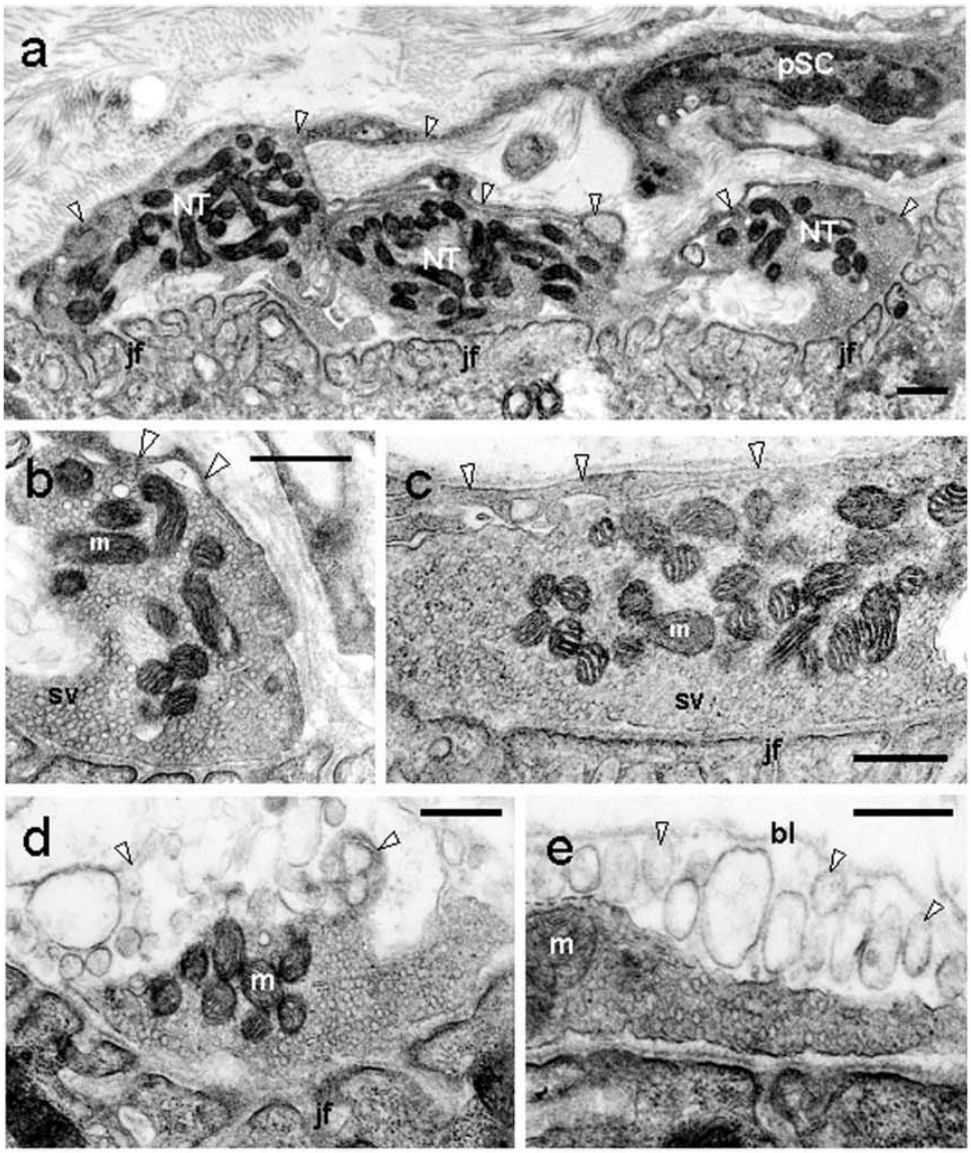

Fig. 3. Ultrastructural characterization of NMJ injury. **a–c:** Control NMJ profiles exposed to Ringer alone appear normal. Nerve terminal (NT) mitochondria (m) are electron-dense with well-defined internal structure. Synaptic vesicles (sv) are abundant, especially in active zones opposed to postsynaptic junctional folds (jf). pSCs extend thin processes (arrowheads) over the surface of the NT, but rarely separate the NT from jf. **d,e:** Group S mAbs injure the pSC only, with pSC processes overlying normal NTs being reduced to a disorganized cluster of spherical bodies (arrowheads, d,e) lying beneath the basal lamina (bl, e). Scale bar 500 nm.

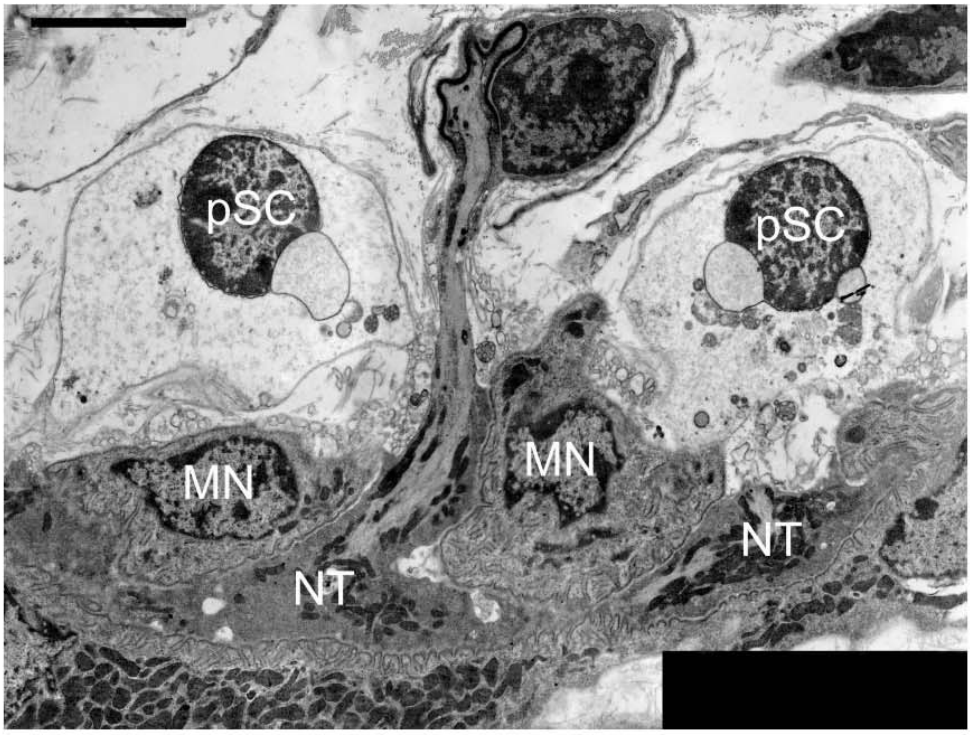

Fig. 4. Ultrastructural characterization of pSC injury induced by Group S mAb, EG-1. Low-magnification electron micrograph illustrating a motor axon wrapped by a myelinating Schwann cell forming nerve terminals (NT) that form synaptic contact with a muscle fiber. The nerve terminals (NT) have a normal morphology, with electron-dense mitochondria and tightly packed synaptic vesicles. Two pSCs sitting either side of the terminal axon appear severely damaged with swollen and electron-lucent cytoplasm, damaged organelles, nuclear membrane blebbing, and perinuclear bodies (arrowheads), all indicative of necrotic cell death. Two myonuclei (MN) beneath the postsynaptic membrane projecting into this plane of section are of normal appearance. Scale bar 5μm.

$\rho = 0.72$, $P < 0.01$). Exposure of NMJs to LTx did not induce pSC injury, assessed either by EthD-1 uptake or by EM (Fig. 2c, 6a last column, LTx).

Characteristics of Motor Nerve Terminal Injury

At the normal NMJ, the neurofilament component of the cytoskeleton extends from the axon over the postsynaptic region to form a branched terminal arborization as visualized with immunofluorescence methods (Fig. 1c). We have previously shown that following exposure to the anti-disialosyl mAb CGM3, a reduction in the NF signal as measured by quantitative immunofluorescence microscopy (Group SN mAb; Fig. 1d) is associated with a profound nerve terminal injury as assessed by EM conducted in parallel (Group SN mAb; Fig. 5). With Group S mAbs, there was no change in NF levels compared with Ringer controls (497 NMJs from six preparations). In contrast, Groups SN and N mAbs produced a significant loss of NF signal over the nerve terminal (Fig. 2b; 990 and 825 NMJs from eight and nine preparations, respectively).

Ultrastructural parameters designed to assess NMJ injury were measured at NMJs exposed to all 10 disialosyl mAbs and NHS (Fig. 6a–d). In comparison with control tissue, mAbs that damaged the nerve terminal (Groups N and SN), as well as LTx, produced swollen and electron-lucent terminals with depletion of synaptic vesicles at active zones. Mitochondria with degenerating internal structures were frequent, often touching the presynaptic membrane. For Group N mAbs and LTx-treated tissue in which pSC viability was unaffected, the damaged nerve terminal was often encircled, either

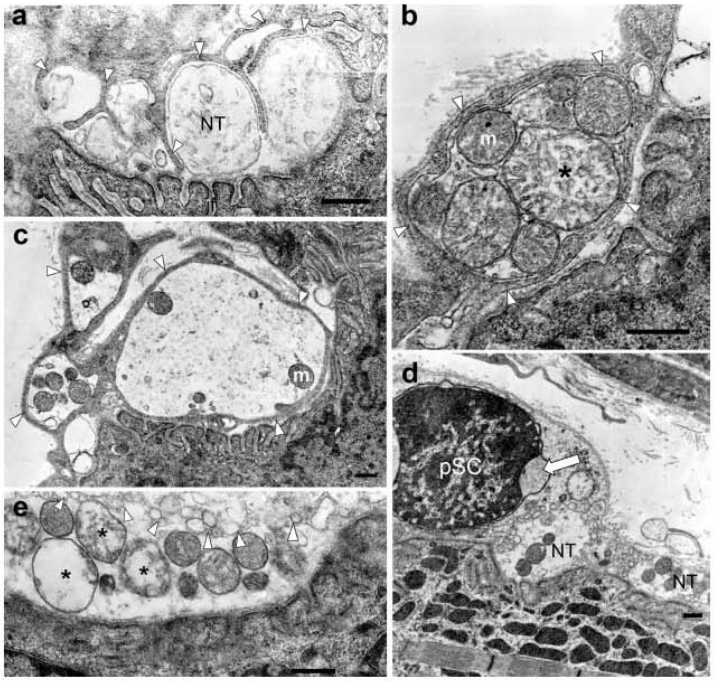

Fig. 5. Ultrastructural characterization of nerve terminal (NT) injury induced by Group N mAbs (a c) and combined pSC and NT injury by Group SN mAbs (d e). **a–c:** The NT is electron-lucent and depleted of synaptic vesicles. Mitochondria (m) are swollen with internal structure degeneration (*). Healthy pSC processes (arrowheads) envelop the terminal profiles, extending into the synaptic cleft between the NT and corresponding postsynaptic junctional folds, forming "full wraps" where there is complete separation (b and c). pSC processes infiltrate the NT, fragmenting it into smaller profiles (a). **d–e:** Group SN mAbs injure both the pSC and NT. The pSC nuclei are swollen and dispersed, with perinuclear bodies (arrow, d). Overlying the damaged NTs, pSC processes are disrupted with circular figures (e). NTs are electron-lucent with reduced numbers of synaptic vesicles and degenerating mitochondria (*). Scale bar 500 nm.

partly or fully ("full wrap") by pSC processes intruding into the synaptic cleft or inserting through the terminal itself (Fig. 5a–c). At NMJs exposed to Group SN mAbs, nerve terminal damage was accompanied by pSC damage, as described above (Fig. 5d,e). As a proportion of affected NMJs exposed to Group SN mAbs were undergoing concurrent pSC injury, the incidence of "full-wraps" formed around nerve terminal profiles by reactive pSC processes were less frequent than with Group N mAbs (Fig. 6b).

Physiological Function at NMJs With Injured Motor Nerve Terminals and Perisynaptic Schwann Cells

Four representative mAbs (Group S, EG1; Group SN, CGM3; Group N, EM2, EM6) were analyzed for acute electrophysiological effects at NMJs. Group SN and N mAb exposure to NMJs induced clear LTx-like effects as previously reported (Fig. 7a,b). Thus, MEPP frequency dramatically increased for ~20–45 min; thereafter, no MEPPs were observed and stimulation of the phrenic nerve did not result in the generation of an EPP (data not shown). These effects did not appear at NMJs pre-incubated with the Group S mAb.

To test for acute effects of pSC injury/ablation, EPPs resulting from 0.3- and 40-Hz nerve stimulation were recorded during NHS incubation in muscle preparations that had been pre-incubated with the Group S mAb. Compared with the Ringer control, (i.e., recorded during NHS incubation without mAb pre-incubation), there were no changes in EPP amplitude and quantal content at 0.3-Hz stimulation, nor in the physiological rundown of EPP amplitude during high-rate (40-Hz) nerve stimulation (Fig. 7c–e). No changes were observed in MEPP frequency, amplitude, or kinetics. These data show that pSC loss has no acute effects on pre- and postsynaptic function at the NMJ.

Susceptibility to perisynaptic Schwann cell injury in different mouse strains In previous studies with young NIH(s) mice (O'Hanlon et al., 2001, 2002), we frequently observed abundant pSC process formation at NMJs exposed to CGM3 mAb. However, a more recent study (Halstead et al., 2004) and the current study with Balb/c mice indicated that CGM3 is a Group SN mAb, causing both pSC death and neuronal injury. Therefore, pSC process formation would be expected to be minor, owing to the competing effects of extensive pSC death. To address this apparent discrepancy, we compared NIH(s), Balb/c, C57BL/6j, and mixed-background C57BL/6 ×

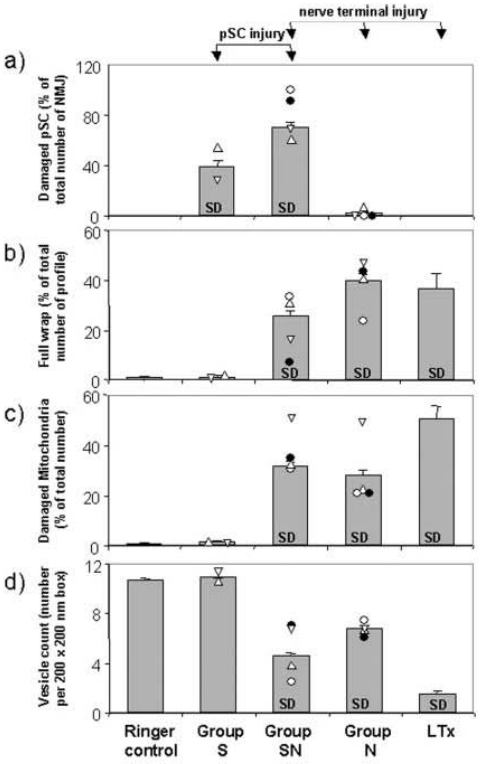

Fig. 6. Quantitative analysis of four key ultrastructural features at injured NMJs, i.e., damaged pSCs, "full wraps" (complete enclosure by pSC processes of nerve terminal fragments with separation from the postsynaptic membrane), damaged mitochondria, and vesicle counts. Ringer-treated samples are negative controls; LTx-treated tissue is a positive control for nerve terminal (NT) injury. **a:** Damaged pSCs were limited to Groups S, SN mAbs. **b:** "Full wraps" were confined to LTx and Group N and SN mAbs. For Group SN mAbs, pSC process formation was slightly muted, owing to concomitant pSC injury. Mitochondrial damage (**c**) and reduced synaptic vesicle counts (**d**) were sensitive markers of LTx and Group SN and N mAbs. Data are mean values ± SEM. The values obtained for individual mAbs within each group are marked as follows. Group S: EG1 (▽); R24 (△); Group SN: CGM1 (●); CGM2 (▽); CGM3 (△); EM1 (○); Group N: EM2 (●); EM3 (▽); EM6 (△); EG2 (○).

129/Sv and C57BL/6 × CBA mice for pSC and nerve terminal effects using the Group SN mAb CGM3. Surprisingly, but nevertheless consistent with previous observations, pSC injury was almost absent in NIH(s) mice but present at typically high levels in other strains tested (Fig. 8). This was not an age-related effect as both young (4–6 weeks, age matched to previous studies) and older (11–13 weeks) mice were similarly resistant.

In addition, we tested Group S mAbs (EG1, R24) and confirmed that the NIH(s) strain resistance to pSC injury by anti-disialosyl antibodies was a general phenomenon (data not shown). We also examined a Group N mAb (EG2) that also had no effect on pSC viability in NIH(s) mice, indicating that a switch in vulnerability had not occurred. Thus NIH(s) mice are resistant to the pSC killing effects of Group S and SN mAbs, and their pSCs remain resistant to Group N mAbs.

Correlation Between mAb Specificity and Injury

We analyzed the data for correlations between the severity of injury to neuronal and glial components of the NMJ and reactivity to the three structurally related disialosyl gangliosides, GD3, GT1a, and GQ1b using the Spearman's rank correlation test (Fig. 9). The strongest correlation was seen between vesicle count and GT1a reactivity (one-tailed test, 1% level of significance; Fig. 9a). GT1a also had a weaker but significant correlation with damaged mitochondria and the presence of "full wraps" of pSC membranes (5% level of significance), but did not reach significance for NF loss. Thus GT1a reactivity was associated with neuronal injury and pSC survival and activation. Both GD3 and GQ1b demonstrated a weak negative correlation (5% level of significance) with vesicle count. GD3 reactivity was also weakly correlated with the presence of damaged mitochondria and GQ1b reactivity was weakly correlated with presence of "full wraps" of pSC membranes around the pre-synaptic nerve terminal (5% level of significance). There was no significant correlation between pSC injury as assessed by EthD-1 uptake and binding reactivities of any individual ganglioside, however, when antibodies were expressed as half-maximal binding ratios of GD3/GT1a or GD3/GQ1b reactivities, there was a positive correlation with pSC injury (1% and 5% level of significance, respectively). This indicates that pSC injury was relatively associated with GD3 reactivity.

DISCUSSION

We have previously shown through morphological and electrophysiological monitoring that the anti-disialosyl ganglioside mAb, CGM3, produces a profound lesion at the mouse NMJ, injuring both the nerve terminal (O'Hanlon et al., 2001, 2002, 2003) and pSC (Halstead et al., 2004). In this study, we have been able to segregate this lesion into its pre-synaptic nerve terminal and pSC components, using anti-disialosyl mAbs that differ in their precise specificity for disialylated gangliosides. As shown in Table 1, the anti-disialosyl antibodies we have cloned bind to disialylated gangliosides including GD3, GT1a, and GQ1b with varying reactivities, thereby allowing them to preferentially target particular ganglioside-containing membranes (Andersen et al., 2004; Boffey et al., 2004; Willison et al., 2004).

The explanation for the difference in vulnerability of pSC and neuronal membranes to anti-disialosyl antibody mediated injury remains unknown, although presumably

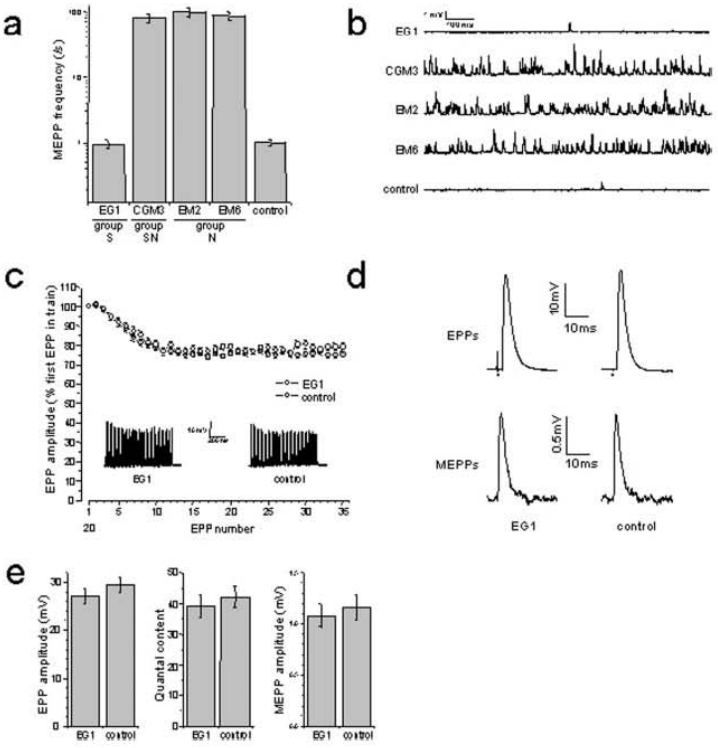

Fig. 7. Electrophysiological analysis of anti-disialosyl mAb effects on NMJ synaptic function in vitro. Balb/c mouse hemidiaphragms were pre-incubated with mAbs; thereafter, normal human serum (1:2) was added as a source of complement. For a period of 1 h, electrophysiological recordings were made at 7 19 neuromuscular junctions (NMJs) per preparation. mAbs had been pre-assigned to Groups S (pSC only), N (nerve terminal only), and SN (pSC and nerve terminal) based on prior morphological studies. **a,b:** Group N and SN mAbs readily induced LTx-like effects, i.e., a dramatic increase in miniature endplate potential (MEPP) frequency followed by block of evoked ACh release (Goodyear et al., 1999), measured as endplate potentials (EPPs). NMJs that were incubated with Group S mAbs lacked LTx-like effects in that spontaneous quantal ACh release rate was not different from that observed in the Ringer control. **c–e:** Further analysis of the effects of the Group S mAbs EG1 on evoked ACh release at either 40-Hz (c) or 0.3-Hz (d,e) nerve stimulation and on spontaneous MEPPs (d) showed no differences from control. These data show that selective pSC ablation does not have acute effects on mouse NMJ function. Data in a, c, and e are mean values ± SEM of 16 35 NMJs sampled in two preparations per mAb. Traces in b and d are representative examples of the electrophysiological recordings. Black dot indicates the moment of nerve stimulation.

reflects underlying differences in the ganglioside composition. We anticipated finding a correlation between the neuronal or glial injury and antibody specificities for different disialosyl-bearing gangliosides. GQ1b, GT1a, and GD3 all possess the terminal NeuNAc(α2–8)NeuNAc(α2–8)Gal disialylgalactose epitope. Our data tentatively suggests a relationship between preferential anti-GD3 reactivity and pSC injury, and conversely, preferential anti-GT1a/GQ1b reactivity and neuronal injury. However these divisions are not absolutely defined as each antibody does not sit perfectly in its respective S, SN, or N group when half-maximal binding values to the different gangliosides are considered. Presumably, there are unidentified confounding factors that distinguish the ganglioside binding behavior of an antibody in a solid-phase ELISA in comparison with its binding behavior in an ordered glial or neuronal membrane. Further work is needed to understand the biophysical basis for these findings. Despite the above caveats, these data suggest that motor neurons innervating the mouse diaphragm express more complex gangliosides (including GT1a and GQ1b) at their terminals than are expressed by pSCs. The regulatory steps in ganglioside biosynthesis that may underlie this have not been explored. We have presented the NMJ injury as segregating into three categories (S, N, and SN). It is very likely that, in some cases, these classifications could form part of a continuous spectrum, based on the interacting combination of antibody specificity and membrane ganglioside profile. By increasing antibody concentration, or exposure times it may be possible to broaden an antibody-induced pSC injury to include the nerve terminal, or vice versa. Indeed, we have observed antibody concentration-dependent variations that affect the degree of glial or neuronal membrane targeting. Another possibility is that alternative gangliosides or nonganglioside, disialylated antigens are targets. However in our previous studies, we have shown that GalNAcT$^{-/-}$ mice (containing GM3 and GD3 only) are vulnerable to anti-disialosyl antibodies that bind GD3 and resistant to those that bind GQ1b, whereas GalNAcT$^{-/-}$ × GD3s$^{-/-}$ double knock-out mice (containing GM3 only) are completely resistant to any anti-disialosyl antibody effects. This indicates it is very likely that disialylated gangliosides are the target antigens.

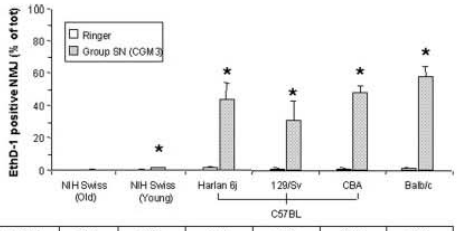

Ringer NMJ	2675	2834	2411	1982	2378	2266
CGM3 NMJ	2994	3355	2214	2134	2224	2755

Fig. 8. Inter-strain comparison of pSC susceptibility to Group SN mAB mediated injury. Diaphragms from Harlan C57BL/6j, 129/Sv, and CBA (both crossed onto the C57Bl background); NIH Swiss old and young and Balb/c mice strains were exposed in vitro to the Group SN mAb, CGM3, with NHS as a source of complement. pSC injury was assessed by nuclear uptake of EthD-1, expressed as percentage of NMJs affected. pSC injury is virtually absent in young and old NIH Swiss mice, compared with all other strains tested. Figures are mean ± SEM from three separate staining runs repeated in three different preparations. *Significantly different from corresponding Ringer control; Chi squared-test, $P < 0.01$. Boxed numbers indicate the total number of NMJs assessed per experimental condition.

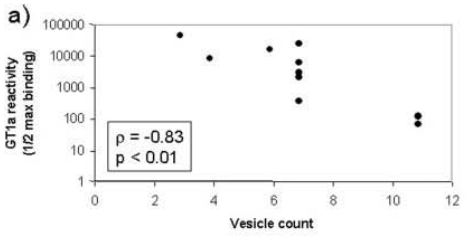

b)

ρ value	EthD-1	Full wrap	Damaged Mito.	NF	Vesicle count
GD3	0.33	0.19	0.61	-0.35	0.64
GT1a	-0.31	0.76	0.59	-0.52	-0.83
GQ1b	-0.13	0.62	0.21	-0.24	0.76
GD3/GT1a	0.84	-0.45	0.05	0.1	-0.12
GD3/GQ1b	0.64	-0.56	0.38	-0.07	0.12

Fig. 9. Correlation between the levels of injury to nerve terminals (damaged mitochondria, neurofilament loss, vesicle counts) or pSCs (EthD-1-positive nuclei) or the presence of "full wraps" and the reactivity of anti-disialosyl mAbs to three structurally related gangliosides, GD3, GT1a, and GQ1b (see Table 1), using Spearman's rank test. **a:** mAb reactivity with GT1a is negatively correlated with vesicle depletion, indicating that nerve terminal injury correlates with GT1a reactivity. **b:** Spearman's rank correlation coefficient, ρ, for comparisons between ganglioside reactivity and five markers of injury. As above, vesicle count and GT1a reactivity strongly correlated ($P < 0.01$). Weaker but significant correlation was also observed between vesicle counts and GD3 or GQ1b reactivity ($P < 0.05$). No correlations were noted between pSC injury and binding to any individual gangliosides tested; however, when mAb ganglioside binding reactivity was expressed ratiometrically, a high GD3:GT1a binding ratio correlated positively with pSC injury. Hatched box, significant at 5% level; shaded box, significant at 1% level.

A curious finding is that of the strains studied here, NIH(s) mice are refractory to anti-disialosyl antibody-mediated pSC injury in this model. This observation explains why anti-disialosyl antibody-mediated pSC injury was not seen in our earlier studies conducted in NIH(s) mice (O'Hanlon et al., 2001), but it is evident in recent studies using Balb/c and C57Bl/6 mice (Halstead et al., 2004). Our preliminary indications are that immunoglobulin deposits over pSCs are lower in NIH(s) mice than in Balb/c mice, suggesting that differences in ganglioside quantity or display underlies these findings, rather than relative resistance of NIH(s) pSCs to complement-mediated injury. It is well recognized that the local microenvironment can have a major effect on ganglioside–antibody interaction (Lloyd et al., 1992; Kremer et al., 1997; Tatewaki et al., 1997), particularly for short core gangliosides such as GD3. Any ganglioside defect in NIH(s) pSCs seems not to affect neuronal gangliosides, as motor nerve terminal vulnerability to anti-disialosyl antibodies was maintained.

Based on pharmacological and Ca^{2+}-imaging studies at frog NMJs, the pSC is believed to play a key role in supporting the underlying nerve terminal and in short-term and long-term modulation of synaptic transmission (Castonguay et al., 2001; Rochon et al., 2001; Auld and Robitaille, 2003b; Colomar and Robitaille, 2004). Surprisingly, in recent immune-mediated pSC ablation studies in the in vivo frog no immediate electrophysiological effects were observed upon pSC loss (Reddy et al., 2003). However, after 1 week, nerve terminal retraction occurs and is accompanied by failure of pre-synaptic function, manifest by a decrease in nerve evoked twitch tension (Reddy et al., 2003). Our present observation that synaptic physiology is unaffected at mouse NMJs acutely ablated of pSCs confirms the observation in the frog. A caveat of our findings is that pSC ablation was not complete at all endplates, and thus any surviving pSCs may be able to provide a sufficient level of support to prevent any acute effects on underlying synaptic function. There is also a range of pSC injury, presumably dependent on variations in the duration of exposure to complement products, in turn dependent on the rate of passive diffusion through the experimental tissues. We are currently performing longer-term passive immunization of mice with pSC-specific anti-disialosyl mAbs to investigate any chronic effects of murine pSC ablation on motor nerve terminal function and integrity.

Conversely, motor nerve terminal damage could influence pSC integrity or function. However, this is excluded by our studies, as pSC viability was not affected at NMJs that displayed severe motor nerve terminal injury resulting from treatment with LTx or Group N mAbs and complement. Indeed the formation of "full wraps" of pSC processes around fragmented nerve terminals within 1 h suggests both a high viability and short response time of pSCs to the underlying nerve terminal injury. The frequency of these profiles in the injured tissue, and their absence in normal control tissue indicates that they have arisen acutely, as previously observed (Halstead et al., 2004).

Although the NMJ is targeted in other antibody mediated autoimmune diseases and toxinopathies (Lennon et al., 1995; McConville and Vincent, 2002; Marvaud et al., 2002; Lang and Vincent, 2003), pSCs have never been identified as specific targets in human disease. However, the observation that pSCs can be killed selectively by certain anti-ganglioside mAbs, especially those directed at GD3, suggests that pSC injury may be involved in distal nerve failure seen in some cases of MFS and GBS (Ho et al., 1997; Uncini and Lugaresi, 1999; Wirguin et al., 2002; Spaans et al., 2003), and possibly in other neuropathic disorders as well. The mAbs characterized in the present study provide interesting tools for the investigation of the relationship between mammalian pSCs and the underlying nerve terminal in healthy and diseased states.

ACKNOWLEDGMENTS

The authors are grateful to Dr. Yuri Ushkaryov for generous provision of alpha latrotoxin. This work was supported by grants from the Wellcome Trust (to S.K.H., G.M.O.H., P.D.H., and H.J.W.), Guillain-Barré syndrome Support Group UK (to J.A.G. and H.J.W.), KNAW (Koninklijke Nederlandse Akademie van Wetenschappen) Van Leersumfonds (to J.J.P.), Prinses Beatrix Fonds grant MAR04-0213 (to J.J.P.).

REFERENCES

Andersen SM, Ling CC, Zhang P, Townson K, Willison HJ, Bundle DR. 2004. Synthesis of ganglioside epitopes for oligosaccharide specific immunoadsorption therapy of Guillian-Barré syndrome. Org Biomol Chem 2:1199–1212.

Ashton AC, Rahman MA, Volynski KE, Manser C, Orlova EV, Matsushita H, Davletov BA, van Heel M, Grishin EV, Ushkaryov YA. 2000. Tetramerisation of alpha-latrotoxin by divalent cations is responsible for toxin-induced non-vesicular release and contributes to the Ca^{2+}-dependent vesicular exocytosis from synaptosomes. Biochimie 82:453–468.

Auld DS, Robitaille R. 2003a. Glial cells and neurotransmission: an inclusive view of synaptic function. Neuron 40:389–400.

Auld DS, Robitaille R. 2003b. Perisynaptic Schwann cells at the neuromuscular junction: nerve- and activity-dependent contributions to synaptic efficacy, plasticity, and reinnervation. Neuroscientist 9:144–157.

Boffey J, Nicholl D, Wagner ER, Townson K, Goodyear C, Furukawa K, Furukawa K, Conner J, Willison HJ. 2004. Innate murine B cells produce anti-disialosyl antibodies reactive with *Campylobacter jejuni* LPS and gangliosides that are polyreactive and encoded by a restricted set of unmutated V genes. J Neuroimmunol 152:98–111.

Bullens RWM, O'Hanlon GM, Goodyear CS, Molenaar P, Conner J, Willison HJ, Plomp JJ. 2000. Anti-GQ1b antibodies and evoked acetylcholine release at mouse motor endplates. Muscle Nerve 23:1035–1043.

Bullens RWM, O'Hanlon GM, Wagner E, Molenaar PC, Furukawa K, Plomp JJ, Willison HJ. 2002. Complex gangliosides at the neuromuscular junction are membrane receptors for autoantibodies and botulinum neurotoxin but redundant for normal synaptic function. J Neurosci 22:6876–6884.

Castonguay A, Levesque S, Robitaille R. 2001. Glial cells as active partners in synaptic functions. Prog Brain Res 132:227–240.

Chapman PB, Yuasa H, Houghton AN. 1990. Homophilic binding of mouse monoclonal antibodies against GD3 ganglioside. J Immunol 145:891–898.

Chiba A, Kusunoki S, Shimizu T, Kanazawa I. 1992. Serum IgG antibody to ganglioside GQ1b is a possible marker of Miller Fisher syndrome. Ann Neurol 31:677–679.

Colomar A, Robitaille R. 2004. Glial modulation of synaptic transmission at the neuromuscular junction. Glia 47:284–289.

Dippold WG, Lloyd KO, Li LT, Ikeda H, Oettgen HF, Old LJ. 1980. Cell surface antigens of human malignant melanoma: definition of six antigenic systems with mouse monoclonal antibodies. Proc Natl Acad Sci USA 77:6114–6118.

Duchen LW, Gomez S, Queiroz LS. 1981. The neuromuscular junction of the mouse after black widow spider venom. J Physiol (Lond) 316: 279–291.

Goodyear CS, O'Hanlon GM, Plomp JJ, Wagner ER, Morrison I, Veitch J, Cochrane L, Bullens RWM, Molenaar PC, Conner J, Willison HJ. 1999. Monoclonal antibodies raised against Guillain Barré syndrome-associated *Campylobacter jejuni* lipopolysaccharides react with neuronal gangliosides and paralyse nerve muscle preparations. J Clin Invest 104:697–708.

Halstead SK, O'Hanlon GM, Humphreys PD, Morrison DB, Morgan BP, Todd AJ, Plomp JJ, Willison HJ. 2004. Anti-disialoside antibodies kill perisynaptic Schwann cells and damage motor nerve terminals via membrane attack complex in a murine model of neuropathy. Brain 127:2109–2123.

Ho TW, Hsieh S-T, Nachamkin I, Willison HJ, Sheikh K, Kiehlbauch J, Flanigan K, McArthur JC, Cornblath DR, McKhann GM, Griffin JW. 1997. Motor nerve terminal degeneration provides a potential mechanism for rapid recovery in acute motor axonal neuropathy after *Campylobacter infection*. Neurology 48:717–724.

Holt DS, Botto M, Bygrave AE, Hanna SM, Walport MJ, Morgan BP. 2001. Targeted deletion of the CD59 gene causes spontaneous intravascular hemolysis and hemoglobinuria. Blood 98:442–449.

Jacobs BC, Bullens RW, O'Hanlon GM, Ang CW, Willison HJ, Plomp JJ. 2002. Detection and prevalence of alpha-latrotoxin-like effects of serum from patients with Guillain-Barré syndrome. Muscle Nerve 25:549–558.

Koga M, Yoshino H, Morimatsu M, Yuki N. 2002. Anti-GT1a IgG in Guillain-Barre syndrome. J Neurol Neurosurg Psychiatry 72:767–771.

Kremer DM, Lopez PHH, Mizutamari RK, Kremer LJ, Bacile EA, Nores GA. 1997. Factors defining target specificity in antibody-mediated neuropathy: density-dependent binding of anti-GD1a polyclonal IgG from a neurological patient. J Neurosci Res 47:636–641.

Lang B, Vincent A. 2003. Autoantibodies to ion channels at the neuromuscular junction. Autoimmun Rev 2:94–100.

Lennon VA, Kryzer TJ, Griesmann GE, O'Suilleabhain PE, Windebank AJ, Woppmann A, Miljanich GP, Lambert EH. 1995. Calcium-channel antibodies in the Lambert-Eaton syndrome and other paraneoplastic syndromes. N Engl J Med 332:1467–1474.

Lloyd KO, Gordon CM, Thampoe IJ, DiBenedetto C. 1992. Cell surface accessibility of individual gangliosides in malignant melanoma cells to antibodies is influenced by the total ganglioside composition of the cells. Cancer Res 52:4948–4953.

Marvaud JC, Raffestin S, Popoff MR. 2002. Botulism: the agent, mode of action of the botulinum neurotoxins, forms of acquisition, treatment and prevention. C R Biol 325:863–878.

McConville J, Vincent A. 2002. Diseases of the neuromuscular junction. Curr Opin Pharmacol 2:296–301.

O'Hanlon GM, Plomp JJ, Chakrabarti M, Morrison I, Wagner ER, Goodyear CS, Yin X, Trapp BD, Conner J, Molenaar PC, Stewart S, Rowan EG, Willison HJ. 2001. Anti-GQ1b ganglioside antibodies mediate complement-dependent destruction of the motor nerve terminal. Brain 124:893–906.

O'Hanlon GM, Bullens RW, Plomp JJ, Willison HJ. 2002. Complex gangliosides as autoantibody targets at the neuromuscular junction in Miller Fisher syndrome: a current perspective. Neurochem Res 27: 697–709.

O'Hanlon GM, Humphreys PD, Goldman RS, Halstead SK, Bullens RW, Plomp JJ, Ushkaryov Y, Willison HJ. 2003. Calpain inhibitors protect against axonal degeneration in a model of anti-ganglioside antibody-mediated motor nerve terminal injury. Brain 126:1–13.

O'Leary CP, Veitch J, Durward WF, Thomas AM, Rees JH, Willison HJ. 1996. Acute oropharyngeal palsy is associated with antibodies to GQ1b and GT1a gangliosides. J Neurol Neurosurg Psychiatry 61: 649–651.

Plomp JJ, Molenaar PC, O'Hanlon GM, Jacobs BC, Veitch J, Daha MR, van Doorn PA, van der Meché FGA, Vincent A, Morgan BP, Willison HJ. 1999. Miller Fisher anti-GQ1b antibodies: a-latrotoxin-like effects on motor end plates. Ann Neurol 45:189–199.

Reddy LV, Koirala S, Sugiura Y, Herrera AA, Ko C-P. 2003. Glial cells maintain synaptic structure and function and promote development of the neuromuscular junction in vivo. Neuron 40:563–580.

Roberts M, Willison H, Vincent A, Newsom-Davis J. 1994. Serum factor in Miller-Fisher variant of Guillain-Barre syndrome and neurotransmitter release. Lancet 343:454–455.

Rochon D, Rousse I, Robitaille R. 2001. Synapse–glia interactions at the mammalian neuromuscular junction. J Neurosci 21:3819–3829.

Spaans F, Vredeveld JW, Morre HH, Jacobs BC, De Baets MH. 2003. Dysfunction at the motor end-plate and axon membrane in Guillain-Barre syndrome: a single-fiber EMG study. Muscle Nerve 27:426–434.

Susuki K, Yuki N, Hirata K. 2001. Fine specificity of anti-GQ1b IgG and clinical features. J Neurol Sci 185:5–9.

Takamiya K, Yamamoto A, Furukawa K, Yamashiro S, Shin M, Okada M, Fukumoto S, Haraguchi M, Takeda N, Fujimura K, Sakae M, Kishikawa M, Shiku H, Furukawa K, Aizawa S. 1996. Mice with disrupted GM2/GD2 synthase gene lack complex gangliosides but exhibit only subtle defects in their nervous system. Proc Natl Acad Sci USA 93:10662–10667.

Tatewaki K, Yamaki T, Maeda Y, Tobioka H, Piao H, Yu H, Ibayashi Y, Sawada N, Hashi K. 1997. Cell density regulates crypticity of GM3 ganglioside on human glioma cells. Exp Cell Res 233:145–154.

Uncini A, Lugaresi A. 1999. Fisher syndrome with tetraparesis and antibody to GQ1b: evidence for motor nerve terminal block. Muscle Nerve 22:640–644.

Willison HJ, O'Hanlon GM. 1999. The immunopathogenesis of Miller Fisher syndrome. J Neuroimmunol 100:3–12.

Willison HJ, O'Hanlon GM, Paterson G, Veitch J, Wilson G, Roberts M, Tang T, Vincent A. 1996. A somatically mutated human antiganglioside IgM antibody that induces experimental neuropathy in mice is encoded by the variable region heavy chain gene, V1–18. J Clin Invest 97:1155–1164.

Willison HJ, Townson K, Veitch J, Boffey J, Isaacs N, Andersen SM, Zhang P, Ling CC, Bundle DR. 2004. Synthetic disialylgalactose immunoadsorbents deplete anti-GQ1b antibodies from autoimmune neuropathy sera. Brain 127:680–691.

Willison HJ, Yuki N. 2002. Peripheral neuropathies and anti-glycolipid antibodies. Brain 125:1–35.

Wirguin I, Ifergane G, Almog Y, Lieberman D, Bersudsky M, Herishanu YO. 2002. Presynaptic neuromuscular transmission block in Guillain-Barre syndrome associated with anti-GQ1b antibodies. Neuromuscul Disord 12:292–293.

References

Aguayo,A.J., Charron,L., and Bray,G.M. 1976. Potential of Schwann cells from unmyelinated nerves to produce myelin: a quantitative ultrastructural and radiographic study. *J.Neurocytol.* 5:565-573.

Al Shekhlee,A., Hachwi,R.N., Preston,D.C., and Katirji,B. 2005. New criteria for early electrodiagnosis of acute inflammatory demyelinating polyneuropathy. *Muscle Nerve* 32:66-72.

Albers,J.W., Donofrio,P.D., and Mcgonagle,T.K. 1985. Sequential Electrodiagnostic Abnormalities in Acute Inflammatory Demyelinating Polyradiculoneuropathy. *Muscle & Nerve* 8:528-539.

Ando,S., Tanaka,Y., Waki,H., Kon,K., Iwamoto,M., and Fukui,F. 1998. Gangliosides and sialylcholesterol as modulators of synaptic functions. *Ann.N.Y.Acad.Sci.* 845:232-239.

Ang,C.W., Jacobs,B.C., and Laman,J.D. 2004. The Guillain-Barré syndrome: a true case of molecular mimicry. *Trends Immunol.* 25:61-66.

Arányi,Z., Szabo,G., Szepesi,B., and Folyovich,A. 2006. Proximal conduction abnormality of the facial nerve in Miller Fisher syndrome: a study using transcranial magnetic stimulation. *Clin.Neurophysiol.* 117:821-827.

Araque,A., Parpura,V., Sanzgiri,R.P., and Haydon,P.G. 1999. Tripartite synapses: glia, the unacknowledged partner. [Review] [61 refs]. *Trends in Neurosciences.* 22:208-215.

Arevalo,J.C. and Wu,S.H. 2006. Neurotrophin signaling: many exciting surprises! *Cell Mol.Life Sci.* 63:1523-1537.

Asbury,A.K., Arnason,B.G., and Adams,R.D. 1969. The inflammatory lesion in idiopathic polyneuritis. Its role in pathogenesis. *Medicine (Baltimore)* 48:173-215.

Asbury,A.K. and Cornblath,D.R. 1990. Assessment of current diagnostic criteria for Guillain-Barré syndrome. *Ann.Neurol.* 27 Suppl:S21-S24.

Astrow,S.H., Son,Y.J., and Thompson,W.J. 1994. Differential neural regulation of a neuromuscular junction-associated antigen in muscle fibers and Schwann cells. *J.Neurobiol.* 25:937-952.

Auld,D.S. and Robitaille,R. 2003a. Perisynaptic Schwann cells at the neuromuscular junction: nerve- and activity-dependent contributions to synaptic efficacy, plasticity, and reinnervation. *Neuroscientist.* 9:144-157.

Auld,D.S. and Robitaille,R. 2003b. Glial cells and neurotransmission: an inclusive view of synaptic function. *Neuron* 40:389-400.

Balice-Gordon,R.J. and Lichtman,J.W. 1990. In vivo visualization of the growth of pre- and postsynaptic elements of neuromuscular junctions in the mouse. *J.Neurosci.* 10:894-908.

Balice-Gordon,R.J. and Lichtman,J.W. 1994. Long-term synapse loss induced by focal blockade of postsynaptic receptors. *Nature* 372:519-524.

Bartus,R.T., Elliott,P.J., Hayward,N.J., Dean,R.L., Harbeson,S., Straub,J.A., Li,Z., and Powers,J.C. 1995. Calpain as a novel target for treating acute neurodegenerative disorders. *Neurol.Res.* 17:249-258.

Bhakdi,S. and Tranum-Jensen,J. 1991. Complement lysis: a hole is a hole. *Immunol.Today* 12:318-320.

Birks,R., Huxley,H.E., and Katz,B. 1960. The fine structure of the neuromuscular junction of the frog. *J.Physiol* 150:134-144.

Bixby,J.L., Lilien,J., and Reichardt,L.F. 1988. Identification of the major proteins that promote neuronal process outgrowth on Schwann cells in vitro. *J.Cell Biol.* 107:353-361.

Boffey,J., Nicholl,D., Wagner,E.R., Townson,K., Goodyear,C., Furukawa,K., Furukawa,K., Conner,J., and Willison,H.J. 2004. Innate murine B cells produce anti-disialosyl antibodies reactive with Campylobacter jejuni LPS and gangliosides that are polyreactive and encoded by a restricted set of unmutated V genes. *J.Neuroimmunol.* 152:98-111.

Boffey,J., Odaka,M., Nicoll,D., Wagner,E.R., Townson,K., Bowes,T., Conner,J., Furukawa,K., and Willison,H.J. 2005. Characterisation of the immunoglobulin variable region gene usage encoding the murine anti-ganglioside antibody repertoire. *J.Neuroimmunol.* 165:92-103.

Bordet, J. 1898. Sur l'agglutination et la dissolution des globules rouges par le serum d'animaux injectes de sang defibrine. Ann. De l'Inst. Pasteur. xii: 688-695.

Boudier,J.L., Jover,E., and Cau,P. 1988. Autoradiographic localization of voltage-dependent sodium channels on the mouse neuromuscular junction using 125I-alpha scorpion toxin. I. Preferential labeling of glial cells on the presynaptic side. *J.Neurosci.* 8:1469-1478.

Bowes,T., Wagner,E.R., Boffey,J., Nicholl,D., Cochrane,L., Benboubetra,M., Conner,J., Furukawa,K., Furukawa,K., and Willison,H.J. 2002. Tolerance to self gangliosides is the major factor restricting the antibody response to lipopolysaccharide core oligosaccharides in Campylobacter jejuni strains associated with Guillain-Barré syndrome. *Infect.Immun.* 70:5008-5018.

Brodbeck,W.G., Mold,C., Atkinson,J.P., and Medof,M.E. 2000. Cooperation between decay-accelerating factor and membrane cofactor protein in protecting cells from autologous complement attack. *J.Immunol.* 165:3999-4006.

Buchwald,B., Ahangari,R., and Toyka,K.V. 2002. Differential blocking effects of the monoclonal anti-GQ1b IgM antibody and alpha-latrotoxin in the absence of complement at the mouse neuromuscular junction. *Neurosci.Lett.* 334:25-28.

Bullens,R.W., O'Hanlon,G.M., Wagner,E., Molenaar,P.C., Furukawa,K., Furukawa,K., Plomp,J.J., and Willison,H.J. 2002. Complex gangliosides at the neuromuscular junction are membrane receptors for autoantibodies and botulinum neurotoxin but redundant for normal synaptic function. *J.Neurosci.* 22:6876-6884.

Buonanno,A. and Fischbach,G.D. 2001. Neuregulin and ErbB receptor signaling pathways in the nervous system. *Curr.Opin.Neurobiol.* 11:287-296.

Buzby,J.C., Allos,B.M., and Roberts,T. 1997. The economic burden of Campylobacter-associated Guillain-Barré syndrome. *J.Infect.Dis.* 176 Suppl 2:S192-S197.

Cardasis,C.A. and Padykula,H.A. 1981. Ultrastructural evidence indicating reorganization at the neuromuscular junction in the normal rat soleus muscle. *Anat.Rec.* 200:41-59.

Caroni,P. and Grandes,P. 1990. Nerve sprouting in innervated adult skeletal muscle induced by exposure to elevated levels of insulin-like growth factors. *J.Cell Biol.* 110:1307-1317.

Caroni,P. 1997. Overexpression of growth-associated proteins in the neurons of adult transgenic mice. *J.Neurosci.Methods* 71:3-9.

Casali,P. and Schettino,E.W. 1996. Structure and function of natural antibodies. *Curr.Top.Microbiol.Immunol.* 210:167-179.

Castonguay,A. and Robitaille,R. 2001. Differential regulation of transmitter release by presynaptic and glial Ca2+ internal stores at the neuromuscular synapse. *J.Neurosci.* 21:1911-1922.

Chalfie,M., Tu,Y., Euskirchen,G., Ward,W.W., and Prasher,D.C. 1994. Green fluorescent protein as a marker for gene expression. *Science* 263:802-805.

Chamberlain,L.H., Burgoyne,R.D., and Gould,G.W. 2001. SNARE proteins are highly enriched in lipid rafts in PC12 cells: implications for the spatial control of exocytosis. *Proc.Natl.Acad.Sci.U.S.A* 98:5619-5624.

Chan,S.L. and Mattson,M.P. 1999. Caspase and calpain substrates: roles in synaptic plasticity and cell death. *J.Neurosci.Res.* 58:167-190.

Cheng,C. and Zochodne,D.W. 2002. In vivo proliferation, migration and phenotypic changes of Schwann cells in the presence of myelinated fibers. *Neuroscience* 115:321-329.

Chiba,A., Kusunoki,S., Obata,H., Machinami,R., and Kanazawa,I. 1993. Serum anti-GQ1b IgG antibody is associated with ophthalmoplegia in Miller Fisher syndrome and Guillain-Barré syndrome: clinical and immunohistochemical studies. *Neurology* 43:1911-1917.

Chiba,A., Kusunoki,S., Obata,H., Machinami,R., and Kanazawa,I. 1997. Ganglioside composition of the human cranial nerves, with special reference to pathophysiology of Miller Fisher syndrome. *Brain Res.* 745:32-36.

Cole,D.S. and Morgan,B.P. 2003. Beyond lysis: how complement influences cell fate. *Clin.Sci.(Lond)* 104:455-466.

Connor,E.A. and McMahan,U.J. 1987. Cell accumulation in the junctional region of denervated muscle. *J.Cell Biol.* 104:109-120.

Corfas,G., Velardez,M.O., Ko,C.P., Ratner,N., and Peles,E. 2004. Mechanisms and roles of axon-Schwann cell interactions. *J.Neurosci.* 24:9250-9260.

Couteaux,R. 73 A.D. Motor end-plate structure. In The structure and function of muscle. G.H.Bourne, editor. Academic Press, New York. 483-530.

Dalakas,M.C. 2004. The use of intravenous immunoglobulin in the treatment of autoimmune neuromuscular diseases: evidence-based indications and safety profile. *Pharmacol.Ther.* 102:177-193.

Dashiell,S.M., Rus,H., and Koski,C.L. 2000. Terminal complement complexes concomitantly stimulate proliferation and rescue of Schwann cells from apoptosis. *Glia* 30:187-198.

Davies,A., Simmons,D.L., Hale,G., Harrison,R.A., Tighe,H., Lachmann,P.J., and Waldmann,H. 1989. CD59, an LY-6-like protein expressed in human lymphoid cells, regulates the action of the complement membrane attack complex on homologous cells. *J.Exp.Med.* 170:637-654.

Dehaene,I., Martin,J.J., Geens,K., and Cras,P. 1986. Guillain-Barré syndrome with ophthalmoplegia: clinicopathologic study of the central and peripheral nervous systems, including the oculomotor nerves. *Neurology* 36:851-854.

Descarries,L.M., Cai,S., and Robitaille,R. 1998. Localization and characterization of nitric oxide synthase at the frog neuromuscular junction. *J.Neurocytol.* 27:829-840.

Durand,M.C., Goulon-Goeau,C., Schweitzer,A., Cheliout-Heraut,F., Raphael,J.C., and Gajdos,P. 2001. [Electrophysiologic study of 10 cases of Miller Fisher syndrome]. *Rev.Neurol.(Paris)* 157:72-79.

The Dutch Guillain-Barré Study Group 1994. Treatment of Guillain-Barré syndrome with high-dose immune globulins combined with methylprednisolone: a pilot study. *Ann.Neurol.* 35:749-752.

Ehrlich,P. and Morgenroth,J. 1899. Zur theorie der lysinwirkung. *Berlin Klin.Wochenchr.* 36:6-9.

Endtz,H.P., Ang,C.W., Van den,B.N., Duim,B., Rigter,A., Price,L.J., Woodward,D.L., Rodgers,F.G., Johnson,W.M., Wagenaar,J.A. *et al*. 2000. Molecular characterization of Campylobacter jejuni from patients with Guillain-Barré and Miller Fisher syndromes. *J.Clin.Microbiol.* 38:2297-2301.

Esser,A.F. 1991. Big MAC attack: complement proteins cause leaky patches. *Immunol.Today* 12:316-318.

Fagarasan,S. and Honjo,T. 2000. T-Independent immune response: new aspects of B cell biology. *Science* 290:89-92.

Feasby,T.E., Gilbert,J.J., Brown,W.F., Bolton,C.F., Hahn,A.F., Koopman,W.F., and Zochodne,D.W. 1986. An acute axonal form of Guillain-Barré polyneuropathy. *Brain* 109 (Pt 6):1115-1126.

Feng,G., Mellor,R.H., Bernstein,M., Keller-Peck,C., Nguyen,Q.T., Wallace,M., Nerbonne,J.M., Lichtman,J.W., and Sanes,J.R. 2000. Imaging neuronal subsets in transgenic mice expressing multiple spectral variants of GFP. *Neuron* 28:41-51.

Fisher,M. 1956. An unusual variant of acute idiopathic polyneuritis (syndrome of ophthalmoplegia, ataxia and areflexia). *New England Journal of Medicine* 255:57-65.

Fisher,M.A. 1998. The contemporary role of F-wave studies. F-wave studies: clinical utility. *Muscle Nerve* 21:1098-1101.

Fross,R.D. and Daube,J.R. 1987. Neuropathy in the Miller Fisher syndrome: clinical and electrophysiologic findings. *Neurology* 37:1493-1498.

Fujinaga,Y., Wolf,A.A., Rodighiero,C., Wheeler,H., Tsai,B., Allen,L., Jobling,M.G., Rapoport,T., Holmes,R.K., and Lencer,W.I. 2003. Gangliosides that associate with lipid rafts mediate transport of cholera and related toxins from the plasma membrane to endoplasmic reticulm. *Mol.Biol.Cell* 14:4783-4793.

Fujita,T., Inoue,T., Ogawa,K., Iida,K., and Tamura,N. 1987. The mechanism of action of decay-accelerating factor (DAF). DAF inhibits the assembly of C3 convertases by dissociating C2a and Bb. *J.Exp.Med.* 166:1221-1228.

Furuse,H., Waki,H., Kaneko,K., Fujii,S., Miura,M., Sasaki,H., Ito,K.I., Kato,H., and Ando,S. 1998. Effect of the mono- and tetra-sialogangliosides, GM1 and GQ1b, on long-term potentiation in the CA1 hippocampal neurons of the guinea pig. *Exp.Brain Res.* 123:307-314.

Gabriel,C.M., Hughes,R.A., Moore,S.E., Smith,K.J., and Walsh,F.S. 1998. Induction of experimental autoimmune neuritis with peripheral myelin protein-22. *Brain* 121 (Pt 10):1895-1902.

Galou,M., Gao,J., Humbert,J., Mericskay,M., Li,Z., Paulin,D., and Vicart,P. 1997. The importance of intermediate filaments in the adaptation of tissues to mechanical stress: evidence from gene knockout studies. *Biol.Cell* 89:85-97.

Ganser,A.L., Kirschner,D.A., and Willinger,M. 1983. Ganglioside localization on myelinated nerve fibres by cholera toxin binding. *J.Neurocytol.* 12:921-938.

Ganser,A.L. and Kirschner,D.A. 1984. Differential expression of gangliosides on the surfaces of myelinated nerve fibers. *J.Neurosci.Res.* 12:245-255.

Gatchalian,C.L., Schachner,M., and Sanes,J.R. 1989. Fibroblasts that proliferate near denervated synaptic sites in skeletal muscle synthesize the adhesive molecules tenascin(J1), N-CAM, fibronectin, and a heparan sulfate proteoglycan. *J.Cell Biol.* 108:1873-1890.

Georgiou,J., Robitaille,R., Trimble,W.S., and Charlton,M.P. 1994. Synaptic regulation of glial protein expression in vivo. *Neuron* 12:443-455.

Georgiou,J. and Charlton,M.P. 1999a. Non-myelin-forming perisynaptic schwann cells express protein zero and myelin-associated glycoprotein. *Glia* 27:101-109.

Georgiou,J., Robitaille,R., and Charlton,M.P. 1999b. Muscarinic control of cytoskeleton in perisynaptic glia. *J.Neurosci.* 19:3836-3846.

Giraudo,C.G., Rosales,F., V, and Maccioni,H.J. 1999. GA2/GM2/GD2 synthase localizes to the trans-golgi network of CHO-K1 cells. *Biochem.J.* 342 Pt 3:633-640.

Gong,Y., Tagawa,Y., Lunn,M.P., Laroy,W., Heffer-Lauc,M., Li,C.Y., Griffin,J.W., Schnaar,R.L., and Sheikh,K.A. 2002. Localization of major gangliosides in the PNS: implications for immune neuropathies. *Brain* 125:2491-2506.

Goodearl,A.D., Yee,A.G., Sandrock,A.W., Jr., Corfas,G., and Fischbach,G.D. 1995. ARIA is concentrated in the synaptic basal lamina of the developing chick neuromuscular junction. *J.Cell Biol.* 130:1423-1434.

Goodfellow,J.A., Bowes,T., Sheikh,K., Odaka,M., Halstead,S.K., Humphreys,P.D., Wagner,E.R., Yuki,N., Furukawa,K., Furukawa,K. *et al*. 2005.

Overexpression of GD1a ganglioside sensitizes motor nerve terminals to anti-GD1a antibody-mediated injury in a model of acute motor axonal neuropathy. *J.Neurosci.* 25:1620-1628.

Goodyear,C.S., O'Hanlon,G.M., Plomp,J.J., Wagner,E.R., Morrison,I., Veitch,J., Cochrane,L., Bullens,R.W., Molenaar,P.C., Conner,J. *et al*. 1999. Monoclonal antibodies raised against Guillain-Barré syndrome-associated Campylobacter jejuni lipopolysaccharides react with neuronal gangliosides and paralyze muscle-nerve preparations. *J.Clin.Invest* 104:697-708.

Gordon,J.W., Chesa,P.G., Nishimura,H., Rettig,W.J., Maccari,J.E., Endo,T., Seravalli,E., Seki,T., and Silver,J. 1987. Regulation of Thy-1 gene expression in transgenic mice. *Cell* 50:445-452.

Gordon,P.H. and Wilbourn,A.J. 2001. Early electrodiagnostic findings in Guillain-Barré syndrome. *Arch.Neurol.* 58:913-917.

Graus,F., Cordon-Cardo,C., Houghton,A.N., Melamed,M.R., and Old,L.J. 1984. Distribution of the ganglioside GD3 in the human nervous system detected by R24 mouse monoclonal antibody. *Brain Res.* 324:190-194.

Griffin,J.W., Drucker,N., Gold,B.G., Rosenfeld,J., Benzaquen,M., Charnas,L.R., Fahnestock,K.E., and Stocks,E.A. 1987. Schwann cell proliferation and migration during paranodal demyelination. *J.Neurosci.* 7:682-699.

Griffin,J.W., Stocks,E.A., Fahnestock,K., Van Praagh,A., and Trapp,B.D. 1990. Schwann cell proliferation following lysolecithin-induced demyelination. *J.Neurocytol.* 19:367-384.

Griffin,J.W., Li,C.Y., Ho,T.W., Tian,M., Gao,C.Y., Xue,P., Mishu,B., Cornblath,D.R., Macko,C., McKhann,G.M. *et al*. 1996. Pathology of the motor-sensory axonal Guillain-Barré syndrome. *Ann.Neurol.* 39:17-28.

Guillain,G., Barré,J.A., and Strohl,A. 1999. [Radiculoneuritis syndrome with hyperalbuminosis of cerebrospinal fluid without cellular reaction. Notes on clinical features and graphs of tendon reflexes. 1916]. *Ann.Med.Interne (Paris)* 150:24-32.

Gurney,M.E. 1984. Suppression of sprouting at the neuromuscular junction by immune sera. *Nature* 307:546-548.

Gurney,M.E., Apatoff,B.R., and Heinrich,S.P. 1986. Suppression of terminal axonal sprouting at the neuromuscular junction by monoclonal antibodies against a muscle-derived antigen of 56,000 daltons. *J.Cell Biol.* 102:2264-2272.

Gussoni,E., Soneoka,Y., Strickland,C.D., Buzney,E.A., Khan,M.K., Flint,A.F., Kunkel,L.M., and Mulligan,R.C. 1999. Dystrophin expression in the mdx mouse restored by stem cell transplantation. *Nature* 401:390-394.

Hafer-Macko,C., Hsieh,S.T., Li,C.Y., Ho,T.W., Sheikh,K., Cornblath,D.R., McKhann,G.M., Asbury,A.K., and Griffin,J.W. 1996a. Acute motor axonal neuropathy: an antibody-mediated attack on axolemma. *Ann.Neurol.* 40:635-644.

Hafer-Macko,C.E., Sheikh,K.A., Li,C.Y., Ho,T.W., Cornblath,D.R., McKhann,G.M., Asbury,A.K., and Griffin,J.W. 1996b. Immune attack on the Schwann cell surface in acute inflammatory demyelinating polyneuropathy. *Ann.Neurol.* 39:625-635.

Hakomori Si,S.I. 2002. Inaugural Article: The glycosynapse. *Proc.Natl.Acad.Sci.U.S.A* 99:225-232.

Hall,S.M. 1986. The effect of inhibiting Schwann cell mitosis on the re-innervation of acellular autografts in the peripheral nervous system of the mouse. *Neuropathol.Appl.Neurobiol.* 12:401-414.

Hall,S.M. 1989. Regeneration in the peripheral nervous system. *Neuropathol.Appl.Neurobiol.* 15:513-529.

Halstead,S.K., O'Hanlon,G.M., Humphreys,P.D., Morrison,D.B., Morgan,B.P., Todd,A.J., Plomp,J.J., and Willison,H.J. 2004. Anti-disialoside antibodies kill perisynaptic Schwann cells and damage motor nerve terminals via membrane attack complex in a murine model of neuropathy. *Brain* 127:2109-2123.

Halstead,S.K., Humphreys,P.D., Goodfellow,J.A., Wagner,E.R., Smith,R.A., and Willison,H.J. 2005a. Complement inhibition abrogates nerve terminal injury in Miller Fisher syndrome. *Ann.Neurol.* 58:203-210.

Halstead,S.K., Morrison,I., O'Hanlon,G.M., Humphreys,P.D., Goodfellow,J.A., Plomp,J.J., and Willison,H.J. 2005b. Anti-disialosyl antibodies mediate selective neuronal or Schwann cell injury at mouse neuromuscular junctions. *Glia* 52:177-189.

Harris,C.L., Hanna,S.M., Mizuno,M., Holt,D.S., Marchbank,K.J., and Morgan,B.P. 2003. Characterization of the mouse analogues of CD59 using novel monoclonal antibodies: tissue distribution and functional comparison. *Immunology* 109:117-126.

Harvey,G.K., Toyka,K.V., Zielasek,J., Kiefer,R., Simonis,C., and Hartung,H.P. 1995. Failure of anti-GM1 IgG or IgM to induce conduction block following intraneural transfer. *Muscle Nerve* 18:388-394.

Haymaker,W. and Kernohan J.W. 1949. The Landry-Guillain-Barré Syndrome: A clinicopathologic report of fifty fatal cases and a critique of the literature. *Medicine (Baltimore)* 28:59-141.

Hayworth,C.R., Moody,S.E., Chodosh,L.A., Krieg,P., Rimer,M., and Thompson,W.J. 2006. Induction of neuregulin signaling in mouse schwann cells in vivo mimics responses to denervation. *J.Neurosci.* 26:6873-6884.

Hila,S., Soane,L., and Koski,C.L. 2001. Sublytic C5b-9-stimulated Schwann cell survival through PI 3-kinase-mediated phosphorylation of BAD. *Glia* 36:58-67.

Ho,T.W., Hsieh,S.T., Nachamkin,I., Willison,H.J., Sheikh,K., Kiehlbauch,J., Flanigan,K., McArthur,J.C., Cornblath,D.R., McKhann,G.M. *et al*. 1997. Motor nerve terminal degeneration provides a potential mechanism for rapid recovery in acute motor axonal neuropathy after Campylobacter infection. *Neurology* 48:717-724.

Holland,R.L. and Brown,M.C. 1980. Postsynaptic transmission block can cause terminal sprouting of a motor nerve. *Science* 207:649-651.

Holmgren,J., Elwing,H., Fredman,P., and Svennerholm,L. 1980. Polystyrene-adsorbed gangliosides for investigation of the structure of the tetanus-toxin receptor. *Eur.J.Biochem.* 106:371-379.

Holt,D.S., Botto,M., Bygrave,A.E., Hanna,S.M., Walport,M.J., and Morgan,B.P. 2001. Targeted deletion of the CD59 gene causes spontaneous intravascular hemolysis and hemoglobinuria. *Blood* 98:442-449.

Hourcade,D.E., Mitchell,L.M., and Medof,M.E. 1999. Decay acceleration of the complement alternative pathway C3 convertase. *Immunopharmacology* 42:167-173.

Hughes,R., Sanders,E., Hall,S., Atkinson,P., Colchester,A., and Payan,P. 1992a. Subacute idiopathic demyelinating polyradiculoneuropathy. *Arch.Neurol.* 49:612-616.

Hughes,R., Atkinson,P., Coates,P., Hall,S., and Leibowitz,S. 1992b. Sural nerve biopsies in Guillain-Barré syndrome: axonal degeneration and macrophage-associated demyelination and absence of cytomegalovirus genome. *Muscle Nerve* 15:568-575.

Hughes,R.A., Hadden,R.D., Gregson,N.A., and Smith,K.J. 1999. Pathogenesis of Guillain-Barré syndrome. *J.Neuroimmunol.* 100:74-97.

Hughes,R.A. and Cornblath,D.R. 2005. Guillain-Barré syndrome. *Lancet* 366:1653-1666.

Hughes,R.A., Raphael,J.C., Swan,A.V., and van Doorn,P.A. 2006a. Intravenous immunoglobulin for Guillain-Barré syndrome. *Cochrane.Database.Syst.Rev.*CD002063.

Hughes,R.A., Swan,A.V., van Koningsveld,R., and van Doorn,P.A. 2006b. Corticosteroids for Guillain-Barré syndrome. *Cochrane.Database.Syst.Rev.*CD001446.

Hughes,R.A., Swan,A.V., Raphael,J.C., Annane,D., van Koningsveld,R., and van Doorn,P.A. 2007. Immunotherapy for Guillain-Barré syndrome: a systematic review. *Brain* 130:2245-2257.

Imbach,P., Barandun,S., Baumgartner,C., Hirt,A., Hofer,F., and Wagner,H.P. 1981. High-dose intravenous gammaglobulin therapy of refractory, in particular idiopathic thrombocytopenia in childhood. *Helv.Paediatr.Acta* 36:81-86.

Jackson,K.A., Mi,T., and Goodell,M.A. 1999. Hematopoietic potential of stem cells isolated from murine skeletal muscle. *Proc.Natl.Acad.Sci.U.S.A* 96:14482-14486.

Jacobs,B.C., Rothbarth,P.H., Van der Meche,F.G., Herbrink,P., Schmitz,P.I., De Klerk,M.A., and van Doorn,P.A. 1998. The spectrum of antecedent infections in Guillain-Barré syndrome: a case-control study. *Neurology* 51:1110-1115.

Jacobs,B.C., O'Hanlon,G.M., Bullens,R.W., Veitch,J., Plomp,J.J., and Willison,H.J. 2003. Immunoglobulins inhibit pathophysiological effects of anti-GQ1b-positive sera at motor nerve terminals through inhibition of antibody binding. *Brain* 126:2220-2234.

Jahromi,B.S., Robitaille,R., and Charlton,M.P. 1992. Transmitter release increases intracellular calcium in perisynaptic Schwann cells in situ. *Neuron* 8:1069-1077.

Jamal,G.A. and Ballantyne,J.P. 1988. The localization of the lesion in patients with acute ophthalmoplegia, ataxia and areflexia (Miller Fisher syndrome). A serial multimodal neurophysiological study. *Brain* 111 (Pt 1):95-114.

Kadlubowski,M. and Hughes,R.A. 1979. Identification of the neuritogen for experimental allergic neuritis. *Nature* 277:140-141.

Kaida,K., Morita,D., Kanzaki,M., Kamakura,K., Motoyoshi,K., Hirakawa,M., and Kusunoki,S. 2004. Ganglioside complexes as new target antigens in Guillain-Barré syndrome. *Ann.Neurol.* 56:567-571.

Kamata,Y., Kozaki,S., Sakaguchi,G., Iwamori,M., and Nagai,Y. 1986. Evidence for direct binding of Clostridium botulinum type E derivative toxin and its fragments to gangliosides and free fatty acids. *Biochem.Biophys.Res.Commun.* 140:1015-1019.

Kang H, Thompson WJ, Mignone J, EnikolopovG (2001) Changes of nestin expression pattern in neonates and adult neuromuscular junction of nesting transgenic mice. Soc Neurosci Abstr 27:694.8.

Kang,H., Tian,L., and Thompson,W. 2003. Terminal Schwann cells guide the reinnervation of muscle after nerve injury. *J.Neurocytol.* 32:975-985.

Kang,H., Tian,L., Son,Y.J., Zuo,Y., Procaccino,D., Love,F., Hayworth,C., Trachtenberg,J., Mikesh,M., Sutton,L. *et al*. 2007. Regulation of the intermediate filament protein nestin at rodent neuromuscular junctions by innervation and activity. *J.Neurosci.* 27:5948-5957.

Kappel,T., Anken,R.H., Hanke,W., and Rahmann,H. 2000. Gangliosides affect membrane-channel activities dependent on ambient temperature. *Cell Mol.Neurobiol.* 20:579-590.

Kearney,J.F., Won,W.J., Benedict,C., Moratz,C., Zimmer,P., Oliver,A., Martin,F., and Shu,F. 1997. B cell development in mice. *Int.Rev.Immunol.* 15:207-241.

Kelley,K.A., Friedrich,V.L., Jr., Sonshine,A., Hu,Y., Lax,J., Li,J., Drinkwater,D., Dressler,H., and Herrup,K. 1994. Expression of Thy-1/lacZ fusion genes in the CNS of transgenic mice. *Brain Res.Mol.Brain Res.* 24:261-274.

Kistner,A., Gossen,M., Zimmermann,F., Jerecic,J., Ullmer,C., Lubbert,H., and Bujard,H. 1996. Doxycycline-mediated quantitative and tissue-specific control of gene expression in transgenic mice. *Proc.Natl.Acad.Sci.U.S.A* 93:10933-10938.

Kitamura,M., Iwamori,M., and Nagai,Y. 1980. Interaction between Clostridium botulinum neurotoxin and gangliosides. *Biochim.Biophys.Acta* 628:328-335.

Kleyweg,R.P., Van der Meche,F.G., and Meulstee,J. 1988. Treatment of Guillain-Barré syndrome with high-dose gammaglobulin. *Neurology* 38:1639-1641.

Kozaki,S., Kamata,Y., Watarai,S., Nishiki,T., and Mochida,S. 1998. Ganglioside GT1b as a complementary receptor component for Clostridium botulinum neurotoxins. *Microb.Pathog.* 25:91-99.

Kornberg,A.J. and Pestronk,A. 1995. Chronic motor neuropathies: diagnosis, therapy, and pathogenesis. *Ann.Neurol.* 37 Suppl 1:S43-S50.

Kuffler,S.W. and Nicholls,J.G. 1966. The physiology of neuroglial cells. *Ergeb.Physiol* 57:1-90.

Kuffler,S.W. and Yoshikami,D. 1975. The number of transmitter molecules in a quantum: an estimate from iontophoretic application of acetylcholine at the neuromuscular synapse. *J.Physiol* 251:465-482.

Kusunoki,S., Chiba,A., Hirabayashi,Y., Irie,F., Kotani,M., Kawashima,I., Tai,T., and Nagai,Y. 1993. Generation of a monoclonal antibody specific for a new class of minor ganglioside antigens, GQ1b alpha and GT1a alpha: its binding to dorsal and lateral horn of human thoracic cord. *Brain Res.* 623:83-88.

Kusunoki,S., Shimizu,J., Chiba,A., Ugawa,Y., Hitoshi,S., and Kanazawa,I. 1996. Experimental sensory neuropathy induced by sensitization with ganglioside GD1b. *Ann.Neurol.* 39:424-431.

Kusunoki,S., Mashiko,H., Mochizuki,N., Chiba,A., Arita,M., Hitoshi,S., and Kanazawa,I. 1997. Binding of antibodies against GM1 and GD1b in human peripheral nerve. *Muscle Nerve* 20:840-845.

Kusunoki,S., Morita,D., Ohminami,S., Hitoshi,S., and Kanazawa,I. 2003. Binding of immunoglobulin G antibodies in Guillain-Barré syndrome sera to a mixture of GM1 and a phospholipid: possible clinical implications. *Muscle Nerve* 27:302-306.

Kyle,R.A. 1992. Monoclonal proteins in neuropathy. *Neurol.Clin.* 10:713-734.

Lee,J.Y., Qu-Petersen,Z., Cao,B., Kimura,S., Jankowski,R., Cummins,J., Usas,A., Gates,C., Robbins,P., Wernig,A. *et al*. 2000. Clonal isolation of muscle-

derived cells capable of enhancing muscle regeneration and bone healing. *J.Cell Biol.* 150:1085-1100.

Léger,J.M., Chassande,B., Musset,L., Meininger,V., Bouche,P., and Baumann,N. 2001. Intravenous immunoglobulin therapy in multifocal motor neuropathy: a double-blind, placebo-controlled study. *Brain* 124:145-153.

Lichtman,J.W., Magrassi,L., and Purves,D. 1987. Visualization of neuromuscular junctions over periods of several months in living mice. *J.Neurosci.* 7:1215-1222.

Lin,F., Salant,D.J., Meyerson,H., Emancipator,S., Morgan,B.P., and Medof,M.E. 2004. Respective roles of decay-accelerating factor and CD59 in circumventing glomerular injury in acute nephrotoxic serum nephritis. *J.Immunol.* 172:2636-2642.

Lichtman,J.W. and Sanes,J.R. 2003. Watching the neuromuscular junction. *J.Neurocytol.* 32:767-775.

Linington,C., Izumo,S., Suzuki,M., Uyemura,K., Meyermann,R., and Wekerle,H. 1984. A permanent rat T cell line that mediates experimental allergic neuritis in the Lewis rat in vivo. *J.Immunol.* 133:1946-1950.

Linington,C., Lassmann,H., Ozawa,K., Kosin,S., and Mongan,L. 1992. Cell adhesion molecules of the immunoglobulin supergene family as tissue-specific autoantigens: induction of experimental allergic neuritis (EAN) by P0 protein-specific T cell lines. *Eur.J.Immunol.* 22:1813-1817.

Loeb,J.A., Hmadcha,A., Fischbach,G.D., Land,S.J., and Zakarian,V.L. 2002. Neuregulin expression at neuromuscular synapses is modulated by synaptic activity and neurotrophic factors. *J.Neurosci.* 22:2206-2214.

Love,F.M. and Thompson,W.J. 1998. Schwann cells proliferate at rat neuromuscular junctions during development and regeneration. *J.Neurosci.* 18:9376-9385.

Love,F.M. and Thompson,W.J. 1999. Glial cells promote muscle reinnervation by responding to activity-dependent postsynaptic signals. *J.Neurosci.* 19:10390-10396.

Love,F.M., Son,Y.J., and Thompson,W.J. 2003. Activity alters muscle reinnervation and terminal sprouting by reducing the number of Schwann cell pathways that grow to link synaptic sites. *J.Neurobiol.* 54:566-576.

Low,P.A., Dyck,P.J., Lambert,E.H., Brimijoin,W.S., Trautmann,J.C., Malagelada,J.R., Fealey,R.D., and Barrétt,D.M. 1983. Acute panautonomic neuropathy. *Ann.Neurol.* 13:412-417.

Low,P.A. 1994. Autonomic neuropathies. *Curr.Opin.Neurol.* 7:402-406.

Lubischer,J.L. and Bebinger,D.M. 1999. Regulation of terminal Schwann cell number at the adult neuromuscular junction. *J.Neurosci.* 19:RC46.

Luijten,J.A. and Baart de la Faille-Kuyp. 1972. The occurrence of IgM and complement factors along myelin sheaths of peripheral nerves. An immunohistochemical study of the Guillain-Barré syndrome. Preliminary communication. *J.Neurol.Sci.* 15:219-224.

Maccioni,H.J., Daniotti,J.L., and Martina,J.A. 1999. Organization of ganglioside synthesis in the Golgi apparatus. *Biochim.Biophys.Acta* 1437:101-118.

Maehara,T., Ono,K., Tsutsui,K., Watarai,S., Yasuda,T., Inoue,H., and Tokunaga,A. 1997. A monoclonal antibody that recognizes ganglioside GD1b in the rat central nervous system. *Neurosci.Res.* 29:9-16.

Martini,R. and Schachner,M. 1986. Immunoelectron microscopic localization of neural cell adhesion molecules (L1, N-CAM, and MAG) and their shared carbohydrate epitope and myelin basic protein in developing sciatic nerve. *J.Cell Biol.* 103:2439-2448.

Marques,M.J., Pereira,E.C., Minatel,E., and Neto,H.S. 2006. Nerve-terminal and Schwann-cell response after nerve injury in the absence of nitric oxide. *Muscle Nerve* 34:225-231.

McFarlin,D.E. 1990. Immunological parameters in Guillain-Barré syndrome. *Ann.Neurol.* 27 Suppl:S25-S29.

McKhann,G.M., Cornblath,D.R., Griffin,J.W., Ho,T.W., Li,C.Y., Jiang,Z., Wu,H.S., Zhaori,G., Liu,Y., Jou,L.P. *et al*. 1993. Acute motor axonal neuropathy: a frequent cause of acute flaccid paralysis in China. *Ann.Neurol.* 33:333-342.

Meri,S., Morgan,B.P., Davies,A., Daniels,R.H., Olavesen,M.G., Waldmann,H., and Lachmann,P.J. 1990. Human protectin (CD59), an 18,000-20,000 MW complement lysis restricting factor, inhibits C5b-8 catalysed insertion of C9 into lipid bilayers. *Immunology* 71:1-9.

Miledi,R. and Slater,C.R. 1968. Electrophysiology and electron-microscopy of rat neuromuscular junctions after nerve degeneration. *Proc.R.Soc.Lond B Biol.Sci.* 169:289-306.

Miledi,R. and Slater,C.R. 1970. On the degeneration of rat neuromuscular junctions after nerve section. *J.Physiol* 207:507-528.

Miwa,T. and Song,W.C. 2001. Membrane complement regulatory proteins: insight from animal studies and relevance to human diseases. *Int.Immunopharmacol.* 1:445-459.

Miwa,T., Zhou,L., Hilliard,B., Molina,H., and Song,W.C. 2002. Crry, but not CD59 and DAF, is indispensable for murine erythrocyte protection in vivo from spontaneous complement attack. *Blood* 99:3707-3716.

Mizoguchi,K. 1998. Anti-GQ1b IgG antibody activities related to the severity of Miller Fisher syndrome. *Neurol.Res.* 20:617-624.

Molander,M., Berthold,C.H., Persson,H., Andersson,K., and Fredman,P. 1997. Monosialoganglioside (GM1) immunofluorescence in rat spinal roots studied with a monoclonal antibody. *J.Neurocytol.* 26:101-111.

Morgan,B.P., Luzio,J.P., and Campbell,A.K. 1986. Intracellular Ca2+ and cell injury: a paradoxical role of Ca2+ in complement membrane attack. *Cell Calcium* 7:399-411.

Mori,M., Kuwabara,S., Fukutake,T., Yuki,N., and Hattori,T. 2001. Clinical features and prognosis of Miller Fisher syndrome. *Neurology* 56:1104-1106.

Morin,J.G. and Hastings,J.W. 1971. Energy transfer in a bioluminescent system. *J.Cell Physiol* 77:313-318.

Morris,R. 1985. Thy-1 in developing nervous tissue. *Dev.Neurosci.* 7:133-160.

Murinson,B.B., Archer,D.R., Li,Y., and Griffin,J.W. 2005. Degeneration of myelinated efferent fibers prompts mitosis in Remak Schwann cells of uninjured C-fiber afferents. *J.Neurosci.* 25:1179-1187.

Nachamkin,I. 2001. Campylobacter Enteritis and the Guillain-Barré Syndrome. *Curr.Infect.Dis.Rep.* 3:116-122.

Nangaku,M. 2003. Complement regulatory proteins: are they important in disease? *J.Am.Soc.Nephrol.* 14:2411-2413.

Newman,E.A. 1986. Physiological properties and possible functions of Muller cells. *Neurosci.Res.Suppl* 4:S209-S220.

Nobile-Orazio,E., Manfredini,E., Carpo,M., Meucci,N., Monaco,S., Ferrari,S., Bonetti,B., Cavaletti,G., Gemignani,F., Durelli,L. *et al*. 1994. Frequency and clinical correlates of anti-neural IgM antibodies in neuropathy associated with IgM monoclonal gammopathy. *Ann.Neurol.* 36:416-424.

O'Hanlon,G.M., Paterson,G.J., Wilson,G., Doyle,D., McHardie,P., and Willison,H.J. 1996. Anti-GM1 ganglioside antibodies cloned from autoimmune neuropathy patients show diverse binding patterns in the rodent nervous system. *J.Neuropathol.Exp.Neurol.* 55:184-195.

O'Hanlon,G.M., Paterson,G.J., Veitch,J., Wilson,G., and Willison,H.J. 1998. Mapping immunoreactive epitopes in the human peripheral nervous system using

human monoclonal anti-GM1 ganglioside antibodies. *Acta Neuropathol.(Berl)* 95:605-616.

O'Hanlon,G.M., Plomp,J.J., Chakrabarti,M., Morrison,I., Wagner,E.R., Goodyear,C.S., Yin,X., Trapp,B.D., Conner,J., Molenaar,P.C. *et al*. 2001. Anti-GQ1b ganglioside antibodies mediate complement-dependent destruction of the motor nerve terminal. *Brain* 124:893-906.

O'Hanlon,G.M., Bullens,R.W., Plomp,J.J., and Willison,H.J. 2002. Complex gangliosides as autoantibody targets at the neuromuscular junction in Miller Fisher syndrome: a current perspective. *Neurochem.Res.* 27:697-709.

O'Hanlon,G.M., Humphreys,P.D., Goldman,R.S., Halstead,S.K., Bullens,R.W., Plomp,J.J., Ushkaryov,Y., and Willison,H.J. 2003. Calpain inhibitors protect against axonal degeneration in a model of anti-ganglioside antibody-mediated motor nerve terminal injury. *Brain* 126:2497-2509.

O'Malley,J.P., Waran,M.T., and Balice-Gordon,R.J. 1999. In vivo observations of terminal Schwann cells at normal, denervated, and reinnervated mouse neuromuscular junctions. *J.Neurobiol.* 38:270-286.

Oaklander,A.L., Miller,M.S., and Spencer,P.S. 1987. Early changes in degenerating mouse sciatic nerve are associated with endothelial cells. *Brain Res.* 419:39-45.

Odaka,M., Yuki,N., and Hirata,K. 2001. Anti-GQ1b IgG antibody syndrome: clinical and immunological range. *J.Neurol.Neurosurg.Psychiatry* 70:50-55.

Odaka,M., Yuki,N., Yamada,M., Koga,M., Takemi,T., Hirata,K., and Kuwabara,S. 2003. Bickerstaff's brainstem encephalitis: clinical features of 62 cases and a subgroup associated with Guillain-Barré syndrome. *Brain* 126:2279-2290.

Ogawa-Goto,K. and Abe,T. 1998. Gangliosides and glycosphingolipids of peripheral nervous system myelins--a minireview. *Neurochem.Res.* 23:305-310.

Ogino,M., Orazio,N., and Latov,N. 1995. IgG anti-GM1 antibodies from patients with acute motor neuropathy are predominantly of the IgG1 and IgG3 subclasses. *J.Neuroimmunol.* 58:77-80.

Overell,J.R., Hsieh,S.T., Odaka,M., Yuki,N., and Willison,H.J. 2007. Treatment for Fisher syndrome, Bickerstaff's brainstem encephalitis and related disorders. *Cochrane.Database.Syst.Rev.*CD004761.

Pamphlett,R. 1989. Early terminal and nodal sprouting of motor axons after botulinum toxin. *J.Neurol.Sci.* 92:181-192.

Paterson,G., Wilson,G., Kennedy,P.G., and Willison,H.J. 1995. Analysis of anti-GM1 ganglioside IgM antibodies cloned from motor neuropathy patients demonstrates diverse V region gene usage with extensive somatic mutation. *J.Immunol.* 155:3049-3059.

Pellegrino,R.G. and Spencer,P.S. 1985. Schwann cell mitosis in response to regenerating peripheral axons in vivo. *Brain Res.* 341:16-25.

Pellegrino,R.G., Politis,M.J., Ritchie,J.M., and Spencer,P.S. 1986. Events in degenerating cat peripheral nerve: induction of Schwann cell S phase and its relation to nerve fibre degeneration. *J.Neurocytol.* 15:17-28.

Pestronk,A. and Li,F. 1991. Motor neuropathies and motor neuron disorders: association with antiglycolipid antibodies. *Adv.Neurol.* 56:427-432.

Pinard,A., Levesque,S., Vallee,J., and Robitaille,R. 2003. Glutamatergic modulation of synaptic plasticity at a PNS vertebrate cholinergic synapse. *Eur.J.Neurosci.* 18:3241-3250.

Plomp,J.J., Molenaar,P.C., O'Hanlon,G.M., Jacobs,B.C., Veitch,J., Daha,M.R., van Doorn,P.A., Van der Meche,F.G., Vincent,A., Morgan,B.P. *et al*. 1999. Miller Fisher anti-GQ1b antibodies: alpha-latrotoxin-like effects on motor end plates. *Ann.Neurol.* 45:189-199.

Podack,E.R. and Tschopp,J. 1984. Membrane attack by complement. *Mol.Immunol.* 21:589-603.

Prasher,D.C., Eckenrode,V.K., Ward,W.W., Prendergast,F.G., and Cormier,M.J. 1992. Primary structure of the Aequorea victoria green-fluorescent protein. *Gene* 111:229-233.

Putzu,G.A., Figarella-Branger,D., Bouvier-Labit,C., Liprandi,A., Bianco,N., and Pellissier,J.F. 2000. Immunohistochemical localization of cytokines, C5b-9 and ICAM-1 in peripheral nerve of Guillain-Barré syndrome. *J.Neurol.Sci.* 174:16-21.

Qu,Z., Huang,X., Ahmadi,P., Stenberg,P., Liebler,J.M., Le,A.C., Planck,S.R., and Rosenbaum,J.T. 1998. Synthesis of basic fibroblast growth factor by murine mast cells. Regulation by transforming growth factor beta, tumor necrosis factor alpha, and stem cell factor. *Int.Arch.Allergy Immunol.* 115:47-54.

Quarles,R.H. and Weiss,M.D. 1999. Autoantibodies associated with peripheral neuropathy. *Muscle Nerve* 22:800-822.

Rafuse,V.F., Gordon,T., and Orozco,R. 1992. Proportional enlargement of motor units after partial denervation of cat triceps surae muscles. *J.Neurophysiol.* 68:1261-1276.

Raphael,J.C., Chevret,S., Hughes,R.A., and Annane,D. 2002. Plasma exchange for Guillain-Barré syndrome. *Cochrane.Database.Syst.Rev.*CD001798.

Reddy,L.V., Koirala,S., Sugiura,Y., Herrera,A.A., and Ko,C.P. 2003. Glial cells maintain synaptic structure and function and promote development of the neuromuscular junction in vivo. *Neuron* 40:563-580.

Rees,J.H., Thompson,R.D., Smeeton,N.C., and Hughes,R.A. 1998. Epidemiological study of Guillain-Barré syndrome in south east England. *J.Neurol.Neurosurg.Psychiatry* 64:74-77.

Reiser,G. and Miledi,R. 1988. Characteristics of Schwann-cell miniature end-plate currents in denervated frog muscle. *Pflügers Arch.* 412:22-28.

Reynolds,M.L. and Woolf,C.J. 1992. Terminal Schwann cells elaborate extensive processes following denervation of the motor endplate. *J.Neurocytol.* 21:50-66.

Rich,M.M. and Lichtman,J.W. 1989. In vivo visualization of pre- and postsynaptic changes during synapse elimination in reinnervated mouse muscle. *J.Neurosci.* 9:1781-1805.

Riethmacher,D., Sonnenberg-Riethmacher,E., Brinkmann,V., Yamaai,T., Lewin,G.R., and Birchmeier,C. 1997. Severe neuropathies in mice with targeted mutations in the ErbB3 receptor. *Nature* 389:725-730.

Roberts,M., Willison,H., Vincent,A., and Newsom-Davis,J. 1994. Serum factor in Miller Fisher variant of Guillain-Barré syndrome and neurotransmitter release. *Lancet* 343:454-455.

Robitaille,R., Garcia,M.L., Kaczorowski,G.J., and Charlton,M.P. 1993. Functional colocalization of calcium and calcium-gated potassium channels in control of transmitter release. *Neuron* 11:645-655.

Robitaille,R., Bourque,M.J., and Vandaele,S. 1996. Localization of L-type Ca2+ channels at perisynaptic glial cells of the frog neuromuscular junction. *J.Neurosci.* 16:148-158.

Robitaille,R., Jahromi,B.S., and Charlton,M.P. 1997. Muscarinic Ca2+ responses resistant to muscarinic antagonists at perisynaptic Schwann cells of the frog neuromuscular junction. *J.Physiol* 504 (Pt 2):337-347.

Robitaille,R. 1998. Modulation of synaptic efficacy and synaptic depression by glial cells at the frog neuromuscular junction. *Neuron* 21:847-855.

Rochon,D., Rousse,I., and Robitaille,R. 2001. Synapse-glia interactions at the mammalian neuromuscular junction. *J.Neurosci.* 21:3819-3829.

Roots,B.I. 1983. Neurofilament accumulation induced in synapses by leupeptin. *Science* 221:971-972.

Ropper,A.H., Wijdicks,E.F., and Shahani,B.T. 1990. Electrodiagnostic abnormalities in 113 consecutive patients with Guillain-Barré syndrome. *Arch.Neurol.* 47:881-887.

Ropper,A.H. 1992. The Guillain-Barré syndrome. *N.Engl.J.Med.* 326:1130-1136.

Rose,N.R. and Bona,C. 1993. Defining criteria for autoimmune diseases (Witebsky's postulates revisited). *Immunol.Today* 14:426-430.

Saida,T., Saida,K., Silberberg,D.H., and Brown,M.J. 1978. Transfer of demyelination by intraneural injection of experimental allergic neuritis serum. *Nature* 272:639-641.

Saida,T., Saida,K., Brown,M.J., and Silberberg,D.H. 1979a. Peripheral nerve demyelination induced by intraneural injection of experimental allergic encephalomyelitis serum. *J.Neuropathol.Exp.Neurol.* 38:498-518.

Saida,T., Saida,K., and Silberberg,D.H. 1979b. Demyelination produced by experimental allergic neuritis serum and anti-galactocerebroside antiserum in CNS cultures. An ultrastructural study. *Acta Neuropathol.* 48:19-25.

Saito,A. and Zacks,S.I. 1969. Ultrastructure of Schwann and perineural sheaths at the mouse neuromuscular junction. *Anat.Rec.* 164:379-390.

Saleh,M.N., Khazaeli,M.B., Wheeler,R.H., Dropcho,E., Liu,T., Urist,M., Miller,D.M., Lawson,S., Dixon,P., Russell,C.H. *et al*. 1992. Phase I trial of the murine monoclonal anti-GD2 antibody 14G2a in metastatic melanoma. *Cancer Res.* 52:4342-4347.

Sanders,M.E., Koski,C.L., Robbins,D., Shin,M.L., Frank,M.M., and Joiner,K.A. 1986. Activated terminal complement in cerebrospinal fluid in Guillain-Barré syndrome and multiple sclerosis. *J.Immunol.* 136:4456-4459.

Sandrock,A.W., Jr., Goodearl,A.D., Yin,Q.W., Chang,D., and Fischbach,G.D. 1995. ARIA is concentrated in nerve terminals at neuromuscular junctions and at other synapses. *J.Neurosci.* 15:6124-6136.

Santoro,M., Uncini,A., Corbo,M., Staugaitis,S.M., Thomas,F.P., Hays,A.P., and Latov,N. 1992. Experimental conduction block induced by serum from a patient with anti-GM1 antibodies. *Ann.Neurol.* 31:385-390.

Sartucci,F., Cafforio,G., Borghetti,D., Domenici,L., Orlandi,G., and Murri,L. 2005. Electrophysiological evidence by single fibre electromyography of neuromuscular transmission impairment in a case of Miller Fisher syndrome. *Neurol.Sci.* 26:125-128.

Sauron,B., Bouche,P., Cathala,H.P., Chain,F., and Castaigne,P. 1984. Miller Fisher syndrome: clinical and electrophysiologic evidence of peripheral origin in 10 cases. *Neurology* 34:953-956.

Schiavo,G., Benfenati,F., Poulain,B., Rossetto,O., Polverino,d.L., Dasgupta,B.R., and Montecucco,C. 1992. Tetanus and botulinum-B neurotoxins block neurotransmitter release by proteolytic cleavage of synaptobrevin. *Nature* 359:832-835.

Schlaepfer,W.W. 1977. Vesicular disruption of myelin simulated by exposure of nerve to calcium ionophore. *Nature* 265:734-736.

Schuman,E.M. and Madison,D.V. 1994. Nitric oxide and synaptic function. *Annu.Rev.Neurosci.* 17:153-183.

Scolding,N.J., Morgan,B.P., Houston,W.A., Linington,C., Campbell,A.K., and Compston,D.A. 1989. Vesicular removal by oligodendrocytes of membrane attack complexes formed by activated complement. *Nature* 339:620-622.

Seale,P., Asakura,A., and Rudnicki,M.A. 2001. The potential of muscle stem cells. *Dev.Cell* 1:333-342.

Shahar,E. 2006. Current therapeutic options in severe Guillain-Barré syndrome. *Clin.Neuropharmacol.* 29:45-51.

Sheikh,K.A., Nachamkin,I., Ho,T.W., Willison,H.J., Veitch,J., Ung,H., Nicholson,M., Li,C.Y., Wu,H.S., Shen,B.Q. *et al*. 1998. Campylobacter jejuni lipopolysaccharides in Guillain-Barré syndrome: molecular mimicry and host susceptibility. *Neurology* 51:371-378.

Sheikh,K.A., Deerinck,T.J., Ellisman,M.H., and Griffin,J.W. 1999. The distribution of ganglioside-like moieties in peripheral nerves. *Brain* 122 (Pt 3):449-460.

Sheikh,K.A. and Griffin,J.W. 2001. Variants of the Guillain Barré syndrome: progress toward fulfilling "Koch's postulates". *Ann.Neurol.* 49:694-696.

Sheng,Z.H., Westenbroek,R.E., and Catterall,W.A. 1998. Physical link and functional coupling of presynaptic calcium channels and the synaptic vesicle docking/fusion machinery. *J.Bioenerg.Biomembr.* 30:335-345.

Shimonura,O., Johnson,F.H., and Saiga,Y. 1962. Extraction, purification and properties of aequorin, a bioluminescent protein from the luminous hydromedusan, Aequorea. *J.Cell Comp Physiol* 59:223-239.

Silverstein,A.M. 2001. Autoimmunity versus horror autotoxicus: the struggle for recognition. *Nat.Immunol.* 2:279-281.

Simons,K. and Ikonen,E. 1997. Functional rafts in cell membranes. *Nature* 387:569-572.

Slater,C.R., Lyons,P.R., Walls,T.J., Fawcett,P.R., and Young,C. 1992. Structure and function of neuromuscular junctions in the vastus lateralis of man. A motor point biopsy study of two groups of patients. *Brain* 115 (Pt 2):451-478.

Smit,A.A., Vermeulen,M., Koelman,J.H., and Wieling,W. 1997. Unusual recovery from acute panautonomic neuropathy after immunoglobulin therapy. *Mayo Clin.Proc.* 72:333-335.

Smith,K.J., Hall,S.M., and Schauf,C.L. 1985. Vesicular demyelination induced by raised intracellular calcium. *J.Neurol.Sci.* 71:19-37.

Snapper,C.M., Yamaguchi,H., Moorman,M.A., and Mond,J.J. 1994. An in vitro model for T cell-independent induction of humoral immunity. A requirement for NK cells. *J.Immunol.* 152:4884-4892.

Son,Y.J. and Thompson,W.J. 1995a. Schwann cell processes guide regeneration of peripheral axons. *Neuron* 14:125-132.

Son,Y.J. and Thompson,W.J. 1995b. Nerve sprouting in muscle is induced and guided by processes extended by Schwann cells. *Neuron* 14:133-141.

Son,Y.J., Trachtenberg,J.T., and Thompson,W.J. 1996. Schwann cells induce and guide sprouting and reinnervation of neuromuscular junctions. *Trends Neurosci.* 19:280-285.

Sontheimer,H., Black,J.A., and Waxman,S.G. 1996. Voltage-gated Na+ channels in glia: properties and possible functions. *Trends Neurosci.* 19:325-331.

Spicer,A.P., Seldin,M.F., and Gendler,S.J. 1995. Molecular cloning and chromosomal localization of the mouse decay-accelerating factor genes. Duplicated genes encode glycosylphosphatidylinositol-anchored and transmembrane forms. *J.Immunol.* 155:3079-3091.

Sun,X., Funk,C.D., Deng,C., Sahu,A., Lambris,J.D., and Song,W.C. 1999. Role of decay-accelerating factor in regulating complement activation on the erythrocyte surface as revealed by gene targeting. *Proc.Natl.Acad.Sci.U.S.A* 96:628-633.

Susuki,K., Odaka,M., Mori,M., Hirata,K., and Yuki,N. 2004. Acute motor axonal neuropathy after Mycoplasma infection: Evidence of molecular mimicry. *Neurology* 62:949-956.

Svennerholm,L., Bostrom,K., Fredman,P., Jungbjer,B., Lekman,A., Mansson,J.E., and Rynmark,B.M. 1994. Gangliosides and allied glycosphingolipids in human peripheral nerve and spinal cord. *Biochim.Biophys.Acta* 1214:115-123.

Tam,S.L., Archibald,V., Jassar,B., Tyreman,N., and Gordon,T. 2001. Increased neuromuscular activity reduces sprouting in partially denervated muscles. *J.Neurosci.* 21:654-667.

Taveggia,C., Zanazzi,G., Petrylak,A., Yano,H., Rosenbluth,J., Einheber,S., Xu,X., Esper,R.M., Loeb,J.A., Shrager,P. *et al*. 2005. Neuregulin-1 type III determines the ensheathment fate of axons. *Neuron* 47:681-694.

Thompson,W. and Jansen,J.K. 1977. The extent of sprouting of remaining motor units in partly denervated immature and adult rat soleus muscle. *Neuroscience* 2:523-535.

Tonnessen,T.I., Nyland,H., and Aarli,J.A. 1982. Complement factors and acute phase reactants in the Guillain-Barré syndrome. *Eur.Neurol.* 21:124-128.

Trachtenberg,J.T. and Thompson,W.J. 1996. Schwann cell apoptosis at developing neuromuscular junctions is regulated by glial growth factor. *Nature* 379:174-177.

Trachtenberg,J.T. and Thompson,W.J. 1997. Nerve terminal withdrawal from rat neuromuscular junctions induced by neuregulin and Schwann cells. *J.Neurosci.* 17:6243-6255.

Trachtenberg,J.T., Chen,B.E., Knott,G.W., Feng,G., Sanes,J.R., Welker,E., and Svoboda,K. 2002. Long-term in vivo imaging of experience-dependent synaptic plasticity in adult cortex. *Nature* 420:788-794.

Tsien,R.Y. 1998. The green fluorescent protein. *Annu.Rev.Biochem.* 67:509-544.

Tucek,S. and Proska,J. 1995. Allosteric modulation of muscarinic acetylcholine receptors. *Trends Pharmacol.Sci.* 16:205-212.

Vaittinen,S., Lukka,R., Sahlgren,C., Rantanen,J., Hurme,T., Lendahl,U., Eriksson,J.E., and Kalimo,H. 1999. Specific and innervation-regulated expression of the intermediate filament protein nestin at neuromuscular and myotendinous junctions in skeletal muscle. *Am.J.Pathol.* 154:591-600.

Van den Berg,L.H., Hays,A.P., NobileOrazio,E., Kinsella,L.J., Manfredini,E., Corbo,M., Rosoklija,G., Younger,D.S., Lovelace,R.E., Trojaborg,W. *et al*. 1996. Anti-MAG and anti-SGPG antibodies in neuropathy. *Muscle & Nerve* 19:637-643.

Vedeler,C.A., Matre,R., and Nyland,H. 1988. Class and IgG subclass distribution of antibodies against peripheral nerve myelin in sera from patients with inflammatory demyelinating polyradiculoneuropathy. *Acta Neurol.Scand.* 78:401-407.

Vidal,M., Morris,R., Grosveld,F., and Spanopoulou,E. 1990. Tissue-specific control elements of the Thy-1 gene. *EMBO J.* 9:833-840.

Wada,M.R., Inagawa-Ogashiwa,M., Shimizu,S., Yasumoto,S., and Hashimoto,N. 2002. Generation of different fates from multipotent muscle stem cells. *Development* 129:2987-2995.

Waksman,B.H. and Adams,R.D. 1955. Allergic neuritis: an experimental disease of rabbits induced by the injection of peripheral nervous tissue and adjuvants. *J.Exp.Med.* 102:213-236.

Walport,M.J. 2001a. Complement. First of two parts. *N.Engl.J.Med.* 344:1058-1066.

Walport,M.J. 2001b. Complement. Second of two parts. *N.Engl.J.Med.* 344:1140-1144.

Walsh,M.K. and Lichtman,J.W. 2003. In vivo time-lapse imaging of synaptic takeover associated with naturally occurring synapse elimination. *Neuron* 37:67-73.

Wang,Z., Low,P.A., Jordan,J., Freeman,R., Gibbons,C.H., Schroeder,C., Sandroni,P., and Vernino,S. 2007. Autoimmune autonomic ganglionopathy: IgG effects on ganglionic acetylcholine receptor current. *Neurology* 68:1917-1921.

Wigston,D.J. 1990. Repeated in vivo visualization of neuromuscular junctions in adult mouse lateral gastrocnemius. *J.Neurosci.* 10:1753-1761.

Willison,H.J. and Kennedy,P.G. 1993. Gangliosides and bacterial toxins in Guillain-Barré syndrome. *J.Neuroimmunol.* 46:105-112.

Willison,H.J., Veitch,J., Paterson,G., and Kennedy,P.G. 1993a. Miller Fisher syndrome is associated with serum antibodies to GQ1b ganglioside. *J.Neurol.Neurosurg.Psychiatry* 56:204-206.

Willison,H.J., Paterson,G., Veitch,J., Inglis,G., and Barnett,S.C. 1993b. Peripheral neuropathy associated with monoclonal IgM anti-Pr2 cold agglutinins. *J.Neurol.Neurosurg.Psychiatry* 56:1178-1183.

Willison,H.J. and Veitch,J. 1994. Immunoglobulin subclass distribution and binding characteristics of anti-GQ1b antibodies in Miller Fisher syndrome. *J.Neuroimmunol.* 50:159-165.

Willison,H.J., O'Hanlon,G.M., Paterson,G., Veitch,J., Wilson,G., Roberts,M., Tang,T., and Vincent,A. 1996. A somatically mutated human antiganglioside IgM

antibody that induces experimental neuropathy in mice is encoded by the variable region heavy chain gene, V1-18. *J.Clin.Invest* 97:1155-1164.

Willison,H.J., Veitch,J., Swan,A.V., Baumann,N., Comi,G., Gregson,N.A., Illa,I., Zielasek,J., and Hughes,R.A. 1999. Inter-laboratory validation of an ELISA for the determination of serum anti-ganglioside antibodies. *Eur.J.Neurol.* 6:71-77.

Willison,H.J., O'Leary,C.P., Veitch,J., Blumhardt,L.D., Busby,M., Donaghy,M., Fuhr,P., Ford,H., Hahn,A., Renaud,S. *et al*. 2001. The clinical and laboratory features of chronic sensory ataxic neuropathy with anti-disialosyl IgM antibodies. *Brain* 124:1968-1977.

Willison,H.J. and Yuki,N. 2002. Peripheral neuropathies and anti-glycolipid antibodies. *Brain* 125:2591-2625.

Willison,H.J., Townson,K., Veitch,J., Boffey,J., Isaacs,N., Andersen,S.M., Zhang,P., Ling,C.C., and Bundle,D.R. 2004. Synthetic disialylgalactose immunoadsorbents deplete anti-GQ1b antibodies from autoimmune neuropathy sera. *Brain* 127:680-691.

Willison,H.J. 2005. Ganglioside complexes: new autoantibody targets in Guillain-Barré syndromes. *Nat.Clin.Pract.Neurol.* 1:2-3.

Wilson,G.F. and Chiu,S.Y. 1990. Ion channels in axon and Schwann cell membranes at paranodes of mammalian myelinated fibers studied with patch clamp. *J.Neurosci.* 10:3263-3274.

Winer,J.B. 2001. Bickerstaff's encephalitis and the Miller Fisher syndrome. *J.Neurol.Neurosurg.Psychiatry* 71:433-435.

Wood,S.J. and Slater,C.R. 2001. Safety factor at the neuromuscular junction. *Prog.Neurobiol.* 64:393-429.

Woolf,C.J., Reynolds,M.L., Chong,M.S., Emson,P., Irwin,N., and Benowitz,L.I. 1992. Denervation of the motor endplate results in the rapid expression by terminal Schwann cells of the growth-associated protein GAP-43. *J.Neurosci.* 12:3999-4010.

Young,W.W., Jr., Lutz,M.S., Mills,S.E., and Lechler-Osborn,S. 1990. Use of brefeldin A to define sites of glycosphingolipid synthesis: GA2/GM2/GD2 synthase is trans to the brefeldin A block. *Proc.Natl.Acad.Sci.U.S.A* 87:6838-6842.

Yu,Z. and Lennon,V.A. 1999. Mechanism of intravenous immune globulin therapy in antibody-mediated autoimmune diseases. *N.Engl.J.Med.* 340:227-228.

Yuki,N., Yoshino,H., Sato,S., Ohno,T., and Miyatake,T. 1990. [An acute axonal form of Guillain-Barré syndrome with antibodies against gangliosides GM1 and GD1b--a case report]. *Rinsho Shinkeigaku* 30:989-993.

Yuki,N., Sato,S., Tsuji,S., Hozumi,I., and Miyatake,T. 1993a. An immunologic abnormality common to Bickerstaff's brain stem encephalitis and Fisher's syndrome. *J.Neurol.Sci.* 118:83-87.

Yuki,N., Taki,T., Inagaki,F., Kasama,T., Takahashi,M., Saito,K., Handa,S., and Miyatake,T. 1993b. A bacterium lipopolysaccharide that elicits Guillain-Barré syndrome has a GM1 ganglioside-like structure. *J.Exp.Med.* 178:1771-1775.

Yuki,N., Sato,S., Tsuji,S., Ohsawa,T., and Miyatake,T. 1993c. Frequent presence of anti-GQ1b antibody in Fisher's syndrome. *Neurology* 43:414-417.

Yuki,N., Yamada,M., Tagawa,Y., Takahashi,H., and Handa,S. 1997. Pathogenesis of the neurotoxicity caused by anti-GD2 antibody therapy. *J.Neurol.Sci.* 149:127-130.

Yuki,N., Yamada,M., Koga,M., Odaka,M., Susuki,K., Tagawa,Y., Ueda,S., Kasama,T., Ohnishi,A., Hayashi,S. *et al*. 2001. Animal model of axonal Guillain-Barré syndrome induced by sensitization with GM1 ganglioside. *Ann.Neurol.* 49:712-720.

Zuo,Y., Lubischer,J.L., Kang,H., Tian,L., Mikesh,M., Marks,A., Scofield,V.L., Maika,S., Newman,C., Krieg,P. *et al*. 2004. Fluorescent proteins expressed in mouse transgenic lines mark subsets of glia, neurons, macrophages, and dendritic cells for vital examination. *J.Neurosci.* 24:10999-11009.